AN ABSTRACT OF THE THESIS OF

Reed S. Lewis for the degree of Doctor of Philosophy in Geology presented on May 21, 1990.

Title: Geology, Geochemistry, and Mineral Potential of Cretaceous and Tertiary Plutons in the Eastern Part of the Soldier Mountains, Idaho

Abstract approved: Redacted for Privacy

Cyrus W. Field

The eastern part of the Soldier Mountains is principally underlain by plutons of Cretaceous and Eocene age. The former are subdivided into a potassic suite, enriched in Rb, Cs, U, B, Mg, Sc, Co, and Cr, and a sodic suite, enriched in Al, Sr, Ba, Zr, and light rare earth elements. The sodic suite was probably derived from one or more sources more depleted in large-ion lithophile elements than the source of the potassic suite. The Eocene plutonic rocks are subdivided into quartz monzodiorite and pink granite suites. On the basis of CaO and Sr content, MgO/(MgO + FeO*) ratios, and initial $^{87}Sr/^{86}Sr$ ratios, the two Eocene suites cannot be related by fractional crystallization.

Plutonic rocks in the eastern part of the Soldier Mountains have undergone propylitic, potassic, and muscovite-quartz alteration. Muscovite-quartz alteration is Cretaceous in age and is localized along joints and fractures, some of which are filled with vein quartz. This alteration type involved relatively high-$\delta^{18}O$ fluids (about 7 permil) of probable magmatic origin. Potassic alteration is probably both Cretaceous and Eocene in age, but is limited in extent. During Eocene time propylitic alteration was pronounced around the pink granites. In propylitized rocks the $\delta^{18}O$ values of feldspars are as low as -5.8 permil, indicating exchange with heated meteoric water. Regardless of a clear association between plutons of pink granite and

widespread propylitic alteration, mineralization associated with the pink granite suite is minimal. Mineralized areas within the quartz monzodiorite suite are characterized by veins and (or) stockworks(?) enriched in Cu, Mo, and Ag.

Most $\delta^{18}O$ values of coexisting feldspars fall near a 1:1 line on a δ-δ plot, but isotopic disequilibrium is indicated by several pairs that differ by up to 3.6 permil. Plagioclase feldspars in propylitized rocks typically have lower $\delta^{18}O$ values than do potassium feldspars, which reflects the more restricted stability of plagioclase feldspar during alteration. In contrast, turbid potassium feldspar in Eocene granite is more depleted in ^{18}O than coexisting plagioclase. Fluid temperature was probably the most important variable controlling the relative stability of different feldspars during alteration.

Geology, Geochemistry and Mineral Potential of Cretaceous and Tertiary Plutons in the Eastern Part of the Soldier Mountains, Idaho

by

Reed S. Lewis

A THESIS

submitted to

Oregon State University

in partial fulfillment of
the requirements for the
degree of

Doctor of Philosophy

Completed May 21, 1990

Commencement June 1991

APPROVED:

Redacted for Privacy

Professor of Geology in charge of major

Redacted for Privacy

Chairman of Department of Geosciences

Redacted for Privacy

Dean of Graduate School

Date thesis is presented May 21, 1990

Typed by Reed S. Lewis for Reed S. Lewis

ACKNOWLEDGEMENTS

Financial support for this project was provided in part by the U.S. Geological Survey as part of the Hailey project. Reactor time and facilitites for instrumental neutron activation analysis were provided by the Oregon State University Radiation Center.

Numerous people helped along the way, including the following: Ron Worl, Thor Kiilsgaard, Wayne Hall, Earl Bennett, Bob Criss, Mary Horan, Larry Snee, Mick Kunk, Bill Leeman, Chris Clarke, Liz Metzen, George Carrico, and Buz Vanskike. I would also like to thank my advisor Cy Field and the members of my committee, Bill Taubeneck, Ed Taylor, Anita Grunder, and Gerald Simonson, for their input. Discussions with Gary Davidson and John Curless were both enjoyable and invaluable. A special thanks to Karen, who has helped the most.

TABLE OF CONTENTS

LIST OF FIGURES

LIST OF TABLES

LIST OF PLATES

GEOLOGY, GEOCHEMISTRY AND MINERAL POTENTIAL OF CRETACEOUS AND TERTIARY PLUTONS IN THE EASTERN PART OF THE SOLDIER MOUNTAINS, IDAHO

INTRODUCTION

The principal objective of this study is to gain a better understanding of the processes related to the formation, crystallization, and subsequent cooling of granitic plutons. Although problems associated with magmatic evolution are addressed, late-stage plutonic processes, particularly hydrothermal alteration, are also evaluated. The study of late-stage phenomena is critical from a petrologic standpoint to understanding the larger question of how granitic rocks are generated and emplaced. Hydrothermal fluids are able to alter magmatic textures, as well as to change the chemical compositions of rock. This latter effect is particularly true with respect to the mobile elements such as potassium and sodium. Thus, to fully understand the formation of granitic rocks, it is expedient to be able to recognize the effects of late-stage hydrothermal activity, and to understand how such processes operated. Aside from basic scientific benefits, this investigation has important economic implications with respect to the formation of ore deposits. It has long been recognized that many ore deposits are related in time and space to igneous activity and, in particular, there has been observed an often-repeated association between the waning stages of plutonism and the development of mineralization. The movement and local concentration of alkalies are features typical of this late-stage activity. This study concentrates on rock-fluid interactions and associated alkali mobility, and thus provides information that may be used in both understanding known ore deposits and searching for new ones.

Location of the study area is given in Figure 1. Reconnaissance of the area in a two-day period during the summer of 1984 revealed a complex series of plutonic rocks overlain in places by younger volcanic rocks. It was noted that the plutonic rocks were locally altered, as distinguished by "pinked-up" zones in otherwise gray granodiorite. The alteration was thought at the time to be potassic, with the potential for associated porphyry-type mineralization. It had been shown by Criss (1981) and Criss and Taylor (1983) that feldspars within plutonic rocks in the study area were depleted in ^{18}O, which they attributed to exchange with heated meteoric waters. Their reconnaissance work indicated that epizonal Eocene plutons, unmapped at that time, were probably responsible for circulation of the meteoric water and resultant feldspar alteration. Because of the complex intrusive relations, and the associated alteration, it was clear that the area was well-suited for a detailed investigation of granite genesis and related hydrothermal alteration.

The approach used in this study has included geologic mapping, petrography, and geochronology. These have been integrated with studies of major- and trace-element geochemistry and oxygen-isotope geochemistry. Data for the ratios of isotopes of Rb, Sr, Sm, and Nd provided by Chris Clarke of the Open University have been incorporated as well. This work was carried out in conjunction with the Hailey CUSMAP (Conterminous United States Mineral Appraisal Program) project undertaken by the U.S. Geological Survey, which involved evaluation of mineral resources in the Hailey 1 by 2 degree quadrangle.

Geologic mapping was conducted during the summers of 1985 and 1986. During the course of this effort seven plutonic rock units of Cretaceous to Eocene age were delineated, as well as four alteration types, and twelve volcanic and surficial units, of Eocene to Quaternary age, were also distinguished. The interrelationships between mineralogic,

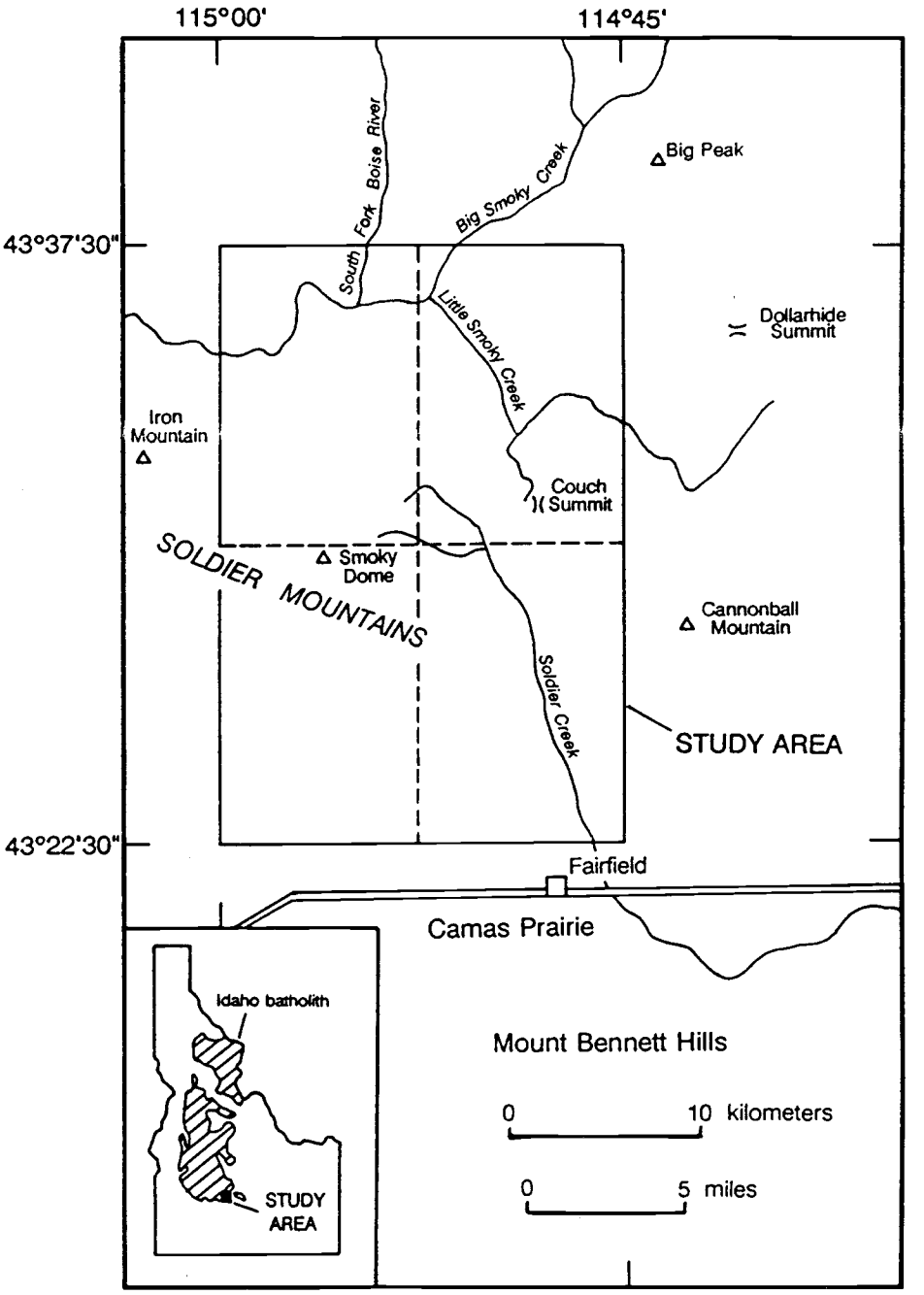

Figure 1. Index map showing the location of the study area.

chemical, and isotopic alteration were determined, and an effort was made to identify primary igneous features that could be utilized in petrogenetic interpretations. This objective was accomplished through detailed petrographic studies of samples of the plutons and their altered equivalents, in conjunction with chemical analyses of whole-rock samples and the determination of $^{18}O/^{16}O$ ratios of constituent minerals.

Nearly all previous geologic mapping in the study area has been of a reconnaissance nature. Piper (1924) made a study of ground water on Camas Prairie, and distinguished between plutonic and volcanic rocks north of Fairfield. The volcanic unit, termed the Mt. Bennett rhyolite, was tentatively assigned to the Late Miocene, and the plutonic rocks were assigned a Late Cretaceous or Early Eocene age. Ross (1930) discussed the geology and ore deposits of the Little Smoky and Willow Creek mining districts, which are largely east and north of the study area. He also constructed a geologic sketch map which included the eastern portion of the study area. Ross correlated the volcanic rocks with the Challis Volcanics found farther to the northeast, and the granitic rocks with the Late Cretaceous Idaho batholith. In more recent studies, Cluer and Cluer (1986) investigated the formation of Camas Prairie, which they concluded was a Late Cenozoic rift (graben) developed as a result of downwarping of the Snake River Plain. Gehlen (1983) and Darling (1987) mapped the Dollarhide Mountain quadrangle, which adjoins the study area to the northeast, and Bennett (unpublished mapping) mapped the quadrangles to the west. The studies by Darling and Bennett were part of the Hailey CUSMAP project.

REGIONAL GEOLOGIC SETTING

The regional distribution of rock types is illustrated in Figure 2. The oldest units are: 1) Paleozoic sedimentary rocks east of the southeastern margin of the Idaho batholith, 2) Precambrian to Ordovician metamorphic rocks in the Pioneer window, 3) metasedimentary rocks of uncertain age as roof pendants in the batholith, and 4) Permian to Jurassic metavolcanic and metasedimentary rocks of the Blue Mountains island arc west of the batholith.

Paleozoic rocks east of the southern lobe of the batholith are continentally-derived sedimentary rocks that have been folded and faulted, but not highly metamorphosed. An axial plane cleavage is present in the Devonian Milligen Formation, but Pennsylvanian and Permian rocks of the Wood River, Dollarhide, and Grand Prize Formations generally exhibit simple contact metamorphic effects. Garnet and diopside are found near intrusive contacts, and tremolite is found over larger areas. A more complex contact zone is present northeast of Willow Creek (about midway between Ketchum and Fairfield), where biotite defines a foliation in metasedimentary rocks of the Carrietown Sequence (Skipp and Hall, 1980). Geslin (1986) and Darling (1987) attributed the biotite to a regional metamorphic event. However, the occurrence of the Carrietown Sequence in a narrow belt parallel the margin of the batholith suggests that it formed as a contact metamorphic zone that was undergoing deformation concurrent with intrusion of the batholith. A similar conclusion was reached by S. Whitman (pers. comm., 1988), who is undertaking a detailed study of this deformed zone.

The Pioneer Window, east of the batholith, exposes a core of Precambrian gneiss, as well as schist, quartzite, and calc-silicate rocks of Precambrian(?) to Ordovician age. Intrusive rocks of Cretaceous(?) and Eocene age are also present in the window (Dover, 1983). The Pioneer Window has been termed a metamorphic core complex (Coney,

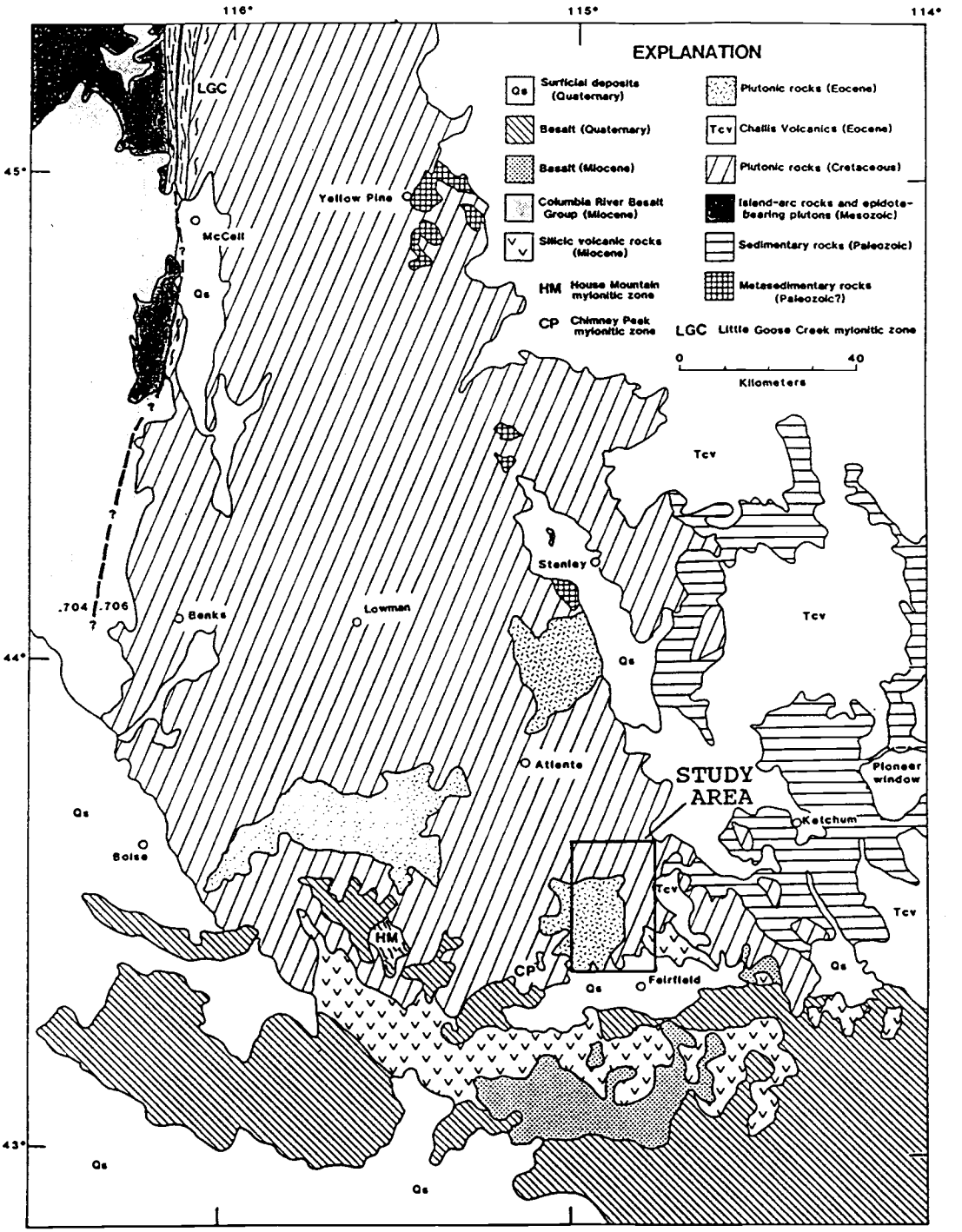

Figure 2. Simplified geologic map showing the regional geologic setting of the southern lobe of the Idaho batholith. Compiled from Bond (1978), Fisher and others (1983), Bonnichsen (1987), Manduca (1988), and Johnson and others (1988).

1980), and the bounding faults have been the subject of recent debate (Pavlis and O'Neill, 1987; Wust, 1987). The debate centers on the nature and timing of movement on the bounding faults, mapped as thrust faults by Dover, and interpreted as Paleogene extensional faults by Wust (1985, 1987), and Wust and Link (1988). O'Neill and Pavlis (1985, 1988) have emphasized that the Paleogene extension is superimposed on Mesozoic compressional structures, and that subsequent Neogene Basin and Range-type extension overprinted previous deformational episodes.

Metasedimentary rocks in the southern part of the Idaho batholith are confined to the House Mountain and Chimney Peak areas (HM and CP in Fig. 2), and to a belt of roof pendants which trends northwest from Stanley. The rocks at House Mountain and Chimney Peak are high-grade (amphibolite facies) gneisses, quartzites and calc-silicate rocks that have been mylonitized (Jacob, 1985a, 1985b; Bennett, unpubl. mapping). The mylonitization is most intense near granite-metasediment contacts, and decreases in an irregular fashion into the batholith. Mylonitic foliation is shallow, dipping about 25° to the east at House Mountain. As noted by Jacob (1985a), deformation is similar to deformation within metamorphic core complexes of the western Cordillera (Coney, 1980). However, chloritic breccias appear to be lacking, as are low-grade, upper-plate rocks. Aplite and pegmatite dikes of presumed Cretaceous age intrude both parallel to and across the foliation, suggesting that mylonitic deformation took place in the Cretaceous during the latest stages of batholith emplacement (Johnson and others, 1988). Jacob (1985b) argues that mylonitization continued into the Eocene, because a few andesite and dacite dikes of probable Eocene age are also deformed. Amphibolite-facies metamorphism and ductile deformation are associated with intrusion of the batholith, but a previous metamorphic event cannot be ruled out. Correlation of the metasedimentary rocks with known formations has not been established, but

they are thought to be Paleozoic and (or) Precambrian in age.

The belt of roof pendants trending northwest from Stanley also consists of high-grade rocks, including biotite schist, calc-silicate gneiss, and quartzite. Although most are probably Paleozoic in age, correlation with previously defined formations has not be made. Sillimanite, and andalusite partly reacted to sillimanite, are present locally (Lewis, 1984). Smitherman (1985) studied the pendants near Yellow Pine and attributed high-grade mineral assemblages to a pre-batholith metamorphic event.

Rocks along the western margin of the batholith are part of an allochthonous Permian to Jurassic island-arc complex, which Vallier and Engebretson (1984) referred to as the Blue Mountains arc. These rocks are largely to the west of the area shown in Figure 2. The eastern part of the Blue Mountain arc consists of low-grade metavolcanic and metasedimentary rocks of the Wallowa terrane, and, adjacent to the batholith, higher grade (up to lower amphibolite facies) volcanic and volcaniclastic schists of the Riggins Group (Hamilton, 1963; Brooks and Vallier, 1978; Lund and Snee, 1988; Aliberti and Manduca, 1988). Amphibolite facies metavolcanic and metasedimentary rocks mapped southwest of McCall (Taubeneck, 1971; Bonnichsen, 1987) are part of the Blue Mountains arc, and may correlate with rocks farther north of the Riggins Group.

The western margin of the batholith is at the edge of the old continental margin, as indicated by a sharp break in initial $^{87}Sr/^{86}Sr$ ratios of igneous rocks in this area (Armstrong and others, 1977; Criss and Fleck, 1987). The transition from low (<0.7043) ratios in the west to high (>0.7055) ratios in the east is across a steeply dipping zone of highly deformed rocks, typically of plutonic origin (Myers, 1982; Lund, 1984; Hoover, 1987; Manduca, 1988). The zone is coincident with changes from roof pendants of continental metasedimentary rocks in the east to pendants of the

Blue Mountains arc rocks to the west. The portion of the zone north of McCall has been termed the Little Goose Creek Complex, and here the mylonitic deformation post-dates emplacement of tonalites of the Idaho batholith (Manduca, 1988). Many of the plutonic rocks just west of the arc-continent boundary contain epidote (Taubeneck, 1971). The epidote has been interpreted by Zen and Hammarstrom (1984) as magmatic, and an indication of deep (>25 km) levels of emplacement.

The metamorphic and intrusive history along the western margin of the batholith is complex. Rocks of the Riggins Group were multiply deformed and metamorphosed during the Cretaceous, and the arc-continent boundary was intruded by numerous plutonic bodies which were subsequently deformed (Onash, 1987; Lund and Snee, 1988; Manduca, 1988). The exact timing of juxtaposition of the island-arc rocks against the continent remains a matter of debate. $^{40}Ar/^{39}Ar$ age-spectrum dating of a 118-Ma metamorphic event in the Riggins Group has led Sutter and others (1984) and Lund and Snee (1988) to postulate movement into the present position along a right-lateral transcurrent fault during the interval between 118 and 93 Ma. However, U-Pb dating by Manduca (1988) in the McCall area suggests that the arc-continent boundary had formed, and subduction west of the Blue Mountain arc had begun, prior to 118 Ma.

The most widely exposed rocks in the region are those of the Idaho batholith, one of several Mesozoic batholiths of the western Cordillera. As indicated in Figure 3, the position of this batholith is farther inland than those of large batholiths to the north (Coast Plutonic Complex) or to the south (Sierra Nevada batholith), and it is more in line with an inner belt of muscovite-bearing granitic plutons that stretches from Mexico to British Columbia (Miller and Bradfish, 1980). Although only the core of the Idaho batholith is muscovite-bearing, its relatively high $^{87}Sr/^{86}Sr$ ratios and dominantly peraluminous character are more

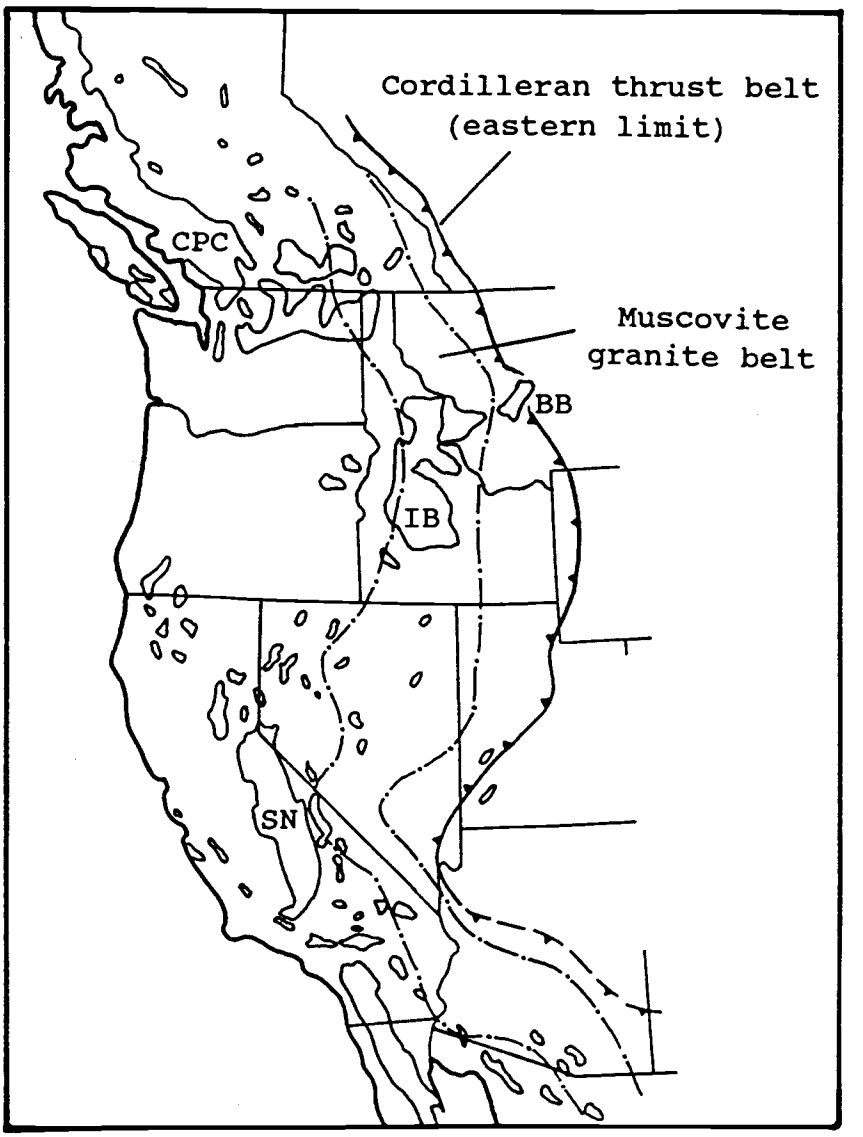

Figure 3. Map showing the locations of batholiths in the western United States and southern British Columbia. CPC = Coast plutonic complex; BB = Boulder batholith; IB = Idaho batholith; SN = Sierra Nevada batholith. Modified from Miller and Bradfish (1980).

characteristic of the inner belt granites. These features presumably reflect a significant contribution of continental crust to the formation of these rocks.

The Idaho batholith consists of a northern (Bitterroot) and southern (Atlanta) lobe. Rocks in the Atlanta lobe have been subdivided into several units by Fisher and others (1983), Kiilsgaard and Lewis (1985), and Kiilsgaard, Bennett, and Lewis (unpublished mapping). These units are illustrated in Figure 4.

A series of hornblende-biotite granodiorites and tonalites are the oldest intrusive bodies now exposed in the Atlanta lobe of the batholith. These hornblende-bearing phases are present in the western part of the batholith, where large areas have yet to be mapped in detail, as well as in smaller areas in the central and eastern parts of the batholith. Reconnaissance geologic mapping of the western margin of the Atlanta lobe by Taubeneck (1971) has revealed a complex foliated border zone dominated by tonalitic rocks. In the southeastern part of the batholith, hornblende-bearing granodiorite (the Hailey granodiorite unit of Schmidt, 1962) intrudes quartz diorite of the Croesus stock. The Croesus stock is unusual in that it contains abundant pyroxene, which is absent in the rest of the Atlanta lobe. Closely related to the early tonalites and granodiorites is a porphyritic (megacryst-bearing) granodiorite phase, which is present in a northwest-trending belt across the northeastern part of the Atlanta lobe. The age of the early hornblende-bearing phases has not been well established, but it is thought to be in the 95-85 Ma range (Lewis and others, 1987).

The dominant rock type in the batholith is biotite granodiorite, which grades into muscovite-biotite granite over a zone as wide as 2 km or more. These two phases crystallized sometime between 85 and 72 Ma (Lewis and others, 1987), but ages are not well constrained. The youngest phases of the batholith consist of leucocratic granite in

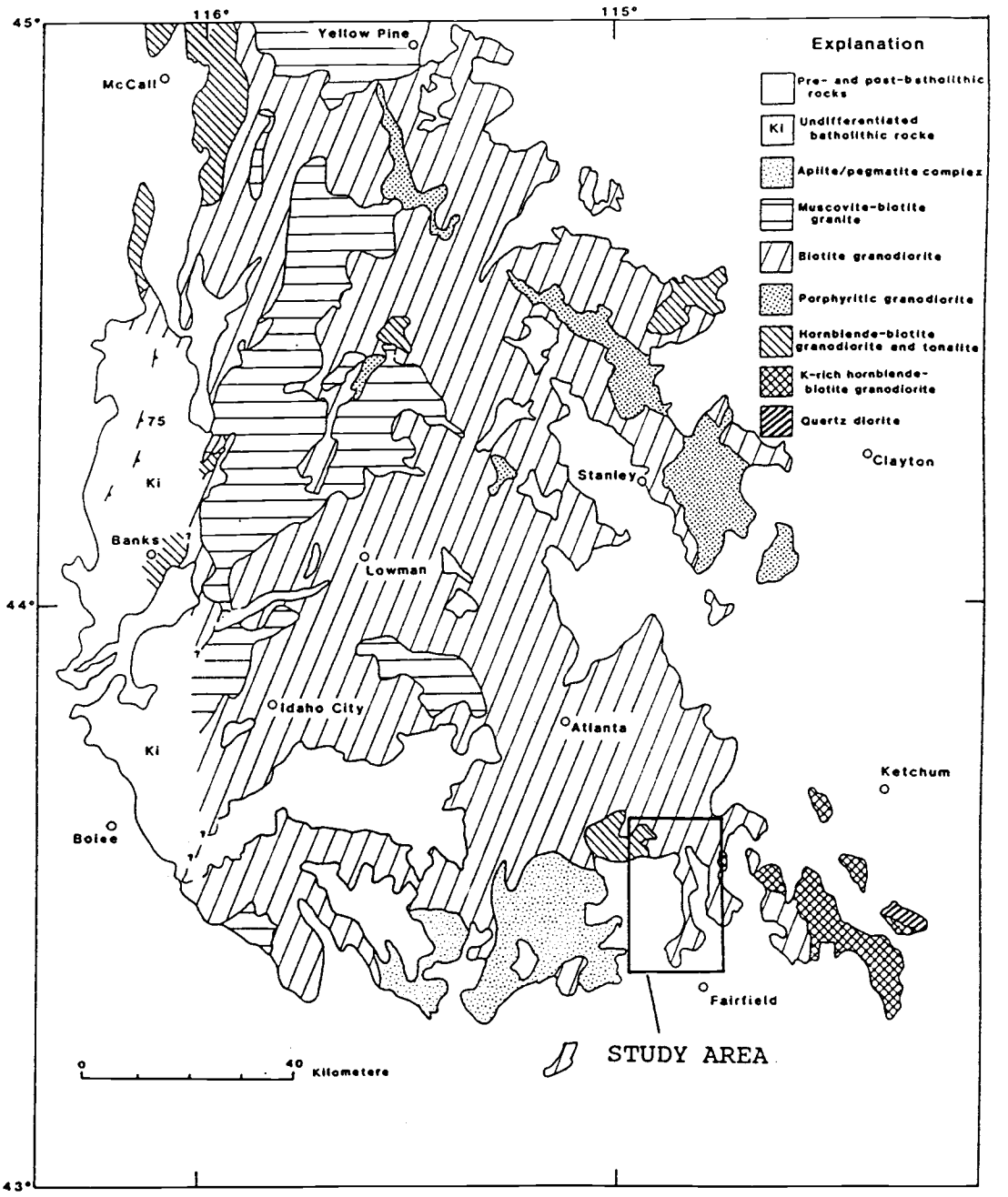

Figure 4. Simplified geologic map showing plutonic rock units of Cretaceous age in the southern lobe of the Idaho batholith. Compiled from Taubeneck (1971), Bond (1978), Fisher and others (1983), and Johnson and others (1988).

dikes, sills and small stocks (not shown in Fig. 4) as well as pegmatite and aplite dikes. An area containing abundant pegmatite and aplite dikes is present in the southern part of the Atlanta lobe.

As illustrated in Figure 5, Eocene plutonic and volcanic rocks are widely exposed in the region. These rocks are part of the Challis magmatic episode, which affected a broad area from British Columbia to Wyoming (Armstrong, 1974; Bennett, 1980a; Moye and others, 1988). In Idaho, the plutonic rocks of Eocene age fall into two suites: 1) pink biotite granite and 2) quartz monzodiorite (Bennett and Knowles, 1985). These plutons are epizonal and intrude the Late Cretaceous Idaho batholith, Paleozoic sedimentary rocks, and broadly coeval volcanic rocks of the Challis Volcanic field. Numerous dike swarms of probable Eocene age are present as well. K-Ar age determinations of the pink granites tend to be younger than those of the quartz monzodiorites (typically 44-48 Ma versus 47-50 Ma), but data are scarce and there is some overlap (Bennett and Knowles, 1985, Fig. F1). The quartz monzodiorite suite is compositionally variable, ranging from hornblende and pyroxene diorite to hornblende-biotite granite. In contrast, the pink granite suite is restricted to the granite field. The Challis Volcanics are characterized by older intermediate to mafic lava flows and tuff breccias, and younger dacitic to rhyolitic tuffs and lava flows (McIntyre and others, 1982; Moye and others, 1988).

Miocene and younger volcanism was widespread in the western and southern parts of the region (Fig. 2). Extensive flows of the Miocene Columbia River Basalt Group are preserved along much of the western margin of the batholith, masking intrusive relations of the batholith in this area. To the south is the Snake River Plain, which has been the locus of voluminous rhyolitic and basaltic magmatism since the Miocene. Some of the Miocene volcanic section is exposed in the Mount Bennett Hills, 10 kilometers south of the

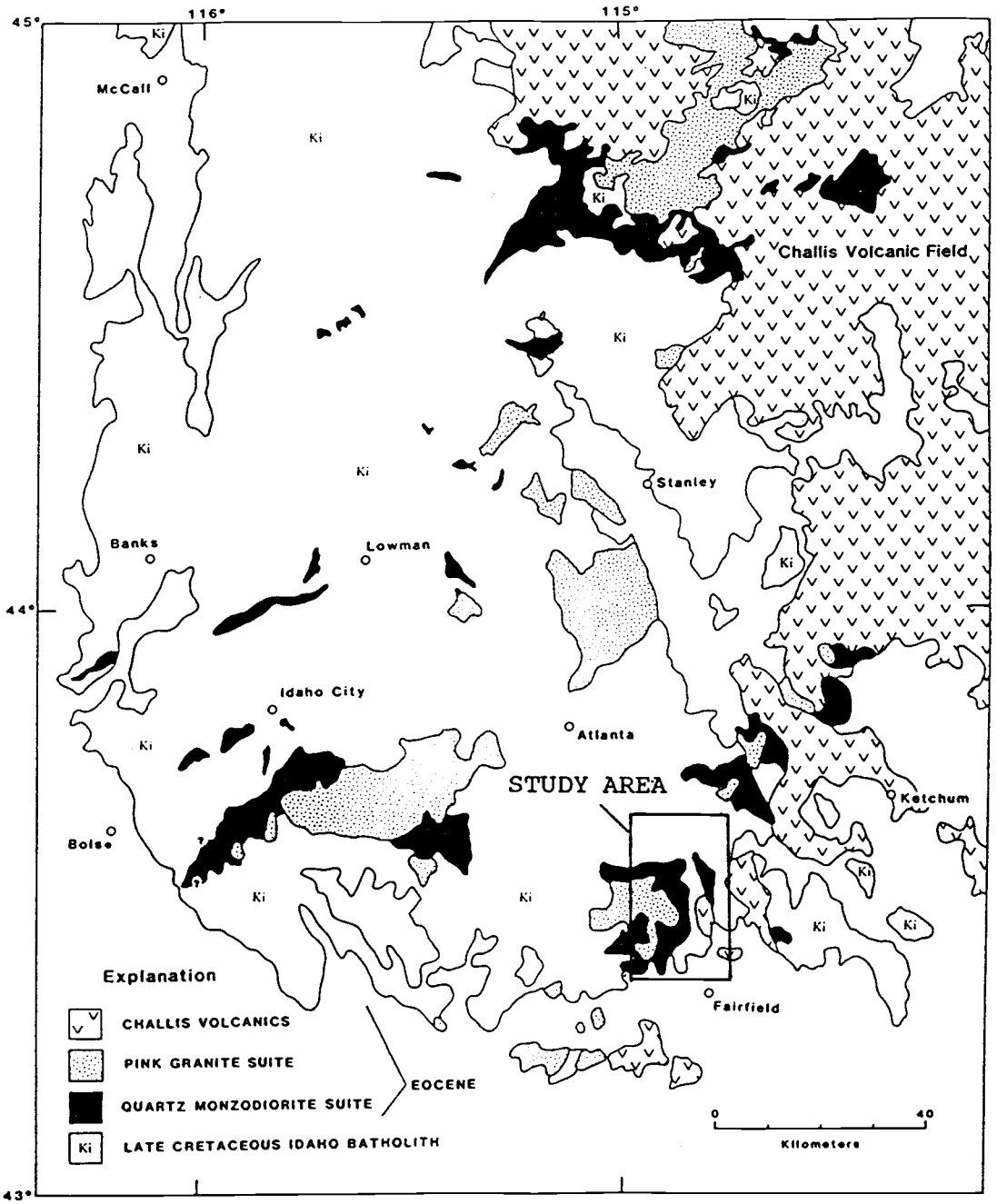

Figure 5. Simplified geologic map showing the locations of plutonic and volcanic rocks of Eocene age in south-central Idaho. Compiled from Anderson (1934a), Bond (1978), Fisher and others (1983), and Johnson and others (1988).

study area, and to the east in the Magic Reservoir area. Present in these two areas are rhyolitic ash-flow tuffs of the Idavada Volcanics, as well as intercalated basalts (Malde and others, 1963; Smith, 1966; Armstrong and others, 1975; Leeman, 1982a; Honjo and others, 1986). Basalt flows of Quaternary age are also widespread. They underlie a large part of the Snake River Plain, and fill several canyons within the Idaho batholith west of the study area.

The structural history of the region is complex. Some of the oldest structures are folds and thrust faults within the Paleozoic section east of the batholith. Most of these features have been attributed to deformation during the Cretaceous Sevier orogeny, but Latest Devonian to Early Mississippian Antler structures may be present as well (Skipp and Hait, 1977; Dover, 1983; Skipp, 1987; Link and others, 1988). The Idaho batholith intruded the western part of the fold and thrust belt during Late Cretaceous time. Locally it intruded along the thrust faults, and in these areas the batholith post-dates the faulting. However, because of the difficulty of recognizing low-angle structures in homogeneous granitic rocks, the existence of thrust faults within the batholith cannot entirely be ruled out. As mentioned previously, deformation probably coincident with intrusion of the batholith has been recognized at House Mountain, Chimney Peak, and Willow Creek.

In addition to the controversial faults bounding the Pioneer Window, other low-angle structures originally mapped as Mesozoic thrust faults have been reinterpreted as Tertiary extensional faults (Skipp and others, 1986; Link and others, 1987). Otto and Turner (1987) have also described a low-angle contact of Eocene Challis Volcanics near Ketchum as a fault contact, rather than depositional. As with the thrust faults, recognition of these low-angle structures is difficult in the batholith. Low-angle zones of crushed and silicified rock have been noted by the author west of the Sawtooth Range, and in the northeastern corner of the study

area. These probably represent Eocene extensional structures, but timing is constrained only by the age of the batholith (i.e. post Late Cretaceous movement).

Anderson (1934b) and Taubeneck (1971) recognized that numerous steep faults cut the Idaho batholith. Recent mapping (e.g. Fisher and others, 1983) has greatly added to the number of known faults. The regional distribution of these structures is illustrated in Figure 6.

Three predominant orientations of steep faults have been described by Kiilsgaard and Lewis (1985). The first is a north-northeast fault set in the western part of the Atlanta lobe, including the Boise Ridge fault and the Deadwood fault zone. There is evidence of significant dip-slip motion along some of these faults, such as the Boise Ridge fault, and an indication of left lateral motion on a few of the faults. The age of initial motion is not known, but offset of Columbia River basalts along several of these faults indicates Miocene or younger movement.

The second set of steep faults trends northeast, and is associated with Eocene extension and graben development. This set of structures, termed the Trans-Challis fault system, was important in localizing andesitic to rhyolitic Eocene dike swarms, which typically have northeast trends. Precious-metal mineralization may also have been controlled by these structures (Kiilsgaard and others, 1986). The Trans-Challis system appears to continue to the northeast into Montana, where it coincides with the Great Falls lineament (O'Neill and Lopez, 1985). To the southwest, a large concentration of these northeast-trending faults disappears under undisturbed Quaternary basalts southwest of Idaho City. Dikes of probable Eocene age are broken by these faults, but are not highly displaced or as altered and sheared as the Cretaceous granitic rocks in the same zones. Thus, much of the movement predated dike emplacement, and is likely to be Late Cretaceous to Early Eocene in age.

The third dominant fault trend is northwest to

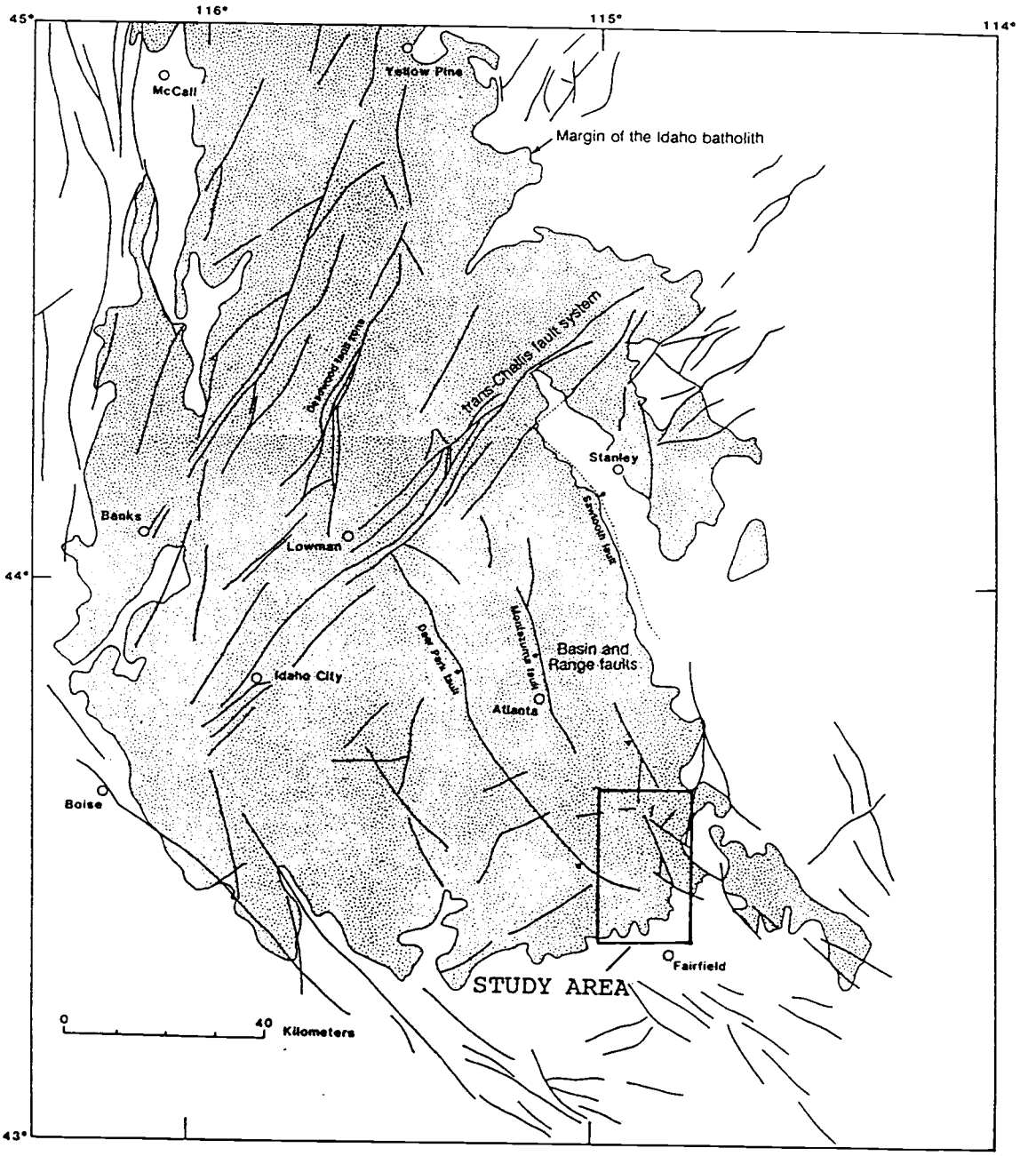

Figure 6. Map showing the locations of steep faults in the southern lobe of the Idaho batholith. Compiled from Bond (1978), Fisher and others (1983), and Johnson and others (1988).

north-northwest. These faults are the easiest to recognize, because dip-slip motion along these structures has resulted in Basin and Range topography. The Sawtooth and Montezuma faults (Reid, 1963) are two examples. Some of these structures remain active, as indicated by the 1983 Borah Peak earthquake south of Challis that was centered along one of these faults. Several northwest- and north-trending high-angle faults in the northern part of the Challis Volcanic field predate deposition of the volcanic rocks (McIntyre and others, 1982). Similar structures are present in the southern part of the Challis Volcanic field (F.J. Moye, pers. comm., 1988). These structural relationships imply that some of the northwest-trending faults in the region were present during the Eocene, and that movement has been recurrent since that time.

ROCK UNITS

Mapping performed in the course of this investigation has defined 23 bedrock units and 4 surficial units in the eastern part of the Soldier Mountains (Plate 1). Cursory descriptions of both surficial and bedrock units are given on Plate 1; the latter are described in greater detail below. Sample localities are on Plate 2.

Plutonic rocks of Late Cretaceous and Eocene age are the predominant lithologies, and are the focus of this study. Plutonic rock names follow the nomenclature of Streckeisen and others (1973); volcanic rocks are classified using nomenclature based on modal mineralogy (Streckeisen, 1978) and chemical composition (LeMaitre, 1984).

METASEDIMENTARY ROCKS

The oldest rocks are metasedimentary rocks preserved in a small (500 m-long) roof pendant in the western part of the area. The pendant is contained within a large mass of Eocene plutonic rocks. Isolated xenoliths of metasedimentary rocks are also found within Eocene plutonic rocks 6 km to the southeast of the pendant, but are too small to show at map scale.

Lithologies within the pendant are garnet-diopside gneiss, quartzite, and minor biotite-sillimanite schist. The garnet-diopside gneiss is a dark-green, fine-grained, equigranular rock which is crudely layered. Diopside, garnet, and labradorite are the most abundant minerals; lesser amounts of quartz, epidote, sphene and opaque minerals are also present. The quartzite was not studied in thin section, but is brown in color and medium grained. The biotite-sillimanite schist is a fine-grained, dark-brown rock. It contains an abundance of prismatic sillimanite a;igned parallel to the foliation defined by biotite. Minor amounts of plagioclase feldspar, sericite (after plagioclase

and biotite), chlorite (after biotite) and opaque minerals comprise the remainder of the rock. Dikes of aplite and pegmatite cross-cut the pendant, and are locally folded.

Because of the minimal exposure of metasedimentary rocks, it is difficult to assess their age or metamorphic history. Lithologically they are similar to Paleozoic(?) pendants northwest of Stanley (Lewis, 1984), as well as Precambrian(?) to Ordovician rocks of the Hyndman and Eastfork Formations described by Dover (1983) in the Pioneer Window. Because of the uncertainty of correlation they are assigned a tentative Paleozoic age.

The fabric developed in the schists, as well as the presence of folded aplite and pegmatite dikes, indicate that metamorphism was not simply high temperature (pyroxene-hornfels) contact metamorphism related to intrusion of the Eocene plutons. Elsewhere in the region these epizonal plutons have very narrow contact aureoles, and therefore it is likely that metamorphism of the pendant is related to either a Late Cretaceous event associated with the Idaho batholith, or to a metamorphic event that predated emplacement of the batholith. The age of metamorphism, as with other pendants in the region, remains poorly constrained.

CRETACEOUS PLUTONIC ROCKS

Three intrusive phases of the Idaho batholith are present. A simplified geologic map of their distribution is in Figure 7. Modal data are listed in Table 1. The Cretaceous plutonic rocks are similar to those mapped to the north by Fisher and others (1983) in the Challis one- by two-degree quadrangle , and described by Kiilsgaard and Lewis (1985), and Lewis and others (1987).

Coarse-grained hornblende-biotite granodiorite

Coarse-grained hornblende-biotite granodiorite crops

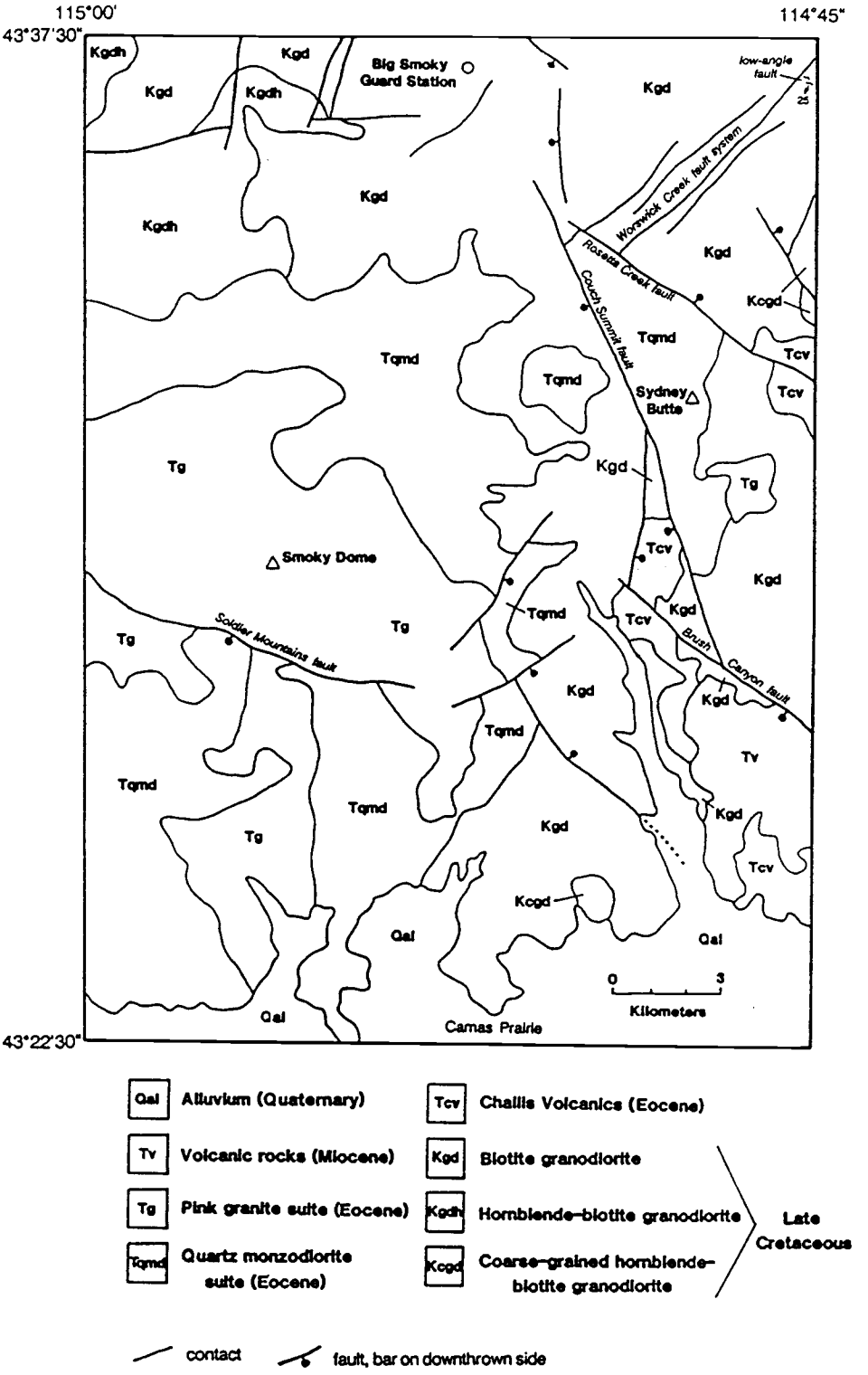

Figure 7. Simplified geologic map of the eastern part of the Soldier Mountains.

CRETACEOUS PLUTONIC ROCKS

	Pf	Kf	Qz	Bt	Hb	Px	Op	Sp	Cl	An
Coarse-grained hornblende-biotite granodiorite										
RL038	37	17	28	8	7	--	2	0.9	17	20-38
RL252	44	12	25	10	7	--	1	0.6	18	20-38
RL331	36	21	30	6	4	--	1	0.5	11	20-37
mean	39	17	28	8	6	--	1	0.7	15	--
Hornblende-biotite granodiorite										
RL278	55	6	24	7	5	--	2	<0.1	14	28-30
RL309	49	10	24	11	6	--	1	0.4	18	28-37
mean	52	8	24	9	6	--	2	<0.3	16	--
Biotite granodiorite										
RL020	47	11	28	11	--	--	1	1.1	13	20-34
RL028	42	21	32	5	--	--	1	<0.1	6	20-38
RL039	49	28	19	3	--	--	1	<0.1	4	20
RL076	47	16	24	6	5	--	1	0.4	12	39-41
RL081	51	9	24	12	2	--	2	0.7	15	29-41
RL092	47	14	30	7	--	--	1	0.4	8	26-40
RL148	46	22	27	3	--	--	1	0.1	5	--
RL154	46	11	29	10	1	--	1	1.5	12	37
RL171	50	10	24	10	5	--	1	0.3	16	--
RL181	41	25	29	2	--	--	2	<0.1	4	20-25
RL210	44	21	24	10	--	--	1	0.4	11	25-35
RL219	50	15	27	6	--	--	1	0.3	7	27-29
RL225	48	13	27	11	--	--	1	0.8	11	27-31
RL230	45	26	21	6	--	--	2	0.1	8	26-39
RL241	45	16	28	10	--	--	1	0.8	10	27
RL244	43	24	26	6	tr	--	1	<0.1	7	27-31
RL249	45	17	30	6	--	--	1	<0.1	7	29-38
RL263	39	21	32	7	--	--	1	0.1	8	20-30
RL266	45	25	26	4	--	--	tr	<0.1	4	--
RL275	50	9	31	9	tr	--	1	0.2	10	31
RL279	41	20	31	7	--	--	1	0.4	7	27-34
mean	46	18	27	7	<1	--	1	<1.0	9	--

EOCENE PLUTONIC ROCKS

Foliated hornblende-biotite granodiorite										
RL170	60	7	13	8	10	--	2	0.4	21	--
RL349	58	6	15	9	11	--	2	<0.1	21	20-46
mean	59	7	14	9	11	--	2	<0.3	21	--

Pf = plagioclase feldspar; Kf = potassium feldspar; Qz = quartz; Bt = biotite; Hb = hornblende; Px = pyroxene; Op = opaque minerals; Sp = sphene; CI = color index; An = range of anorthite content

Table 1. Modal data from plutonic rocks of the eastern part of the Soldier Mountains. Modes determined by counting approximately 1000 points on slabs stained for potassium feldspar.

EOCENE PLUTONIC ROCKS

	Pf	Kf	Qz	Bt	Hb	Px	Op	Sp	CI	An
Hornblende diorite										
RL339	42	2	1	6	48	--	3	<0.1	56	--
Biotite-hornblende granodiorite										
RL008	45	20	21	8	6	--	1	<0.1	15	16-37
RL010	37	31	20	5	5	1	2	<0.1	13	--
RL059	45	23	22	5	5	--	1	<0.1	11	14-35
RL062	43	21	20	6	8	tr	2	0.4	16	20-35
RL090	45	20	24	5	5	tr	1	<0.1	12	16-37
RL096	39	25	25	5	6	--	1	<0.1	11	16-35
RL097	35	30	22	6	6	tr	1	0.2	13	16-38
RL104	46	22	16	8	6	tr	2	0.4	16	18-41
RL113	37	23	21	5	9	1	3	0.9	18	16-42
RL119	37	24	26	5	5	1	2	<0.1	13	15-38
RL129	37	28	22	5	6	tr	2	<0.1	13	15-44
RL159	40	26	25	8	--	--	1	<0.1	9	--
RL160	42	23	19	7	6	1	2	0.5	16	16-42
RL161	46	23	15	6	7	tr	2	0.4	16	20-44
RL167	40	25	19	5	7	1	2	0.3	16	20-45
RL299	32	35	21	5	6	tr	1	0.4	11	16-45
RL340	43	22	18	6	7	1	3	0.4	18	20-48
RL345	52	12	12	9	12	tr	2	0.2	24	20-47
RL355	41	28	15	5	8	tr	2	<0.1	16	20-46
RL367	45	20	17	6	10	tr	2	0.2	18	17-41
RL372	37	27	22	5	6	tr	2	0.3	14	15-47
mean	41	24	20	6	6	<1	2	0.3	15	--
Pink granite										
RL066	25	38	36	tr	--	--	1	<0.1	1.1	11
RL073	27	36	33	3	--	--	tr	<0.1	3.6	15-20
RL085**	32	32	27	8	tr	--	1	<0.1	9.0	20-28
RL158	33	34	28	5	--	--	1	<0.1	5.8	18-30
RL182	26	40	31	1	1	--	1	0.2	3.2	12-18
RL187*	36	32	24	4	3	tr	1	0.1	8.3	20-36
RL188	25	41	32	2	--	--	1	<0.1	2.7	10-15
RL293	28	34	32	5	tr	--	1	<0.1	5.7	--
RL338**	25	37	32	5	2	--	1	<0.1	7.1	16-28
RL341	26	39	33	2	--	--	1	<0.1	2.7	--
RL373**	28	36	29	5	2	tr	1	<0.1	8.0	20-41
RL374**	26	41	28	4	1	tr	1	0.1	5.6	14-34
mean	28	37	30	4	<1	--	1	<0.1	5.2	--

Pf = plagioclase feldspar; Kf = potassium feldspar; Qz = quartz; Bt = biotite; Hb = hornblende; Px = pyroxene; Op = opaque minerals; Sp = sphene; CI = color index; An = range of anorthite content

* hybrid rock with intermediate pink granite and biotite-hornblende granodiorite characteristics and mafic inclusions
** possible hybrid rocks with 5 percent or less mafic inclusions

Table 1 (continued). Modal data from plutonic rocks of the eastern part of the Soldier Mountains.

out along Carrie Creek, near the northeastern margin of the study area, and west of McCan Gulch, immediately north of Camas Prairie. Exposures west of McCan Gulch are poor, so the extent of the unit in that area is not well known. Although rocks at both localities are similar in appearance, they are separated by a distance of 15 km and may have different origins. Thus, correlation is tentative, and more detailed work is needed to establish their relationship. The exposures along Carrie Creek extend out of the study area to the east where they correspond to the hornblende-biotite granodiorite unit of Darling (1987) in the Dollarhide Mountain quadrangle. Similar rocks present southeast of the Dollarhide Mountain quadrangle were termed the Hailey granodiorite unit by Schmidt (1962). Contacts between the coarse-grained hornblende-biotite unit and the other plutonic rocks in the area are not exposed.

Rocks of this unit are medium to dark gray, and equigranular. Grain size is medium to coarse, and thus slightly coarser than the other Cretaceous granodiorites in the area. Coarse books of biotite (up to 6 mm thick) are characteristic, and contrast with the smaller "shreddy" biotites found in other Cretaceous units. As indicated in Figure 8, samples of this plutonic unit plot in the granodiorite and granite fields on a QAP diagram.

Plagioclase feldspar is white in color and oligoclase-andesine in composition; it exhibits normal and lesser oscillatory zoning. Potassium feldspar is microcline and white to pale pink in color. It displays poorly to strongly developed grid twins and weak microperthitic textures. Quartz is present in polycrystalline aggregates up to 10 mm across, and locally contains rutile inclusions. Hornblende is present as subhedral crystals 1 to 7 mm in length. Magnetite is the predominant opaque mineral. Sphene and apatite are the most abundant accessory minerals, whereas allanite and zircon are less common.

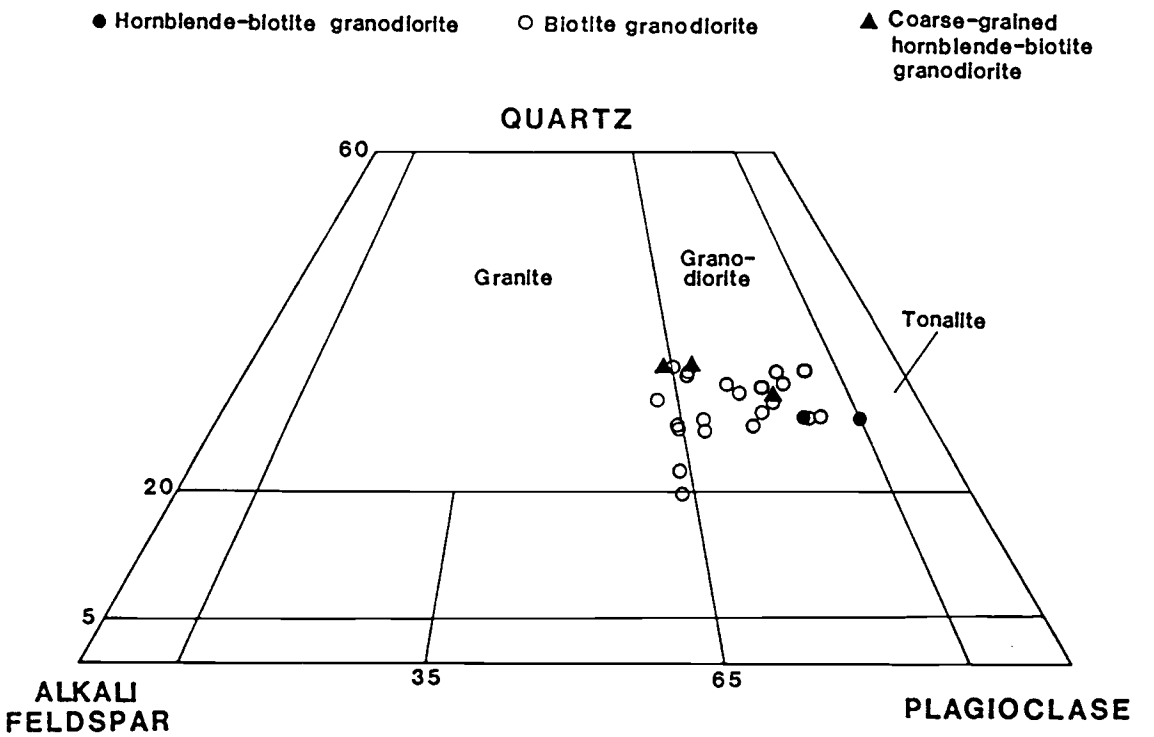

Figure 8. Plot of modal determinations (Table 1) of Cretaceous plutonic rocks from the eastern part of the Soldier Mountains.

Hornblende-biotite granodiorite

This plutonic unit is exposed in the northwestern part of the study area where it is a relatively resistant, cliff-forming unit. The rock is medium gray, equigranular, and medium grained. Biotite locally defines a weak foliation, and biotite-rich schlieren are present in a few localities. The hornblende-biotite granodiorites plot in the granodiorite field in a QAP diagram (Fig. 8), near or at the tonalite boundary. The unit is cross-cut by numerous aplite and pegmatite dikes, and, to a much lesser extent, by fine-grained granitic dikes that may be offshoots of the biotite granodiorite unit discussed below. Although this dike relationship suggests that the hornblende-biotite granodiorite predates the biotite granodiorite, several of the contact areas between the two units appear to be gradational. Thus, it is likely that the two units are similar in age.

Plagioclase feldspar is white, anhedral, and consists of normally zoned calcic oligoclase and andesine. Zonation is uniform, and lacks oscillatory complexities. Potassium feldspar is white, anhedral, and lacks albite-pericline grid twins; microperthitic textures are weakly developed or absent. In hand specimen the quartz appears similar in size to the feldspars (typically 3-6 mm), but in thin-section it is present as aggregates of smaller (0.5 mm) crystals formed by recrystallization of larger strained crystals. Biotite is subhedral and small (0.2-2 mm) in length. The hornblende is present as stubby, subhedral crystals up to 6 mm in length. Magnetite is the predominant opaque mineral. Apatite and sphene are conspicuous accessory minerals and lesser amounts of allanite and zircon are also present.

Biotite granodiorite

Biotite granodiorite is extensively exposed in the

eastern part of the study area. Locally it contains up to 5 percent hornblende, but generally biotite and magnetite are the only mafic minerals. Samples of this unit plot in the granodiorite and granite fields of the QAP diagram (Fig. 8). Exposures are poor, particularly in the southern half of the area. The biotite granodiorite unit is cross-cut by dikes of aplite and pegmatite, which resist weathering and form many of the outcrops.

Rocks of the biotite granodiorite unit are typically light gray and medium grained. Finer-grained variants are present in the Rosetta and Grindstone Creek drainages in the northeastern part of the area, and coarser-grained varieties crop out near Camas Prairie. The granodiorite is typically equigranular, but phenocrysts of potassium feldspar 1 to 5 cm in length are present locally. These phenocrysts appear to have crystallized late relative to other minerals, contain numerous inclusions of plagioclase feldspar and quartz, and have irregular margins.

Plagioclase feldspar is white, and consists of subhedral to anhedral oligoclase-andesine, mostly in the An_{20-35} range. Zonation is weak, with single crystals typically having rims 5 to 15 percent lower in An content than the cores. Potassium feldspar is white to pale pink, and weakly perthitic; turbidity is moderate to low, and grid twins are well developed in a majority of the crystals. X-ray diffraction analysis of the potassium feldspar indicates that it is predominantly intermediate microcline. The d spacings match well with the calculated intermediate microcline d spacings described by Borg and Smith (1969). A mixture of low and intermediate microcline appears to be present at two localities. The diffraction patterns also indicate that the relative abundance of included albite (as micro- and cryptoperthite) is low. Quartz is present as large (3-8 mm) strained crystals, or as polycrystalline aggregates resulting from recrystallization of the large crystals. Rutile is a common inclusion in the quartz. Crystals of biotite are

small (0.2-2 mm) in size and anhedral to subhedral in shape. Hornblende, where present, is in stubby crystals up to 6 mm long. Magnetite is the predominant opaque mineral. Sphene, allanite (± epidote rims), and apatite are the most abundant accessory minerals, whereas zircon is less common. Zircon is present as elongate euhedral crystals, and as anhedral round to elongate crystals which tend to be larger than those with well developed crystal faces. Myrmekite, formed at the margins of feldspar crystals, is a common feature of these rocks.

EOCENE PLUTONIC ROCKS

Eocene plutonic rocks are much more extensive in the area than previously recognized. Mapping has delineated four intrusive phases, of which three continue to the west beyond the area of study. The earliest three units consist of relatively mafic rocks. They range from diorite to granite in composition and are collectively referred to as the quartz monzodiorite suite. They are similar in age, lithology, and chemistry to Eocene plutonic rocks mapped to the north in the Challis one- by two-degree quadrangle (Fisher and others, 1983; Bennett and Knowles, 1985). The fourth intrusive phase is a pink granite, which is similar to Eocene pink granite mapped to the north and west by Reid (1963), Kiilsgaard and others (1970), Bennett (1980b), and Fisher and others (1983). The pink granite plutons are collectively referred to as the pink granite suite. The distributions of these two suites are shown in Figure 7, and modal data are in Table 1.

Foliated hornblende-biotite granodiorite

This unit is well exposed in an upthrown fault block west of Worswick Hot Springs. It is resistant to erosion and has formed steep canyon walls along Little Smoky Creek.

Compositionally and texturally similar intrusive rocks are found in the southwestern part of the study area near the head of Rough Creek. They are poorly exposed in this area and their distribution is not well known.

The foliated hornblende-biotite granodiorite unit is heterogeneous, ranging from quartz diorite to granite in composition. Detailed modal analyses of the various lithologies of the unit were not undertaken. Two samples of a common lithology plot near the quartz monzodiorite-quartz diorite boundary, as indicated in Figure 9. The unit varies from strongly foliated to massive, with alternating layers of mafic and subordinate felsic phases defining the foliation of this unit. Foliation strikes northeast, and typically dips steeply. Cross-cutting dikes of andesite and dacite are common. The unit is intruded by non-foliated rocks of the biotite-hornblende granodiorite unit described below.

Locally, the foliated hornblende-biotite granodiorite contains outcrop-size inclusions similar to the biotite granodiorite unit of the Cretaceous batholith. These are interpreted as stoped blocks of the older rock. Sharp contacts between the biotite granodiorite and the foliated rocks are not apparent, so it may be inferred that some assimilation of the stoped blocks took place.

Mafic rocks in the foliated hornblende-biotite granodiorite unit are medium- to fine-grained and equigranular. Plagioclase feldspar is white, and consists of euhedral to subhedral oligoclase-andesine. Normal and oscillatory zoning is pronounced, with core compositions in one sample about 20 to 25 percent richer in An content than the rims (Table 1). Hornblende and biotite are the predominant mafic minerals, and augite is present locally. Potassium feldspar is interstitial, lacks grid twins, and is moderately perthitic. Quartz is also interstitial. Apatite, sphene, allanite and zircon comprise the accessory minerals.

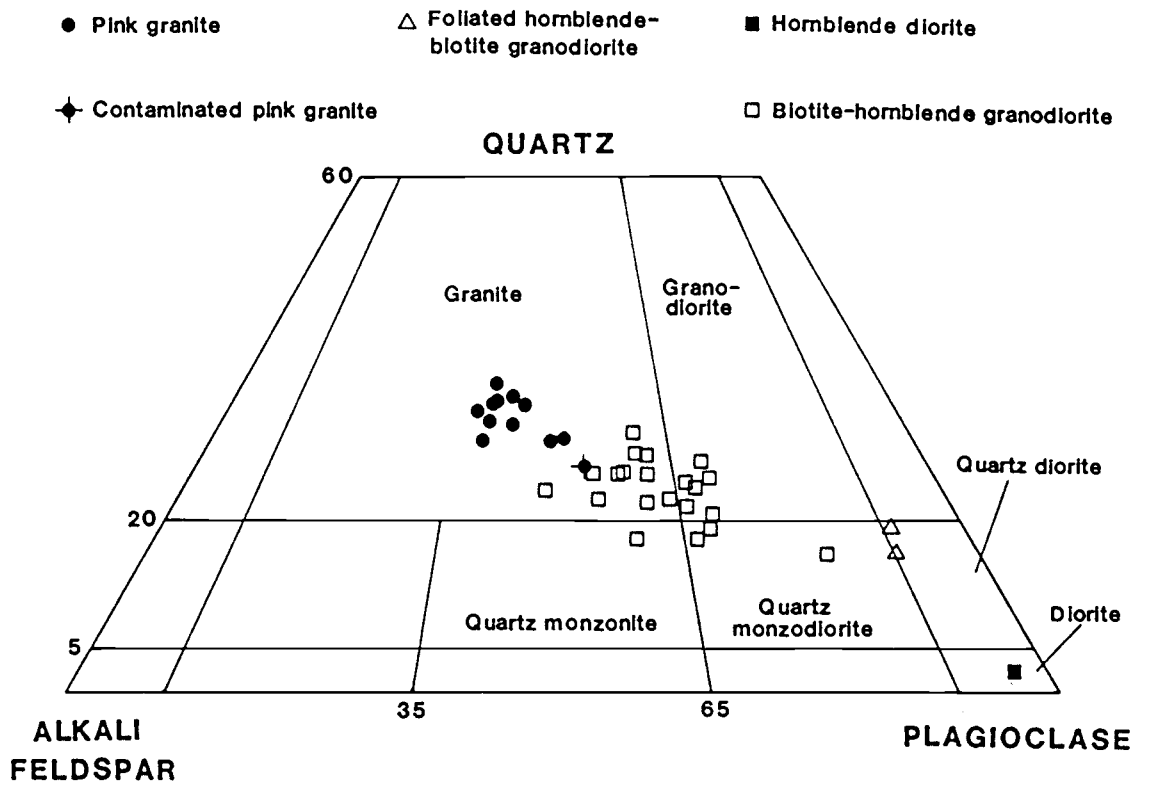

Figure 9. Plot of modal determinations (Table 1) of Eocene plutonic rocks from the eastern part of the Soldier Mountains.

The felsic rocks within the unit are fine-grained, equigranular, biotite granodiorite and granite, some of which is aplitic. Quartz, oligoclase, and perthitic potassium feldspar are the predominant minerals. The mafic minerals are biotite, and minor hornblende and opaques. Apatite, sphene, allanite, and zircon are present in trace amounts.

Hornblende diorite

Hornblende diorite is exposed in the southwestern part of the study area. The unit is poorly exposed, but characteristically weathers to a dark-brown soil. Outcrops commonly show evidence of shearing and propylitic alteration. The hornblende diorite is dark, equigranular, and medium- to fine-grained. Modal analyses plot in the diorite/gabbro field (Fig. 9). Contact relations with other units are not exposed, but the mafic character and large extent of alteration suggest that it is one of the older Eocene units.

Hornblende is the predominant mineral in this unit, and it is present both as an interstitial inclusion-rich phase and as euhedral pseudomorphs after pyroxene. The plagioclase feldspar is euhedral andesine, which is highly altered to sericite and epidote. Biotite is anhedral and extensively chloritized. Potassium feldspar and opaque minerals are minor constituents. Apatite is relatively abundant, constituting an estimated 1 percent of the rock.

Biotite-hornblende granodiorite

Biotite-hornblende granodiorite is exposed in the central and eastern parts of the study area. Textures vary from equigranular to porphyritic, and fine-grained to coarse-grained, but most of the rocks are medium-grained and seriate to porphyritic. Hornblende-rich inclusions (enclaves), commonly 3 to 10 cm across, are typical of this

unit. The more mafic phases of this unit are most common near contacts with older rocks, but they are not restricted to these areas. Aplite dikes are narrow and sparse, and pegmatite dikes are rare. Samples from this plutonic unit plot in the granite, granodiorite, quartz monzonite, and quartz monzodiorite fields (Fig. 9).

Plagioclase feldspar in the biotite-hornblende granodiorite unit is white, and consists of subhedral, strongly zoned crystals of sodic oligoclase and andesine. Core compositions are about 21 to 27 percent higher in An content than the rims (Table 1). The zonation is normal, but also has oscillatory and patchy domains. Potassium feldspar is present as small phenocrysts and as an interstitial component. It has poorly to moderately developed microperthitic textures, and is generally pink in color, but may be gray, particularly in the cores of phenocrysts. Turbidity is variable, but generally is highest in crystals that are pink. X-ray diffraction patterns indicate that the potassium feldspar is intermediate microcline, although grid twins are not discernable in thin section. Quartz is present as small (<4 mm) equant crystals and interstitial matrix material. Myrmekitic intergrowths are rare.

Pseudohexagonal books of biotite are a common feature of the biotite-hornblende granodiorite unit. Hornblende is typically euhedral, acicular, and glomerocrystic. Magnetite is abundant in the hornblende-rich glomerocrysts, which are small-scale versions of the mafic inclusions observed in outcrops. Apatite is a relatively abundant accessory mineral, and is characteristically found as inclusions in biotite and hornblende. Sphene, allanite, and zircon are also present in trace amounts.

Some of the most mafic rocks in this unit have textures and mineralogies that suggest a cumulate origin. Specifically, they contain about 40 percent euhedral hornblende (up to 6 mm in length) and about 15 percent euhedral clinopyroxene surrounded by interstitial plagioclase feldspar,

quartz, and K-feldspar. A few small euhedral plagioclase feldspar crystals are included within the larger hornblende crystals. Magnetite is relatively abundant and comprises about 4 percent of these rocks. Apatite and rare sphene are the only accessory minerals.

Pink granite

The pink granite unit is exposed in the high peaks around Smoky Dome in the western part of the area and in three small outlying stocks east of Couch Summit. The large mass in the western part of the area forms the central core of Eocene plutonic rock exposures in the study area, being rimmed by more mafic Eocene rocks of the quartz monzodiorite suite. This type of distribution is suggestive of a genetic link between the two suites of rocks, with the felsic rocks forming a differentiated core. However, to the west of the study area, the rim of more mafic rocks is lacking, and the pink granite is in contact with the Cretaceous batholith (Fig. 5). Also, the contact between these two rock suites, though usually not exposed, is abrupt. Chemical data presented in a later section indicate that the two rock suites represent distinct magma types derived from different sources. One locality, where the contact between pink granite and biotite-hornblende granodiorite can be observed, is just north of the metasedimentary roof pendant in the western part of the area. Here, neither phase exhibits a chilled margin, but a dike of pink granite cross-cuts the biotite-hornblende granodiorite, indicating that the pink granite is slightly younger.

Rocks of the pink granite unit are medium- to fine-grained, and typically equigranular. Subordinate porphyritic variants contain small potassium feldspar phenocrysts. Dikes of aplite and pegmatite cross-cut the unit, but are not common. Rock samples of the pink granite unit plot entirely within the granite field on a QAP diagram

(Fig. 9). One sample (RL187), is notably richer in plagioclase feldspar, and plots in an area that lies between the average pink granite and the average biotite-hornblende granodiorite. It is labeled as contaminated pink granite on Figure 9, because of an abundance of small (1 cm and less) mafic inclusions that are atypical for this unit. Three other samples (RL338, RL373, and RL374) also contain mafic inclusions, but these inclusions are in much lower abundance and the modal values are not significantly different from pink granite that lacks mafic inclusions. The mafic inclusions are identical to those found in the biotite-hornblende granodiorite unit described previously.

Pink, turbid, highly perthitic potassium feldspar is the most abundant mineral in the pink granite unit, and is responsible for the overall pink color of these rocks. Phenocrysts of potassium feldspar, where present, commonly have gray cores which are less turbid than the pink rims. X-ray diffraction patterns indicate that the potassium feldspar is intermediate microcline, but grid twins are not discernable in thin section. The diffraction patterns also indicate that the relative abundance of included albite (as microperthite) is high. Quartz is equant, up to 8 mm across in single crystals, and as polycrystalline aggregates of recrystallized strained crystals. Unlike in most of the other pink granites in Idaho, the quartz is not particularly smoky. Granophyric intergrowths of quartz and K-feldspar are common, but myrmekitic textures are at most weakly developed.

The plagioclase feldspar is predominantly white oligoclase with albitic rims. Zonation is weak to moderate, and normal, with minor oscillatory and patchy areas. Crystals as calcic as An_{41} are present in rocks that contain mafic inclusions. Rapakivi texture is developed locally. The plagioclase feldspar rims on the rapakivi feldspars are albitic and probably resulted from extensive exsolution. Unlike many other pink granites in Idaho, those in the

eastern part of the Soldier Mountains only rarely contain miarolitic cavities.

Subhedral to anhedral biotite, and anhedral magnetite, are the predominant mafic minerals in the pink granite. Hornblende is present in small mafic inclusions, as mentioned above, and as discrete crystals in a few of the samples. Some of the hornblende contains relict cores of pyroxene. Apatite, sphene, allanite and zircon comprise the accessory minerals.

One sample of fine-grained pink granite (RL245) from a small outlier was stained for potassium feldspar and found to be layered. It contains one layer, three cm or more in thickness, which consists of potassium feldspar, lesser quartz, and minor plagioclase feldspar and magnetite. Another layer is about four cm in thickness and contains roughly equal amounts of plagioclase feldspar, quartz, and potassium feldspar, with minor magnetite. Boundaries between the layers are diffuse. The origin of the layering is unknown, but it is clear that some process has, at least at a small scale, caused local enrichments in potassium feldspar relative to plagioclase feldspar.

Contrasts between Eocene and Cretaceous plutonic rocks

The petrographic characteristics of the plutonic rocks are summarized in Table 2. The large quartz crystals present in all of the Late Cretaceous plutonic rocks serve as the most useful field guide when trying to differentiate between Eocene and Cretaceous granodiorites. The distinct color of the Eocene pink granite unit is usually sufficient to distinguish these rocks, but the highly perthitic potassium feldspar is diagnostic. Care must be taken when considering color of the rock, because albitization (discussed in the Hydrothermal Alteration section) results in a pink color as well. Useful petrographic criteria in recognizing rocks of the Cretaceous biotite granodiorite unit include

EOCENE		CRETACEOUS
Quartz monzodiorite suite	Pink granite suite	Idaho batholith
seriate to porphyritic	equigranular	equigranular to porphyritic
highly variable texture and composition	monotonous texture and composition	monotonous texture and composition
strongly and complexly zoned andesine is dominant plagioclase	oligoclase is dominant plagioclase	weakly and sporatically zoned oligoclase is dominant plagioclase
moderately perthitic K-feldspar	highly perthitic K-feldspar	weakly perthitic K-feldspar
microcline grid twins absent	microcline grid twins absent	well developed microcline grid twins
low quartz content in mafic phases (diorites)	high quartz content	high quartz content, even in mafic phases (tonalites)
interstitial quartz	large quartz grains	large quartz grains or clusters of quartz grains
color index 9-56	color index 1-9	color index 4-18
euhedral biotite	anhedral biotite	anhedral biotite
hornblende commonly acicular; abundant	hornblende rare	stubby hornblende in some phases

Table 2. Petrographic characteristics of Eocene and Cretaceous plutonic rocks of central Idaho.

abundant myrmekitic textures and albite-pericline grid twins in potassium feldspar.

Rocks of the Cretaceous Idaho batholith are dominated by granodiorite (Fig. 8). All are rich in quartz, even those that contain abundant mafic minerals. The pink granite suite has a restricted compositional range, but is also enriched in quartz (Fig. 9). In contrast, rocks of the Eocene quartz monzodiorite suite have variable contents of quartz. Rock samples of this suite trend in a line toward the plagioclase feldspar apex on the QAP diagram, similar to calc-alkaline suites such as plutons in the Sierra Nevada batholith (Bateman and others, 1963). Lameyre and Bowden (1982) have interpreted modal distributions that trend toward the plagioclase feldspar apex as an indication that crystal fractionation processes have operated, particularly with respect to removal or addition of plagioclase feldspar. In contrast, they interpret plutonic rocks with consistently high quartz contents as mobilized crustal material (e.g. granitoids of Stone Mountain, Georgia). Using these criteria, both the Cretaceous batholithic rocks and the Eocene pink granite suite would be classified as mobilized crustal rocks. The quartz monzodiorite suite would be classified by Lameyre and Bowden (1982) as a typical calc-alkaline suite that had undergone crystal fractionation.

Although these relationships represent a crude system of evaluating the genesis of plutonic rocks, they point to differences in evolutionary history. It should be noted that petrographic evidence of crystal fractionation, in the form of cumulate rocks, has been recognized for the quartz monzodiorite suite. However, the layering in the one sample of pink granite is also indicative of crystal fractionation. Geochemical data presented in a subsequent section confirm that crystal fractionation was important in generating at least some of the variation within each suite, particularly the quartz monzodiorite suite.

Plagioclase feldspar within the Eocene plutonic rocks is more strongly zoned than that in the Cretaceous rocks. This relationship has been noted elsewhere (Anderson, 1952; Lewis, 1984) and is attributed to differences in cooling rates between the two groups of rocks. The cooling rate is in turn related to depth of emplacement and size of the intrusive body. Large Cretaceous plutons were emplaced at deeper levels and cooled more slowly, thus allowing plagioclase feldspar crystals to more closely equilibrate with fractionating melt. Smaller Eocene plutons, emplaced at epizonal levels, cooled more rapidly; in these plutons plagioclase feldspar was unable to equilibrate with the melt and is strongly zoned. Granophyric textures and miarolitic cavities present in many of the Eocene pink granites are also features common to epizonal plutons (Buddington, 1959).

Textures of potassium feldspar vary between the Cretaceous and Eocene plutonic rock units. Microscopically visible grid twins are lacking in microclines in the Eocene plutons, whereas perthite is common, particularly in the pink granite. The reverse is true of potassium feldspars in the Cretaceous biotite granodiorite and coarse-grained hornblende-biotite granodiorite units. Grid twins in these rocks are common, and perthite is poorly developed. The Cretaceous hornblende-biotite granodiorite unit has poorly developed perthite and visible microcline grid twins are also lacking.

The presence of well developed grid twins in most of the Cretaceous plutonic rocks is consistent with the evidence of slow cooling at relatively deep crustal levels. Other factors, such as deformation concurrent with cooling, or the amount of water present, may also have contributed to their formation. Numerous studies indicate that deformation enhances grid twin development (see summary by Smith, 1974). The presence of strained and recrystallized quartz crystals in the Cretaceous plutons is indicative of deformation, and lends support to the idea of strain-induced grid twinning.

The lack of microscopic grid twins in the Eocene microclines can be explained by relatively rapid cooling at epizonal levels. Although quartz in rocks of the Eocene plutons is locally strained, the degree of deformation appears to have been less than that in the Cretaceous plutons. The stress involved was apparently not sufficient to affect grid twin development. The presence of water may facilitate ordering of feldspars (Parsons, 1978), and perhaps contributed to the development of coarse microcline grid twinning in the Cretaceous plutons. The presence of numerous pegmatites in the Cretaceous plutons is evidence of available water. There is some indication that water also interacted with the cooling Eocene plutons. The pink color and turbid nature of potassium feldspar in these rocks suggest that they interacted with an oxidizing fluid phase following crystallization. This hypothesis is supported by oxygen isotope data, and is developed further in subsequent sections. As noted by Parsons (1978), the water needs to be present over the temperature interval during which ordering takes place. It may be that fluid-rock interaction in the Eocene plutons was at a lower (or higher?) temperature than the Cretaceous plutons and did not affect the coarseness of grid twin development.

The abundance of perthite in the Eocene plutons, and its paucity in the Cretaceous rocks, cannot be explained by differences in rates of cooling. If cooling rate was the controlling factor, then the Cretaceous rocks should have the coarsest perthite. This is not the case. Other factors to consider are the composition of the magma, its water content, and the amount of water present during subsolidus cooling.

If a magma has a low Ca content, then most or all of the crystallizing feldspar will be a single alkali feldspar relatively rich in Na (Tuttle, 1952). Considerable albite could exsolve upon cooling, forming a coarse perthitic texture. Such a scenario is likely for the pink granites

because they are low in Ca (<1.8 weight percent CaO). Both the Eocene quartz monzodiorites and the Cretaceous granodiorites have CaO contents greater than 2.5 weight percent. Neither contains abundant perthite, though it is better developed in the Eocene quartz monzodiorite suite. The relatively high proportion of total albite in alkali feldspars of the pink granites lends support to the hypothesis that magma composition was an important factor in controlling the degree of eventual perthite development.

The amount of water dissolved in the magma is another consideration with regard to the development of perthite. The addition of water under pressure depresses the solidus and enables subsolvus (2-feldspar) granites to crystallize (Tuttle and Bowen, 1958). Strictly speaking, the Eocene pink granites are subsolvus, because they contain discrete plagioclase feldspar crystals. Nonetheless, because the predominant feldspar is perthite, they resemble the hypersolvus (1-feldspar) granites. The hypersolvus granites are thought to form from relatively dry magmas that crystallize at temperatures above the alkali feldspar solvus (Tuttle and Bowen, 1958). Subsequent cooling results in the formation of perthite. By analogy, the highly perthitic Eocene pink granites may also have crystallized from relatively dry magmas. The fact that pegmatites are rare in the pink granite is supportive evidence of a relatively dry system, as is their shallow emplacement level. Had the rising magmas been water-rich, crystallization would have commenced at deeper levels.

The amount of water present during subsolidus cooling may also have influenced the degree of perthite development. Parsons (1978) and Parsons and Brown (1984) have emphasized the importance of water in perthite development, and documented cases of "catastrophic coarsening" brought about by interaction of deuteric or hydrothermal fluids with alkali feldspars. The coarse perthitic textures thus formed cut across preexisting exsolution textures and often include the

development of turbidity. They also suggest that in some rocks this coarsening may have taken place a relatively high temperatures (>400°C) and completely masked preexisting coherent exsolution features. Evidence for the latter process is more difficult to obtain than for localized coarse overprints. There is no petrographic evidence that the perthite in the Eocene plutons post-dates a preexisting exsolution texture. Thus, any "catastrophic coarsening" would have had to have been pervasive, and would be difficult to prove.

In summary, the controls of potassium feldspar textures are complex, and no single process can account for all of the textures observed. The microcline grid twins in the Cretaceous plutons probably result from slow cooling at relatively deep crustal levels, perhaps enhanced by concurrent deformation. The lack of coarse twins in the Eocene plutons is likely an indication of higher cooling rates with less applied stress. Also, water may not have been as abundant in the Eocene rocks during the temperature interval at which twinning took place. The coarse perthitic textures in the Eocene granites is most easily explained by low Ca content of the magma, but may also be indicative of a relatively dry system during crystallization.

Though sparse, mafic inclusions are anomalously abundant in pink granite of the Soldier Mountains. The pink granite elsewhere in the region is either devoid of inclusions or, as reported by Stewart (1987), it contains rare inclusions. This relative abundance of inclusions is most easily explained by the distribution of pink granite relative to the more mafic Eocene rocks. The pink granite was intruded into the center of a slightly older mass of biotite-hornblende granodiorite, and could easily have either collected xenoliths of the more mafic rocks, or partly mixed with a magma of the more mafic suite. Although either mechanism is possible, the fact that the inclusions are rounded suggests that they were at least partly molten when

incorporated into the presumably cooler granite magma. Xenoliths of country rock (quartzite) in the Eocene plutons tend to be angular rather than rounded. A restite origin for the mafic inclusions in the pink granite is less likely, because of their characteristic absence in the Eocene granites elsewhere in the region.

Inclusions in the quartz monzodiorite suite are probably not xenoliths of unrelated rock, because mineralogically they are similar, although generally more mafic, than typical rocks of this suite. Whether or not they are restite, cognate inclusions, or of mixed magmatic origin, remains a topic for more detailed sampling and study.

EOCENE DIKE ROCKS

Dike rocks of probable Eocene age are abundant in the area, and cross-cut both Cretaceous and Eocene plutonic rocks. None of the dikes have been dated radiometrically, but they are spatially associated with plutonic rocks of known Eocene age. The dikes are resistant to erosion and typically form prominent outcrops; strikes are predominantly northeast. In the southwestern part of the area exposures are poor and dike float is abundant. In this area the mapped dikes are in part schematic as shown on Plate 1, and a larger mass of hypabyssal rock, perhaps of stock dimensions, may be present. Classification of the dikes is difficult because they are fine grained and exhibit subtle textural and mineralogical variations. Textures also vary from interior to margins within some of the dikes, with the margins having fewer phenocrysts than the interiors. Nonetheless, four types of dikes were distinguished in this reconnaissance investigation.

Dacite and andesite dikes are green to gray in color and weakly to moderately porphyritic. Phenocrysts are typically 2 to 4 mm in size, and consist of plagioclase feldspar and hornblende. Other phenocrysts may include

pyroxene and (or) biotite. The groundmass is composed largely of plagioclase feldspar.

Dikes of rhyodacite are pink to gray-green in color and moderately to highly porphyritic. Phenocrysts are typically 2 to 5 mm in size, and consist of plagioclase feldspar and hornblende, with lesser amounts of biotite and embayed quartz. The groundmass is characterized by granophyric intergrowths of quartz and potassium feldspar.

Rhyolite porphyry dikes are pink to light gray in color and highly porphyritic. They contain potassium feldspar phenocrysts up to 15 mm in length and smaller phenocrysts of plagioclase feldspar, quartz, hornblende, and biotite. The groundmass is typically granophyric.

Rhyolite dikes are tan to light brownish red in color and medium to weakly porphyritic. Phenocrysts are generally 2 mm and less in size and they consist of plagioclase feldspar, quartz, and potassium feldspar. Minor hornblende and biotite are typically restricted to the groundmass. Crude spherulitic textures are developed in the groundmass, along with subordinate granophyric textures.

MIOCENE DIKE ROCKS

Three pyroxene basalt dikes are exposed west and northwest of Smoky Dome, and one crops out north of River Bend Campground. All four have north-northwest trends. The dikes are dark green, microporphyritic, and contain sparse vesicles filled with zeolite and calcite. Similar dikes are widely scattered throughout the Atlanta lobe of the batholith and have been termed "diabase" by Reid (1963), Kiilsgaard (1983a), and Fisher and others (1983). Reid (1963) noted that their northwest trends contrast with those of the northeast-trending dikes of Eocene age. He also speculated that they were feeders to basalts of the Columbia River Group of Miocene age. A basaltic dike sample collected near Anderson Ranch Dam (40 km west of the study area) by

W.H. Taubeneck yielded a K-Ar age of 15.5 ± 0.7 Ma (recalculated from Armstrong, 1975). Although this is probably a minimum age, it is compatible with the published ages of the Columbia River Basalt flows (Hooper, 1982).

Euhedral crystals of labradorite range from 0.2 to 1 mm in length and form the predominant microphenocrysts in the pyroxene basalt dikes. They are accompanied by lesser amounts of augite subhedra that range from 0.1 to 5 mm in size. The groundmass consists of dark-brown glass and contains skeletal plagioclase feldspar, acicular augite(?), and opaque minerals. Rare xenocrysts of quartz are rimmed with augite.

A whole-rock chemical analysis for one sample (RL220) of a pyroxene basalt dike from the northern part of the study area is listed in Table 3. Also listed are C.I.P.W. normative minerals. This sample plots in the basaltic andesite field on an alkalies versus silica diagram, as illustrated in Figure 10. The term basalt is used for this unit because of similarities in age and composition to the Columbia River Basalts, many of which are also basaltic andesites by the chemical classification system used in Figure 10. The dike is a relatively siliceous quartz tholeiite similar to Grande Ronde Basalt of the Columbia River Basalt Group. Comparison of RL220 with 13 analyses of a high-Mg Grande Ronde flow (Swanson and others, 1979) shows similar concentrations of major elements (Table 3). The lack of large phenocrysts, and the pyroxene-plagioclase feldspar mineralogy, is also characteristic of Grande Ronde Basalt. Although the pyroxene basalt dikes that were mapped are texturally and compositionally similar to the Grande Ronde flows, more analyses of these and other basaltic dikes in the Atlanta lobe are needed to verify this correlation.

A single north-northeast-trending dike of dark-gray, porphyritic pyroxene-olivine basalt is present near the head of Lawrence Creek, in the southeastern part of the area. It cross-cuts flows of olivine basalt and is assumed to be a

unit	Tdb	Trd	Tgs	Ttc	Ttc	dike	Tb	Tb	Tb	CRB
sample	RL258	RL292	RL318	RL375	RL511	RL220	RL173	RL503	RL520	high Mg
Major-element oxides in weight percent										
SiO_2	62.3	67.7	73.4	74.4	75.3	53.0	50.0	47.3	47.4	53.78
TiO_2	0.60	0.42	0.39	0.22	0.19	1.86	2.33	1.48	1.53	1.78
Al_2O_3	14.7	14.7	11.9	11.1	11.6	13.7	14.7	16.2	16.3	14.45
Fe_2O_3	5.05	1.30	2.69	2.51	1.51	5.64	4.11	3.95	3.88	—
FeO	0.14	1.51	0.21	1.00	1.00	5.72	9.71	8.05	8.12	11.35
MgO	3.47	1.01	0.17	0.11	<0.10	4.49	4.19	6.75	6.27	5.25
MnO	0.07	0.05	<0.02	0.05	0.02	0.17	0.23	0.20	0.20	0.19
CaO	3.96	2.58	0.71	0.20	0.04	7.91	7.49	9.56	10.1	9.07
Na_2O	3.49	3.17	2.88	3.95	4.12	2.66	3.54	3.10	3.04	2.83
K_2O	3.05	4.50	4.81	4.86	4.97	1.73	1.94	0.92	0.89	1.05
P_2O_5	0.22	0.14	<0.05	<0.05	0.05	0.28	0.59	0.31	0.31	0.28
H_2O^+	0.96	2.09	0.78	0.37	0.25	0.66	0.72	1.67	1.01	—
H_2O^-	0.95	0.11	0.55	0.21	<0.05	1.25	0.46	0.41	0.32	—
CO_2	0.01	<0.01	0.01	0.70	<0.01	0.17	0.48	0.01	0.71	—
total	99.0	99.3	98.6	99.7	99.2	99.2	100.5	99.9	100.1	100[1]
Trace elements in parts per million										
Ba	1500	1200	1100	16	—	530	1200	—	—	—
Sr	560	370	71	11	—	300	499	—	—	—
Rb	64	150	180	267	—	48	26	—	—	—
Nb	—	—	—	88	—	—	—	—	—	—
Zr	—	—	—	837	—	—	163	—	—	—
La	—	—	—	64	—	—	—	—	—	—
Ce	—	—	—	155	—	—	—	—	—	—
Y	—	—	—	73	—	—	—	—	—	—
C.I.P.W. norms in weight percent										
Q	15.7	24.8	35.5	33.1	32.4	10.5	0.09	—	—	—
C	—	0.13	0.75	—	0.04	—	—	—	—	—
Or	18.0	26.6	28.4	28.7	29.4	10.2	11.5	5.4	5.3	—
Ab	29.5	26.8	24.4	30.0	32.0	22.5	30.0	26.2	25.7	—
An	15.4	12.2	3.4	—	—	20.3	18.5	27.6	28.2	—
Ac	—	—	—	3.0	2.5	—	—	—	—	—
Di	1.78	—	—	0.26	—	10.4	5.3	9.7	8.2	—
Hd	0.81	—	—	0.29	—	2.5	4.8	4.7	4.4	—
En	7.8	2.5	0.42	0.15	0.24	6.3	8.0	2.1	5.2	—
Fs	4.1	1.1	2.4	0.18	1.0	1.8	8.4	1.2	3.2	—
Fo	—	—	—	—	—	—	—	7.1	4.6	—
Fa	—	—	—	—	—	—	—	4.4	3.1	—
Mt	1.9	1.9	1.1	2.1	0.92	8.2	6.0	5.7	5.6	—
Il	1.1	0.79	0.74	0.41	0.36	3.5	4.4	2.8	2.9	—
Ap	0.52	0.33	0.11	0.11	0.11	0.66	1.4	0.73	0.73	—
Cc	0.02	—	0.02	—	—	0.38	1.1	0.02	1.61	—
Zr	—	—	—	0.16	—	—	0.03	—	—	—

Tdb = dacite lava flow (Challis Volcanics); Trd = rhyodacite lava flow (Challis Volcanics); Tgs = Gwin Spring Formation; Ttc = tuff of Cannonball Mountain; dike = pyroxene basalt dike; Tb = basalt flows; CRB = Mg-rich flow of the Grand Ronde Basalt of the Columbia River Basalt Group (average of 13 analyses from Swanson and others, 1979); [1] normalized to 100 percent anhydrous; norm of RL375 calculated without CO_2 (negative An values obtained with CO_2 included); norms of highly oxidized samples RL258 and RL318 calculated with assumed FeO/FeO* = 0.75.

Table 3. Chemical analyses and C.I.P.W. norms of volcanic rocks of the study area, and comparative samples. Major-element oxides were determined using X-ray fluorescence spectroscopy (XRF) and trace elements were determined using inductively-coupled plasma spectroscopy and atomic-absorption spectroscopy; trace elements in RL375 determined by energy-dispersive XRF. Analyses by J. Taggart, A. Bartel, D. Siems, E. Brandt, J.H. Christie, L. Jackson, J. Evans, and K. Slaughter at U.S. Geological Survey laboratories in Denver, Colorado, and Reston, Virginia.

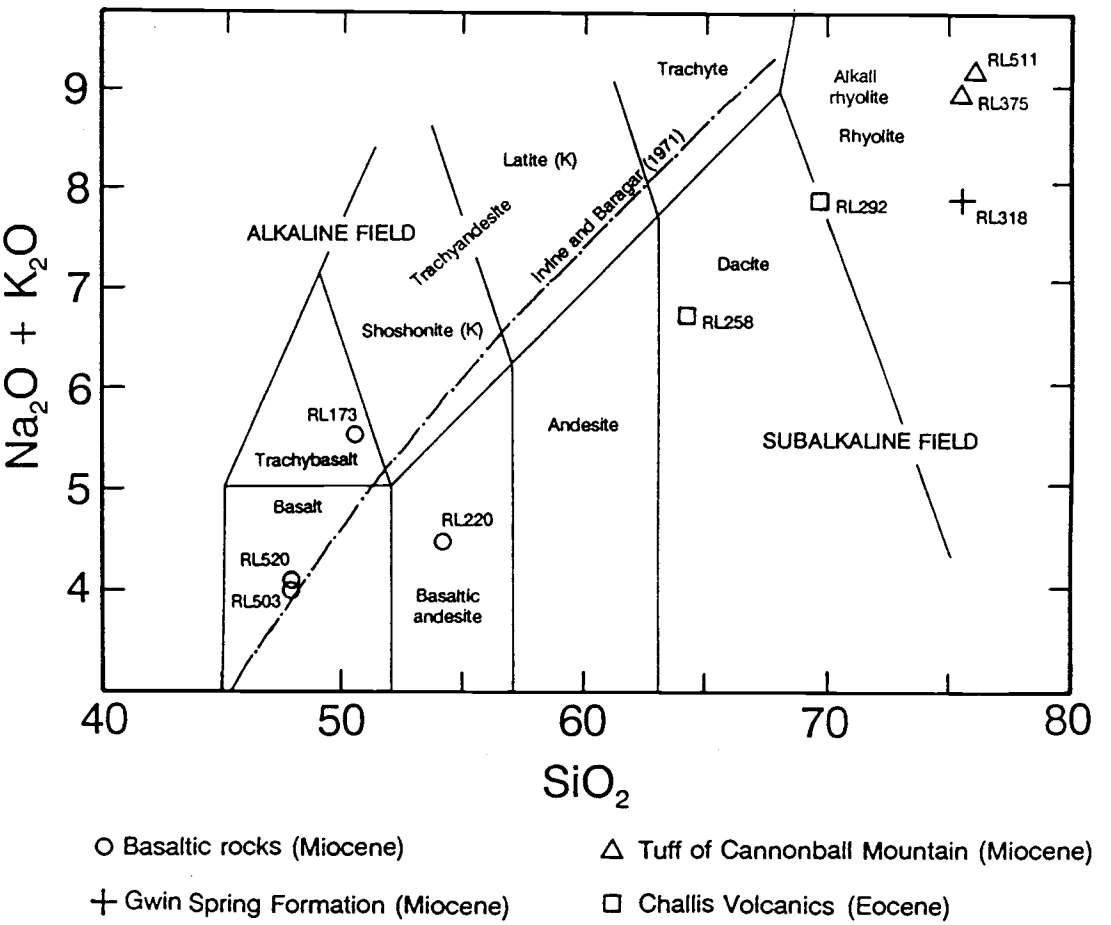

Figure 10. Plot of K_2O + Na_2O versus SiO_2 for volcanic rocks from the eastern part of the Soldier Mountains. Alkaline and subalkaline fields are from Irvine and Baragar (1971) and rock nomenclature is from LeMaitre (1984).

feeder to one of the younger, pyroxene-phyric flows found east of the study area. The predominant phenocryst is euhedral labradorite, which averages about 0.5 mm in length and is commonly embayed. Olivine phenocrysts, mostly 0.3 mm across, are also embayed. Clinopyroxene is a phenocryst phase, a feature that is lacking in most basalts of the Snake River Plain. The clinopyroxene phenocrysts are similar in size to the olivine, but less abundant. The groundmass is holocrystalline, and consists of plagioclase feldspar, clinopyroxene, and opaque minerals. A whole-rock K-Ar age determination of 6.4 $\pm$ 0.2 Ma was obtained on a sample from this dike, the results of which are listed in Table 4. This young age is compatible with field relations.

EOCENE VOLCANIC ROCKS (CHALLIS VOLCANICS)

Volcanic rocks correlative with the Challis Volcanics are exposed in the eastern part of the study area. They are locally preserved in down-dropped fault blocks and rest on an uneven erosional surface of Cretaceous granodiorite. Presumably these exposures represent remnants of a once-extensive volcanic cover.

Dacite and andesite lava flows and breccias

A complex sequence of poorly exposed dacite and andesite lava flows and breccias is present along Owen's Creek and Soldier Creek. Individual flows are meters to tens of meters thick and accumulations of multiple flows locally amount to several hundred meters. Colors range from purple to red to green, and textures are porphyritic to nearly aphyric. Most flows are porphyritic, and contain phenocrysts of andesine and hornblende, $\pm$ biotite, $\pm$ augite. Quartz is present locally as small embayed phenocrysts. The groundmass consists of plagioclase feldspar, opaque minerals, and minor glass. The glass is generally devitrified.

rock unit	sample number	material dated	K (wt.%)	Ar_{rad} (cm^3/g)	$^{40}Ar_{rad}$ (%)	date (Ma)
porphyritic rhyodacite	RL292	hornblende	0.962	1.8897 E-6	30	49.9±0.6
		biotite	7.12	1.3272 E-5	70	47.4±0.5*
tuff of Cannonball Mtn.	RL375	sanidine	6.01	2.3833 E-6	9	10.2±0.3
Gwin Spring Formation	RL179	obsidian	4.04	1.3788 E-6	26	8.8±0.1*
olivine basalt (dike)	RL195	whole rock	0.979	2.4249 E-7	28	6.4±0.2

*Ar loss suspected (see text)

Table 4. Potassium-argon age determinations of volcanic rocks in the eastern part of the Soldier Mountains. Analyses were conducted by D. Pyle at Oregon State University.

The breccias in this unit are typically monolithologic, and contain small (<10 cm) rounded devitrified clasts which have phenocrysts of plagioclase feldspar, hornblende and biotite. The coarseness of devitrification products differs from clast to clast. The breccia matrix mineralogically is similar to the clasts, differing mainly in the degree of devitrification. Coarser, heterolithologic breccias are present as well, but are less common.

A whole-rock analysis of one of the flows in the dacite and andesite unit is given in Table 3. The rock is subalkaline, and plots in the dacite field on an alkalies versus silica diagram (Fig. 10).

Porphyritic rhyodacite lava flow

A porphyritic rhyodacite is exposed in erosional windows through Miocene volcanic rocks in the southeastern part of the area. The rock is reddish in color, with the exception of local dark-gray vitrophyres. It is distinguished from the dacite and andesite flows described previously by the abundance of phenocrysts and the presence of quartz as a ubiquitous phenocryst phase. Outcrops of porphyritic rhyodacite exhibit well-developed flow foliation that varies in attitude and is locally folded. Absolute thickness of the unit is unknown, but local exposures exceed 15 m. Normal magnetic polarity was measured at two localities.

A K-Ar age determination on hornblende from a vitrophyre of the porphyritic rhyodacite unit yielded a 49.9 $\pm$ 0.6 Ma date (Table 4). Biotite from the same sample yielded a 47.4 $\pm$ 0.5 Ma date. The younger age of the biotite is interpreted to be a result of argon loss, whereas the hornblende age is considered more reliable, and is consistent with the normal polarity of the unit.

Phenocrysts of andesine, biotite, hornblende and quartz constitute about 45 percent of the rock. They are set in a groundmass of glass, which is locally devitrified and

spherulitic. Quartz is embayed.

The results of a whole-rock analysis of the porphyritic rhyodacite unit are given in Table 3. A plot of alkalies versus silica (Fig. 10) indicates that this unit is transitional between dacite and rhyolite. The field term of rhyodacite has been retained for this unit, which applies to transitional dacite/rhyolite rocks in the modal classification scheme of Streckeisen (1978).

MIOCENE VOLCANIC AND SEDIMENTARY ROCKS

Volcanic rocks and interbedded gravels of Miocene age are present in the southeastern part of the study area where they rest unconformably on Eocene Challis Volcanics and Cretaceous biotite granodiorite. The volcanic units consist of alkali rhyolite (comendite) tuff, rhyolite tuff, and basalt, and are related to Snake River Plain volcanism.

Tuff of Cannonball Mountain

The oldest Miocene unit is the alkali rhyolite (comendite) tuff of Cannonball Mountain, which crops out in the upper parts of both Powell Creek and Sampson Creek. Exposures continue as far east as Willow Creek, 15 km east of the study area boundary. Evidence for a pyroclastic origin is lacking in the study area, but a pumice-rich zone that resisted devitrification is exposed in Elk Creek, 7 km east of the study area boundary. The informal name "tuff of Cannonball Mountain" is proposed, and refers to exposures on Cannonball Mountain, 3 km east of the study area boundary.

Overall, the unit is poorly exposed, and thickness is difficult to estimate. Attitudes of flow foliation are highly variable, and locally are folded. The folds indicate that the tuff remobilized after deposition, and may have thickened locally by infilling topographically low areas.

The tuff is present over a vertical distance of about 300 m in the Cannonball Mountain area. Thus, despite the possibility of unmapped faults having thickened the section, local accumulations of at least 100 to 200 m are likely. The age of this unit is about 10.2 ± 0.3 Ma, based on a sanidine K-Ar age determination (Table 4).

The tuff of Cannonball Mountain is light gray, porphyritic, and vesicular. It weathers brown and forms thin soils which are particularly conducive to growth of ponderosa pine and Douglas fir, even on dry, south-facing slopes. Although nodules of obsidian are common in float, it was never found in outcrops. Phenocrysts of sanidine and quartz, 0.2 to 0.3 mm in size, comprise about 2 to 6 percent of the rock. Both minerals are embayed, and the sanidine commonly exhibits light blue chatoyancy. The groundmass is thoroughly devitrified, and is composed of spherulites or, more commonly, intergrowths of equant feldspar and quartz crystals. Small radial sprays of both opaque minerals and amphibole are intergrown with the quartz and feldspar. Amphibole is also present in vesicles, along with quartz and zeolite. The amphibole is a strongly pleochroic alkali amphibole (X = dark blue-green to blue, Y = olive green, Z = dark brownish gray). X-ray diffraction patterns indicate that it is arfvedsonitic in composition. Mafic phenocrysts are lacking in these rocks within the study area, but rare green pyroxene (aegerine-augite?) is present near Willow Creek. The extensive reconstitution of the groundmass, coupled with late formation of amphibole, is suggestive of intense vapor-phase alteration.

Two samples of the tuff of Cannonball Mountain were analyzed (Table 3) and found to contain molecular $Na_2O + K_2O$ in excess of Al_2O_3 and normative acmite; they are thus peralkaline. On an alkalies versus silica diagram (Fig.10), these samples plot in the alkali rhyolite field. They are designated comendite using the classification of MacDonald (1974) for peralkaline rocks oversaturated with silica. The

presence of alkali amphibole in the groundmass and in vesicles is a characteristic of comendites, as is thorough devitrification (Sutherland, 1974; Schminke, 1974).

When compared to other Miocene rhyolitic rocks of the Snake River Plain, the tuff of Cannonball Mountain is chemically and mineralogically unique. Typical rhyolites of the Snake River Plain are metaluminous or peraluminous, and they lack late-stage sodic amphiboles (see Leeman, 1982b, for summary). The only previously recognized peralkaline rocks in the region are comendite lavas of Quaternary age at Big Southern Butte, 120 km east of the study area (Noble and Parker, 1974; Spear and King, 1982). The closest peralkaline rocks of Miocene age are comendite tuffs in southeastern Oregon and northwestern Nevada (Rytuba and McKee, 1984; Conrad, 1984).

Gwin Spring Formation

A crystal-poor rhyolite tuff is exposed in several localities east of Soldier Creek. This unit is correlated with the Gwin Spring Formation of Smith (1966), the type section of which is exposed in the Mount Bennett Hills 20 km south of the study area. Formation status for this unit has never been established, but the name is retained and used in an informal sense. A K-Ar age determination on glass from the upper vitrophrye yielded a 8.8 $\pm$ 0.1 Ma date (Table 4). This is slightly younger than the age of the Gwin Springs Formation in the Mount Bennett Hills, which has been bracketed between 9.4 $\pm$ 0.1 and 9.8 $\pm$ 0.3 Ma (Leeman, 1982a; Honjo and others, 1986). Argon loss from the glass is suspected. Weak normal polarity was measured at one locality. The type section of the Gwin Spring Formation has normal polarity as well (Leeman, 1982a).

The unit is flow foliated and vesicular. Flow foliation varies in attitude and is locally folded. Vesicles are typically lined with zeolite, flattened, and elongated in

one direction. Most of the vesicles are 0.5 to 2 cm long, but rare vesicles over 30 cm in length are present as well. The folded flow foliation and elongate vesicles are an indication of movement following compaction and welding of the tuff. Smith (1966) noted these features from exposures of the Gwin Spring Formation in the Mount Bennett Hills, and attributed them to shearing and folding of unusually hot and fluid ash flows as they moved down southerly-sloping surfaces.

The lower and upper parts of this rhyolite tuff are locally defined by vitrophyres that range from 1 to 4 m and 1 to 2 m in thickness, respectively. Both are dark gray in color. The lower vitrophyre contains welded glass shards, sparse pumice fiame, and rare clasts of granite grus. Phenocrysts in this vitrophyre are sparse (about 1-3 percent), and consist of plagioclase feldspar and lesser clinopyroxene, quartz, and opaque minerals. They are 1 mm and less in size. The upper vitrophyre is similar, but contains less than 1 percent phenocrysts. Between the upper and lower vitrophyres the tuff is entirely devitrified, red-brown in color, and breaks into platy fragments parallel to the flow foliation. Here, the groundmass is extremely fine-grained and is composed of equant feldspars(?), quartz(?), and opaque minerals. Phenocrysts are similar to those in the lower vitrophyre, but less abundant. Clinopyroxene has been replaced by biotite and chlorite. Total thickness of the tuff is variable, but rarely exceeds 30 m.

In contrast to the tuff of Cannonball Mountain, the Gwin Spring Formation is a "typical" rhyolite tuff of the Snake River Plain. It is similar in composition and phenocryst mineralogy to other rhyolitic units grouped loosely as the Idavada Volcanics. Examples include the Cougar Point tuff (Bonnichsen and Citron, 1982) and the tuff of Swisher Mountain (Ekren and others, 1982). The Idavada tuffs are characteristically crystal-poor, and commonly contain only anhydrous mafic phenocryst phases (usually clinopyroxene ±

orthopyroxene). They apparently were erupted at high temperatures (some ≥ 1000°C) and coalesced to form liquids before final emplacement and cooling (Ekren and others, 1984). Many resemble rhyolite lava flows, but have broad areal distributions, and pyroclastic textures that are preserved locally at the bases, tops, and distal ends of some of the deposits (Ekren and others, 1984).

Gravels

Poorly sorted gravels were deposited locally on Cretaceous biotite granodiorite and Challis Volcanics. Pebbles and cobbles of granitic rock, and the tuff of Cannonball Mountain, are the predominant clasts. These gravels underlie the Miocene olivine basalt flows. In most cases they are 1 m or less in thickness and do not show at map scale. However, thicker accumulations near the mouth of Powell Creek are mappable as a unit, and are shown on Plate 1.

Olivine basalt

Porphyritic olivine basalt flows are exposed in the vicinity of Wardrop Creek, and continue an additional 15 km east and northeast of the study area. Dips on the flows are less than 20 degrees. Those in the study area extruded over a relatively gentle topography, but to the east they filled canyons. Individual flows vary in the phenocryst content, and in the presence or absence of clinopyroxene as a phenocryst phase. Flow tops are vesiculated, but most of the rock is dense and dark gray, and lacks the diktytaxitic texture common to many basalt flows of the Snake River Plain. Local accumulations exceed 120 m. Impure diatomite is interbedded among the flows in Brush Canyon.

Plagioclase feldspar, mostly 0.5 to 1.5 mm in length, is the predominant phenocryst; lesser amounts of olivine

Collectively, these mineral phases make up about 30 to 40 percent of the rock. The plagioclase feldspars are aligned as a consequence of flowage. Larger crystals of plagioclase feldspar (up to 12 mm) locally comprise as much as 10 percent of the rock, and are probably xenocrysts. They are more equant than the smaller crystals, and some are embayed and filled with inclusions. Clinopyroxene is a rare phenocryst phase in flows within the study area, but is more common in basalt to the east on Cannonball Mountain. The groundmass in the olivine basalt is holocrystalline and consists of plagioclase feldspar, clinopyroxene, and opaque minerals. Chlorite, and calcite are present, as well as trace amounts of interstitial biotite.

One single and highly oxidized olivine basalt flow was mapped as a separate unit (Plate 1). It is exposed east of Wardrop Creek, and is one of the younger basalt flows. It is similar to the flows described above, but is reddish in color and richer in opaque minerals.

None of the flows of olivine basalt from the study area were analyzed chemically. However, three basalts collected within 10 km to the east of the study area were analyzed and the results are listed in Table 3. Sample RL173 contains clinopyroxene phenocrysts, which are lacking in the other two samples. Samples of olivine basalt in the study area are petrographically most similar to RL503 and RL520, which have normative olivine and orthopyroxene, and lack normative quartz. These two samples are olivine tholeiites according to the classification of Yoder and Tilley (1962) and they plot in the basalt field on an alkalies versus silica diagram (Fig. 10). The pyroxene-phyric sample plots in the trachybasalt field. Note that all are alkaline according to the classification of Irvine and Baragar (1971), despite a lack of normative nepheline. According to Leeman and Vitaliano (1976) many basalts of the Snake River Plain have sufficient $Na_2O + K_2O$ for a given SiO_2 content to be classified as alkaline.

Ages of the olivine basalt flows in the study area, and those immediately to the east, are not precisely known. In many places the flows rest on the Gwin Spring Formation, and thus are 9.4 Ma or younger. The pyroxene-olivine basalt dike described previously, and dated at 6.4 Ma, is similar mineralogically to a clinopyroxene-phyric flow east of the study area on the north side of Cannonball Mountain. This flow appears to be one of the youngest of the basalt flows in the area. Consequently, the age of most (or all) of the flows is probably between 6.4 and 9.4 Ma. Additional geochronologic and stratigraphic work is clearly needed.

LATE MIOCENE(?) OR PLIOCENE(?) SEDIMENTARY ROCKS

Poorly consolidated arkose and interbedded water-lain ash are exposed along Lick Creek, 1.5 km southeast of Big Smoky Guard Station. These sediments were deposited in a small basin within the Cretaceous biotite granodiorite. The beds dip to the northeast at 20 to 30 degrees, and are partly covered by flat-lying terrace gravels of Pleistocene age. The section is not well exposed, but its thickness exceeds 600 m, assuming no repetition by faulting or slumping.

Arkose and siltstone are the predominant lithologies, and water-lain ash and conglomerate are less abundant. The arkose, siltstone, and conglomerate are poorly sorted and consist of locally-derived granitic material. The arkose has been quarried for road metal. The water-lain ash is thinly laminated and is present in at least two beds averaging 4 m in thickness. Unaltered glass shards, 0.2 to 0.5 mm in size, are the main constituent, whereas plagioclase feldspar, quartz, biotite (after pyroxene?), and lithics comprise about 5 percent of the rock.

Plant fossils (sedge and pollen) were collected from siltstones within the arkose and ash unit south of Lick Creek (RL319, Plate 2). The age of these rocks, on the

basis of this collection, is thought to be Late Miocene(?) or Pliocene(?) (William C. Rember, pers. comm., 1986). The grass-like fossils were identified as sedge (Cyperaceae) by Douglass M. Henderson (pers. comm., 1986). The pollen was studied by William Rember, who identified pine and fir, and noted a lack of grass or sagebrush pollen, which are now common in the area.

STRUCTURE

Prominent structures in the eastern Soldier Mountains are faults, and swarms of dikes that follow zones of structural weakness (Plate 1). Distributions of the major faults are shown in simplified fashion in Figure 7. The majority of the faults dip steeply and were recognized by topographic expression, changes of rock type, and (or) zones of cataclasis. The only low-angle fault that could be traced any distance is present in the extreme northeastern corner of the study area. Numerous other low-angle structures probably are present, but were not recognized with certainty because of poor exposures and lack of marker units.

HIGH-ANGLE FAULTS

The Worswick Creek fault system (WCFS) is probably one of the oldest high-angle structures in the area. It consists of a series of northeast-trending faults characterized by easily eroded zones of sheared rock that have influenced the drainage pattern of Worswick Creek. Some of these faults may continue southwest of the Rosetta Creek fault, but none could be traced because of poor exposures. The northeast trend of the WCFS parallels the predominant trend of Eocene dikes in the area, and thus, the fault system is likely to have been present during Eocene time. The northeast trend is the same as that of the much larger Trans-Challis fault system mapped to the north (Kiilsgaard and Lewis, 1985). The two structures are considered contemporaneous. Direction of displacement along the WCFS is unknown, but there is no topographic break that would indicate recent dip-slip motion. Although rocks along the fault zone are crushed and broken, hydrothermal alteration is minimal.

Propylitic alteration of probable Eocene age is localized along some of the faults in the study area. This

imprint of hydrothermal activity suggests that these faults were present in the Eocene, but movement may have been recurrent since that time. Examples include the east-west-trending fault 2.5 km southwest of U.S. Forest Service Big Smoky guard station, and the northwest-trending fault 2.5 km east of the guard station (Fig. 7). In addition, propylitic alteration is pronounced along the northwestern part of the Rosetta Creek fault, but this may reflect alteration at an intrusive contact which was later the site of fault motion.

The Brush Canyon, Couch Summit, Rosetta Creek, and Soldier Mountains faults are characterized by topographic breaks, and probably have had dip-slip motion within the past several hundred thousand years. Some or all of these faults may yet be active. Their west-northwest to north-northwest trends parallel Basin and Range structures present in the region, and all are interpreted as steep normal faults. Hydrothermal alteration along these faults is not pronounced. Rocks along the Couch Summit fault are the most altered, having been propylitized. This alteration is thought to have been Eocene in age, and thus the Couch Summit fault has probably been the site of recurrent movement over the past 50 Ma. The other steep normal faults are probably younger, but age of initial movement is difficult to establish. The Soldier Mountains fault is the southernmost part of a structure 80 km in length that extends as far north as the South Fork of the Payette River, east of Lowman, Idaho (Fig. 6). The northern part of the fault, recognized by Anderson (1934b), is termed the Deer Park fault. Net vertical displacement on the Soldier Mountains fault, based exclusively on topographic relief, is roughly 700 m (2300 ft). Vertical displacement on the order of 500 m (1600 ft) is likely along the Brush Canyon fault and along the southern end of the Couch Summit fault.

LOW-ANGLE FAULTS

The low-angle fault in the northeastern corner of the study area dips about 25 degrees to the south. It continues east into the Dollarhide Mountain quadrangle, where it forms a resistant ridge of propylitized and crushed Cretaceous biotite granodiorite. The map by Darling (1987), of the Dollarhide Mountain quadrangle, does not show this feature as a fault, but does show a sericitized and propylitized zone within the biotite granodiorite. The origin of this structure is uncertain, but it is probably a low-angle extensional fault of Eocene age. Propylitic alteration, such as found in this fault zone, is commonly associated with Eocene plutonism elsewhere in the region. Darling (1987) has mapped a propylitized hornblende quartz monzonite of Eocene age below the altered and sheared biotite granodiorite, and has inferred an Eocene age for alteration in this part of the Dollarhide Mountain quadrangle.

Low-angle shear zones were also noted during underground mapping of the Richard Allen mine west of Soldier Creek. Alteration along these shear zones is characterized by coarsely crystalline secondary muscovite rather than a propylitic assemblage. Similar alteration elsewhere in the study area has been dated as Cretaceous (approximately 70 Ma), as indicated in the section entitled "Geochronology of plutonic rocks". Because of poor exposure, none of these muscovite-bearing shear zones are recognizable at the surface.

DIKES

The andesitic to rhyolitic dikes of probable Eocene age have a pronounced northeast trend (Plate 1). This trend is common for dikes throughout the region, and reflects a northwest-southeast extensional regime during the Eocene. In contrast, dikes of pyroxene basalt probably correlative

to the Miocene Columbia River Basalt Group have north-northwest trends, much like the orientation of Columbia River Basalt feeder dikes in eastern Oregon and Washington. Thus, by Miocene time the extensional direction was oriented west-southwest-east-northeast. The northwesterly trends of the active(?) normal faults mentioned previously (e.g. Brush Canyon and Couch Summit faults) indicate that the direction of extension in the eastern Soldier Mountains has maintained a more or less west-southwest-east-northeast orientation since Miocene time.

GEOCHRONOLOGY OF PLUTONIC ROCKS

Previous radiometric dating in the region has been by the K-Ar method and is summarized by Criss and others (1982), Bennett and Knowles (1985), and Lewis and others (1987). Efforts to determine the crystallization ages of the Cretaceous plutons have been hampered by the effects of slow cooling, excess Ar in hornblende, and resetting during Eocene time. Dates by the K-Ar method from the Eocene plutons are more consistent than those of the Cretaceous rock units, but the geochronology of the region remains poorly known. Thermochronologic data to indicate how fast the Cretaceous rocks rocks cooled are also lacking. However, textural evidence presented in a previous section suggests a slow cooling rate for the Cretaceous plutons in the eastern part of the Soldier Mountains. Thus, all K-Ar and $^{40}Ar/^{39}Ar$ age determinations from these rocks have to be regarded as cooling ages, rather than crystallization ages. Because of the epizonal emplacement levels and relatively rapid cooling rates of the Eocene plutons, the cooling ages are probably within a few million years (or less?) of the crystallization ages.

Two 84 Ma K-Ar age determinations on biotite from the Hailey granodiorite unit (Berry and others, 1976; Lewis and others, 1987) are at present the best estimates of the cooling age of this unit, which crops out east of the study area. The coarse-grained hornblende-biotite granodiorite unit (Plate 1) is considered correlative to these rocks. Muscovite collected by W.E. Hall from a pegmatite in the biotite granodiorite unit 9 km east of the study area was dated at 76.4 $\pm$ 1.5 Ma (sample H23; Lewis and others, 1987). The younger date on the muscovite, relative to the 84 Ma biotite, cannot be attributed to differences in Ar blocking temperature because muscovite has a slightly higher blocking temperature than biotite (300 $\pm$ 30°C versus 280 $\pm$ 40°C, Harrison and McDougall, 1980; Snee, 1982; Snee and others,

1988). Assuming that post-Cretaceous Ar loss from these samples was negligible, the biotite granodiorite is either younger than the Hailey granodiorite unit (perhaps by as much as 8 Ma), or it cooled at a slower rate.

Previous workers obtained two K-Ar mineral dates on rocks of Eocene age from the eastern part of the Soldier Mountains. Criss and others (1982) obtained a 46.1 Ma date on biotite from the foliated hornblende-biotite granodiorite unit (sample RH85d), and W.E. Hall (pers. comm., 1984) obtained a 43.5 ± 1.3 Ma date from biotite in the same unit (sample P-87). Locations of these two samples are shown on Plate 2, and interpretation of the dates is given in Table 5.

TECHNIQUES AND RESULTS OF PRESENT STUDY

Samples for $^{40}Ar/^{39}Ar$ dating were collected by Larry Snee, Mick Kunk, and the author. Because hornblende has a relatively high Ar blocking temperature (530 ± 50°C, Harrison, 1981) an attempt was made to collect hornblende-bearing lithologies. Mineral separation and subsequent analytical work was carried out by Snee and Kunk, and by technicians under their supervision at U.S. Geological Survey laboratories in Reston, Virginia, and Denver, Colorado. Samples and standards were irradiated in a TRIGA reactor and isotopic ratios were measured with a mass spectrometer. Corrections were made for ^{40}Ar, ^{39}Ar, ^{37}Ar, and ^{36}Ar produced by irradiation, as well as for atmospheric ^{40}Ar. Details of the $^{40}Ar/^{39}Ar$ technique are given in Dalrymple and others (1981) and Snee and others (1988).

Results of the $^{40}Ar/^{39}Ar$ age determinations are presented in Figures 11 to 13. Errors shown in these figures represent 1 sigma confidence levels. Interpretations of individual mineral spectra are presented in Table 5. Data used to construct these figures are tabulated in Table 6, and sample localities are given on Plate 2.

Sample	Unit	Mineral	Result	Interpretation
RL169	Kgd	hb	steps up from 75 to 84 Ma	disturbed by Eocene event; upper "date" may approximate cooling age; sample was propylitized
		bt	arched release pattern 47-49 Ma	reflects Eocene resetting at about 47-48 Ma; arched pattern may indicate minor chlorite contaminant (L. Snee, pers. comm., 1988)
		K-spar	irregular release pattern 46-59 Ma	reflects partial resetting during Eocene time
RL171	Kgd	hb	steps up from about 61 to 73 Ma then decreases	severe Ar loss during Eocene time or at about 61 Ma; sample from within Worswick Creek fault system; cataclastic texture
		bt	arched release pattern mostly 49-51 Ma	reflects partial(?) Eocene resetting; arched pattern may indicate minor chlorite contaminant
RL168	Kgd	secondary musc	plateau at 70.3 ± 0.4 Ma	reflects Late Cretaceous alteration associated with cooling of Idaho batholith; qtz-musc alteration in selvages along fractures; local associated vein quartz
H23	Kgd	musc (pegmatite)	conventional K-Ar date of 76.4 ± 1.5 Ma	probable cooling age; collected by W.E. Hall (Lewis and others, 1987)
RL170	Tfgd	hb	slightly higher dates at either end of spectra	probably reflects excess Ar; "plateau" at 55.2 Ma is single heating step; field relations support contamination by Cretaceous biotite granodiorite; K-spar considered more reliable for age
		bt	plateau at 47.4 ± 0.2 Ma	cooling age of Tfgd unit, or reset by biotite-hornblende granodiorite unit
		K-spar	plateau at 48.0 ± 0.3 Ma	probable cooling age of Tfgd unit
P-87	Tfgd	bt	conventional K-Ar date of 43.5 ± 1.3 Ma	partial argon loss; probably is 47-48 Ma pluton; date from W.E. Hall (pers. comm., 1984)
RH85d	Tfgd	bt	conventional K-Ar date of 46.1 Ma	partial argon loss; probably is 47-48 Ma pluton; date from Criss and others, 1982

Kgd = biotite granodiorite unit; Tfgd = foliated hornblende-biotite granodiorite unit

Table 5. Interpretation of radiometric age determinations of plutonic rocks from the eastern part of the Soldier Mountains. Minerals: hb = hornblende; bt = biotite; K-spar = potassium feldspar; musc = muscovite.

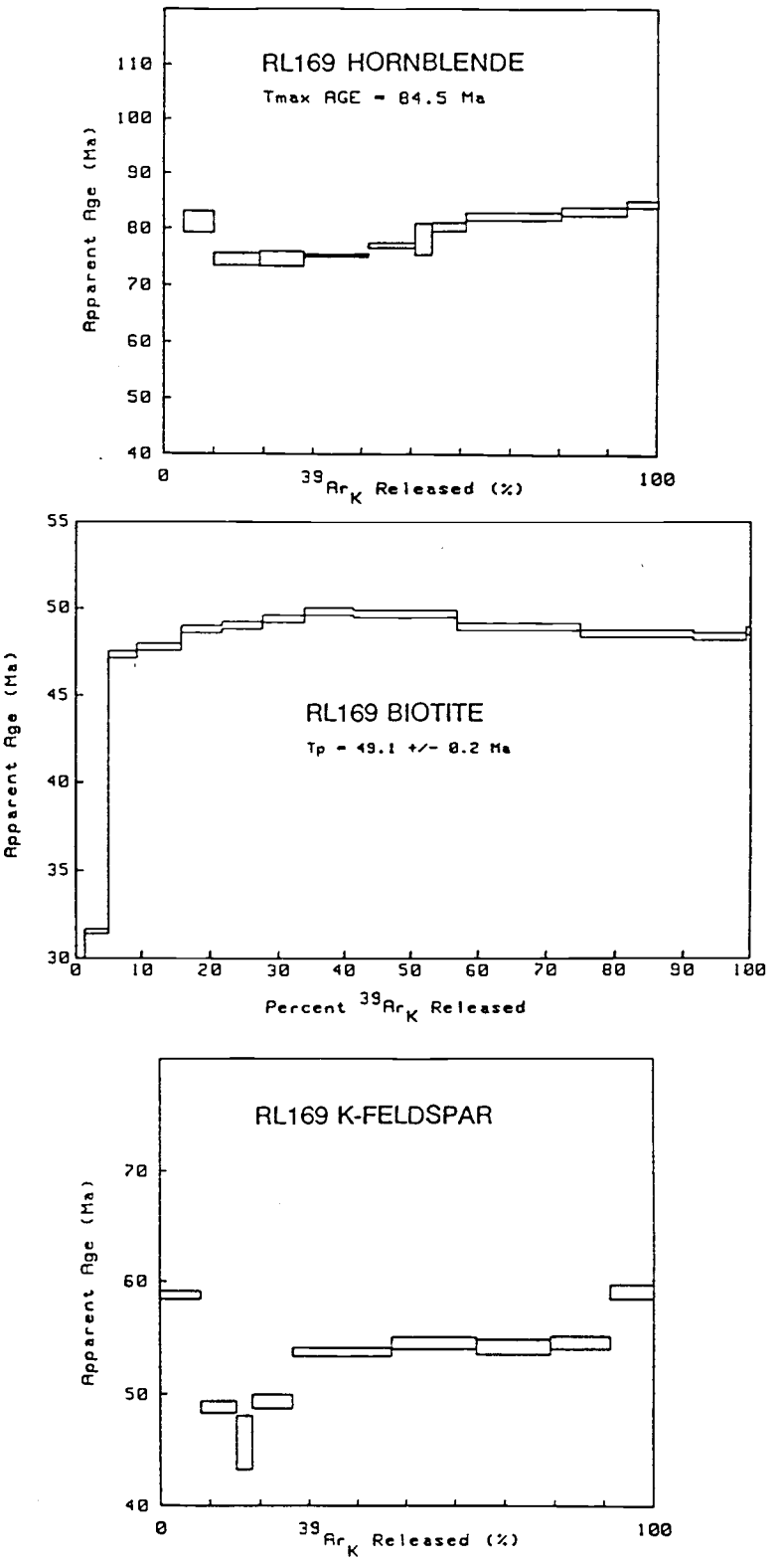

Figure 11. $^{40}Ar/^{39}Ar$ age spectra of hornblende, potassium feldspar, and biotite from sample RL169 of the biotite granodiorite unit.

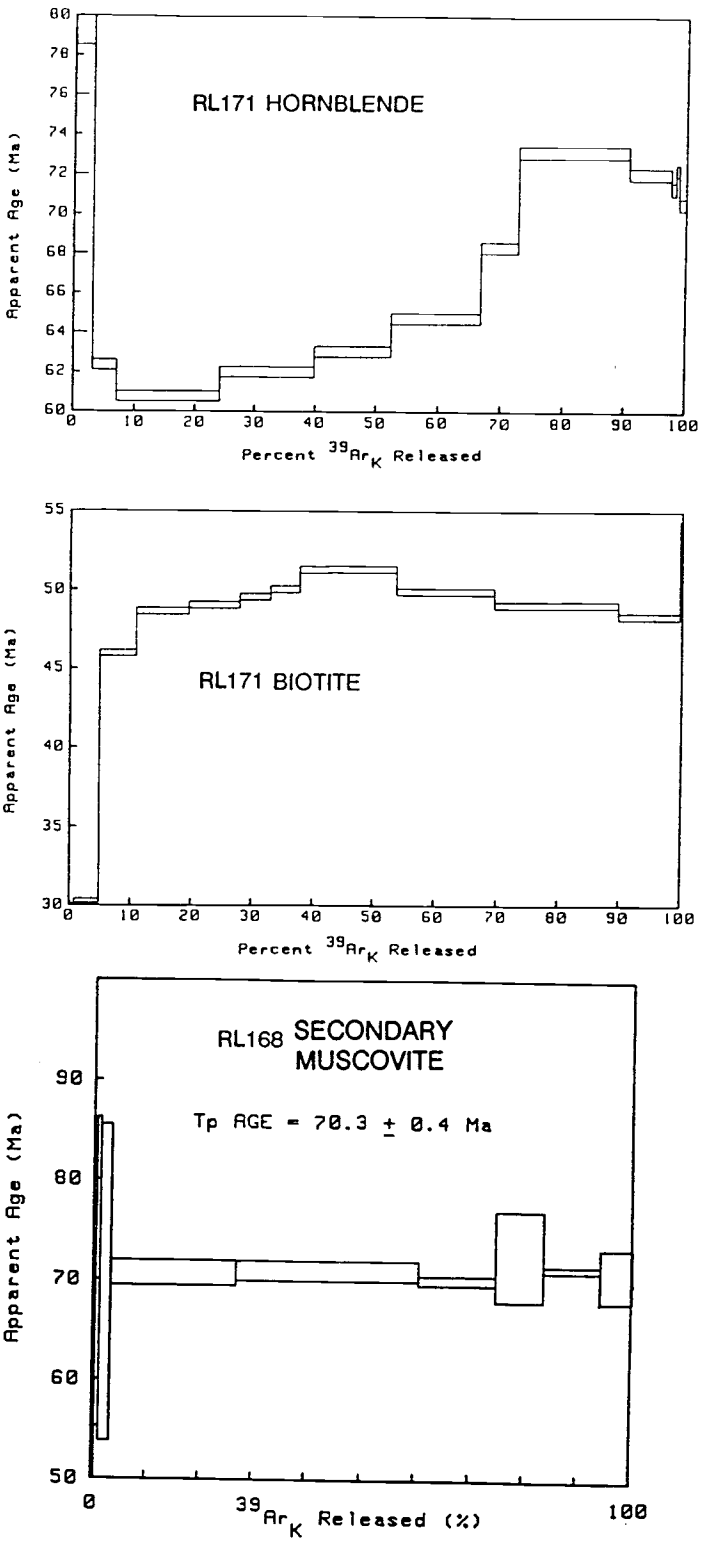

Figure 12. $^{40}Ar/^{39}Ar$ age spectra of hornblende and biotite from sample RL171 of the biotite granodiorite unit and secondary muscovite from sample RL168 of the biotite granodiorite unit.

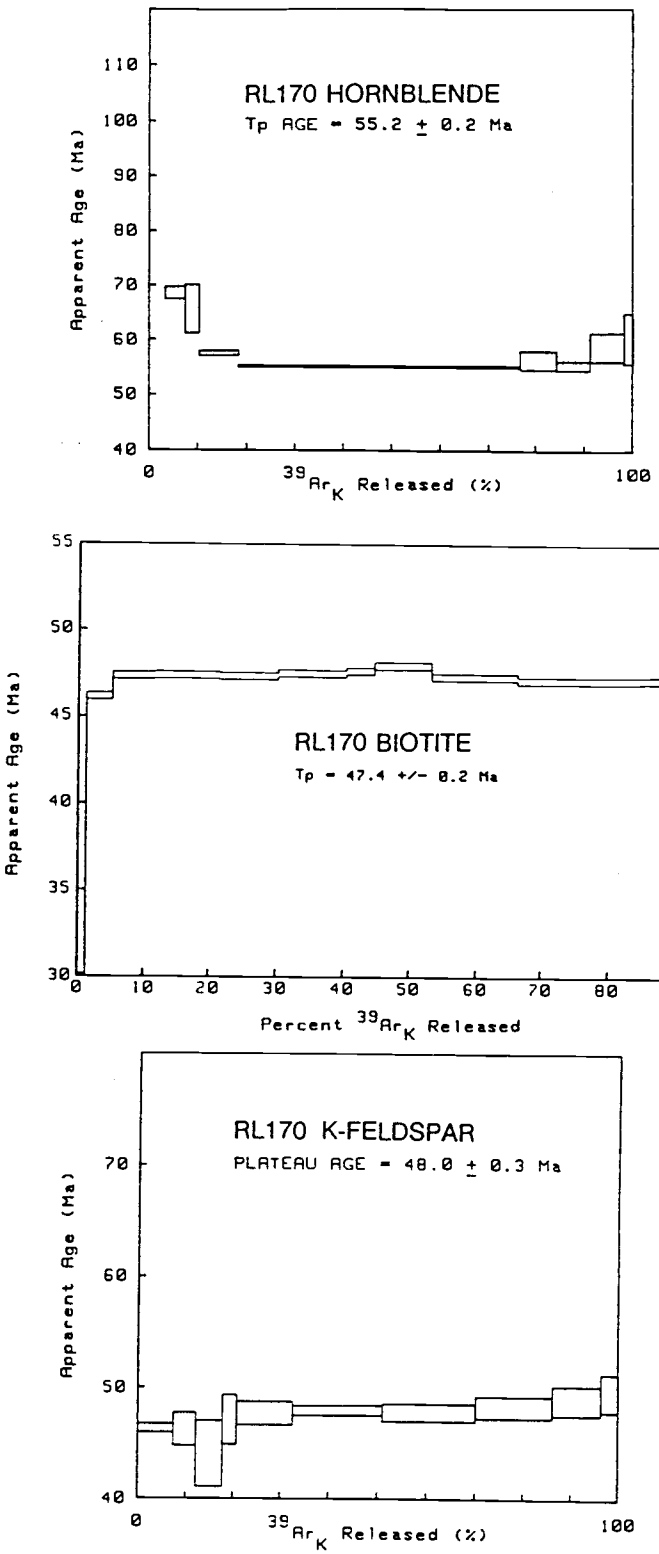

Figure 13. $^{40}Ar/^{39}Ar$ age spectra of hornblende, biotite, and potassium feldspar from sample RL170 of the biotite-hornblende granodiorite unit.

unit	sample no.	mineral	temp °C	$^{39}Ar_K$ %	apparent age Ma
Kgd	RL169	hornblende	850	3.9	135.1 ± 1.1
			950	6.0	81.2 ± 1.1
			1000	9.2	74.6 ± 0.7
			1025	9.0	74.7 ± 0.8
			1050	13.3	75.3 ± 0.4
			1075	9.4	77.1 ± 0.5
			1100	3.4	78.2 ± 1.5
			1150	6.8	80.4 ± 0.6
			1250	19.3	82.3 ± 0.6
			1350	13.3	83.2 ± 0.6
			1550	6.5	84.5 ± 0.5
			total gas		81.5
Kgd	RL169	biotite	500	1.3	9.2 ± 0.1
			600	3.7	31.5 ± 0.1
			650	4.3	47.3 ± 0.2
			700	6.5	47.8 ± 0.2
			750	5.9	48.8 ± 0.2
			800	5.9	49.0 ± 0.2
			850	6.3	49.4 ± 0.2
			900	7.4	49.8 ± 0.2
			950	15.6	49.7 ± 0.2
			1000	18.1	48.9 ± 0.2
			1050	16.5	48.6 ± 0.2
			1150	8.0	48.4 ± 0.2
			1300	0.7	48.7 ± 0.2
			total gas		47.7
Kgd	RL169	K-spar	450	8.2	58.7 ± 0.3
			750	7.1	48.8 ± 0.4
			850	3.1	45.6 ± 1.2
			950	8.1	49.3 ± 0.4
			1150	20.5	53.7 ± 0.3
			1250	17.2	54.5 ± 0.4
			1350	14.9	54.2 ± 0.4
			1450	12.1	54.6 ± 0.4
			1550	8.9	59.1 ± 0.4
			total gas		54.0
Kgd	RL171	hornblende	850	3.1	380.8 ± 1.5
			950	3.9	62.4 ± 0.3
			1000	17.1	60.8 ± 0.3
			1025	15.7	62.0 ± 0.3
			1050	12.6	63.1 ± 0.3
			1075	14.3	64.7 ± 0.3
			1100	6.0	68.3 ± 0.3
			1150	17.9	73.2 ± 0.3
			1200	6.9	72.0 ± 0.3
			1250	0.8	71.3 ± 0.3
			1300	0.5	72.3 ± 0.3
			1500	1.2	70.5 ± 0.3
			total gas		76.5
Kgd	RL171	biotite	500	0.8	18.4 ± 0.1
			600	4.0	30.3 ± 0.1
			650	6.0	46.0 ± 0.2
			700	8.7	48.6 ± 0.2
			750	8.4	49.0 ± 0.2
			800	5.1	49.6 ± 0.2

Kgd = biotite granodiorite unit

Table 6. $^{40}Ar/^{39}Ar$ age spectra of minerals from plutonic rocks in the eastern part of the Soldier Mountains.

unit	sample no.	mineral	temp °C	$^{39}Ar_K$ %	apparent age Ma	
Kgd	RL171	biotite	850	4.7	50.0 ± 0.2	
			900	4.5	51.3 ± 0.2	
			950	11.5	51.3 ± 0.2	
			1000	15.7	49.9 ± 0.2	
			1050	20.2	49.0 ± 0.2	
			1150	10.1	48.3 ± 0.2	
			1300	0.4	53.7 ± 0.8	
			total gas		48.3	
Kgd	RL168	secondary muscovite	350	0.4	31.1 ± 21.9	
			450	0.8	70.7 ± 7.8	
			650	2.0	69.6 ± 7.9	
			850	23.3	70.7 ± 0.7	
			950	33.9	70.9 ± 0.6	
			1000	14.1	70.0 ± 0.4	
			1050	9.0	72.5 ± 2.3	
			1150	10.6	71.2 ± 0.4	
			1350	5.9	70.5 ± 1.4	
			total gas		70.7	plateau age of 70.3 ± 0.4
Tfgd	RL170	hornblende	850	3.2	125.2 ± 1.8	
			950	4.2	68.6 ± 0.8	
			1000	2.9	65.6 ± 2.3	
			1050	8.1	57.5 ± 0.4	
			1150	58.3	55.1 ± 0.2	
			1200	7.6	56.3 ± 0.9	
			1250	6.9	55.3 ± 0.5	
			1350	7.0	58.7 ± 1.3	
			1450	1.9	60.3 ± 2.3	
			total gas		58.9	
Tfgd	RL170	biotite	500	1.2	29.2 ± 0.2	
			600	3.9	46.2 ± 0.2	
			650	6.2	47.4 ± 0.2	
			700	10.1	47.4 ± 0.2	
			750	8.7	47.3 ± 0.2	
			800	5.6	47.5 ± 0.2	
			850	4.6	47.5 ± 0.2	
			900	4.3	47.7 ± 0.2	
			950	8.5	48.0 ± 0.2	
			1000	13.1	47.3 ± 0.2	
			1050	18.7	47.1 ± 0.2	
			1150	15.1	47.2 ± 0.2	
			1300	0.1	42.1 ± 1.2	
			total gas		47.1	plateau age of 47.4 ± 0.2
Tfgd	RL170	K-spar	750	7.3	46.3 ± 0.2	
			850	4.8	46.2 ± 0.8	
			950	5.6	44.0 ± 1.5	
			1050	3.0	47.1 ± 1.1	
			1150	11.8	47.7 ± 0.5	
			1250	18.4	47.9 ± 0.2	
			1350	19.1	47.7 ± 0.4	
			1450	16.1	48.2 ± 0.5	
			1550	10.2	48.8 ± 0.7	
			1650	3.7	49.5 ± 0.9	
						plateau age of 48.0 ± 0.3

Kgd = biotite granodiorite unit; Tfgd = foliated hornblende-biotite granodiorite unit

Table 6 (continued). $^{40}Ar/^{39}Ar$ age spectra of minerals from plutonic rocks in the eastern part of the Soldier Mountains.

DISCUSSION

Ages of various plutonic phases of the Idaho batholith in the eastern part of the Soldier Mountains are, as elsewhere, not well constrained. A hornblende cooling age (time when hornblende reached the 530 ± 50°C blocking temperature) of 84 Ma for the biotite granodiorite unit is one interpretation. This interpretation is based on assignment of a reliable geologic meaning to the upper date (last amount of Ar released) of hornblende in RL169 (Fig. 11). It is also possible that the upper date is not geologically significant. If Ar loss was extensive, the upper date is only a minimum cooling age. A further complication involves possible excess Ar in heating steps at higher temperatures. Excess Ar in hornblende has been a problem in the region, and an Ar loss pattern superimposed on that caused by excess Ar could render the upper date meaningless. If the tentative assumption of a 84 Ma cooling age is correct, then crystallization of the biotite granodiorite may have only post-dated crystallization of the Hailey granodiorite unit (with its 84 Ma biotite cooling age) by a few million years. Assuming Ar was not lost from the muscovite in the pegmatite in the biotite granodiorite unit (sample H23), the biotite granodiorite unit cooled below the muscovite blocking temperature (300 ± 30°C) at about 76 Ma. The above interpretations are speculative, as undisturbed spectra will need to be obtained from these rocks for more reliable dates.

Quartz-muscovite alteration along fractures at about 70 Ma marks the end of Cretaceous activity in the eastern Soldier Mountains. The older (76 Ma) K-Ar age from muscovite in a pegmatite in the same unit suggests that the 70 Ma date is a crystallization age, and that the rocks had cooled below the blocking temperature of muscovite by the time alteration had taken place. Similar types of alteration apparently continued sporadically over the next 13 Ma both west and north of the study area (L. Snee, pers. comm.,

1988).

Disturbance of Ar systematics in Cretaceous rocks by Eocene plutons is clearly demonstrated. Hornblende was the least affected, and potassium feldspar more so. Biotite was the most strongly affected, and reset to Eocene ages. Youngest "dates" (i.e. lowest dates in spectra) of disturbed hornblendes in RL169 (75 Ma) and RL171 (61 Ma) might reflect only partial Ar loss and, thus, would not be geologically significant. However, the 61 Ma "date" roughly corresponds to mineralization ages between 57 and 63 Ma (from $^{40}Ar/^{39}Ar$ age-spectra plateaus on sericite) at the Ida Elmore and Hermada mines northwest of the study area (L. Snee, pers. comm., 1988). Thus, two thermal events (Paleocene and Eocene in age) cannot be dismissed.

Eocene intrusive activity in the study area apparently began at about 47 to 48 Ma. The older (55.2 Ma) date on hornblende from RL170 is thought to be the result of excess Ar. However, additional samples of hornblende from this unit need to be analyzed to verify this interpretation. Dates have not been obtained on the younger Eocene intrusive units. Based on ages of comparable rocks elsewhere in the region (Criss and others, 1982; Bennett and Knowles, 1985), Eocene plutonism probably continued for another 2 to 5 Ma.

CHEMICAL CHARACTERISTICS OF PLUTONIC ROCKS

The analysis of 34 whole-rock samples for this study represents a significant addition to the data base for plutonic rocks of south-central Idaho, particularly with regard to trace elements. When combined with field relations, four distinct geochemical suites of plutonic rocks are recognized: two of Cretaceous age and two of Eocene age. It can be demonstrated that each suite had a different parental composition, and that these compositions reflect differences in source regions. The chemical data are further used to constrain hypotheses that explain the development of within-suite variations.

METHODS

Approximately 1 kg of rock was collected at each sample site and later pulverized in a porcelain-lined jaw crusher to less than 5 mm. One fourth of this material was run though a porcelain-lined shatterbox to obtain minus 120 mesh powder for analysis. Pairs of duplicate samples from four outcrops were analyzed for major-element oxides, and, as indicated in Table 7, each pair yielded similar results.

Major-element oxides were determined using X-ray fluorescence spectroscopy (XRF) at U.S. Geological Survey laboratories in Denver, Colorado, by personnel under the direction of J. Taggart. Samples RL073 and RL167 were analyzed at the same facility by P. Briggs using inductively-coupled plasma spectroscopy for Ba, Sr, and Zr, and atomic-absorption spectroscopy for Rb. Energy-dispersive XRF methods by J. Evans (U.S. Geological Survey, Reston, Virginia) were utilized for Rb, Sr, Nb, Y, and Zr determinations of the remainder of the samples. Details of all of these methods are given in Baedecker (1987). Twelve boron determinations (by neutron activation methods) were provided by W.P. Leeman (pers. comm., 1989).

Analyses of duplicate whole-rock samples

	RL219A	RL219B	RL309A	RL309B	RL322A	RL322B	RL323A	RL323B
	major-element oxides in weight percent							
SiO_2	68.6	68.7	64.7	64.9	67.6	66.9	67.5	67.5
TiO_2	0.43	0.43	0.73	0.72	0.56	0.57	0.53	0.52
Al_2O_3	15.7	15.6	16.5	16.4	15.7	15.8	15.2	15.2
Fe_2O_3	1.22	1.39	1.91	1.72	1.63	3.50*	1.70	3.16*
FeO	1.40	1.24	2.25	2.15	1.60	--	1.31	--
MnO	0.03	0.03	0.06	0.06	0.04	0.04	0.04	0.04
MgO	0.88	0.86	1.69	1.62	1.04	1.29	1.11	1.17
CaO	3.13	3.11	4.59	4.55	3.56	3.53	3.16	3.15
Na_2O	3.54	3.60	3.73	3.76	3.55	3.64	4.28	4.46
K_2O	3.44	3.25	2.46	2.35	2.94	3.08	3.00	3.01
P_2O_5	0.14	0.14	0.24	0.23	0.19	0.21	0.17	0.18
H_2O^+	0.54	0.54	0.66	0.55	0.69	0.71**	0.95	1.11**
H_2O^-	0.15	0.31	<0.05	0.22	0.10	--	0.18	--
CO_2	0.08	0.08	<0.01	0.02	<0.01	--	0.03	--
total	99.3	99.3	99.6	99.3	99.2	99.3	99.2	99.5
	trace elements in parts per million							
Ba	--	--	--	1270	1590	--	1540	--
Nb	--	15	--	19	18	--	16	--
Rb	--	86	--	77	86	--	76	--
Sr	--	778	--	752	775	--	690	--
Zr	--	239	--	223	234	--	229	--
Y	--	8	--	13	11	--	11	--

*Total Fe as Fe_2O_3
**Loss on ignition at 900°C

Analyses of duplicate powders from one whole-rock sample

	RL309C	RL309D
	trace elements in parts per million	
Sc	7.8	7.9
Cr	10	11
Co	6.7	6.8
Sb	0.15	--
Cs	1.6	1.6
Ba	1270	1270
La	70	66
Ce	148	141
Nd	37	42
Sm	7.06	6.98
Eu	1.70	1.73
Tb	0.70	0.75
Yb	1.46	1.49
Lu	0.18	0.16
Hf	6.7	6.6
Ta	1.5	1.5
Th	15	14
U	2.2	2.2

Table 7. Results of analysis of duplicate whole-rock samples and of duplicate powders from a single sample.

The remainder of the trace elements were determined by instrumental neutron activation analysis (INAA) at Oregon State University. Samples were irradiated along with U.S. Bureau of Standards SRM1633a (fly ash) and an in-house standard equivalent to the U.S. Geological Survey's BCR-1 (Columbia River Basalt). Gamma-ray spectral analyses were run using Ge(Li) detectors one week after irradiation (for short counts) and again one month after irradiation (for long counts). Computer-assisted data reduction was performed using EG&G ORTEC software. Long counts on one detector yielded systematically lower values (about 5 percent) for Fe and Sc when compared to short counts for the same elements, and all elements determined on this detector were adjusted upward by 5 percent. Reason for the discrepancy is unknown, but may reflect counting geometry errors. Duplicate powders of one rock (RL309C and RL309D) were analyzed, and the results are reported in Table 7. Relative differences between the two duplicate powders, combined with error determinations from repeated measurements of standards by workers at the reactor, indicate that most elements are known to within about 5 to 10 percent.

Sodium values determined by INAA were higher by 4 to 9 percent than values determined from the same samples by XRF methods. The lower XRF values are probably the result of error introduced by calibration over a wide SiO_2 range (J. Taggart, pers. comm., 1988). Because INAA values are only available on a limited number of samples, all reported Na_2O data are from XRF analysis, despite the systematic error.

CRETACEOUS PLUTONIC ROCKS

Major- and trace-element determinations of unaltered and weakly altered (mostly propylitized) rock samples are in Table 8. Sample localities are on Plate 2. The weak alteration did not measurably affect major- and trace-element compositions, whereas moderately and highly altered rocks,

	SODIC SUITE						
	Hornblende-biotite granodiorite unit		Biotite granodiorite unit				
	RL278	RL309	RL241	RL266[1]	RL244	RL263	RL275[2]
	major-element oxides in weight percent						
SiO_2	64.8	64.8	68.3	68.9	68.1	70.0	66.0
TiO_2	0.71	0.73	0.52	0.33	0.57	0.36	0.76
Al_2O_3	16.5	16.5	15.5	15.9	15.6	15.5	16.4
Fe_2O_3	1.90	1.82	1.23	1.23	1.58	1.10	1.61
FeO	2.15	2.20	1.50	1.01	1.67	1.01	2.02
MnO	0.07	0.06	0.04	0.03	0.04	0.04	0.05
MgO	1.67	1.66	0.96	0.56	1.04	0.65	1.34
CaO	4.49	4.57	3.22	2.56	3.47	2.48	4.12
Na_2O	3.92	3.75	3.48	3.83	3.57	3.76	3.67
K_2O	2.18	2.41	3.22	4.09	2.97	3.64	2.58
P_2O_5	0.23	0.24	0.17	0.10	0.19	0.12	0.24
H_2O^+	0.71**	0.61	0.57	0.60**	0.56**	0.38	0.62
H_2O^-	–	0.14	0.21	–	–	0.20	0.20
CO_2	0.01	0.01	<0.01	<0.01	<0.01	<0.01	<0.01
total	99.3	99.5	98.9	99.2	99.4	99.3	99.6
A/CNK***	0.97	0.96	1.03	1.03	1.01	1.06	1.00
SG#	2.69	2.71	2.65	–	2.64	2.62	2.66
	trace elements in parts per million						
Sc	7.9	7.9	5.8	2.5	–	–	8.5
Cr	12	11	3.8	3.5	–	–	5.8
Co	6.7	6.8	3.6	2.1	–	–	4.9
Rb	89	77	100	113	98	131	99
Sr	805	752	665	665	715	688	719
Y	19	13	8	15	10	7	15
Zr	232	223	175	230	242	195	223
Nb	24	19	17	18	20	17	21
Sb	0.18	0.15	0.22	0.15	–	–	0.18
Cs	1.8	1.6	2.0	1.1	–	–	2.0
Ba	1510	1270	1410	1470	–	–	1280
La	59	68	50	61	–	–	51
Ce	120	150	110	130	–	–	120
Nd	39	40	28	40	–	–	42
Sm	6.7	7.0	5.2	6.5	–	–	7.5
Eu	1.6	1.7	1.2	1.6	–	–	1.7
Tb	0.63	0.73	0.48	0.63	–	–	0.71
Yb	1.4	1.5	1.0	1.2	–	–	1.6
Lu	0.16	0.17	0.13	0.16	–	–	0.18
Hf	6.3	6.7	5.3	6.6	–	–	6.9
Ta	1.3	1.5	1.1	1.7	–	–	2.0
Th	13	15	13	18	–	–	12
U	2.4	2.2	2.9	2.1	–	–	3.1
B	–	2.7	5.9	3.4	–	–	–

[1] Sample probably has undergone potassic metasomatism
[2] Sample has undergone weak propylitic alteration
** Loss on ignition at 900°C
*** Molecular $Al_2O_3/(CaO+Na_2O+K_2O)$
# Specific gravity

Table 8. Major- and trace-element analyses of Cretaceous plutonic rocks from the eastern part of the Soldier Mountains. Analysts: J. Taggart, A. Bartel, D. Siems, C. Papp, E. Brandt, N. Elsheimer, and J. Evans.

	SODIC SUITE						POTASSIC SUITE[4]	
	biotite granodiorite unit[3]							
	RL210	RL225	RL219	RL249	RL279	RL230	RL252	RL452
	major-element oxides in weight percent							
SiO_2	68.7	67.0	68.7	68.4	69.1	69.8	65.0	68.0
TiO_2	0.54	0.68	0.43	0.45	0.42	0.39	0.67	0.49
Al_2O_3	15.5	16.0	15.7	15.7	15.2	15.2	15.7	15.3
Fe_2O_3	1.37	1.31	1.31	1.58	1.20	1.30	2.10	1.46
FeO	1.55	1.90	1.32	1.30	1.19	1.12	2.19	1.57
MnO	0.05	0.04	0.03	0.05	0.03	0.04	0.07	0.05
MgO	1.01	1.12	0.87	0.85	0.82	0.71	2.24	1.35
CaO	3.57	3.90	3.12	2.95	2.99	2.71	4.50	3.66
Na_2O	3.56	3.61	3.57	3.70	3.31	3.66	3.30	3.12
K_2O	2.69	2.52	3.35	3.05	3.43	3.62	2.78	3.54
P_2O_5	0.16	0.23	0.14	0.15	0.14	0.14	0.22	0.16
H_2O^+	0.64	0.56	0.54	0.73	0.55	0.60**	0.72	0.87
H_2O^-	0.18	0.27	0.21	0.21	0.16	–	0.11	0.11
CO_2	0.03	<0.01	0.08	<0.01	0.01	0.01	0.09	0.09
total	99.6	99.2	99.4	99.1	98.6	99.3	99.7	99.8
A/CNK***	1.01	1.01	1.03	1.06	1.04	1.02	0.94	0.98
SG#	2.65	2.66	2.64	2.63	2.64	2.64	2.70	–
	trace elements in parts per million							
Sc	4.2	4.5	–	–	–	–	10.6	6.4
Cr	6.1	5.0	–	–	–	–	42	9.7
Co	4.1	4.1	–	–	–	–	9.0	5.2
Rb	111	89	86	89	105	108	122	110
Sr	727	745	778	867	745	735	588	533
Y	16	14	8	11	10	14	15	8
Zr	239	208	239	233	184	211	162	138
Nb	23	20	15	17	17	18	21	16
Sb	0.09	0.18	–	–	–	–	0.28	0.23
Cs	2.1	1.6	–	–	–	–	3.4	2.2
Ba	1370	1390	–	–	–	–	912	943
La	65	56	–	–	–	–	35	41
Ce	140	120	–	–	–	–	71	78
Nd	39	40	–	–	–	–	24	21
Sm	5.9	7.1	–	–	–	–	4.2	4.2
Eu	1.4	1.6	–	–	–	–	1.1	1.0
Tb	0.53	0.66	–	–	–	–	0.48	0.38
Yb	1.5	1.5	–	–	–	–	1.4	1.4
Lu	0.20	0.17	–	–	–	–	0.17	0.17
Hf	6.7	6.2	–	–	–	–	4.9	4.5
Ta	2.5	1.7	–	–	–	–	1.2	1.6
Th	15	12	–	–	–	–	15	18
U	2.8	2.9	–	–	–	–	4.3	3.0
B	–	–	–	–	–	3.0	–	9.2

[3] Samples have undergone weak propylitization except RL230 which underwent weak potassic alteration
[4] RL252 = coarse-grained hornblende-biotite granodiorite; RL452 = Hailey granodiorite (30 km east of study area)
** Loss on ignition at 900°C
*** Molecular $Al_2O_3/(CaO+Na_2O+K_2O)$
# Specific gravity

Table 8 (continued). Major- and trace-element analyses of Cretaceous plutonic rocks from the eastern part of the Soldier Mountains.

discussed in a following section, were chemically modified.

Major-element variation

Harker variation diagrams of samples of unaltered and weakly altered Cretaceous plutonic rocks are depicted in Figure 14. Data from this study have been supplemented with samples from nearby quadrangles (Lewis and others, 1987; and unpublished data), particularly with regard to the coarse-grained hornblende biotite granodiorite unit. Data from one sample of this unit (RL252) have been included with eight samples of the Hailey granodiorite unit (exposed to the east), which has similar chemical and mineralogical characteristics.

Values of the major-element oxides define two distinct geochemical suites. One suite consists of the hornblende-biotite granodiorite and biotite granodiorite units, which have high Al_2O_3 and Na_2O contents (at a given SiO_2 value) when compared to the coarse-grained hornblende-biotite granodiorite and Hailey granodiorite. The latter have higher K_2O, MgO, and possibly FeO* (total Fe as FeO) contents. Both suites have similar concentrations of TiO_2, CaO, P_2O_5, and $Na_2O + K_2O$.

Although there is some scatter, major oxides vary regularly with SiO_2. An exception is sample RL266 (shown as a half-filled circle on Fig. 14), which contains numerous inclusion-rich potassium feldspar phenocrysts. It has an unusually high K_2O content (4.09 percent) for the biotite granodiorite unit, and the highest $Na_2O + K_2O$ value (7.92 percent) for any Cretaceous rock analyzed. In addition, Al_2O_3, TiO_2, and MgO fall off the general trend of the biotite granodiorite unit. These deviations may refect local late-stage metasomatic effects and related growth of potassium feldspar phenocrysts. Similar metasomatic effects involving growth of potassium feldspar phenocrysts (megacrysts) have been described within the batholith to the

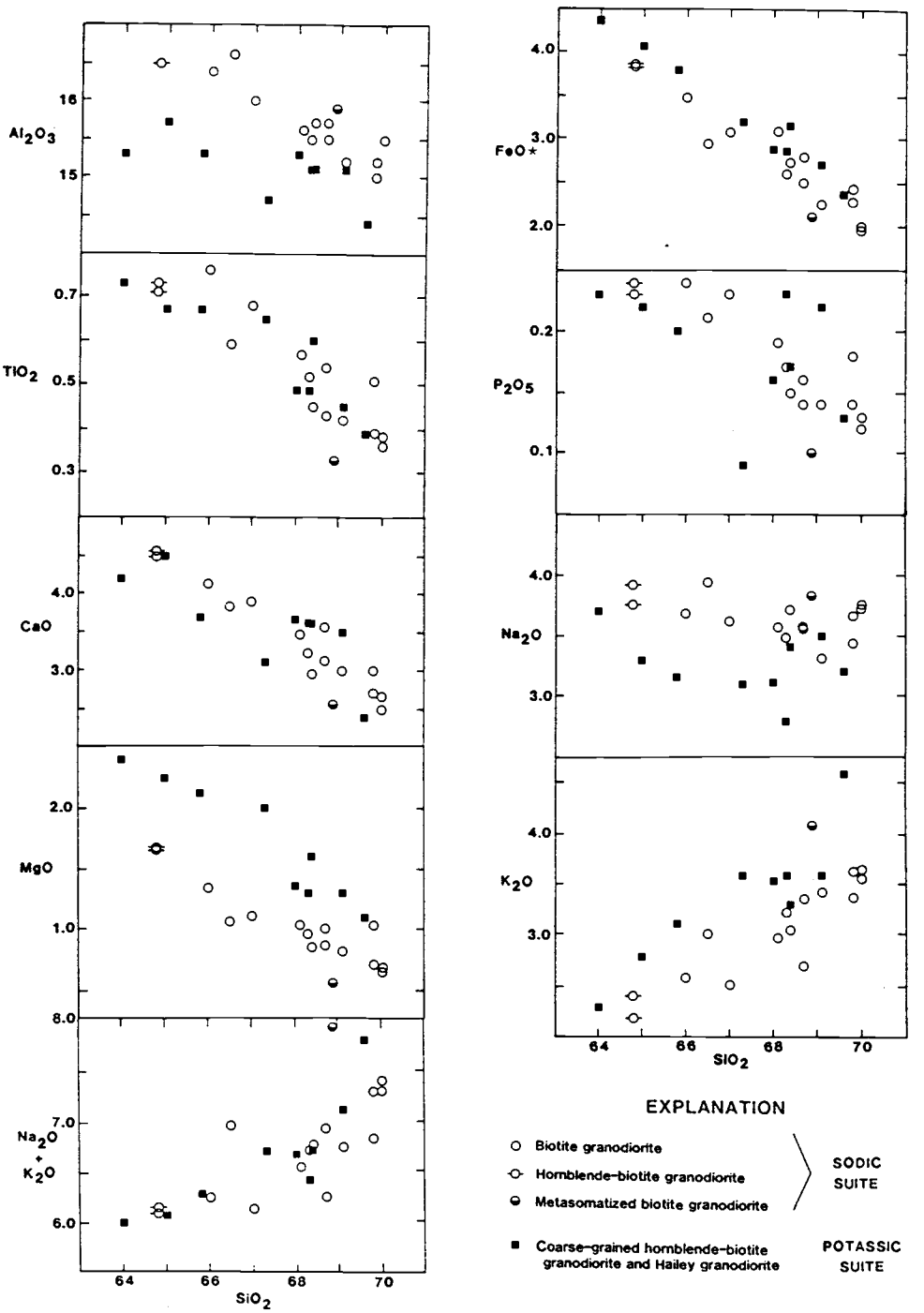

Figure 14. Harker plots of major-element oxides versus silica for plutonic rocks of Cretaceous age from the southeastern part of the Idaho batholith. Values are in weight percent.

north (Hyndman, 1984; Lewis and others, 1987), although they have not been characterized chemically. The preliminary results presented here suggest that high $Na_2O + K_2O$ may prove to be a useful discriminant in recognizing metasomatized rocks in the batholith. Wide scatter of K_2O and Na_2O values for the data set as a whole reflect the mobility of alkalies in plutonic environments.

Although only two samples of hornblende-biotite granodiorite were analyzed, they lie on the extension of the trend defined by the biotite granodiorite. The smooth transition suggests a common parent magma, as is the gradational nature of the contacts between the two units in the field. However, isotopic data presented below indicate a marked difference in ϵ_{Nd} values. Because both units are relatively enriched in Na they will be referred to as the "sodic suite". The coarse-grained biotite granodiorite and Hailey granodiorite are enriched in K, and will be referred to as the "potassic suite". As discussed previously, both suites are similar in age, but have not been precisely dated. The potassic suite is either older (possibly by as much as 8 Ma), or was emplaced at shallower levels and cooled more rapidly than the sodic suite.

The most distinctive petrographic feature of the potassic suite is the presence of thick subhedral books of biotite, which contrast with the small anhedral books present in the sodic suite. The higher K content of the magmas of the potassic suite may have stabilized biotite relatively early in the crystallization sequence. Alternatively, the potassic suite magmas may have had a higher water content which also would have brought about early biotite crystallization.

The existence of both a sodic and potassic suite in the Late Cretaceous Boulder batholith of Montana was recognized by Tilling (1973). Tilling referred to these contemporaneous suites as the "sodic series" and the "main series", respectively. Rocks in the Bitterroot and Atlanta lobes of

the Idaho batholith have been likened to the sodic series (Hyndman, 1983; Lewis and others, 1987) and until this study the main series had no known analogues in the Idaho batholith. Although the potassic suite is volumetrically minor in the Idaho batholith, in the Boulder batholith the bulk of the rocks belong to the potassic suite, the largest pluton of which is the Butte Quartz Monzonite.

The sodic suite in the study area is metaluminous to weakly peraluminous, with molecular $Al_2O_3/(CaO + Na_2O + K_2O)$ values of 0.96 to 1.06 (A/CNK in Table 8). The potassic suite is slightly less aluminous on average (A/CNK = 0.94-1.00; Table 8, and Lewis and others, 1987). Both are less aluminous than average values of biotite granodiorite in the central part of the Atlanta lobe (A/CNK mostly 1.05-1.13, Lewis and others, 1987).

Main-phase biotite granodiorites and two-mica granites of the Idaho batholith are transitional between I- and S-type granites of Chappell and White (1974), and, as noted by Hyndman (1984), and Lewis and others (1987), this classification scheme is not useful in categorizing these units. The metaluminous composition of the two suites in the study area indicates they are more I-type than S-type, but the exact nature of the protoliths remains unclear.

Trace-element variation

Trace-element contents of the sodic and potassic suites of this study also differ (Table 8 and Figures 15, 16, and 17). For a given SiO_2 content the sodic suite is enriched relative to the potassic suite in Ba, Sr, light rare earth elements (LREE), Hf, and, in all but one sample, Zr. The potassic suite tends to be enriched in Rb, and, although data are limited, concentrations of Sc, Cr, Co, Sb, Cs, U, and B are higher at a given SiO_2 value in this suite than in the sodic suite. The two suites have similar values for heavy rare earth elements (HREE), Y, Nb, and Ta.

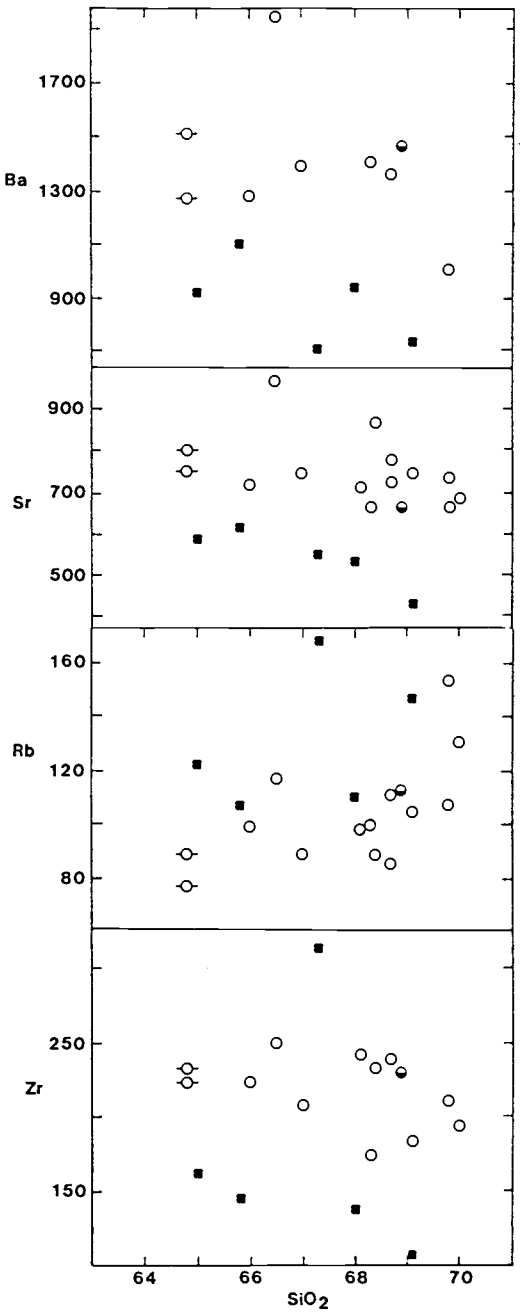

Figure 15. Plots of Ba, Sr, Rb, and Zr versus silica for plutonic rocks of Cretaceous age from the southeastern part of the Idaho batholith. Symbols are the same as in Figure 14. Values in parts per million.

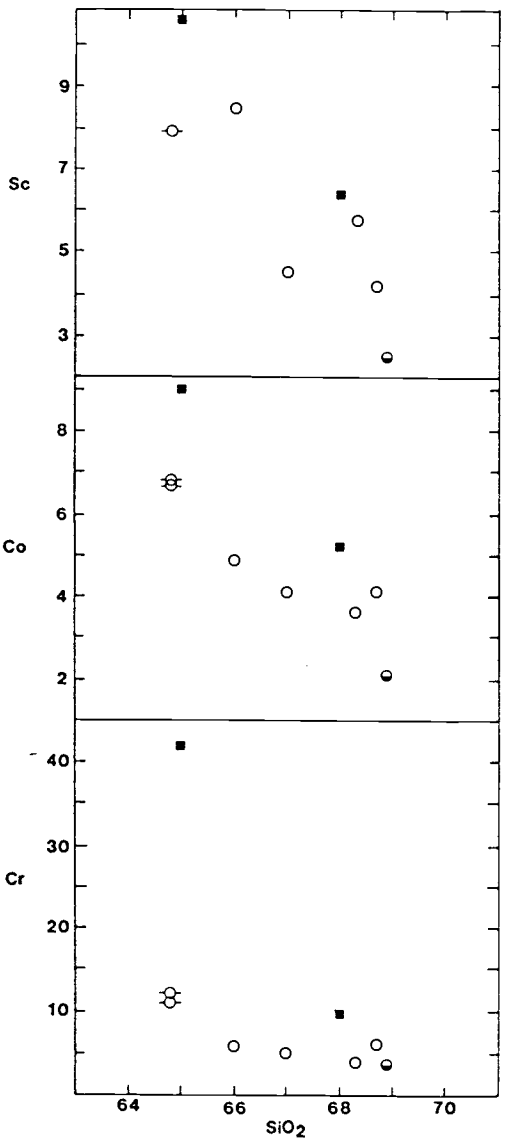

Figure 16. Plots of Sc, Co, and Cr versus silica for plutonic rocks of Cretaceous age from the southeastern part of the Idaho batholith. Values are in parts per million. Symbols are the same as in Figure 14.

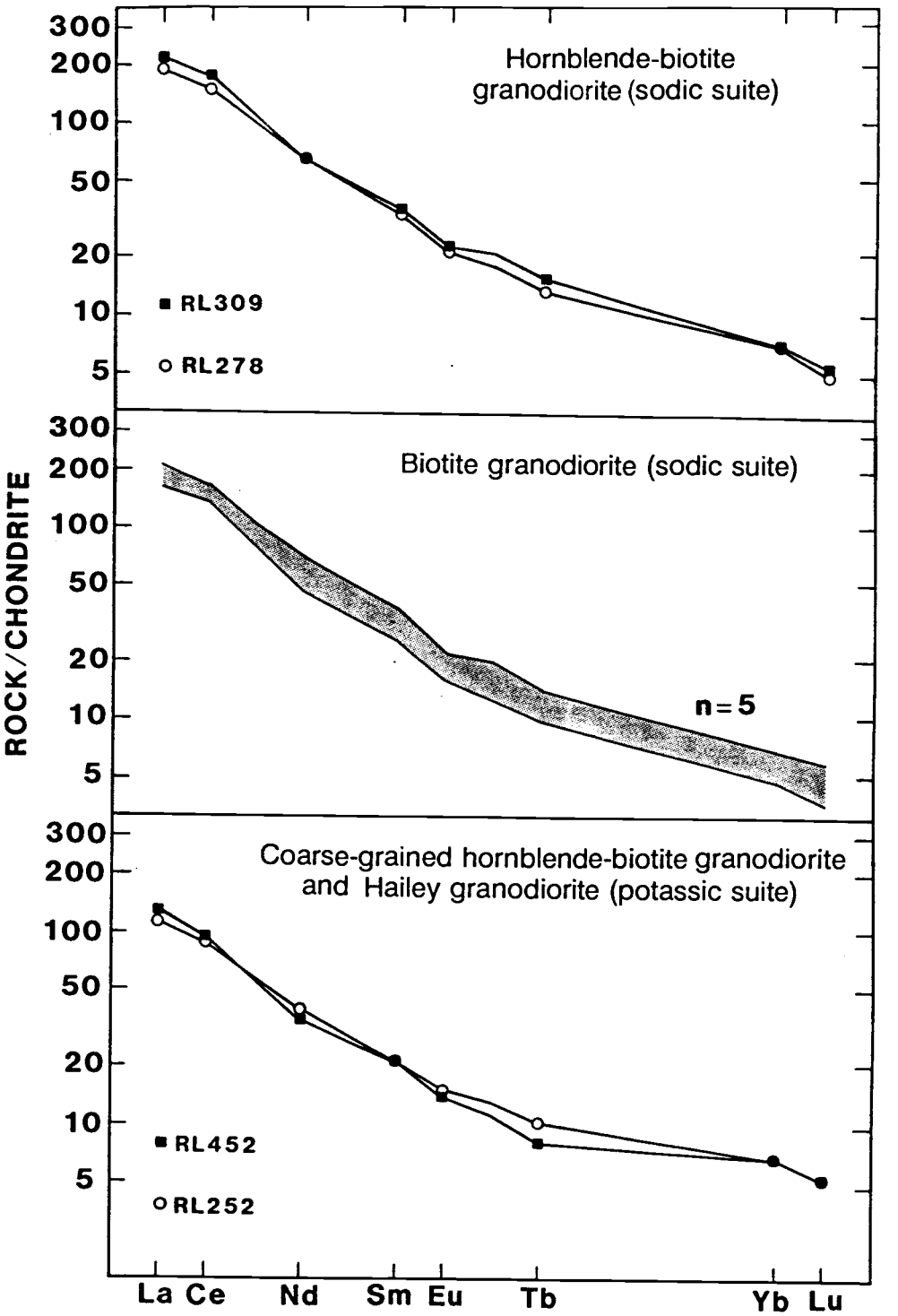

Figure 17. Chondrite-normalized plots of rare-earth element abundances for plutonic rocks of the southeastern part of the Idaho batholith. Chondrite values used for normalization are from Anders and Ebihara (1982).

Concentrations of Th are variable, but they do reach high values in some rocks of the potassic suite.

The trace-element data presented here are similar to the results of Tilling (1973) who reported higher Ba and Sr contents in the sodic series of the Boulder batholith, and higher Rb and U + Th contents in the main series. In addition to the work of Tilling (1973), Noyes and others (1983) have recognized nearly adjacent coeval plutons in the Sierra Nevada batholith with potassic and sodic affinities. As in the Boulder and Idaho batholiths, the Na-rich suite (Red Lake pluton) of Noyes and others (1983) is enriched in Sr and Ba, and depleted in Rb, U and Th. Concentrations of Ta and Cs are also lower in these rocks relative to their K-rich suite (Eagle Peak pluton and Mount Givens granodiorite).

Tilling (1973) attributed the differences in the two suites to differences in source region. He hypothesized that the rocks depleted in K, Rb, and U + Th (sodic series) came from one or more sources at a level deeper than that of the main series. This vertical variation was attributed to decreases in these elements with increasing metamorphic grade (or depth). The source for both series was thought to be in the lower crust or upper mantle. A similar view was held by Noyes and others (1983), who argued for a depleted lower crustal source for the sodic suite. The close spatial and temporal relations between respective suites in Montana and California was put forth as evidence for vertical rather than lateral (or temporal) variation in source region. The ages of the two Idaho suites are not well known, but the more mafic composition (higher MgO + FeO) of the potassic suite suggests that it is not an early derived melt from the same source that gave rise to the sodic suite.

A relatively depleted source area for the sodic suite explains many of the differences between the two Cretaceous rock suites. As shown by Heier (1973) and Tarney and Windley (1977) the large-ion lithophile (LIL) elements (K,

Rb, Cs, Th, and U) are typically depleted in granulites relative to lower-grade metamorphic rocks, although this need not always be the case (e.g. Rudnick and others, 1985). In addition to low K, Rb, Cs and U, the sodic suite has low boron contents (2.7-5.9 ppm), which suggest derivation from a depleted source area. Boron is one of the most mobile elements, and generally decreases in abundance with increasing degrees of metamorphism. Granulite xenoliths from Snake River Plain lavas contain 3 ppm or less boron (W.P. Leeman, pers. comm., 1989). The one boron determination for the potassic suite is higher (9.2 ppm) than those from the sodic suite, consistent with a source relatively less depleted in LIL elements.

It is also likely that protolith differences existed prior to any enrichment or depletion by metamorphism, as suggested by the more mafic composition of the potassic suite. This is in contrast to the findings of Tilling (1973) and Noyes and others (1983), who do not report differences in Mg or Fe between their K-rich and Na-rich suites. The higher concentrations of Al, LREE, and Zr in the sodic suite may also result from original protolith differences, or they may have been enriched during mobilization of the LIL elements. Although relative depletions and enrichment of LIL elements can be demonstrated, absolute direction of element mobility is not known. Thus, the source of the potassic suite may have undergone enrichment, or the source of the sodic suite depletion, with respect to these elements.

As with the studies in the Boulder and Sierra Nevada batholiths, the more depleted source for the sodic suite is assumed to be at deeper levels. The argument for vertical rather than lateral variation is not as strong in the Idaho batholith because the potassic suite is largely exposed in the extreme southeastern part of the batholith. However, if the small body of coarse-grained hornblende-biotite granodiorite north of Camas Prairie (Fig. 7; Plate 1) belongs to

the potassic suite (it is similar petrographically, but has not been chemically analyzed), then the potassic suite is not laterally restricted. This would imply a vertical rather than lateral variation in source area characteristics.

Within-suite variation

Variation within the Cretaceous rock suites is not dramatic. Both have a relatively restricted range of SiO_2 content (64-70 percent), and show a modest decrease in most major-element oxides with increasing SiO_2 (Fig. 14). At the present sample density, spatial control on chemical content is not evident within either suite. Concentrations of FeO*, MgO, and TiO_2 show the most pronounced decrease (with increasing SiO_2), and may indicate fractionation of hornblende or magnetite. Decreases in Sc, Co, and Cr can be accounted for by crystal fractionation of small amounts (a few percent) of these minerals.

The term "crystal fractionation" is used here to indicate segregation of minerals, but the crystals need not have been removed (segregated) from the system. This is in contrast to Rayleigh crystal fractionation, whereby the crystals are entirely removed from the system. Rocks with obvious cumulate texture are lacking, as is common in granitic bodies. However, because of viscosity constraints in silicic magmas it is likely that any removal of crystals was not an efficient process. Thus, the rocks sampled probably reflect magmas variably enriched and depleted in crystals and thus constituent elements, rather than "melts" along a liquid line of descent (see discussions by McCarthy and Hasty, 1976; Simmons and Hedge, 1978; and Cullers and Graf, 1984). It is assumed then that the sample set represents the entire range of magma compositions (crystals plus melt) that developed. Consequently, the parent magma would have had a composition somewhere in the range between the lowest

and highest SiO_2 values, rather than at the low SiO_2 end of the spectrum. If this assumption is correct, then the SiO_2 content of the parent magma of the biotite granodiorite unit was probably between about 65 and 69 percent.

Chondrite-normalized rare-earth element (REE) concentrations within each suite have limited ranges, and correlations between REE contents and SiO_2 contents are lacking in both suites (Fig. 17). These features are indicative of minimal fractionation of minerals with high distribution coefficients (Kds) for REE (e.g. sphene or allanite, Gromet and Silver, 1983). The REE patterns of the hornblende-biotite granodiorite and the biotite granodiorite units are essentially identical. Although the sodic suite has higher LREE contents, both suites are strongly enriched in LREE relative to HREE, suggestive of residual garnet (or possibly amphibole) in their respective source regions. A similar enrichment in LREE was noted by Hoover (1987) in the northern part of the Atlanta lobe and was ascribed to residual garnet.

The change in Sr with increasing SiO_2 is minimal, particularly within the sodic suite (Fig. 15). This constancy of Sr content indicates that plagioclase feldspar removal was not extensive. Assuming a Kd for plagioclase feldspar of 4.1 (Mittlefehldt and Miller, 1983) the decrease from about 600 to about 430 ppm Sr can be accounted for by complete removal of about 10 percent plagioclase feldspar from a magma represented by the low silica rocks. If the rocks with low silica contents contain cumulate plagioclase feldspar, then the amount of plagioclase feldspar removal needed to explain the Sr range would be even less. The lack of significant Eu anomalies also suggests that removal of plagioclase feldspar was not an important process.

White and Chappell (1977) and Chappell and others (1987) have suggested that variable unmixing of restite is a viable means of creating a suite of related igneous rocks. The modest variation in major-element oxides in the

Cretaceous plutons may well have originated from separation of variable amounts of restite brought up from the source region, rather than (or in addition to) fractionation of minerals that crystallized from a melt. The large, rounded zircon grains in these rocks are almost certainly restite material. Cores of zircons from the batholith commonly contain larger amounts of radiogenic Pb than the rims, which has complicated the dating of these rocks by the U-Pb method (Bickford and others, 1981). Zircon is probably not the only restite phase, but the relatively slow cooling rate of the Cretaceous plutons, and subsequent textural and mineralogical equilibration, has obscured textural evidence for additional restite phases. Nevertheless, some of the plagioclase feldspar crystals are likely restite, as implied by Reid (1987), who reported relict crystalloblastic textures between plagioclase feldspar crystals in some of the granodiorites in the Bitterroot lobe of the Idaho batholith.

White and Chappell (1977) show that variable amounts of restite separation will result in linear trends on variation diagrams. However, Wall and others (1987) have pointed out the equivocal nature of White and Chappell's chemical criteria for recognizing restite, and, in particular, have emphasized the near linearity of trends on variation diagrams during crystal fractionation of mineral assemblages with bulk Kds in the 0.3 to 3.0 range. The scatter in data and limited SiO_2 range of the Cretaceous suites makes evaluation of restite removal versus crystal removal impossible. As with crystal fractionation, any removal of restite would probably not be an efficient process, and the rocks would record varying amounts of enrichment or depletion in restite phases.

Other means of generating the modest amounts of variability in these rocks include heterogeneities in the respective source regions, and variable amounts of assimilation of country rock at either shallow or deep crustal levels. These controls are probably best evaluated with

isotopic data. C.B. Clarke, of the Open University in England, is currently undertaking a Sr and Nd isotopic study of the region, and has analyzed samples from the study area. His results are in Table 9. All of the Cretaceous plutonic rocks analyzed were of the sodic suite.

Samples of the hornblende-biotite granodiorite and biotite granodiorite units (sodic suite) have similiar initial $^{87}Sr/^{86}Sr$ ratios (0.7072 ± 0.0003), suggesting that their source regions were relatively homogeneous with respect to Sr isotopes. These ratios are not thought to have been changed by interaction with exposed country rocks. Metamorphic country rocks in the northern part of the Atlanta lobe have initial $^{87}Sr/^{86}Sr$ ratios (calculated to 80 Ma) of greater than 0.730 (Fleck and Criss, 1985), and thus significant contamination by similar rock types in the eastern Soldier Mountains can be ruled out. Measurement of Sr isotopes in samples from a country rock contact inward in the Bitterroot lobe indicates only a local effect (Shuster and Bickford, 1985). Preliminary Sr isotopic data from the Atlanta lobe also indicate that mixing of batholith magmas with upper crustal country rocks is unlikely to have occurred (C.B. Clarke, pers. comm., 1988).

Initial ϵ_{Nd} values are similar in the three samples of biotite granodiorite of the sodic suite (-5.9 to -7.8) but are much lower in the hornblende-biotite granodiorite of the sodic suite (-19.5). It is clear that in spite of the major and trace-element similarities between the two rock types (and the locally gradational contact), their sources were not uniform in Nd isotopes. The lower ϵ_{Nd} value for the hornblende-biotite granodiorite is most easily explained by an older source for this unit. Its more mafic composition probably also reflects this difference in protolith. However, both sources appear to have been depleted in LIL elements relative to the potassic suite, and have similar Sr isotopic compositions. The gradational contact between the two units indicates that both magmas rose at about the same

Cretaceous plutonic rocks (sodic suite)

	Kgdh RL309	Kgd RL219	Kgd RL249	Kgd RL387
$^{87}Sr/^{86}Sr$	0.70749	0.70786	0.70778	0.70735
Rb/Sr	0.128	0.129	0.086	0.120
$^{143}Nd/^{144}Nd$	0.51160	0.51229	0.51225	0.51220
Sm/Nd	0.175	0.153	0.166	0.173
ϵ_{Sr}	39.5	44.8	43.8	37.6
ϵ_{Nd}	-20.3	-6.9	-7.5	-8.5
$(^{87}Sr/^{86}Sr)_i^*$	0.70706	0.70743	0.70750	0.70696
$(^{143}Nd/^{144}Nd)_i^*$	0.51154	0.51224	0.51220	0.51214
$(\epsilon_{Sr})_i^*$	33.5	38.8	39.7	32.0
$(\epsilon_{Nd})_i^*$	-19.5	-5.9	-6.6	-7.8

Eocene plutonic rocks

	quartz monzodiorite suite			pink granite suite		
	Tgd L86-26	Tgd RL385	Tgd RL388	Tg RL338	Tg RL384	Tg RL386
$^{87}Sr/^{86}Sr$	0.70694	0.70949	0.70928	0.71383	0.71394	0.71731
Rb/Sr	0.147	0.239	0.199	0.799	0.550	3.13
$^{143}Nd/^{144}Nd$	0.51218	–	–	0.51226	0.51166	–
Sm/Nd	–	–	–	0.156	–	–
ϵ_{Sr}	31.8	67.9	65.0	130	131	179
ϵ_{Nd}	-9.0	–	–	-7.4	-19.1	–
$(^{87}Sr/^{86}Sr)_i^*$	0.70667	0.70905	0.70891	0.71235	0.71293	0.71153
$(^{143}Nd/^{144}Nd)_i^*$	–	–	–	0.51223	–	–
$(\epsilon_{Sr})_i^*$	28.0	61.7	59.8	109	117	96.9
$(\epsilon_{Nd})_i^*$	–	–	–	-6.8	–	–

*Initial ratios calculated assuming age of 80 Ma for Cretaceous plutons and 45 Ma for Eocene plutons

Kgdh = hornblende-biotite granodiorite unit; Kgd = biotite granodiorite unit; Tgd = biotite-hornblende granodiorite unit; Tg = pink granite unit

Table 9. Rb/Sr and Sm/Nd isotopic data of plutonic rocks in the eastern part of the Soldier Mountains. Data used with permission of C.B. Clarke (pers. comm., 1988).

time from their respective sources, but were incompletely mixed. Such source heterogeneity is to be expected given the complexity of the crust, and will result in heterogeneous plutonic rock bodies, particularly if convection was not pronounced (Miller and others, 1988).

In summary, the Cretaceous plutonic rocks in the area can be subdivided into a sodic suite and a potassic suite. The characteristics of these suites are listed in Table 10. The sodic suite is the most voluminous, and was derived from a source region in which the values of K, Rb, Cs, U, B, Mg, Sc, Cr, Co, Sb, and possibly Th, are lower relative to the potassic suite. The high Mg, Sc, Cr, and Co contents of the potassic suite may reflect differences in protolith composition prior to mobilization of the LIL elements during high-grade metamorphism or melting. During this mobilization, the source of the sodic suite was enriched relative to the potassic suite in Na, Sr, and Ba. Concentrations of Al, LREE, and Zr are higher in the sodic suite, either as a result of original protolith differences, or as a result of enrichment during mobilization of LIL elements. The potassic suite was derived from a less depleted source region, probably at shallower levels in the crust. Garnet and (or) amphibole were likely residual minerals in each source region. Within-suite variations in major- and trace-element abundances are minimal, and can be explained by minor amounts of crystal segregation and (or) restite segregation. Source region heterogeneity also played a role in development of compositional variations in the two plutonic suites. Source regions of the hornblende-biotite granodiorite and the biotite granodiorite were similar with respect to Sr isotopes, but distinct with respect to Nd isotopes. The hornblende-biotite granodiorite magma was probably derived from an older and more mafic source region, and was incompletely mixed with coeval magma of the biotite granodiorite unit.

POTASSIC SUITE	SODIC SUITE
consists of coarse-grained hornblende-biotite granodiorite unit and Hailey granodiorite unit	consists of biotite granodiorite unit and hornblende-biotite granodiorite unit
contains large books of biotite	contains small "shreddy" biotite books
higher K, Rb, Cs, U, B, Mg, Sc, Co, and Cr	higher Na, Al, Sr, Ba, LREE, and Zr
values of $^{87}Sr/^{86}Sr$ and ϵ_{Nd} unknown	initial $^{87}Sr/^{86}Sr$ is 0.7072 $\pm$ 0.0003; initial ϵ_{Nd} is -6.8 $\pm$ 1 in biotite granodiorite unit and -19.5 in hornblende-biotite granodiorite unit
relatively enriched, but more mafic source	relatively depleted source(s) with source of hornblende-biotite granodiorite unit possibly older than that of biotite granodiorite unit
shallower source?	deeper source(s)?

Table 10. Characteristics of potassic and sodic suites in the southeastern part of the Idaho batholith.

Origin of Cretaceous magmas

A model proposed to explain the generation of Cretaceous magmas in the eastern Soldier Mountains must account for an initial $^{87}Sr/^{86}Sr$ ratio of 0.7072 ± 0.0003 and for granodiorite as a predominant rock type, with a compositional range of 64 to 70 percent SiO_2. Potential magma components include the following: 1) mantle-derived magmas; 2) lower- to mid-crustal granulite facies rocks, such as intermediate to felsic granulite xenoliths present in Snake River Plain volcanics (Leeman and others, 1985); and 3) mid- to upper-crustal rocks such as the gneisses, schists, quartzites, and calc-silicate rocks of Precambrian to Paleozoic age present to the east of the batholith and as pendants within the batholith (Dover, 1983; Fisher and others, 1983).

The mass contribution from the mantle in Cretaceous rocks in the eastern Soldier Mountains is thought to be minor. Although the initial Sr ratios of about 0.7072 would permit a mantle component, the abundance of granodiorite, and lack of gabbro and diorite, suggests that any mantle-derived melt originally present has mixed extensively with crustal material. Most Cretaceous rocks in the Atlanta lobe east of the Sr 0.704/0.706 line have initial ratios of 0.707 to 0.710 (Armstrong and others, 1977; R.J. Fleck, pers. comm., 1985; C.B. Clarke, pers. comm., 1988). Armstrong and others (1977) have argued that these ratios are too low to represent melts entirely crustal in origin. However, chemical data from the sodic suite suggest derivation from a depleted lower crustal source (e.g. high concentrations of Na, Al, Sr, and Ba and low concentrations of K, Rb, Cs, and U). Such a source would be low in radiogenic Sr, and could presumably give rise to rocks with initial ratios in the 0.707 to 0.710 range, as has been previously suggested by workers in the Bitterroot lobe and the northern part of the Atlanta lobe (Fleck and Criss, 1985; Shuster and Bickford,

1985; Criss and Fleck, 1987). These studies indicated that the main-phase magmas primarily originated from melting of ancient continental basement.

Exposures of basement rocks with appropriate low initial ratios, if present, have yet to be found. Country rocks in the vicinity of the batholith typically have initial ratios (calculated to 80 Ma) of 0.73 and greater (Fleck and Criss, 1985). Granulite xenoliths from Snake River Plain lavas (Leeman and others, 1985) are representative of possible source rocks, and have a wide range of $^{87}Sr/^{86}Sr$ ratios. Those from extreme eastern Idaho have initial ratios (calculated to 80 Ma) as low as 0.7024. However, xenoliths from lavas immediately south of the Idaho batholith have initial ratios of 0.72 and greater (calculated to 80 Ma), and thus contain too much radiogenic Sr to have been source rocks for the batholith.

A further complication is that the isotopic composition of the mantle in the region is uncertain. The existence of a relatively radiogenic mantle beneath Idaho has been proposed by Leeman (1982c), who reported moderately high initial ratios (mostly 0.706-0.707) for basalts of the Snake River Plain which otherwise lack petrologic evidence of crustal contamination. Because the isotopic composition of the crust and mantle beneath the Idaho batholith is poorly known, the resolution of protolith-related questions remains elusive. Thus, the Sr data allow a mantle component within the batholith rocks, but do not require it.

Although significant mass transfer from the mantle is considered unlikely, heat transfer is more plausible, and would account for the large volume of magma that was generated. The idea of generating large-scale crustal melting by underplating of mantle-derived magmas has gained wide acceptance (e.g. Pitcher, 1987; Huppert and Sparks, 1988), and Hyndman and Foster (1988) have invoked this process to explain magma generation for the Bitterroot lobe of the batholith. They suggested that melting took place within

the crust as a consequence of prolonged injection of high-temperature mantle magmas, now represented by synplutonic mafic dikes in the Bitterroot lobe of the batholith. The synplutonic mafic dikes in the Bitterroot lobe are evidence for a mafic precursor, as are diorites and gabbros in the western part of the Atlanta lobe near Banks (Russell, 1987), but direct evidence that such a process formed the central and eastern part of the Atlanta lobe of the Idaho batholith is lacking. Rare Cretaceous(?) lamprophyre dikes are present in the Atlanta lobe, but they are not convincingly synplutonic.

Another means by which to generate the Cretaceous magmas is by crustal thickening and anatexis resulting from the stacking of thrust plates during the Sevier orogeny of Cretaceous age. If the crust was thickened to 50 km, then a modest geothermal gradient of 15°C/km would provide adequate temperatures for anatexis in the lower 10 km of crust. A higher geothermal gradient would allow melting at mid-crustal levels. Wickham (1987) has suggested gradients as high as 80 to 100°C/km in the Hercynian metamorphic belt, with anatexis at 10 to 12 km.

Zen (1988) has modeled the relationship of thrusting and anatexis and has concluded that anatexis is likely in a sialic crust thickened by thrust slices of upper crustal material. He also noted that a time lag (several tens of millions of years) is likely between thrusting and anatexis. Patino-Douce and Humphreys (1989) modeled thickening and anatexis in the Sevier hinterland and found a 10 to 15 Ma time lag between deformation and generation of volumes of melt large enough to allow migration.

It is not known if a sufficient time lag existed between thrusting (and crustal thickening) and formation of the Idaho batholith. Plutonism probably spanned from about 85 to 72 Ma in the central and southern parts of the Atlanta lobe. The initiation of Sevier thrusting in western Wyoming has been estimated as Aptian or younger (<119 Ma; Heller and

others, 1986), and at 100 Ma in Nevada (Miller and Gans, 1989). The age of the thrust faults immediately east of the Idaho batholith is uncertain. Those that are east of the Bitterroot lobe are perhaps in the 80 to 85 Ma range, and they become progressively younger (up to early Tertiary in age) farther to the east (J. Whipple, pers. comm., 1989). Because the thrust faults young to the east, it is likely that the Idaho batholith now occupies the area that once contained the oldest faults, perhaps faults as old as 100 Ma. The White Cloud stock, east of the Atlanta lobe, intrudes a thrust fault and has been dated at 85 Ma (K-Ar biotite; Lewis and others, 1987). Thus, thrusting appears to have preceded, and been coincident with, crystallization of the Idaho batholith. Additional age constraints on thrusting and plutonism are needed, but the available data do not rule out a genetic link between the two processes. If thrusting began at about 100 Ma, sufficient thickening may have occurred by 85 Ma to produce melting. A thrust-related, anatectic origin for the batholith might also explain why Late Cretaceous plutonism in Idaho and Montana occurred across a belt 300 km wide that lacks any chemical progression to the east of the Sr 0.704/0.706 line.

Best and others (1974) have suggested that two-mica granites in the Kern Mountain range of northeastern Nevada were possibly mobilized crustal material. Miller and Gans (1989) also believe that these two-mica granites are anatectic in origin, and have suggested that the melts formed in a crust structurally thickened by Sevier thrusting. As noted by Miller and Bradfish (1980), the "inner Cordilleran belt" of muscovite-bearing plutons (which includes granites of the Kern Mountain range and those of the Idaho batholith) is in the hinterland of the thrust belt and is coincident with a north-south band that has undergone Mesozoic and (or) Cenozoic regional metamorphism. They have concluded that the distribution, composition, and ages of these granitoids collectively argue against a simple subduction-zone model

for their origin. In contrast, Cretaceous plutons in the coastal batholiths (e.g. central and western Penninsular Range batholith, central and western parts of the Sierra Nevada batholith, and perhaps the western part of the Idaho batholith) are most easily explained by subduction of oceanic crust under the continent and the subsequent rise of arc magma, as is commonly assumed. Plutonism of Cretaceous age in the western U.S. can thus be divided into that with "typical" continental-arc characteristics, and an eastern back-arc setting associated with the Sevier fold and thrust belt. Depending on the amount of anatectic magma generated, either "back-arc plutons" (as in Nevada) or "back-arc batholiths" (as in Idaho), have developed.

In summary, melting of lower to mid-crustal granulites, aided by underplated basalts from the mantle, is an acceptable hypothesis for generating magmas of the Idaho batholith. However, crustal thickening and anatexis resulting from stacking of Cretaceous thrust sheets is also a viable hypothesis, and may explain the wide belt of Late Cretaceous plutonism in Idaho and western Montana.

EOCENE PLUTONIC ROCKS

Intrusive rocks of this age group are represented by ten samples from the eastern Soldier Mountains. Results of major- and trace-element analyses are presented in Table 11, and the locations of these samples are shown on Plate 2. The data set from the eastern Soldier Mountains has been augmented with 78 samples of Eocene plutonic rocks from the Hailey and Challis one by two degree quadrangles (Table 11, and Lewis and Kiilsgaard, unpublished data), and the results are presented in Figures 18 to 23. The combined sets of data are from 9 stocks and 3 batholiths of the pink granite suite and 21 stocks of the quartz monzodiorite suite. They represent rocks of similar age, mineralogy, and geologic setting, and are useful for contrasting the two Eocene rock suites and for comparing them with Cretaceous plutonic rocks in the area. When combining the data from a number of stocks the assumption is made that processes active in the various Eocene magma chambers were probably similar, and resulted in similar chemical trends. This assumption allows qualitative assessment of petrogenetic processes that may have given rise to the two Eocene rock suites. The compilation of data presented here represents a regional reconnaissance effort. However, the next phase of research in the region will require detailed mapping and sampling of the individual stocks.

Major-element variation

The quartz monzodiorite suite ranges in SiO_2 content from 48 to 70 percent, and the pink granite suite ranges from 70 to 77 percent (Figure 18). Samples from the eastern Soldier Mountains span much of the range of silica contents of the entire region (Table 11). Although SiO_2 content may be used to distinguish the pink granites from the quartz monzodiorites, they were originally defined by Fisher and

	QUARTZ MONZODIORITE SUITE							PINK GRANITE SUITE				
	Tgd RL299	Tgd RL253	Tgd RL167	Tfgd 8636K	Cum RL391	Thd RL496[1]	Tgd RL497[1]	Tg RL293	Tg RL324	Tg RL338	Tg RL073	Tg RL374
	major-element oxides in weight percent											
SiO_2	68.6	61.4	62.5	59.8	53.7	54.9	68.4	73.1	71.9	71.7	74.9	73.7
TiO_2	0.45	0.82	0.63	0.73	0.99	0.86	0.47	0.25	0.27	0.31	0.19	0.24
Al_2O_3	14.6	16.2	16.6	17.5	9.63	12.7	14.7	13.7	14.4	14.1	13.3	13.5
Fe_2O_3	1.34	2.36	2.02	2.01	11.30*	3.02	1.62	0.86	0.96	1.07	0.63	0.86
FeO	1.60	2.81	2.29	3.52	–	5.87	1.42	0.83	0.84	0.92	0.62	0.75
MnO	0.05	0.08	0.07	0.09	0.18	0.14	0.04	0.03	0.03	0.03	0.03	0.03
MgO	1.33	2.58	2.07	2.65	9.23	7.47	1.37	0.46	0.54	0.63	0.34	0.45
CaO	2.62	4.25	3.70	5.30	8.95	8.23	2.72	1.26	1.72	1.68	0.90	1.20
Na_2O	3.55	3.87	3.88	4.23	1.75	2.53	3.54	3.52	3.82	3.53	3.45	3.48
K_2O	4.22	3.43	4.65	2.46	2.20	2.07	4.25	4.75	4.19	4.51	4.85	4.71
P_2O_5	0.14	0.28	0.23	0.30	0.28	0.40	0.15	0.09	0.09	0.12	0.05	0.08
H_2O^+	0.41	0.74	0.70	0.74	1.31**	1.44	0.53	0.29	0.38**	0.26	0.44	0.31
H_2O^-	0.17	0.15	0.06	0.08	–	0.12	0.13	0.22	–	0.21	0.07	0.15
CO_2	<0.01	0.14	<0.01	<0.01	–	0.12	0.08	<0.01	0.01	0.10	<0.01	<0.01
total	99.1	99.1	99.4	99.4	99.5	99.7	99.5	99.4	99.2	99.2	99.8	99.5
A/CNK***	0.96	0.91	0.91	0.91	0.45	0.59	0.96	1.03	1.03	1.02	1.06	1.04
	trace elements in parts per million											
Sc	6.3	11	–	–	40	26	6.4	2.1	2.9	2.5	–	–
Cr	40	89	–	–	330	360	41	8.2	7.9	7.2	–	–
Co	7.9	14	–	–	50	38	7.6	3.0	3.4	3.6	–	–
Rb	136	97	120	–	–	55	123	190	197	184	240	200
Sr	427	719	631	–	–	600	470	206	314	251	92	–
Y	17	18	–	–	–	16	22	18	18	15	–	–
Zr	219	261	217	–	–	93	185	173	151	176	104	–
Nb	19	20	–	–	–	12	25	21	35	21	–	–
Sb	0.12	0.13	–	–	0.3	–	0.12	0.15	–	0.10	–	–
Cs	2.3	2.1	–	–	1.6	0.95	1.7	3.3	3.0	3.0	–	–
Ba	1300	2120	2270	–	1220	762	1530	846	1190	924	388	710
La	55	71	–	–	39	43	60	56	49	65	–	–
Ce	110	140	–	–	81	88	130	110	87	120	–	–
Nd	32	45	–	–	43	44	35	28	26	34	–	–
Sm	5.7	7.6	–	–	8.3	7.0	6.7	5.1	4.8	5.3	–	–
Eu	1.1	1.8	–	–	1.9	1.7	1.3	0.76	0.85	0.93	–	–
Tb	0.61	0.79	–	–	0.92	0.52	0.71	0.45	0.38	0.47	–	–
Yb	2.2	2.3	–	–	2.0	1.7	2.1	2.2	2.0	2.0	–	–
Lu	0.23	0.27	–	–	0.36	0.29	0.26	0.22	0.24	0.20	–	–
Hf	6.6	8.2	–	–	4.0	4.1	6.7	5.0	4.6	5.3	–	–
Ta	1.5	1.2	–	–	0.8	1.1	1.8	1.6	2.7	1.8	–	–
Th	25	17	–	–	6.5	8.6	19	33	21	34	–	–
U	4.9	3.0	–	–	1.2	2.4	4.2	5.7	13	5.8	–	–
B	4.5	4.8	–	–	–	3.3	5.5	1.9	2.3	2.8	–	–

[1] Sample from the Willow Creek stock, 20 km east of the study area

* Total Fe as Fe_2O_3; ** Loss on ignition at 900°C; *** Molecular $Al_2O_3/(CaO+Na_2O+K_2O)$

Tgd = biotite-hornblende granodiorite unit; Tfgd = foliated hornblende-biotite granodiorite unit; Cum = pyroxene-hornblende diorite (cumulate phase) of Tgd unit; Thd = hornblende diorite; Tg = pink granite unit

Table 11. Major- and trace-element analyses of Eocene plutonic rocks from the eastern part of the Soldier Mountains and nearby areas. Analysts: J. Taggart, A. Bartel, D. Siems, C. Papp, J.H. Christie, L. Jackson, E. Brandt, N. Elsheimer, K. Slaughter, P.H. Briggs, and J. Evans.

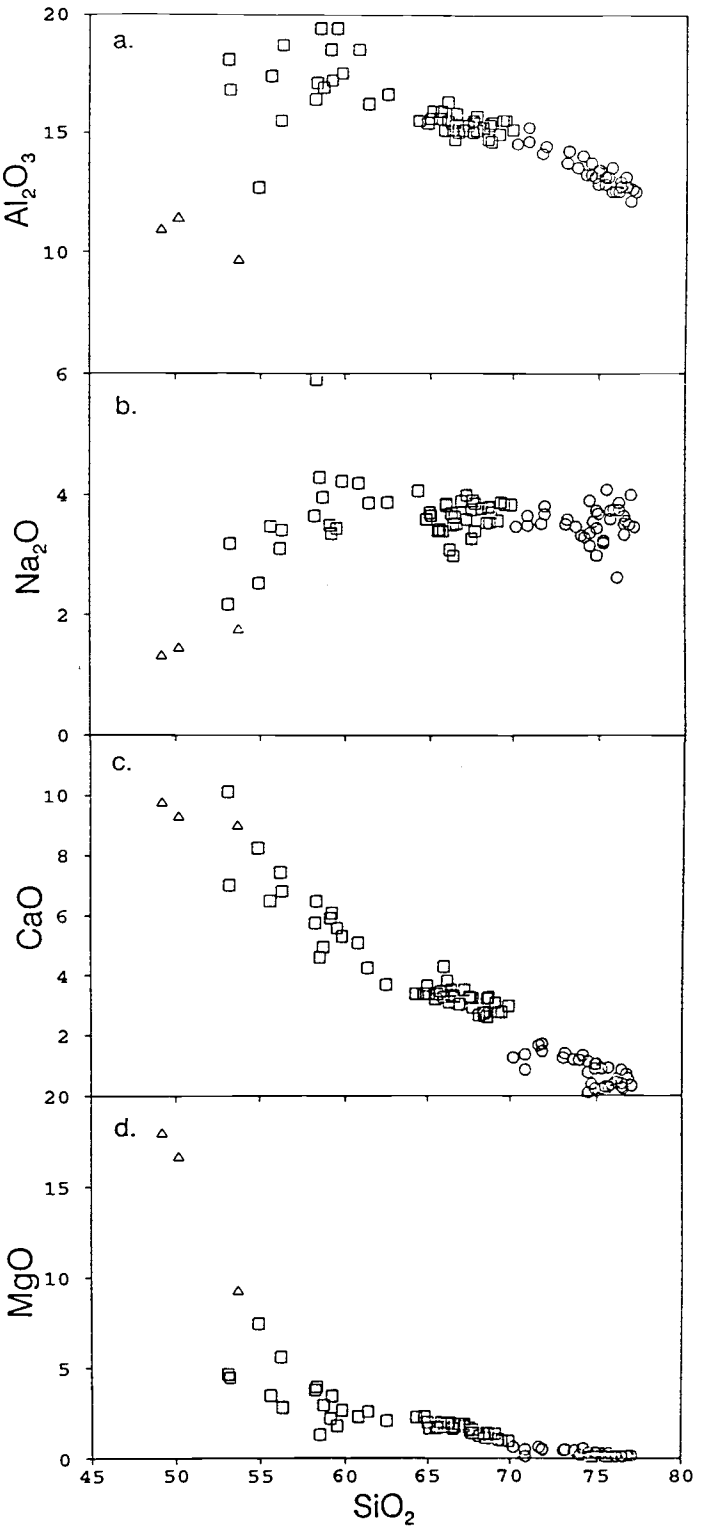

Figure 18. Harker plots of (a) Al_2O_3, (b) Na_2O, (c) CaO, and (d) MgO versus silica for plutonic rocks of Eocene age from central Idaho. Symbols: circles = pink granite suite; squares = quartz monzodiorite suite; triangles = cumulates.

others (1983) and Bennett and Knowles (1985) on the basis of field relations and rock types, not chemical characteristics.

For purposes of this discussion, two chemical subgroups of rocks are designated within the quartz monzodiorite suite. One subgroup is mafic in composition and contains less than 63 percent SiO_2, whereas the other is intermediate in composition with 63 to 70 percent SiO_2 (Fig. 18). Included in the mafic subgroup are cumulate rocks, which contain less than 54 percent SiO_2 and are plotted as triangles on Figure 18. They include rocks rich in hornblende or hornblende and pyroxene, as well as layered intrusive phases containing olivine and pyroxene. All are characterized by plagioclase feldspar as an interstitial phase. The olivine-pyroxene cumulates have only been found in the Thorn Creek stock, 70 km west of the study area. Pyroxene-hornblende cumulates are more common, and are represented by sample RL391 (SiO_2 = 53.7 percent) from the eastern part of the Soldier Mountains. These pyroxene-hornblende rocks are not layered, but are cumulates in the sense that they probably represent rocks that were enriched in early-formed mafic minerals by some fractionation process. Because the cumulate rocks are enriched in mafic minerals, they are not representative of the least evolved (parental) magma compositions. Samples of the mafic subgroup that lack cumulate textures are more likely to represent parental magma compositions. Sample RL496 (SiO_2 = 54.9 percent) is a hornblende diorite from the Willow Creek stock. This sample lacks cumulate textures, and therefore is assumed to represent the least-evolved magma yet recognized in the quartz monzodiorite suite.

Because the two suites have different ranges of SiO_2, their chemical compositions are not as easily compared as the two suites of Cretaceous plutonic rocks. Average abundances listed in Table 12 indicate that the pink granite suite has higher concentrations of K_2O, and lower TiO_2,

	QUARTZ MONZODIORITE SUITE						PINK GRANITE SUITE[3]			A-TYPE[4]			FELSIC I-TYPE[5]	FELSIC S-TYPE[6]	IDAHO BATHOLITH		
	Mafic Subgroup[1]			Intermediate Subgroup[2]											2-Mica Granite[7]	Na Suite[8]	K Suite[9]
	x	s	range	x	s	range	x	s	range	x	s	range	x	x	x	x	x
	major-element oxides in weight percent																
SiO_2	56.9	3.6	49.2-62.5	67.2	1.5	64.3-69.9	74.6	1.9	70.2-77.1	73.81	3.25	60.4-79.8	73.39	73.39	73.8	68.1	67.30
TiO_2	0.87	0.28	0.31-1.49	0.51	0.10	0.33-0.7	0.15	0.09	0.03-0.32	0.26	0.18	0.04-1.25	0.26	0.28	0.10	0.52	0.57
Al_2O_3	16.2	2.8	9.6-19.4	15.3	0.4	14.6-16.3	13.3	0.70	12.1-15.2	12.40	1.40	7.3-17.5	13.43	13.45	14.6	15.8	15.1
Fe_2O_3	1.66	0.70	0.84-3.02	1.12	0.39	0.42-1.88	0.68	0.32	0.31-1.58	1.24	1.13	0.14-8.7	0.60	0.36	0.97	1.49	1.62
FeO	4.63	1.88	2.29-8.0	2.04	0.43	1.34-2.86	0.66	0.25	0.28-1.45	1.58	1.07	0.33-6.1	1.32	1.73	--	1.50	2.03
MnO	0.11	0.04	0.06-0.18	0.06	0.01	0.03-0.08	0.03	0.01	0.02-0.05	0.06	0.04	<0.01-0.24	0.05	0.04	0.03	0.04	0.06
MgO	5.06	4.60	1.29-17.9	1.61	0.37	0.89-2.30	0.26	0.18	<0.10-0.63	0.20	0.24	0.01-1.60	0.55	0.58	0.3	1.00	1.71
CaO	6.58	1.86	3.70-10.1	3.20	0.38	2.29-4.29	0.80	0.47	0.12-1.72	0.75	0.60	0.08-3.7	1.71	1.28	1.52	3.35	3.58
Na_2O	3.34	1.09	1.31-5.92	3.65	0.24	2.99-4.07	3.53	0.29	2.63-4.09	4.07	0.66	2.8-6.1	3.33	2.81	3.9	3.66	3.25
K_2O	2.34	1.03	0.46-4.65	3.52	0.49	2.36-4.25	4.78	0.51	4.17-6.08	4.65	0.49	2.4-6.5	4.13	4.56	3.31	3.11	3.88
P_2O_5	0.30	0.13	0.05-0.59	0.19	0.05	0.11-0.31	0.06	0.02	<0.05-0.12	0.04	0.06	<0.01-0.46	0.07	0.14	0.04	0.17	0.18
	trace elements in parts per million																
Ba	1150	590	373-2270	1270	140	940-1530	666	374	120-1280	352	281	2-1530	510	388	1450	1410	878
Rb	59	31	11-120	103	20	70-140	168	44	110-250	169	76	40-475	194	277	74	104	131
Sr	679	119	445-854	595	89	420-709	189	92	45-321	48	52	0.5-250	143	81	652	749	543
Th	11	5	7-17	22	4	19-25	35	9	21-43	23	11	<1.0-87	22	18	--	14	20
U	2.2	0.9	1.2-3.0	4.6	0.5	4.2-4.9	8	8	5.7-13	5	3	<1.0-23	5	6	--	2.6	5.3
Zr	134	72	27-261	147	29	107-199	127	61	58-252	528	414	82-3530	144	136	120	220	173
Nb	16	6	12-20	19	6	14-25	28	7	21-35	37	37	11-348	12	13	--	19	18
Y	15	4	8-19	14	5	8-22	17	4	10-26	75	29	9-190	34	33	8	12	16
Ce	88	42	41-142	94	33	59-131	98	33	33-136	137	58	18-560	68	53	--	119	98
Sc	26	15	11-40	6.4	0.1	6.3-6.4	2.7	0.5	2.1-3.3	4	5	<1-22	8	8	--	5.9	8.5

x = mean; s = one standard deviation; leaders (--) not determined

[1] This study and unpublished data; average of 20 analyses for major elements and 3 to 11 analyses for trace elements.
[2] This study and unpublished data; average of 34 analyses for major elements and 2 to 25 analyses for trace elements.
[3] This study and unpublished data; average of 35 analyses for major elements and 5 to 18 analyses for trace elements.
[4] Whalen and others (1987); average of 148 analyses; samples collected worldwide.
[5] Whalen and others (1987); average of 421 analyses; Lachlan Fold Belt, Australia.
[6] Whalen and others (1987); average of 205 analyses; Lachlan Fold Belt, Australia.
[7] Lewis and others (1987) and unpublished data; average of 17 analyses for major elements and 4 analyses for trace elements.
[8] This study and unpublished data; average of 16 analyses for major elements and 7 to 15 analyses for trace elements.
[9] This study and unpublished data; average of 9 analyses for major elements and 2 to 5 analyses for trace elements.

Table 12. Average abundances of major and trace elements in plutonic rocks of the eastern part of the Soldier Mountains, and comparative rocks.

Al_2O_3, FeO*, MgO, CaO, and P_2O_5 than the quartz monzodiorite suite. The quartz monzodiorite suite is metaluminous to weakly peraluminous, whereas the pink granites are entirely peraluminous (see A/CNK ratios in Table 11).

The two subgroups within the quartz monzodiorite suite have different chemical characteristics. Relative to the intermediate rocks, those of the mafic group are characterized by: 1) a large amount of scatter on Harker plots, particularly with regard to Al_2O_3; 2) a sharp decrease in MgO with increasing SiO2; and 3) an increase in Al_2O_3 and Na2O with increasing SiO_2. These characteristics are probably controlled in part by compositional variations of the parental magmas, and by fractionation or accumulation of variable amounts of hornblende, pyroxene and olivine. Olivine is present only in cumulates and, in part, accounts for the high MgO contents of these rocks.

The relationship between the mafic rocks and the intermediate rocks is problematic. If fractional crystallization in magmas above about 60 percent SiO_2 was dominated by fairly calcic plagioclase feldspar, the result would be a decrease in Al_2O_3 content, and a flattening of the Na_2O trend, as is observed. However, other processes, such as contamination of the magma of the mafic subgroup with more silicic material, could also be invoked to explain the intermediate group.

Trends for Na_2O and CaO are poorly developed within the pink granite suite (Fig. 18). The variable contents of these oxides may reflect regional variations and (or) deuteric alteration effects. A discontinuity exists in CaO content between the pink granite suite and the quartz monzodiorite suite. This discontinuity indicates that the two suites are not related along a simple liquid line of descent. The decrease in Al_2O_3 content in the pink granite suite with increasing SiO_2 is regular, and is suggestive of feldspar fractionation.

Trace-element variation

Samples from each of the two Eocene plutonic suites exhibit wide and overlapping ranges in the contents of most trace elements (Table 11, Figures 19 and 20). Concentrations of Rb and Ba increase (albeit erratically) with increasing SiO_2 in the mafic subgroup of the quartz monzodiorite suite (Figure 19). Behavior of Sr is not systematic in this subgroup. The intermediate rocks of the quartz monzodiorite suite (63-70 percent SiO_2) show the least variation in trace-element concentrations, and in these rocks the trace elements are not correlated with SiO_2 content. Contents of Ba and Sr in the pink granite suite decrease sharply with increasing SiO_2. Abundance of Sr in the pink granite suite is less than 320 ppm, and a discontinuity exists between these plutonic rocks and those of the intermediate subgroup of the quartz monzodiorite suite. Concentrations of Rb in the pink granite suite are variable, and are not correlated with SiO_2.

The relatively large range of Ba (and to a lesser extent Sr) in the pink granite suite is suggestive of potassium feldspar fractionation. Potassium feldspar readily partitions both Ba and Sr (Kd's of 6.1-12.9 for the former and 3.6-3.9 for the latter; Arth and Hanson, 1975; Mittlefehldt and Miller, 1983). Biotite removal would also deplete a melt in Ba, but, unlike potassium feldspar, it is in low abundance (generally less than 6 percent) in all of the pink granite suite and is less likely to have caused the major variation in Ba content. Variability in Ba content may, in part, be caused by differing parental magma composition (and sources) which is likely given the wide distribution of the pink granite suite. However, large ranges within single stocks (1190 to 388 ppm Ba and 314 to 92 ppm Sr in the eastern Soldier Mountains) are suggestive of fractionation. Because of the good correlation between these trace elements and SiO_2, alteration is unlikely to

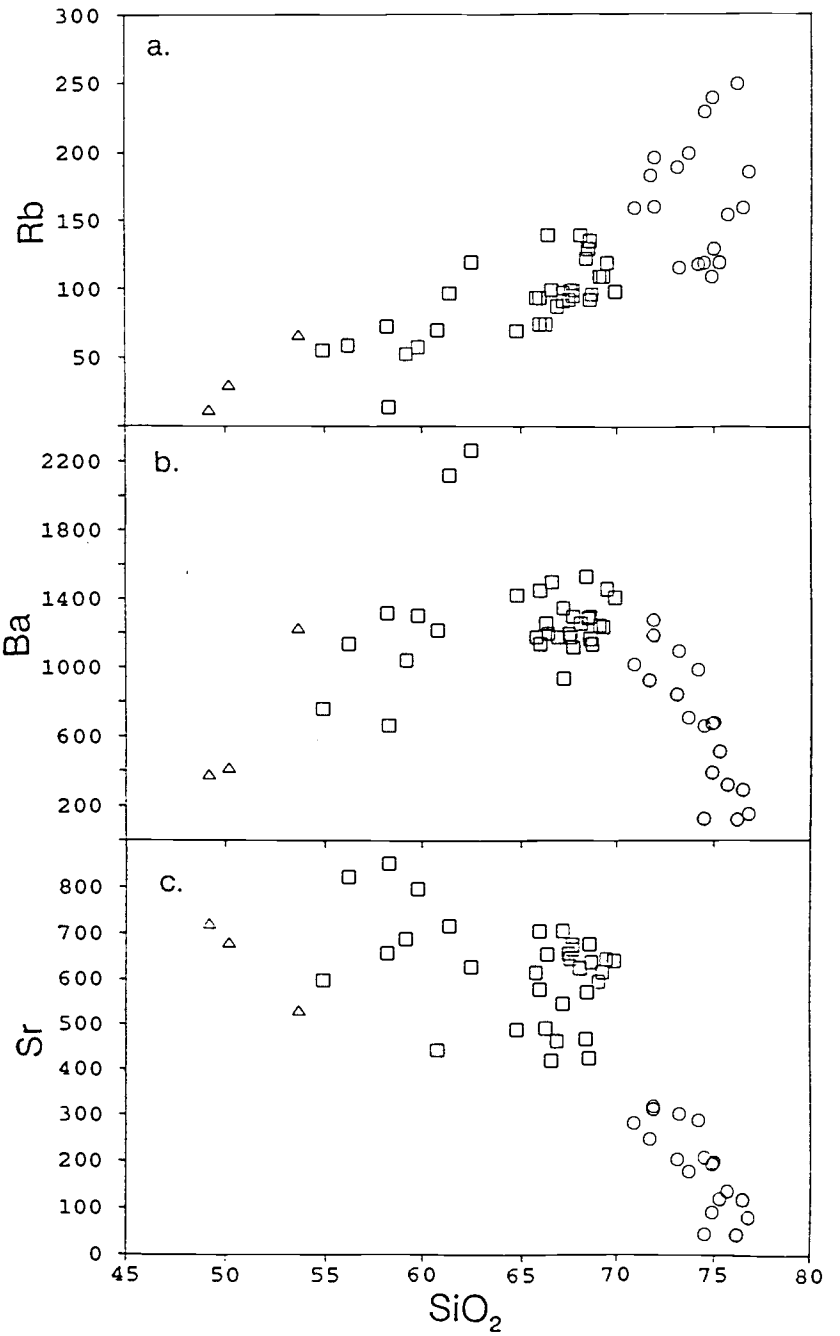

Figure 19. Plots of (a) Rb, (b) Ba, and (c) Sr versus silica for plutonic rocks of Eocene age from central Idaho. Symbols: circles = pink granite suite; squares = quartz monzodiorite suite; triangles = cumulates.

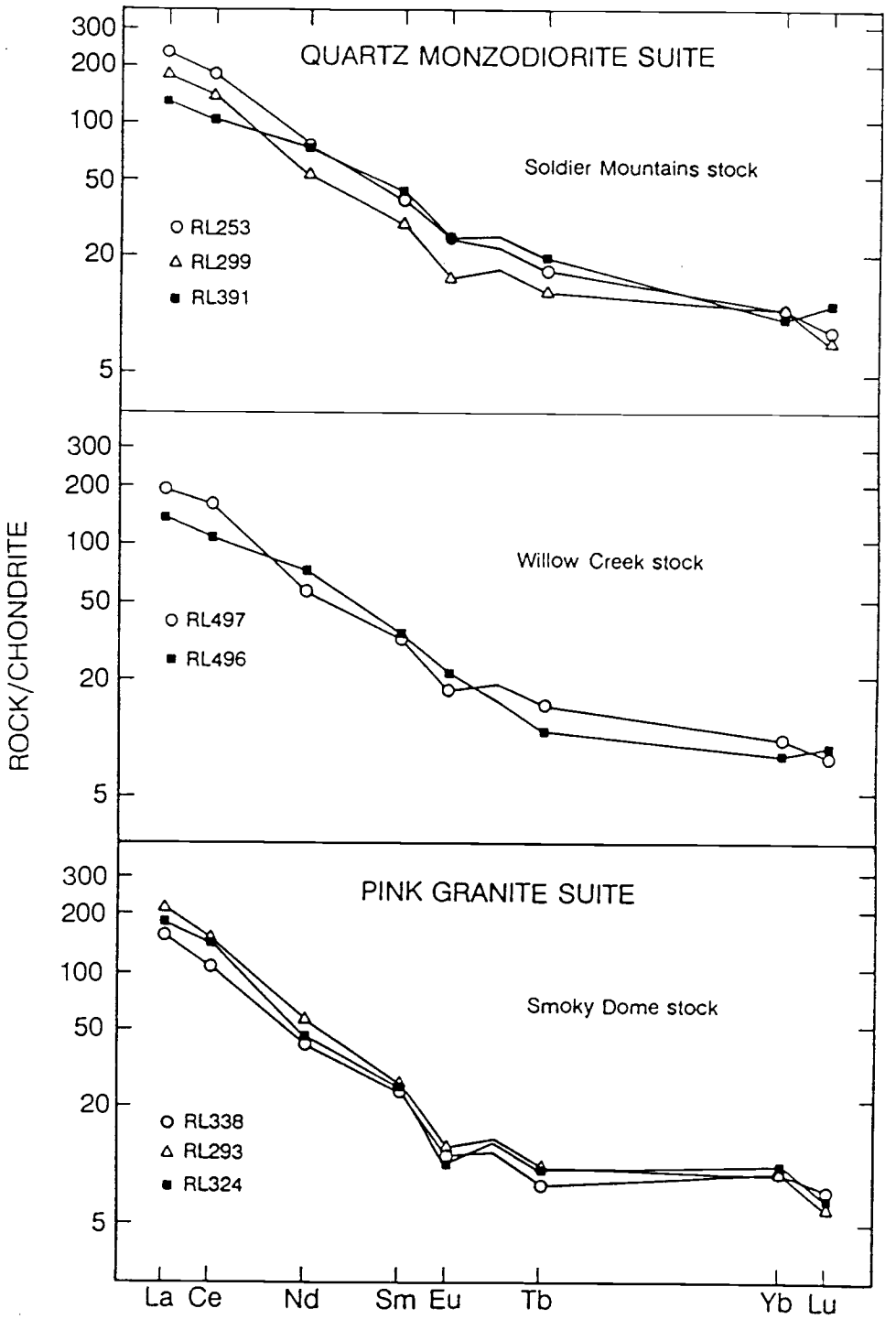

Figure 20. Chondrite-normalized plots of rare-earth element abundances for plutonic rocks of Eocene age from central Idaho. Chondrite values used for normalization are from Anders and Ebihara (1982).

have caused the large variation present within single stocks. In addition, it is unlikely that this variation is a result of differing degrees of partial melting. Concentrations of Ba and Sr, which are elements with high bulk distribution coefficients, should not vary significantly with differing but large amounts of partial melting (Hanson, 1978). Field evidence for crystal-liquid fractionation within the pink granite suite is rare. However, one sample from the eastern Soldier Mountains (RL245) contains layers enriched in potassium feldspar, which may be interpreted as evidence that fractional crystallization processes have operated at least locally.

Concentrations of Sc, Cr, and Co in the Eocene rock suites are known only for eight samples (Table 11). Values in the most mafic rocks decrease markedly with increasing SiO_2 (e.g. Sc decreases from 40 to 11 ppm as SiO_2 increases from 54 to 61 percent). Fractional crystallization of mafic minerals likely controls these variations. Decreases in Sc, Cr, and Co contents with increasing SiO_2 are less dramatic in the samples of intermediate composition. As mentioned previously, RL496 is assumed to represent the least evolved magma of the quartz monzodiorite suite. Concentrations of Sc (26 ppm) and Co (38 ppm) in this sample are second only to the hornblende-pyroxene cumulate (RL391), and Cr values are the highest measured in this study (360 ppm). In contrast, these same elements are in low abundance in the pink granite suite and vary little with changes in SiO_2 content.

Boron content is low in the pink granite (1.9-2.8 ppm), and U concentrations are high (5.7-13 ppm), relative to the quartz monzodiorite suite. The low boron contents in the pink granites are probably not a primary characteristic, because these rocks are enriched in other incompatible elements such as K and Rb. Instead, boron may have been lost to vapor phase (melt/vapor Kd value = 0.33; Pichavant, 1981), or during deuteric alteration. Boron in the quartz monzodiorite suite ranges from 3.3 to 5.5 ppm, and U and Th

increase with increasing SiO_2 from 1.2 to 4.9 ppm and 6.5 to 25 ppm, respectively.

Samples analyzed for REE are from the eastern part of the Soldier Mountains and from the Willow Creek stock 20 km to the east of the study area. The pink granite and quartz monzodiorite suites are strongly enriched in LREE relative to chondritic values, as depicted in Figure 20. Both suites have similar La and Lu contents, but the pink granite suite differs in that the LREE are more strongly enriched and the HREE have a flat unfractionated pattern. Although both suites have negative Eu anomalies, those of the pink granite suite are more pronounced. The negative Eu anomalies of the pink granite suite are suggestive of feldspar fractionation, but are not useful in determining which type of feldspar was removed because both potassium feldspar and plagioclase feldspar incorporate Eu in preference to the other REE (Kds of 3.5-6.5 for potassium feldspar and 3.8-7.9 for plagioclase; Nash and Crecraft, 1985). Hornblende diorite from the Willow Creek stock (RL496) lacks a Eu anomaly, and, as mentioned previously, is assumed to represent the least-evolved magma of the quartz monzodiorite suite. The lack of a Eu anomaly suggests that either plagioclase feldspar was not an important residual phase in its source, or that the fugacity of oxygen in the source region at the time of melting was relatively high.

Relationships between rock suites

The pink granite and quartz monzodiorite suites are broadly related in time and space. However, the contact between these two suites is abrupt. Rare exposures of the contact show that neither suite has a chilled margin, but dikes of pink granite cross-cut the quartz monzodiorite suite, suggesting that the pink granite is slightly younger. Radiometric dating is consistent with the interpretation that the quartz monzodiorite suite is slightly older, but

the number of radiometric dates is limited (see compilation in Bennett and Knowles, 1985).

Several lines of evidence indicate that the two suites represent two distinct magma types from different source regions, and that they are not related by processes of fractional crystallization. Field relations indicate that the two suites are present within discrete stocks, or in adjacent stocks with abrupt contacts. The stocks of the quartz monzodiorite suite are not cored by rocks of the pink granite suite, a relationship that might be expected were they comagmatic. The only exception to this relationship is in the eastern part of the Soldier Mountains, where the quartz monzodiorite suite partly encloses a core of pink granite (Fig. 5). This close spatial association in the Soldier Mountains apparently resulted in local mixing between the two suites, as discussed in the following section.

Geochemical evidence also indicates that a fractionation relationship between the two suites is unlikely. The pink granite suite contains little MgO relative to FeO*, as illustrated in Figure 21, which is a plot of MgO/(MgO + FeO*) versus SiO_2. In contrast, all of the intermediate rocks of the quartz monzodiorite suite have MgO/(MgO+FeO*) ratios greater than 0.3. To derive compositions such as those of the pink granite by fractionation from magmas of intermediate compositions would require removal of an Mg-rich assemblage such as the pyroxene-olivine cumulates (open triangles in Fig. 21). However, these Mg-rich mineral phases are not present in the intermediate rocks of the quartz monzodiorite suite. Hornblende and biotite are the predominant mafic minerals in the intermediate rocks, and these minerals do not contain sufficient Mg to cause the necessary decrease.

The hypothesis that two separate magma types with different sources might account for the pink granite and the quartz monzodiorite suites is also supported by differing initial $^{87}Sr/^{86}Sr$ ratios. Ratios for the pink granite suite

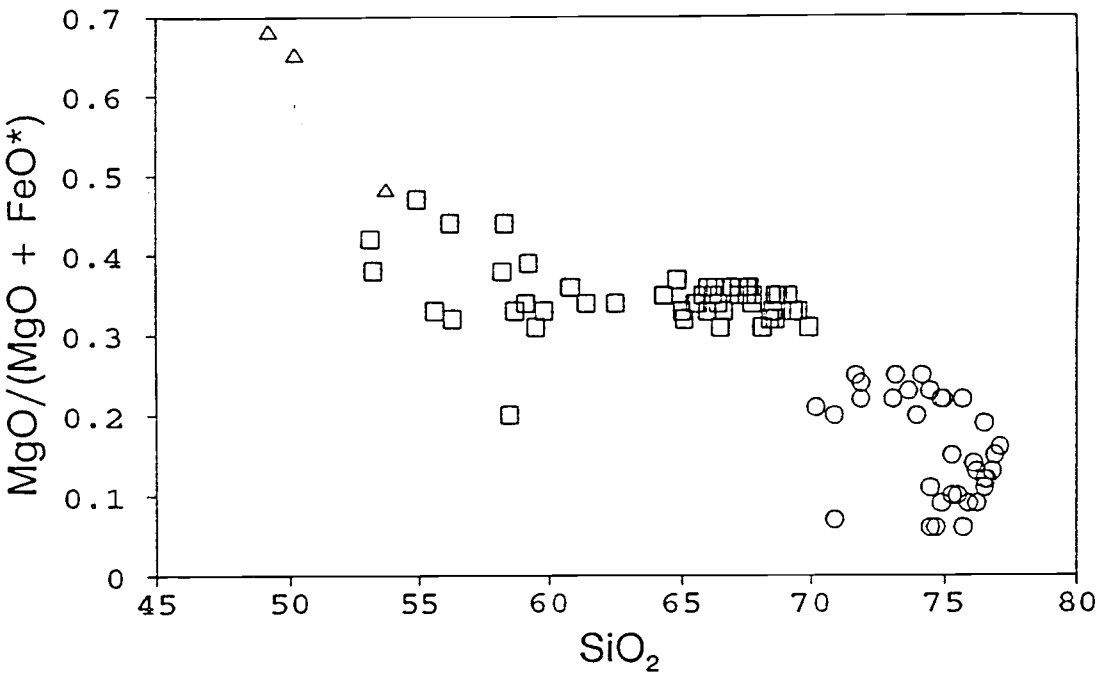

Figure 21. Plot of MgO/(MgO + FeO*) versus silica for plutonic rocks of Eocene age from central Idaho. Symbols: circles = pink granite suite; squares = quartz monzodiorite suite; triangles = cumulates.

in the eastern Soldier Mountains are higher (0.712-0.713; Table 9) than those of the quartz monzodiorite suite (0.707-0.709). These differences in the initial $^{87}Sr/^{86}Sr$ ratios are consistent with an interpretation that requires two distinct magma types (and sources) for the two rock suites.

Other workers have speculated about the relationship between the two Eocene rock suites. Luthy (1981) recognized two distinct comagmatic suites of Eocene plutons northwest of Stanley, and suggested the possibility of a single source at depth. Bennett and Knowles (1985) have interpreted them as a bimodal suite, consisting of crustally derived pink granite and a quartz monzodiorite complex of mantle origin that was partially modified by interaction with the crust. Lewis (1984) and Stewart (1987) concluded that the two suites probably represented two distinct magmas unrelated through fractional crystallization. Stewart (1987) found marked discontinuites in plots of CaO, K_2O, Rb, Sr, Zr, and Mg/Fe versus SiO_2 contents. Chemical discontinuities between the two plutonic suites are evident only on CaO, Sr, and MgO/(MgO + FeO*) plots in the present study. The absence of discontinuities on other diagrams is perhaps caused by scatter introduced by the regional compilation, and by complications induced by local mixing between the two suites, as discussed below.

Mixing between Eocene suites

It is clear from differences in initial $^{87}Sr/^{86}Sr$ ratios, and discontinuities in CaO, Sr, and MgO/(MgO + FeO*), that the two suites are not related by fractional crystallization of a single magma type. However, local mixing between magmas of the pink granite suite and the intermediate rocks of the quartz monzodiorite suite did occur. Evidence for this mixing is most pronounced in outcrops within the eastern Soldier Mountains. Pink granites of this area contain mafic inclusions, which in other exposures are rare

or absent. Their presence in the Soldier Mountains is a result of contamination as the pink granite magma was intruded into the center of a slightly older mass of biotite-hornblende granodiorite. Whether or not the pink granite contains xenoliths of the more mafic rocks, or partly mixed with a magma of the more mafic suite, is unknown. A sample of the pink granite (RL338) with sparse inclusions was analyzed and found to have a relatively low SiO_2 content (71.7 percent), probably a result of contamination. Contamination was not extensive, as overall the sample has major and trace-element concentrations similar to those of the other pink granites. Other samples of pink granite in the region with relatively low SiO_2 contents (<72 percent) also contain mafic inclusions and probably were contaminated with material from the quartz monzodiorite suite. However, the fact that inclusion-rich "hybrid" rocks are rare, combined with the lack of linear arrays of chemical data between the intermediate group and the pink granite suite on plots such as Ba versus SiO_2 (Fig. 19), indicates that contamination of the pink granites has been minimal.

Derivation of the intermediate group of the quartz monzodiorite suite by mixing of the mafic subgroup and the pink granite suite is unlikely. The intermediate group has MgO/(MgO + FeO*) ratios too high to have resulted from simple mixing (Fig. 21), and concentrations of Sr are higher in the intermediate subgroup than predicted by simple mixing of the mafic subgroup and the pink granite suite (Fig. 19).

Contamination of Eocene suites by older rocks

Contamination of the Eocene magmas by assimilation of Cretaceous plutonic rocks may have occurred locally. The foliated hornblende-biotite granodiorite unit in the Eastern Soldier Mountains contains xenoliths of rock that appear similar to the biotite granodiorite of Cretaceous age (sodic suite), and the margins of these xenoliths are diffuse.

These features are suggestive of assimilation at crustal levels now exposed. However, the contacts between the Eocene plutons and the Cretaceous granodiorites are typically sharp, indicating that high-level contamination was not extensive. The possibility of contamination of the Eocene magmas at depth with unexposed and unsampled rock types is more speculative. Isotopic data from the intermediate subgroup (initial $^{87}Sr/^{86}Sr$ ratios of 0.7069-0.7095; Table 9) suggest that these rocks have a crustal component. If parental magmas of the quartz monzodiorite suite originated in the mantle, as suggested by Lewis (1984) and Bennett and Knowles (1985) on the basis of their more mafic composition, then significant contamination had to take place at some level in the crust, particularly with respect to the intermediate subgroup.

Comparison with other granite types

Concentrations of CaO and MgO in the pink granites are low even for granites with high silica contents, and, as noted by Bennett and Knowles (1985), they are thus similar to the A-type granites of Loiselle and Wones (1979). Such A-type granites are usually mildly alkaline, and enriched in incompatable trace elements such as REE (except Eu), Zr, Y, Nb, Ga, and Ta. Loiselle and Wones (1979) have also noted depletion of Co, Sc, Cr, Ni, Ba, and Sr relative to other granite types. The composition of average pink granite is compared to those of average A-type granites from a number of localities in Table 12. Also listed are felsic I-type and felsic S-type granites from the Lachlan Fold Belt of Australia, which have SiO_2 contents similar to the A-types and can be directly compared. Concentrations of CaO, MgO, K_2O, Rb, and Sc in the pink granites are similar to those of average A-type values, but values of FeO, Fe_2O_3, Zr, Nb, Ce, and Y are lower in the pink granite, and Al_2O_3, Ba, and Sr concentrations are higher.

Although the pink granites are not as enriched in Y, Nb, Zr, and Ce as the average A-type granites, they do have compositions that are well within the range of values reported by Whalen and others (1987) for A-type granites (Table 12). These authors noted that although concentrations of Y, Nb, Zr, and Ce are high in alkaline A-type granites, the subalkaline varieties typically are less enriched in these elements. The pink granite suite also is subalkaline, and, as noted above, is not enriched in these trace elements. That the pink granites do not exhibit the strong enrichment in incompatable elements seen in the A-type granites could be a result of several factors: 1) the pink granites mayhave been derived from a source more depleted in incompatible elements than that of "average" A-type granites; 2) magmas that gave rise to the pink granites may have contained lower total alkalies and (or) been at lower temperatures than many A-type granites, which would reduce the solubility of elements such as Zr in the melt (Watson, 1979; Watson and Harrison, 1983); 3) pink granite magmas may have had a lower F content than typical A-type granites, which would reduce the ability of the highly charged cations to enter the melt during anatexis (Collins and others, 1982); and 4) removal of REE, Zr, Nb, Ta, and Y by fractional crystallization of accessory minerals, which are enriched in these elements. Some combination of the above controls are likely responsible for the lower abundance of incompatible trace elements in the pink granite suite.

The higher average Ba and Sr content in the pink granite relative to A-type granite is somewhat misleading. The content of both elements ranges widely in pink granite (Ba from 120 to 1280 ppm and Sr from 45 to 321 ppm), probably as a result of removal or accumulation of variable amounts of potassium feldspar during crystallization of the rocks.

Despite the lack of strong enrichment in Y, Nb, Zr,

and Ce in many samples of the pink granite, the suite has other characteristics of A-type granite. These include Fe-rich biotite compositions (Bennett and Knowles, 1985) and shallow emplacement levels. That pink granite magma was able to rise to shallow levels in the crust before solidification is evidence that the magma was relative dry; water-rich magma will solidify at greater depths as the water-saturated solidus is crossed (Hyndman, 1981). Exposures of A-type granite in the Lachlan Fold Belt of Australia are thought to have formed from relatively dry magma, and characteristically contain Fe-rich biotite (Collins and others, 1982).

Plutonic rocks of Eocene age in the eastern part of the Soldier Mountains exhibit more extreme compositional variations than plutonic rocks of Cretaceous age. The Cretaceous plutons contain 64 to 70 percent SiO_2 (Table 8), whereas SiO_2 in the Eocene plutons ranges from 48 to 77 percent. The intermediate group of the quartz monzodiorite suite is most similar geochemically to the Cretaceous plutons, having characteristics of both the potassic and sodic suites (Table 12). The $^{87}Sr/^{86}Sr$ ratios of the intermediate group of the quartz monzodiorite suite and the Cretaceous plutons are also similar. In the eastern Soldier Mountains, the quartz monzodiorite suite has initial ratios that range from 0.7067 to 0.7091, whereas the sodic suite ranges from 0.7070 to 0.7075 (Table 9). The only Cretaceous rock unit with a SiO_2 content comparable to the pink granite suite is two-mica granite (Table 12). However, other oxide concentrations (and trace-element contents) in the pink granite contrast greatly with those of the two-mica granite. Compared to the two-mica granite, the pink granite has a lower average concentration of Al_2O_3, CaO, Sr, Zr, and Ba, and a higher concentration of K_2O and Rb. These chemical differences between the Cretaceous and Eocene intrusive rocks require a different petrogenetic history for the two rock groups.

Origin of Eocene magmas

As discussed previously, the pink granite of south-central Idaho is similar in many respects to subalkaline examples of A-type granites. The A-type granites are thought to form as a result of partial melting of lower crustal rocks under high temperature, vapor-absent conditions (Collins and others, 1982; Whalen and others, 1987; Anderson, 1983). Such conditions would yield a relatively anhydrous melt that could rise to high crustal levels before solidifying. The initial $^{87}Sr/^{86}Sr$ ratios of pink granite in the Smoky Dome stock are elevated (0.712-0.713, Table 9) and suggestive of a crustal origin for the rock.

Experimental work by Clemens and others (1986) indicates that A-type magmas are water-undersaturated, high-temperature (>830°C), and completely molten (i.e. restite-free). Although the term "A-type" was used partly in reference to their anorogenic setting (Loiselle and Wones, 1979), Whalen and others (1987) have concluded that these types of magmas are generated in a variety of tectonic settings.

The origin of the quartz monzodiorite suite is problematic. Lewis (1984) and Bennett and Knowles (1985) have suggested that heat for generation of the pink granite suite may have come from a mantle-derived magma that underwent subsequent fractional crystallization and assimilation to form the quartz monzodiorite suite. This hypothesis is largely based on the gross spatial and temporal association of the two rock suites, and the less evolved nature of the quartz monzodiorite suite. The chemical data presented in this report are insufficient to identify a source or sources for the quartz monzodiorite suite. Some of the mafic subgroup rocks may have a significant mantle component, as suggested by their low silica content and high MgO, Sc, Co, and Cr contents (e.g. RL496, Table 11). The initial $^{87}Sr/^{86}Sr$ ratios range from 0.707 to 0.709 in the intermediate subgroup and suggest crustal input. However, isotopic data are

needed from rocks of the mafic subgroup in order to more precisely establish their source (or sources).

Summary

The two Eocene plutonic rock suites are chemically distinct. The pink granite suite has silica contents in excess of 70 percent, whereas those of the quartz monzodiorite suite range from 48 to 70 percent. The quartz monzodiorite suite is further subdivided geochemically into mafic and intermediate subgroups. On the basis of field relations, CaO and Sr content, MgO/(MgO + FeO*) ratios, and initial $^{87}Sr/^{86}Sr$ ratios, the two suites are clearly not related by fractional crystallization. However, large ranges in MgO, Sc, Cr, and Co content indicate that fractional crystallization of mafic minerals was important in controlling at least some of the chemical variability within the mafic subgroup of the quartz monzodiorite suite. Differing parental magma composition may also have contributed to diverse compositions of the mafic subgroup. A relatively large variation in Ba content of the pink granite suite probably is a result of removal or accumulation of variable amounts of potassium feldspar. These variations in trace-element concentrations in the Eocene plutons are in contrast to those in the Cretaceous plutons, which have undergone lesser amounts of fractional crystallization and lack marked variations of major and trace elements.

Mixing between the two Eocene suites has not been extensive, but some hybrid pink granites were generated which contain mafic inclusions and have SiO_2 contents of less than 72 percent. The pink granite suite has geochemical affinities with A-type granites, but is not always enriched in the incompatible elements such as Zr, Nb, Y, and Ce. By analogy to other A-type granites, the pink granite probably originated from partial melting of lower crustal rocks under high temperature, vapor-absent conditions.

HYDROTHERMAL ALTERATION

Cretaceous and Eocene plutonic rocks in the eastern part of the Soldier Mountains area have undergone varying amounts and types of hydrothermal alteration. Propylitic, potassic, and muscovite-quartz alteration are present, and are defined on the basis of secondary minerals observed in the field or in petrographic studies. The muscovite-quartz alteration is equivalent to quartz-sericite (or phyllic) alteration. A fourth type of alteration involves widespread "turbidization" of potassium feldspars in the Eocene plutonic rocks, particularly those of the pink granite unit. The only hydrothermally altered volcanic rocks are those of the Challis Volcanics, which are characteristically propylitized. Because the focus of this study concerned the alteration in plutonic rocks, the following discussion is restricted to these rock types. This study of alteration was centered on plutonic rocks in the central and northern parts of the area, as a paucity of exposures prevented adequate sampling in the southern part of the area.

The characteristics of each alteration type are summarized in Table 13. A distinction is made between mineralogic alteration, as described in this section, and isotopic alteration, described in a subseqent section, which may or may not be obvious mineralogically. This distinction is particularly important with respect to the oxygen isotopic compositions of feldspars. Feldspars that appear "fresh" petrographically have in some cases exchanged considerable amounts of oxygen without the formation of visible secondary minerals.

MUSCOVITE-QUARTZ ALTERATION

Muscovite-quartz alteration is most pronounced in the northeastern part of the area, particularly in the drainage of Grindstone Creek. This type of alteration is localized

	Muscovite-quartz	Potassic	Propylitic	"Turbidization"
distribution	localized along fractures in Cretaceous granodiorite; local quartz vein association	locally present adjacent to veins, dikes and Eocene granodiorite	common along fractures and locally pervasive in Cretaceous and Eocene units; common in vicinity of pink granite unit	pervasive in pink granite unit and to a lesser extent in quartz monzodiorite suite
mineralogy	muscovite quartz pyrite ± albite ± calcite	± K-spar ± biotite (new minerals or recrystallized preexisting minerals)	albite epidote chlorite sericite ± magnetite ± hematite(?) ± K-feldspar ± leucoxene ± calcite ± quartz ± fluorite	hematite(?) imparts pink color, but turbidity is probably a result of open spaces in feldspars
age	Cretaceous	Cretaceous and Eocene	Eocene	Eocene

Table 13. Characteristics of alteration types in the eastern part of the Soldier Mountains.

along joints and fractures, some of which are filled with vein quartz, and is restricted to rocks of the Cretaceous batholith. It differs from the weak sericitization, which affects propylitized rocks of all ages in the study area, in that the secondary mica is coarsely crystalline, typically 1 to 4 mm across. In addition to muscovite, primary and fine-grained secondary quartz are abundant. Pale pink, secondary albite is generally the only feldspar; unlike albite in the propylitized rocks, it is not turbid. Euhedral secondary pyrite is common, and protrudes into small cavities in these rocks. Calcite is present locally. Many of the weakly altered Cretacous granodiorites contain populations of both coarse- and fine-grained secondary muscovite replacing plagioclase feldspar. The coarse-grained muscovite is probably indicative of weak muscovite-quartz alteration, later overprinted by propylitic alteration which formed the fine-grained mica.

Coarse secondary muscovite is common around quartz veins throughout the southeastern part of the Idaho batholith. The fact that it is absent in the Eocene plutonic rocks suggests that this type of alteration is Cretaceous in age. One sample of this coarse muscovite from the study area was dated by the $^{40}Ar/^{39}Ar$ method and a stepwise release plateau of 70.3 Ma was obtained (see "Geochronology of Plutonic Rocks" section). This result confirms the Cretaceous age of muscovite-quartz alteration in the study area, and implies that similar alteration in the region may also be of this age.

POTASSIC ALTERATION

Potassic alteration of Cretaceous granodiorite was recognized in just three localities of the study area, and only as a result of petrographic study. Other areas are undoubtedly affected, but this type of alteration appears to be areally limited. Temperatures of alteration are high

(>400°C) because biotite and potassium feldspar are stable phases.

The most pronounced potassic alteration is at the Texas Star mine north of Camas Prairie (sample locality RL036, Plate 2). Here rocks of the coarse-grained hornblende-biotite granodiorite unit are cross-cut by widely spaced quartz veins, adjacent to which fine-grained secondary potassium feldspar has formed. The second area that underwent potassic alteration is about 100 m above the Couch Summit fault near Lawrence Creek (sample locality RL033, Plate 2). Biotite granodiorite at this locality contains finely crystalline secondary biotite and potassium feldspar. Alteration is fracture controlled, and not extensive. Small dikes of fine-grained pink granite and dacite are present in this area, and may have been the source of the potassium-rich fluids. The third locality affected by potassic alteration is on the ridge at the head of Bowns Creek (sample locality RL230, Plate 2). Here, Cretaceous biotite granodiorite collected about 75 m from the contact with Eocene biotite-hornblende granodiorite contains patches of secondary potassium feldspar and recrystallized, fine-grained biotite. The potassium feldspar has partially replaced plagioclase feldspar. Geochemical data presented in a subsequent section indicate that alteration at this locality involved high-temperature recrystallization of existing minerals, but without significant addition of potassium to the rock.

The age of the alteration at these three localities is not well constrained. Alteration and associated mineralization at the Texas Star mine may be Cretaceous in age, as Eocene plutonic rocks are some distance away. The Lawrence and Bowns Creek localities are more likely a result of Eocene alteration, especially the latter, because it is located about 75 m from a contact with Eocene granodiorite.

A variant of the potassic alteration type described above involves local enrichment of Cretaceous biotite grano-

diorite in potassium feldspar, possibly as a result of metasomatism late in the crystallization history of these rocks. The potassium feldspar is present as inclusion-rich phenocrysts and as interstitial crystals. Dikes of aplite and pegmatite are common in phenocryst-rich areas and may have been a source of potassium-rich metasomatic fluids. Chemical data presented in the previous section entitled "Geochemistry of plutonic rocks" indicate an enrichment in potassium and total alkalies in one sample of metasomatized biotite granodiorite (RL266).

PROPYLITIC ALTERATION

Propylitic alteration is by far the most prevalent alteration type within the eastern Soldier Mountains. The hydrothermally altered areas are only part of an areally more extensive altered region recognized by Taylor and Margaritz (1976, 1978), and Criss and Taylor (1983), which was defined on the basis of lowered $\delta^{18}O$ values of feldspars (+6 to -8 permil) and lowered δD values of biotites (-90 to -180 permil). These investigators demonstrated that the propylitic alteration was related to large-scale circulation of heated meteoric waters around the epizonal Eocene plutons.

The Cretaceous biotite granodiorite unit has been propylitized in many areas, but the most widely altered rocks in the study area are those of the Eocene biotite-hornblende granodiorite unit. The pink granite unit is only propylitized locally. Important alteration controls are proximity to Eocene intrusive rocks (particularly the pink granite), as well as to faults, joints, and veinlets of epidote. The altered areas are typically restricted to a few centimeters or less away from the veinlets and joint surfaces, but in some cases the alteration is pervasive over several hundred square meters. This type of alteration implies relatively low temperatures (160-325°C), based on

measurements in active geothermal systems (McDowell and Elders, 1980) and fluid inclusion studies (Kerrich and Kamineni, 1988). Mineralization in the study area does not appear to be linked to this alteration type, but rather is found in association with muscovite-quartz alteration of Late Cretaceous age.

A characteristic feature of the propylitic alteration is albitization of the plagioclase feldspar. The albite, which is generally pink, was initially mistaken for potassium feldspar. However, feldspars etched in HF and treated with sodium cobaltinitrite did not stain yellow, but remained pink. Because they did not turn chalky white, as did plagioclase feldspars of oligoclase-andesine composition, albite was suspected. Subsequent X-ray diffraction analyses verified their sodic composition. These albitized feldspars are turbid, and in thin section it is difficult to find twinned, a-normal sections that exhibit cleavage. A few were found, however, and the albitic character of the plagioclase feldspar was confirmed.

Secondary albite has been reported elsewhere in the region. Reid (1963) has described albite in altered zones of Cretaceous granodiorite several hundred yards wide adjacent to the pink granite in the Sawtooth range, 40 km north of the study area. In addition, clay, sericite, chlorite, and epidote were reported. Albite and epidote that postdate silicification and sericitization along quartz veins have been noted by Allen (1952) in the Volcano mining district, 30 km southwest of the study area. The veins reportedly cross-cut early Tertiary granophyric dikes.

The albite in the propylitized rock is unzoned and compositionally close to An_0, with d spacings matching well with the low albite d spacings reported by Smith (1974). The cause of turbidity in these feldspars is not known. Most feldspars contain small to moderate amounts of sericite, but the sericite does not appear to cloud the crystals significantly. There may be other fine-grained

constituents, such as clay, chlorite, or calcite that are causing the turbidity. Although the X-ray diffraction patterns of the feldspars lack peaks from these minerals, their presence in small amounts could go undetected. The pink color of the albite presumably results from inclusions of finely crystalline hematite, which could contribute to the turbidity as well. The X-ray diffraction patterns did not exhibit peaks for hematite, but their absence could simply be the result of only minute quantities. More likely causes of the turbidity are fluid inclusions and (or) open spaces created during replacement of more calcic plagioclase feldspar by sodic plagioclase feldspar. Open spaces have been suggested as the cause of turbidity commonly associated with potassium feldspars (Martin and LaLonde, 1979), as discussed in the following section. Turbidity, regardless of its cause, commonly indicates that the feldspars have exchanged oxygen with a fluid under subsolidus conditions (Taylor, 1967, 1968; O'Neil and Taylor, 1967). Locally, the albitized plagioclase feldspar is itself partially replaced by potassium feldspar, although secondary potassium feldspar is generally confined to veinlets. Minor epidote, in addition to albite and sericite, has replaced the plagioclase feldspars.

Potassium feldspar appears to be less affected by the propylitic alteration than plagioclase feldspar. However, in a few localities, turbid "pinked-up" potassium feldspar is present. Epidote and more rarely chlorite also formed as secondary minerals after potassium feldspar. Where altered, the turbidity of the potassium feldspar increases, but not to as great an extent as that of albitized plagioclase feldspar. Regardless of feldspar type, those that are pink in color are more turbid than those that are gray.

Another diagnostic characteristic of propylitization is the destruction of biotite. It has been replaced by chlorite, and lesser amounts of epidote, sphene, sericite, and leucoxene. As recognized by Criss (1981), chloritization of

biotite has been widespread in the southern lobe of the batholith. Magnetite appears to be largely unaffected by the propylitic alteration, except in some of the most strongly propylitized samples. Disseminated magnetite, in some cases, may be of secondary origin. Magnetite does not directly replace chloritized biotite, a relationship noted throughout the region by Criss and Champion (1984). Hornblende is replaced by chlorite and epidote, but has been less affected by hydrothermal alteration than biotite. Sphene has been altered to leucoxene and, in strongly propylitized rocks, epidote, as was allanite. Not unexpectedly, apatite and zircon resisted alteration.

Boone (1969), in a study of a granite porphyry in eastern Canada, found zones with phenocrysts of red albite which graded into areas with gray phenocrysts of oligoclase-andesine. Chlorite was abundant in the rocks containing red albite, but sparse in the gray porphyries. Boone attributed the red color of the albite to inclusions of hematite formed during concurrent breakdown of biotite and albitization of plagioclase feldspar under relatively oxidizing conditions. Similar reactions and conditions may have been responsible for the pink color of the albitized feldspars in the eastern Soldier Mountains. The biotite in albitized areas is invariably chloritized, and was a likely source of iron needed for the formation of hematite.

Epidote veinlets, typically 2 mm or less in width, are another common feature of the propylitized rocks. Most veinlets are entirely filled, but some contain central cavities into which euhedral epidote has grown. Plagioclase feldspar is preferentially albitized adjacent to these veinlets. Magnetite and potassium feldspar are present as subordinate minerals within the epidote veinlets. The presence of secondary magnetite within veinlets may in part explain the variability in magnetic susceptability of altered rocks in the southern part of the Idaho batholith which was documented by Criss and Champion (1984). As with

hematite in the feldspars, secondary magnetite probably results from the breakdown of biotite and the subsequent release of iron. Potassium feldspar in the veinlets is typically anhedral, and has poorly developed grid twins. Rarely, it forms euhedral rhombs, characteristic of adularia. Sericite, albite, chlorite, quartz, and fluorite are also found in the epidote veinlets, but they are of negligible abundance. Calcite is found locally and is more common in rocks that do not contain appreciable epidote.

The presence of secondary albite indicates an enrichment of sodium in these rocks, which is borne out by major-element oxide data presented in a subsequent section. Calcium, displaced by the formation of albite, went to form epidote, and less commonly, calcite. Calcium was also removed from some of the rocks during propylitic alteration, as demonstrated in a subsequent section.

The presence of epidote, magnetite, and hematite (as probable inclusions in albite) indicate that the fluids were relatively oxidizing. It is curious that both hematite and magnetite appear to be present. Because the magnetite is largely confined to veinlets, perhaps the paragenetically latest fluids were less oxidizing than the earlier fluids responsible for the pink color of the albite. Alternatively, the fugacity of oxygen may have been near the equilibrium boundary between hematite and magnetite.

"TURBIDIZATION" OF EOCENE FELDSPARS

A clear correlation exists between turbidity and the pink color of the feldspar. Except for local phenocrysts with gray cores, all of the potassium feldspar in the Eocene granite is pink and turbid. The gray cores of phenocrysts are less turbid than the pink rims. Potassium feldspar in the Eocene quartz monzodiorite suite is either gray or pink, and plagioclase feldspar in all of the Eocene rocks is white, and less turbid than the potassium feldspar.

Cretaceous granodiorites contain gray to pale pink potassium feldspar which is less turbid than potassium feldspar in the Eocene rocks.

The turbidity and pink color of the potassium feldspar in the Eocene rocks, particularly the pink granite, is a pervasive feature not related to large-scale faults or joint surfaces. Martin and LaLonde (1979) have suggested that turbidity in potassium feldspar results not from mineral inclusions, but from open spaces produced by reconstitution of a feldspar in the presence of water. They suggest that reconstitution and concomitant volume decrease can result from 1) anisotropic thermal contraction; 2) exsolution; 3) nucleation of strain-free potassic domains; 4) increase in Si-Al order; or 5) removal of matter by dissolution. Any of these causes could explain why the potassium feldspar in the Eocene plutons are more turbid than plagioclase feldspar in the same rocks. However, dissolution and reprecipitation of new feldspar may have been key factors, based on oxygen isotopic systematics presented in a following section. The important point is that the feldspars appear to have interacted with a pervasive fluid phase which affected potassium feldspar more so than plagioclase feldspar. This process caused (or enhanced) the turbid nature and pink color of the potassium feldspar. Turbid areas of the feldspars are cross-cut by microfractures which probably facilitated alteration by enhancing fluid access. The less-turbid (and more gray) potassium feldspars in the Cretaceous granodiorites apparently had little or no interaction with this type of fluid. The higher level of emplacement of the Eocene plutons relative to their Cretaceous counterparts may have facilitated both an increased porosity and greater availability of meteoric waters, thus promoting "turbidization". The pink color of the feldspars presumably has resulted from inclusions of hematite, and indicates that fluids were relatively oxidizing. The pervasive character of the "turbidization" suggests that access by fluids was

along grain boundaries and microfractures, not large-scale fractures. In contrast, albitized plagioclase feldspar in the Cretaceous rocks, though also pink and turbid, formed only adjacent to fractures and veinlets. Space for fluid movement in the Eocene plutons may have been enhanced by volume reduction of quartz during transition from ß to α polymorphs (about 4.3 percent, Robie and others, 1967). This process, suggested by Ferry (1985) for similarly "turbidized" granites on the Isle of Skye, would result in the crystals of quartz and feldspar pulling apart from one another, thus increasing permeability. Ferry (1985) estimated a temperature of 350-400°C for formation of turbid alkali feldspar in the granites of Skye on the basis of compositions of coexisting feldspars. Compositional data that could be used to make temperature estimates are not available for the plutons in Idaho. However, because low temperature mineral assemblages (i.e. propylitic assemblages) are generally not present in the turbidized samples, turbidization probably took place at temperatures in excess of 350°C.

SUMMARY OF ALTERATION HISTORY

Local potassium metasomatism was probably the first type of alteration to form in the area. This process is believed to have occurred late in the crystallization history of the Cretaceous biotite granodiorite, and may have been a subsolidus phenomenon. The first structurally controlled alteration event took place at about 70 Ma as rocks of the Idaho batholith cooled, and hydrothermal fluids migrated along fractures to form alteration selvages of quartz and muscovite. Veins of quartz were also developed along some of these fractures at this time. Following a period of uplift, hydrothermal activity resumed in Eocene time, concurrent with the intrusion of epizonal plutons. Potassic alteration occurred locally, but propylitization was the

predominant and widespread alteration type. Propylitic alteration around the youngest of these plutons (the pink granites) was particularly pronounced, and the rocks of both Eocene and Cretaceous plutons were affected. Faults and joint surfaces served as conduits for fluid circulation. Concurrent(?) movement of heated oxygenated fluids within the cooling plutons of pink granite caused "turbidization" of potassium feldspar, which simultaneously imparted an overall pink color to these rocks. The fluids involved in this process were hotter (perhaps 350-400°C) than those associated with the peripheral propylitic zone, and movement of the fluids was along grain boundaries and microfractures rather than along the larger through-going structures. Processes of hydrothermal alteration in the area appear to have been negligible since Eocene time, as is consistent with the absence of subsequent plutonic activity.

MOBILITY OF MAJOR AND TRACE ELEMENTS

Whole-rock analysis of 12 granodiorite samples was undertaken to characterize the chemical changes caused by hydrothermal alteration in the eastern part of the Soldier Mountains. The results, listed in Table 14, are grouped by pairs of "less altered" and "more altered" samples. Each pair was collected from either the same outcrop, or from nearby outcrops. Also included are two samples (RL307, RL389) for which a less altered equivalent was not collected. All of the samples were from the sodic suite of Late Cretaceous age. Sample locations are noted on Plate 2.

One problem with the study of chemical changes during alteration is estimating the original composition of the host rock. Enough variability is present between unaltered rocks of the sodic suite that there is not a single "starting point" for reference (e.g. TiO_2 ranges from 0.73 to 0.36 percent in unaltered samples, Table 8). The less altered and more altered pairs of samples in Table 14 represent an

	Propylitic								Muscovite-quartz		Potassic	
	weak	strong	weak	strong	mod	mod	strong	mod	mod*	strong	weak+	weak
	RL225	RL224	RL275	RL311	RL307	RL322	RL323	RL389	RL321	RL168	RL279	RL230
	major-element oxides in weight percent											
SiO_2	67.0	64.7	66.0	65.9	63.9	67.1	67.7	72.3	69.7	70.0	69.1	69.8
TiO_2	0.68	0.71	0.76	0.69	0.79	0.58	0.54	0.18	0.41	0.42	0.42	0.39
Al_2O_3	16.0	16.3	16.4	15.8	16.2	15.8	15.1	14.0	15.0	13.6	15.2	15.2
Fe_2O_3	1.31	2.12	1.61	2.13	1.73	1.72	1.77	1.38	1.29	1.67	1.20	1.30
FeO	1.90	1.50	2.02	1.26	2.54	1.53	1.26	0.12	1.13	0.42	1.19	1.12
MnO	0.04	0.05	0.05	0.05	0.07	0.04	0.04	0.03	0.03	0.05	0.03	0.04
MgO	1.12	1.26	1.34	1.17	1.93	1.18	1.15	0.23	0.74	0.65	0.82	0.71
CaO	3.90	3.07	4.12	3.31	4.23	3.58	3.13	1.55	2.26	2.94	2.99	2.71
Na_2O	3.61	4.03	3.67	4.01	3.65	3.59	4.37	3.63	3.58	2.17	3.31	3.66
K_2O	2.52	3.80	2.58	2.23	2.51	3.05	2.97	3.95	3.09	3.57	3.43	3.62
P_2O_5	0.23	0.24	0.24	0.24	0.25	0.20	0.18	0.06	0.14	0.14	0.14	0.14
H_2O^+	0.56	1.67**	0.62	2.02	1.32	0.61	0.94	1.12**	2.44	0.44	0.55	0.60**
H_2O^-	0.27	–	0.20	0.35	0.28	0.15	0.17	–	0.11	1.31	0.16	–
CO_2	<0.01	0.18	<0.01	<0.01	0.10	<0.01	0.03	<0.01	0.38	2.12	0.01	0.01
total	99.2	99.6	99.6	99.2	99.5	99.1	99.4	98.6	100.3	99.5	98.6	99.3
A/CNK#	1.01	1.00	1.00	1.05	0.99	1.00	0.94	1.07	1.12	1.06	1.04	1.02
SG##	2.66	2.63	2.66	2.58	2.67	2.65	2.66	2.58	2.59	2.62	2.64	2.64
	trace elements in parts per million											
Sc	4.5	4.6	8.5	3.2	–	3.9	3.7	–	3.3	3.3	–	–
Cr	5.0	5.2	5.8	4.8	–	7.4	5.7	–	5.2	3.6	–	–
Co	4.1	4.6	4.9	4.1	–	4.5	3.9	–	2.8	0.67	–	–
Rb	89	182	99	68	79	89	74	150	89	195	105	108
Sr	745	889	719	597	939	789	682	453	743	134	745	735
Y	14	16	15	14	19	12	11	8	15	15	10	14
Zr	208	227	223	222	195	232	227	132	221	236	184	211
Nb	20	22	21	20	18	19	19	21	18	26	17	18
Sb	0.18	0.08	0.18	0.29	–	0.09	0.13	–	0.18	0.16	–	–
Cs	1.6	1.5	2.0	1.8	–	1.8	0.77	–	1.7	2.9	–	–
Ba	1390	1820	1280	1360	–	1590	1540	–	1510	973	–	–
La	56	66	51	55	–	82	62	–	59	56	–	–
Ce	120	130	120	130	–	160	130	–	120	120	–	–
Nd	40	42	42	43	–	39	34	–	37	38	–	–
Sm	7.1	7.3	7.5	7.0	–	5.8	5.0	–	6.3	6.2	–	–
Eu	1.6	1.7	1.7	1.6	–	1.3	1.1	–	1.4	1.5	–	–
Tb	0.66	0.64	0.71	0.65	–	0.47	0.51	–	0.50	0.51	–	–
Yb	1.5	1.6	1.6	1.4	–	1.3	1.2	–	1.1	1.1	–	–
Lu	0.17	0.18	0.18	0.16	–	0.13	0.11	–	0.12	0.11	–	–
Hf	6.2	6.6	6.9	6.0	–	6.6	6.1	–	6.1	6.8	–	–
Ta	1.7	1.7	2.0	1.6	–	1.4	1.3	–	1.2	1.6	–	–
Th	12	14	12	15	–	19	16	–	15	15	–	–
U	2.9	2.7	3.1	2.1	–	2.7	2.5	–	2.2	2.3	–	–
B	–	–	–	–	–	–	–	–	–	–	–	3.0

* Sample has undergone moderate propylitic alteration and weak muscovite-quartz alteration
\+ Sample has undergone weak propylitic alteration and lacks potassic alteration
** Loss on ignition at 900°C
\# Molecular $Al_2O_3/(CaO+Na_2O+K_2O)$
\#\# Specific gravity

Table 14. Major- and trace-element analyses of altered plutonic rocks of Cretaceous age from the eastern part of the Soldier Mountains. All samples are from the biotite granodiorite unit of the sodic suite except RL307, which is from the hornblende-biotite granodiorite unit of the sodic suite. Analysts: J. Taggart, A. Bartel, D. Siems, C. Papp, E. Brandt, N. Elsheimer, and J. Evans.

attempt to match rocks that were once similar in composition. Specific gravities of the more altered rocks vary by less than 3.2 percent with respect to the less altered rocks (Table 14), and thus weight percent values (rather than g/100 cm^3) are used for comparison of samples.

Effects of propylitic alteration

Three strongly propylitized samples were analyzed (Table 14). Two of the samples (RL311 and RL323) are typical of propylitized rocks in the area in that they contain abundant secondary albite, chlorite, and epidote. The third sample (RL224) differs in having a cataclastic texture and numerous veinlets of potassium feldspar. The two more typical samples have undergone similar changes in chemical composition, and will be used in the following discussion to characterize element mobility during propylitic alteration.

The effects of strong propylitic alteration on major-element oxide concentrations are illustrated in Figure 22. Oxide values of the more altered samples are plotted against oxide values of less altered samples. The latter are assumed to represent starting compositions. The dashed 1:1 line on this diagram represents identical starting and ending compositions; those oxides which plot below the 1:1 line have increased in amount during alteration whereas those that plot above the 1:1 line have decreased in amount during alteration. Also plotted is an envelope on either side of the 1:1 line. Oxide values that plot within this envelope differ by less than 10 percent in altered versus unaltered samples. Any changes in excess of this amount are assumed to be more than those expected from either analytical error or inhomogeneity between rock samples.

Concentrations of CaO and FeO decreased by more than 10 percent in both RL311 and RL323 as a result of strong propylitic alteration (Fig. 22). In sample RL311 both MgO and K_2O decreased. Concentrations of H_2O^+, Na_2O, and Fe_2O_3

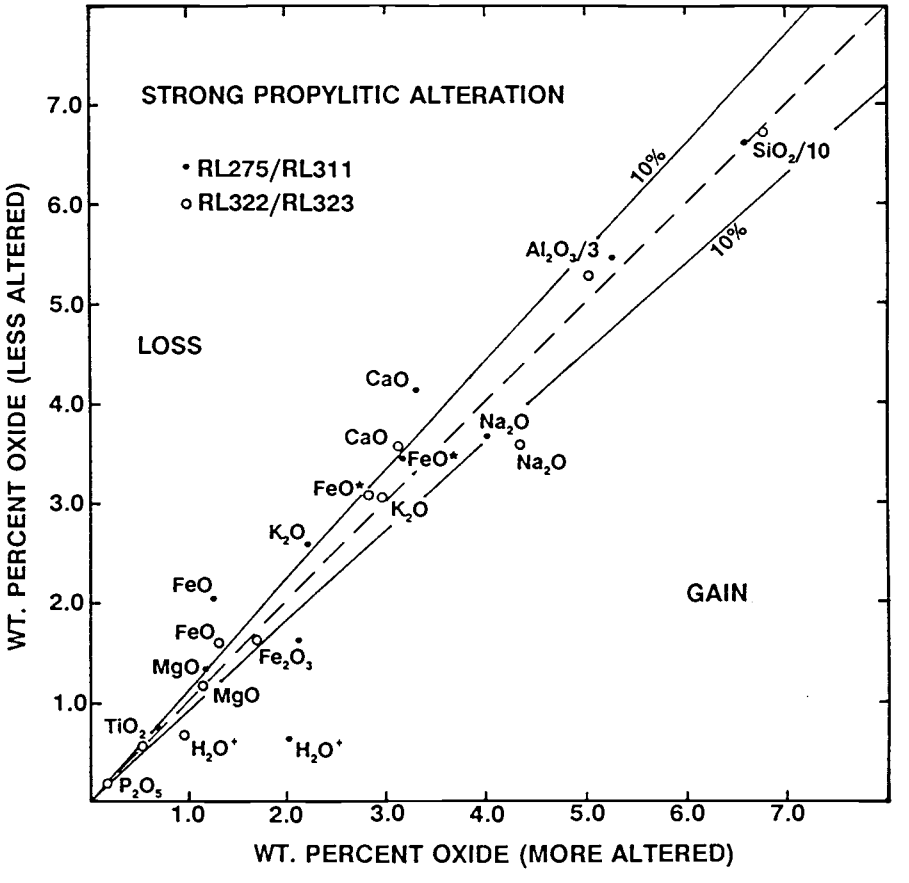

Figure 22. Plot of oxide concentrations of strongly propylitized samples versus those of equivalent less altered samples.

increased in both strongly propylitized samples. Concentrations of SiO_2, Al_2O_3,FeO* (total Fe as FeO), TiO_2, and P_2O_5 vary by 10 percent or less in the more altered versus the less altered rocks. The decrease in CaO and the increase in Na_2O reflect the replacement of oligoclase-andesine by albite. The decrease in MgO in RL311 is likely related to the destruction of biotite, and the reduction in K_2O in this sample is probably a reflection of the partial replacement of potassium feldspar by albite and the destruction of biotite. The increase in H_2O^+ in both RL323 and RL311 has resulted from the formation of hydrous secondary minerals. Decreases in FeO and increases in Fe_2O_3 are a result of oxidation during alteration. In summary, the elements Si, Al, Fe, Ti, and P were relatively immobile during conditions of strong propylitic alteration, whereas Ca, Na, and K were mobile.

A simple base exchange equation that describes the process of albitization is as follows:

sodic andesine → albite

(1) $Na_2CaAl_4Si_8O_{24} + 2Na^+ + 4SiO_2 \Rightarrow 4NaAlSi_3O_8 + Ca^{++}$

Alternatively, both epidote and albite may have formed at the expense of sodic andesine, as described by equation (2). This is a type of hydrolysis reaction in which H^+ is produced.

sodic andesine → epidote + albite

(2) $Na_2CaAl_4Si_8O_{24} + 2.5SiO_2 + Na^+ + 0.5Fe^{+++} + 1.5H_2O \Rightarrow 0.5Ca_2FeAl_2Si_3O_{12}(OH) + 3NaAlSi_3O_8 + 2.5H^+$

In those instances where both potassium feldspar and oligoclase-andesine were replaced (by albite and sericite), a hydrolysis reaction such as (3) may best describe the alteration process.

K-feldspar + sodic andesine → muscovite + albite + quartz

(3) $KAlSi_3O_8 + Na_2CaAl_4Si_8O_{24} + 2H^+ \Rightarrow KAl_3Si_3O_{10}(OH)_2 + 2NaAlSi_3O_8 + Ca^{++} + 2SiO_2$

Equations (1) and (2) require input of Na^+, and equations (1) and (3) require a loss of Ca^{++}. These requirements are consistent with major-element data presented in Figure 22. Equation (2) also requires the input of Fe, which was probably mobilized during the alteration of biotite to chlorite, as represented in equation (4).

$$(4)\quad \underset{\text{biotite}}{2K(Mg,Fe)_3AlSi_3O_{10}(OH)_2} + 4H^+ \Rightarrow \underset{\text{chlorite}}{Al(Mg,Fe)_5AlSi_3O_{10}(OH)_8} + (Mg,Fe)^{++} + 2K^+ + \underset{\text{quartz}}{3SiO_2}$$

The pink color of the secondary albite in the propylitized rocks is presumably a result of hematite inclusions. As discussed in a previous section, the breakdown of biotite to form chlorite is a probable source for the Fe necessary to form hematite. A likely hematite-forming reaction, discussed in detail by Boone (1969), is given in equation (5).

$$(5)\quad 2Fe^{++} + 3H_2O \Rightarrow \underset{\text{hematite}}{Fe_2O_3} + H_2 + 4H^+$$

Figures 23a and 23b illustrate the effects of strong propylitic alteration on trace-element concentrations. These diagrams are similar to Figure 22, except that the scale is logrithmic. A 10 percent envelope is plotted as before. Losses in excess of 10 percent are noted for Sr, Rb, Cs, Cr, Co, and Lu in both RL311 and RL323. The only significant gains are those of Th and Sb in RL311. The elements Y, Zr, Nb, Ba, Hf and Ta appear to have been relatively immobile. The decrease in Sr, Rb, and Cs parallels decreases in CaO and K_2O contents and probably relates to the replacement of oligoclase by albite and biotite by chlorite. The loss of Cr and Co probably reflects the breakdown of biotite and the partial destruction of magnetite during strong propylitic alteration, as does the depletion in Sc in RL311. The behavior of the REE during propylitic alteration in the eastern Soldier Mountains is problematic. Alteration of sample RL311 did not significantly affect the REE, but in RL323 the LREE (La, Ce, Nd, Sm and

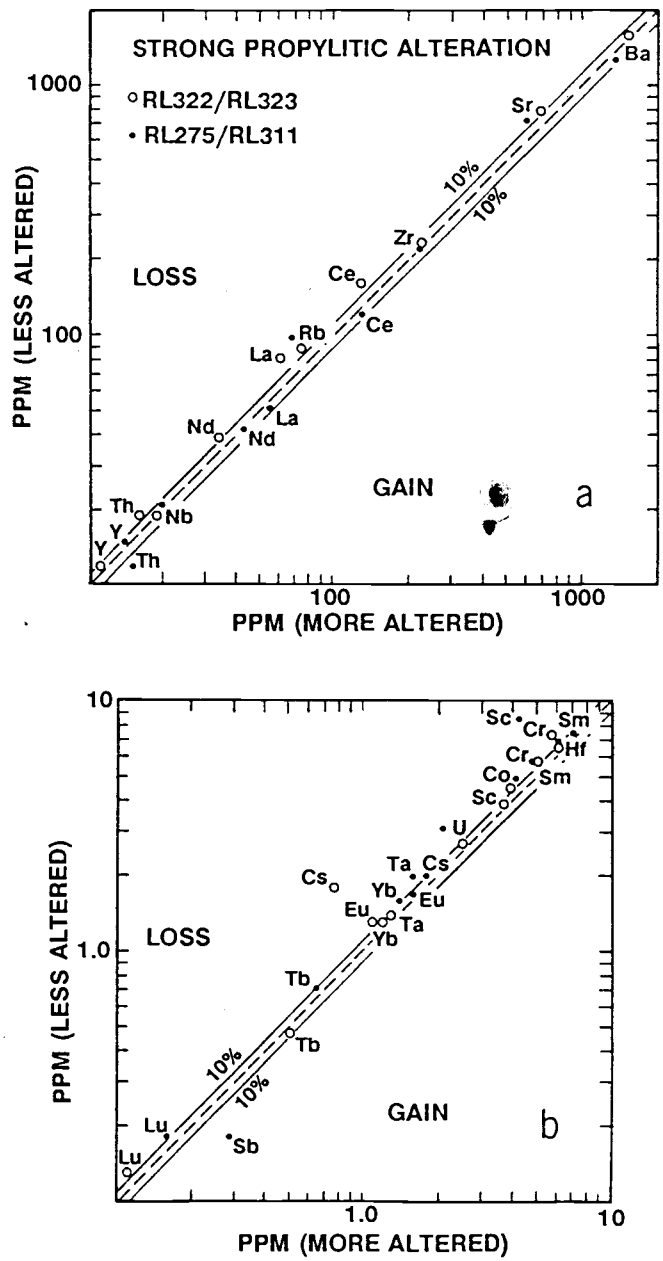

Figure 23. Plots of trace-element concentrations of strongly propylitized samples versus those of equivalent, less altered samples; (a) trace elements with concentrations of >10 ppm; (b) trace elements with concentrations <10 ppm.

Eu) appear to have been depleted relative to the LREE in the less altered equivalent collected 10 meters away (RL322). Allanite and sphene are the LREE-rich phases present in these rocks. Both are present in RL323, but they appear to have been partially replaced by epidote during hydrothermal alteration. The textural evidence for replacement is equivocal, but epidote is present along the margins of many crystals of sphene and allanite. Partial replacement of the sphene and allanite is the most likely cause of LREE depletion in RL323. The REE elements are typically immobile during hydrothermal alteration, but Baker (1985) has reported lowered LREE in an albitized granite in south-central Sweden and Alderton and others (1980) have reported lowered LREE in chloritized granites in southwest England.

Effects of muscovite-quartz alteration

The effects of muscovite-quartz alteration on major-element oxide concentrations are depicted in Figure 24. Deviation from the 1:1 line is more pronounced than was found with the propylitic alteration, which indicates greater element mobility under the conditions of muscovite-quartz alteration. Concentrations of Na_2O, FeO*, FeO, and H_2O^+ decreased, whereas concentrations of CaO, K_2O, Fe_2O_3 and CO_2 increased. The decrease in Na_2O has resulted from replacement of oligoclase-andesine by muscovite and quartz, and the decrease in FeO* is a reflection of replacement of biotite and magnetite. The decrease in H_2O^+ is opposite to what might be expected for this alteration type. It probably has resulted from comparison to an artificially high H_2O^+ value for the less altered equivalent, sample RL321, which is moderately propylitized. Increases in CaO, CO_2, and K_2O have resulted from the presence of calcite and muscovite, and the increase in Fe_2O_3 is a reflection of oxidation during alteration.

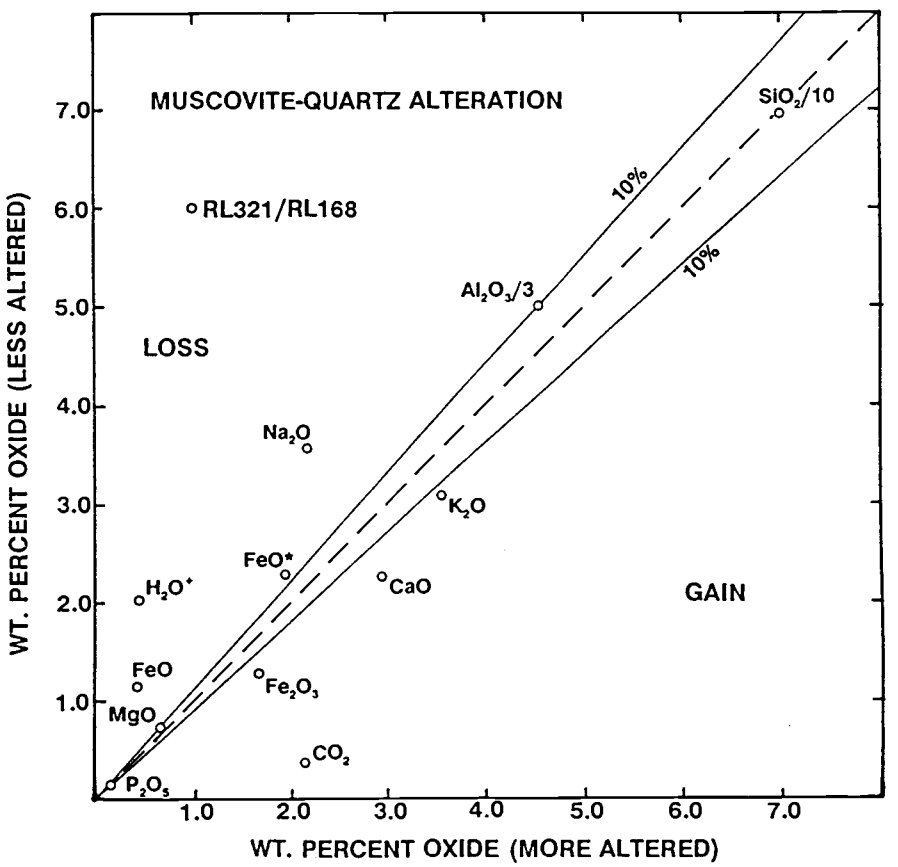

Figure 24. Plot of oxide concentrations following muscovite-quartz alteration versus those of an equivalent, less altered sample.

Changes in mineralogy are more pronounced with muscovite-quartz alteration than with propylitic alteration. Both the potassium feldspar and the oligoclase-andesine in these rocks have been replaced by muscovite, quartz, albite, and calcite. Hypothetical equations that describe the replacement process are as follows:

K-feldspar → muscovite + quartz

(6) $3KAlSi_3O_8 + 2H^+ \Rightarrow KAl_3Si_3O_{10}(OH)_2 + 2K^+ + 6SiO_2$

sodic andesine → muscovite + quartz

(7) $3Na_2CaAl_4Si_8O_{24} + 8H^+ + 4K^+ \Rightarrow 4KAl_3Si_3O_{10}(OH)_2 + 6Na^+ + 12SiO_2 + 3Ca^{++}$

K-feldspar + sodic andesine → muscovite + albite + quartz

(8) $KAlSi_3O_8 + Na_2CaAl_4Si_8O_{24} + 2H^+ \Rightarrow KAl_3Si_3O_{10}(OH)_2 + 2NaAlSi_3O_8 + Ca^{++} + 2SiO_2$

calcite

(9) $Ca^{++} + HCO_3^- \Rightarrow CaCO_3 + H^+$

All four equations involve hydrolysis reactions. In the first three equations H^+ is consumed, and in the fourth equation H^+ is produced. A reaction such as equation (7) would account for the loss in Na_2O and gain in K_2O that occurred during muscovite-quartz alteration. The Ca^{++} produced by equations (7) and (8) would be available to form calcite, but additional Ca^{++} also had to be added to the rock according to the sample analysis.

The effects of muscovite-quartz alteration on trace element concentrations are depicted in Figures 25a and 25b. Losses in excess of 10 percent are noted for Sr, Ba, Co, and Cr. The loss of Sr and Ba is probably a result of the breakdown of oligoclase and potassium feldspar. The decrease in Sr content is opposite the behavior of CaO, which increased. Apparently the Sr was not incorporated to any great extent in the secondary calcite. The reduction in Co and Cr during muscovite-quartz alteration is probably a reflection of the breakdown of magnetite.

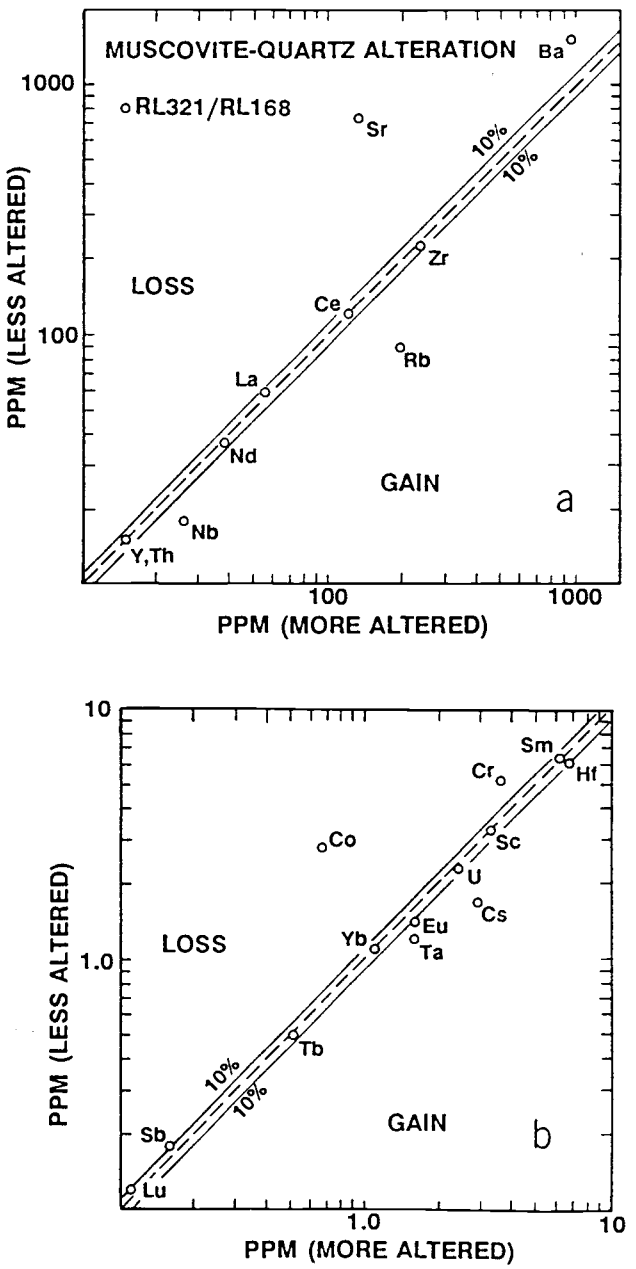

Figure 25. Plot of trace-element concentrations following muscovite-quartz alteration versus those of an equivalent, less altered sample; (a) trace elements with concentrations of >10 ppm; (b) trace elements with concentrations <10 ppm.

Gains in excess of 10 percent are noted for Rb, Cs, Nb, Ta, and Eu. The increase in Rb and Cs parallels that of K_2O, and corresponds to the abundance of secondary muscovite. The increase in Eu parallels that of CaO, and suggests that Eu is more likely than Sr to partition into calcite under conditions of muscovite-quartz alteration. The increase in Nb and Ta during the alteration process is of uncertain origin.

Effects of potassic alteration

The effects of potassic alteration on major-element oxide concentrations are depicted in Figure 26. Gains and losses are 10 percent or less for all of the oxides, including K_2O. The alteration of RL230 apparently involved recrystallization under high-temperature (biotite-stable) conditions, but with little mobility of the major elements. Despite the lack of potassium enrichment in this sample, the term potassic alteration is applied because the potassium-bearing minerals biotite and potassium feldspar were stable. Only a limited number of trace elements were determined in RL230 (Table 14). The concentrations of those analyzed, as with the major elements, were not significantly affected by the potassic alteration.

OXYGEN ISOTOPES

Oxygen-isotope ratios of 58 mineral separates and 7 whole-rock samples from the eastern part of the Soldier Mountains were measured in order to: 1) determine the extent of interaction of hydrothermal fluids with granitic rocks in the study area, 2) relate changes in isotopic ratios to alteration type, and 3) ascertain the source (or sources) of the hydrothermal fluids. Although rocks of both Cretaceous and Eocene age are altered, the relatively uniform mineral and chemical compositions of the Cretaceous units provide a

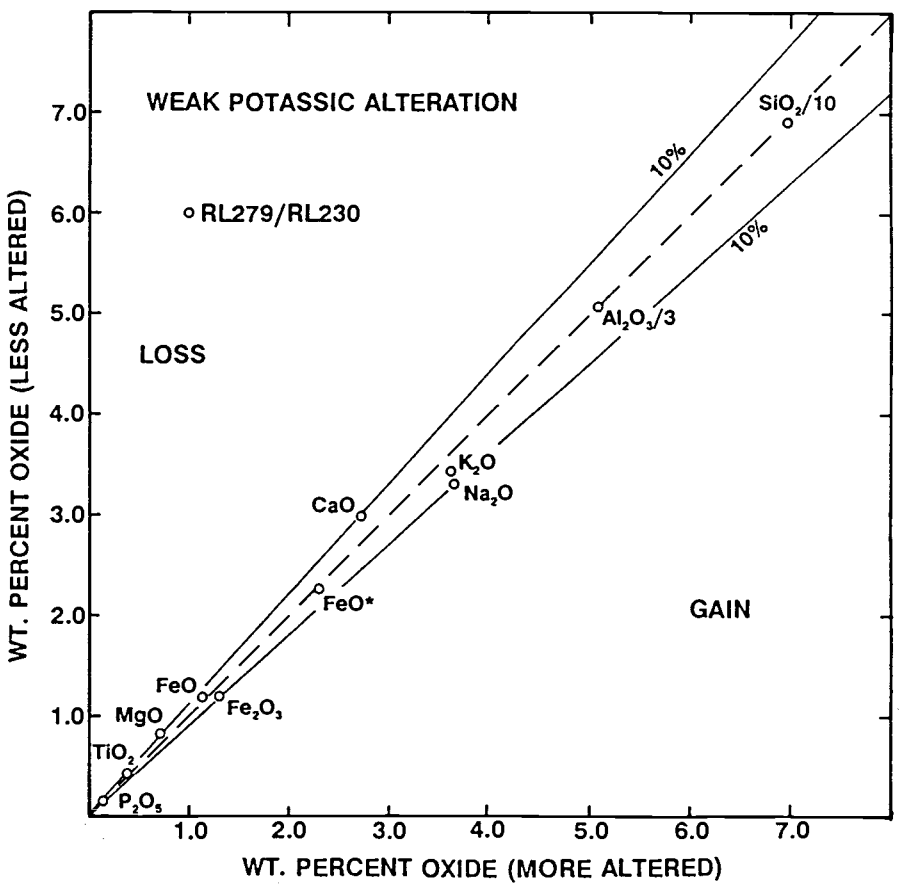

Figure 26. Plot of oxide concentrations following weak potassic alteration versus those of an equivalent less altered sample.

better background against which the effects of alteration can be measured. Thus, most of the samples collected were of Cretaceous plutonic rocks.

Methods

Rock samples were about 1 kg in size, with compositions that ranged from unaltered to strongly altered. These samples were crushed to 4 to 16 mesh and the minerals hand-picked into quartz "concentrate", plagioclase feldspar "concentrate" and so forth. Each concentrate was then crushed in a mortar and pestal to 16 to 32 mesh and impure grains picked out under a binocular microscope. The fine-grained secondary minerals contained in the feldspars were not separated. Also, the potassium feldspar contained small inclusions of plagioclase feldspar, about 5 volume percent, which could not be separated by this method. X-ray diffraction analysis of the feldspar separates indicated that minor amounts of quartz were present, but secondary hydrous minerals (sericite and epidote) were not abundant enough to form distinguishable peaks.

Oxygen extraction was carried out by the author and by Mary Horan at U.S. Geological Survey laboratories in Reston, Virginia. Oxygen was extracted using chlorine trifluoride in vessels heated to 550°C for 12 to 16 hours. The oxygen was reacted with a heated carbon rod, and the resultant CO_2 was analyzed for isotopic ratios with a mass spectrometer by U.S. Geological Survey personnel.

Results

Oxygen-isotope data on mineral separates and whole-rock samples are listed in Table 15, and plotted by alteration type in Figure 27. Results are reported in typical δ notation, which represents deviation in $^{18}O/^{16}O$ ratios from standard mean ocean water (SMOW), measured in parts per

	unaltered				weak propylitic							
	Kgd RL244	Kgd RL263	Kgd RL266	Kgdh RL278	Kgd RL154	Kgd RL210	Kgd RL219	Kgd RL225	Kgd RL249	Kgd RL275	Kgd RL279	Kgdh RL309
	$\delta^{18}O$ in permil											
quartz	–	–	9.5	10.1	–	9.8	10.2	10.8	10.0	10.9	10.4	10.3
K-feldspar	9.0	–	8.2	8.2	4.2	6.7	6.6	5.6	7.6	–	7.5	7.6
alt. K-spar*	–	–	–	–	–	–	–	–	1.0	–	–	–
oligoclase	9.0	–	8.2	8.0	3.9	6.8	7.4	–	5.6	8.4	7.2	7.8
albite	–	–	–	–	–	–	–	–	–	–	–	–
feldspar	–	8.3**	–	–	–	–	–	–	–	–	–	–
bt/chl***	–	–	–	–	–	–	–	0.6	–	-3.9	–	–
2° muscovite	–	–	–	–	–	–	–	–	–	–	–	–
whole rock	–	–	–	–	–	–	–	4.7	4.8	–	–	–
whole-rock (calculated)	9	8	8	7	5	7	8	–	–	8	8	7

	moderate propylitic			strong propylitic			weak potassic	musc-quartz		Eocene rocks+	
	Kgd RL321	Kgd RL322	Kgd RL389	Kgd RL224	Kgd RL311	Kgd RL323	Kgd RL230	Kgd RL168	Kgd RL232	Tg RL293	Tgd RL299
	$\delta^{18}O$ in permil										
quartz	11.1	9.9	9.4	–	6.4	8.7	10.2	11.6	–	–	9.1
K-feldspar	7.1	1.7	–	–	–	-3.5	8.6	–	–	4.4	6.7
alt. K-spar*	–	–	–	–	–	–	–	–	–	–	–
oligoclase	5.4	-1.4	–	–	–	-2.0++	8.5	–	–	5.7	6.0
albite	–	–	–	–	-4.7	-3.2	–	–	–	–	–
feldspar	–	–	–	–	–	–	–	–	–	–	–
bt/chl***	–	–	–	–	–	-11.3	–	–	–	–	–
2° muscovite	–	–	–	–	–	–	–	7.7	8.0	–	–
whole-rock	6.4	1.1	–	-5.7	–	-1.4	–	8.4	–	–	–
whole-rock (calculated)	–	–	–	–	-1	–	8	–	8#	6	6

* "pinked-up" K-feldspar adjacent to fractures
** potassium feldspar > plagioclase feldspar
*** mixture of biotite and chlorite
\# assumed to be similar to RL168
\+ RL293 = turbidized and weakly propylitized
RL299 = weakly propylitized
++ partly albitized

Kgd = biotite granodiorite
Kgdh = hornblende-biotite granodiorite
Tg = pink granite
Tgd = biotite-hornblende granodiorite

Table 15. $\delta^{18}O$ values of plutonic rocks and their constituent minerals from the eastern part of the Soldier Mountains.

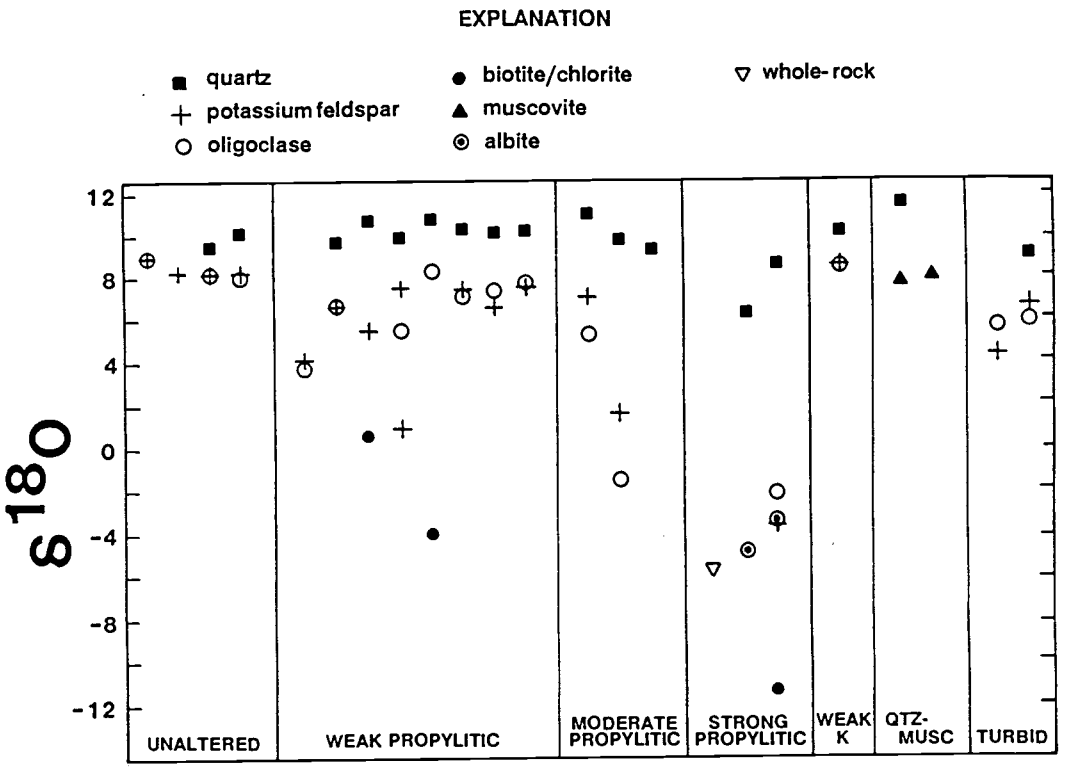

Figure 27. Oxygen-isotope data on mineral separates and whole-rock samples from the eastern Soldier Mountains plotted by alteration type.

thousand (permil). Analytical precision of the values is within ± 0.2 permil. The $\delta^{18}O$ values of rocks and minerals collected within the study area by Criss (1981) and Criss and Fleck (unpub. data, with permission) are listed in Table 16. Sample locations are on Plate 2.

The Cretaceous and Eocene plutonic rocks in Table 15 and Figure 27 are categorized as: 1) unaltered, with high $\delta^{18}O$ feldspar values (8.0 to 9.0 permil) and pristine composition as determined by thin section study; 2) weakly propylitized, with slightly lowered $\delta^{18}O$ feldspar values (8.4 to 3.9 permil) and pristine to slightly altered composition (mostly chloritized); 3) moderately propylitized, with lowered $\delta^{18}O$ feldspar values (7.1 to -1.4 permil) and epidote, chlorite and sericite common; 4) strongly propylitized, with extreme ^{18}O depletion in feldspars (values of -2.0 to -4.7 permil) and albite, epidote, secondary potassium feldspar and chlorite pervasive; 5) weakly potassically altered (recrystallized under biotite-stable conditions) without a change in $\delta^{18}O$ values; and 6) samples strongly altered to muscovite and quartz with a minor increase in $\delta^{18}O$ values of quartz (to 11.6 permil). The sample of Eocene pink granite is "turbidized", and weakly propylitized. It has $\delta^{18}O$ values of plagioclase feldspar (5.7 permil) and potassium feldspar (4.4 permil) that are lower than those of about 8 permil for unaltered Eocene feldspars reported by Criss and Taylor (1983).

Effects of propylitization on minerals

Quartz in the study area has primary (magmatic) $\delta^{18}O$ values averaging about 10.2 permil, identical to those that Criss and Taylor (1983) found for average primary quartz throughout the southern lobe of the batholith. Quartz from the one sample of Eocene granodiorite has a slightly lower value of 9.1 permil. In strongly propylitized rocks, such as RL323 and RL311, the quartz is 8.7 and

Criss (1981)

	unit	quartz	feldspar	K-spar	biotite	whole-rock	calculated whole-rock#
			$\delta^{18}O$ in permil				
RB180a	Kgdh	–	-3.8	–	–	–	0
RH88	Kgdh	9.8	-1.1	–	–	–	2
RH86	Kgd	–	8.8	–	–	–	8
RH85b	Tfgd	–	2.3	–	–	–	3
RH85d	Tfgd	–	–	-0.8	-2.3	–	1
RB167	Tgd	–	6.0	–	–	–	6
RH83	Tgd	–	-0.5	–	–	–	1
RB163	Tgd	–	-5.8	–	–	–	-2
RB169a	Kgd	–	8.7	–	–	–	8

Criss and Fleck (unpublished data)

	unit	quartz	feldspar	K-spar	biotite	whole-rock	calculated whole-rock#
87715G	Tgd	–	–	–	–	2.2	–
87715H	Tgd	–	–	–	–	4.6	–
87715I	Tgd	–	–	–	–	-4.7	–
87715F	Kgd	–	–	–	–	4.8	–

calculated using average modal abundances from Table 1 and assuming quartz = 10.2 permil in Cretaceous units and 9.1 permil in Eocene units

Kgdh = hornblende-biotite granodiorite unit; Kgd = biotite granodiorite unit; Tfgd = foliated hornblende-biotite granodiorite unit; Tgd = biotite-hornblende granodiorite unit

Table 16. $\delta^{18}O$ data of other investigators from plutonic rocks in the eastern part of the Soldier Mountains. Unpublished data of R.E. Criss and R.F. Fleck used with permission.

6.4 permil, indicating reaction with heated low-^{18}O waters. The only water capable of such depletion is meteoric water, which in the region today has $\delta^{18}O$ values that range from -15 to -20 permil (Taylor, 1979), and which is estimated to have been about -15 permil during Eocene time in central Idaho (Criss and Taylor, 1983). Quartz is known to resist isotopic exchange, but extensive reaction with low ^{18}O meteoric waters (i.e. high water/rock ratios), or reaction at high temperatures, will eventually lower the $\delta^{18}O$ values of coexisting quartz. Both of the samples with ^{18}O-depleted quartz were collected within fault zones, the presence of which would have allowed ready access of large volumes of meteoric water.

Potassium feldspar and plagioclase feldspar in unaltered granodiorites have $\delta^{18}O$ values that are 1.3 to 2.1 permil less than coexisting quartz, which is consistent with fractionation at relatively high temperatures. Because the fractionation factor for quartz-potassium feldspar is not agreed upon, it is difficult to accurately estimate a temperature from the quartz-feldspar data, or to assess possible disequilibrium between the two. If the fractionation curves of Botinga and Javoy (1973) are used, the $\Delta_{qtz\text{-}feld}$ values between 1.3 and 2.1 represent temperatures between about 600 and 400°C. The primary fractionation between the plagioclase (average composition about An_{28}) and potassium feldspar cannot be discerned. This is not unexpected, because the fractionation should only be about 0.2 to 0.4 permil between 600 and 400°C (O'Neil and Taylor, 1967).

Unaltered feldspars have $\delta^{18}O$ values of 8.0 to 9.0 permil. Propylitized rocks contain oligoclase that ranges from 8.4 permil down to -1.4 permil, and albitized plagioclase feldspar that ranges from -2.0 to -4.7 permil; potassium feldspar values are as low as -3.5 permil. Criss (1981) found feldspars in the study area with $\delta^{18}O$ values as low as -5.8 permil (Table 16). Clearly the feldspars have exchanged with low-^{18}O fluids (i.e. meteoric water) during

propylitic alteration.

A plot of $\delta^{18}O$ feldspar versus $\delta^{18}O$ quartz in Figure 28 illustrates the relative amount to which quartz and feldspar have exchanged oxygen during propylitic alteration. A reference line with $\blacktriangle_{qtz\text{-}feld}$ of 2 permil is included, which approximates primary, unaltered values. A field is shown which contains the data from Criss and Taylor (1983) for the Atlanta lobe of the Idaho batholith. There is a general agreement between the two sets of data for the propylitized samples, although feldspars in the study area do not reach the extremely low values (down to -8.2 permil) of some of the samples collected by the previous investigators.

Isotopic effects caused by propylitic alteration are first toward lower $\delta^{18}O$ in feldspar, and then reduction of $\delta^{18}O$ in quartz in the most altered samples. This trend is consistent with numerous isotopic studies in which feldspars were found to have exchanged oxygen more readily than quartz. Sample RH14a was left out of the field of Criss and Taylor (1983) because it contains quartz abnormally low in ^{18}O relative to feldspar. This is a sample of Cretaceous granodiorite collected near a contact with Eocene pink granite of the Twin Springs pluton. It is the only sample in their data set for which secondary biotite is reported, and thus it should be considered separately from the propylitized samples. Temperatures during alteration of this rock were high enough for biotite to be stable, and yet meteoric-dominated waters lowered $\delta^{18}O$ values of the component minerals. Quartz appears to have been less resistant to depletion at these temperatures than in the lower temperature propylitic regime.

All of the biotites analyzed contain at least a small amount of chlorite, and all have been shifted to lower $\delta^{18}O$ values. One sample of essentially pure chlorite has an extremely low $\delta^{18}O$ value of -11.3 per mil (RL323). Albite and potassium feldspar in this sample have respective $\delta^{18}O$ values of -3.2 and -3.5 permil. The -11.3 permil value is

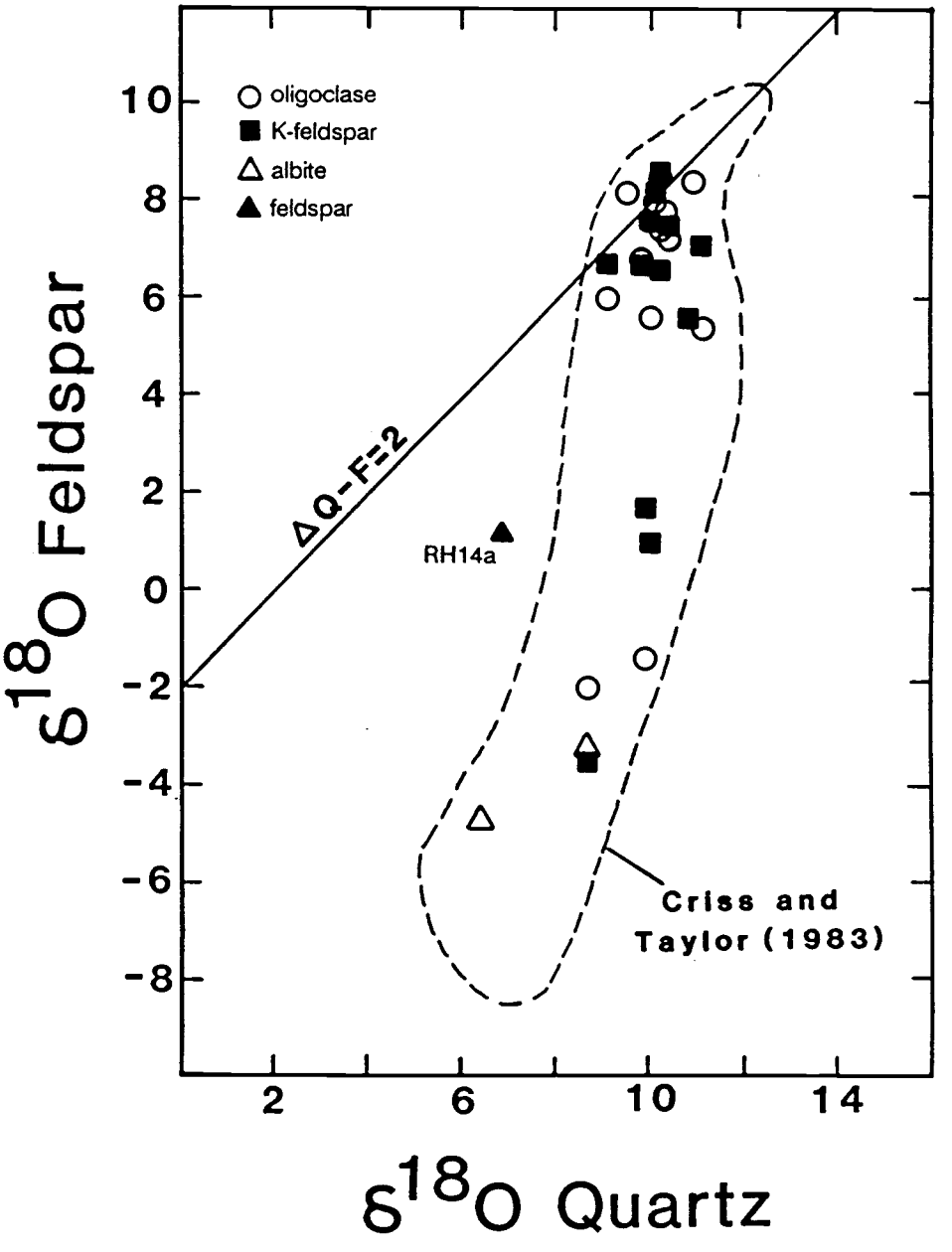

Figure 28. Plot of $\delta^{18}O$ feldspar versus $\delta^{18}O$ quartz in plutonic rocks from central Idaho. All individual samples are from this study except RH14a, which is from Criss and Taylor (1983).

lower than any chlorite analyzed by Criss and Taylor (1983) in rocks to the west and north, which ranged mostly from -2 to -8. Using fractionation data of O'Neil and Taylor (1967), water in equilibrium with the albite and potassium feldspar would be about -10 permil, assuming a temperature of 250°C. Criss and Taylor (1983) estimated a $\delta^{18}O$ value of -15 permil for meteoric water in the Atlanta lobe during Eocene time, but thought that those waters had been shifted to about -9 to -3 by interaction with wallrocks. The -10 permil value based on albite-water equilibrium is considered a rough approximation of the composition of some of the isotopically least-shifted hydrothermal waters in the study area during Eocene time. The lack of a strong shift in isotopic composition of the water at sample locality RL323 is explained by high water/rock ratios within the fault zone.

The amount to which ^{18}O was depleted in the propylitized rocks is a function of the initial isotopic composition of the water and rock, temperature, water/rock ratio, and the extent to which equilibrium was achieved. Calculations of approximate water/rock ratios can be made following the method outlined by Taylor (1979). Given the following assumptions: 1) a closed system with an initial $\delta^{18}O$ value of 8 permil for the rock and -15 permil for the water; 2) a temperature of 250°C; and 3) a $\Delta_{rock\text{-}water}$ fractionation equal to that of andesine-water (6.3 permil), water/rock ratios of 0.2, 0.9, and 3.5 (atom percent oxygen) were calculated for rocks with final $\delta^{18}O$ rock values of 5, 0, and -5 permil. The -5 permil value approximates the extremely ^{18}O-depleted samples present within fault zones in the study area. Thus, variable water/rock ratios of 0.2 to 3.5 can account for much of the range in $\delta^{18}O$ values in the propylitized rocks. Temperature probably played less of a role in controlling the final $\delta^{18}O$ values of the altered rocks. By changing temperature from 250°C to 350°C in the calculation, and maintaining a water/rock ratio of 0.9, the final rock compo-

sition only changes from 0 to -1 permil. The extent to which equilibrium was achieved is another important factor, and is discussed in detail in a following section.

Spatial relations of ^{18}O depletion

The spatial relationships of ^{18}O depletion are illustrated in Figure 29, which is a simplified geologic map of the northern part of the study area. Whole-rock values determined analytically are plotted, as are calculated whole-rock values. The calculated values are based on measured $\delta^{18}O$ values of quartz and feldspar and modes of the respective samples. Mafic minerals are assumed to have $\delta^{18}O$ values of 0 permil. The estimated whole-rock $\delta^{18}O$ values are only approximate, but they allow comparisons of a larger data set than is possible with the feldspar values alone.

It is clear from Figure 29 that both Cretaceous and Eocene granodiorites have been affected by exchange with low-^{18}O waters. The one sample of Eocene granite has undergone moderate exchange as well. Note also that three samples of Cretaceous granodiorite collected within 100 m of contacts with Eocene granodiorite do not show $\delta^{18}O$ depletion ($\delta^{18}O$ of 8-9 permil). This indicates that meteoric water did not circulate near the margins of the Eocene granodiorite pluton at these localities. Circulation of meteoric waters was either insignificant, or farther out from the contact. Although typically not propylitized, some rocks adjacent to the Eocene granodiorite pluton contain secondary biotite and have undergone weak potassic alteration (e.g. sample RL230) as is discussed in a following section.

The absence of meteoric-hydrothermal alteration adjacent to rocks of the Eocene quartz monzodiorite suite is evident elsewhere in the region. A sample of Cretaceous granodiorite collected 40 m from the contact with the Pearl-Horseshoe Bend diorite contains feldspar with a primary $\delta^{18}O$ value of 9.0 permil (sample RB161f; Criss, 1981). In

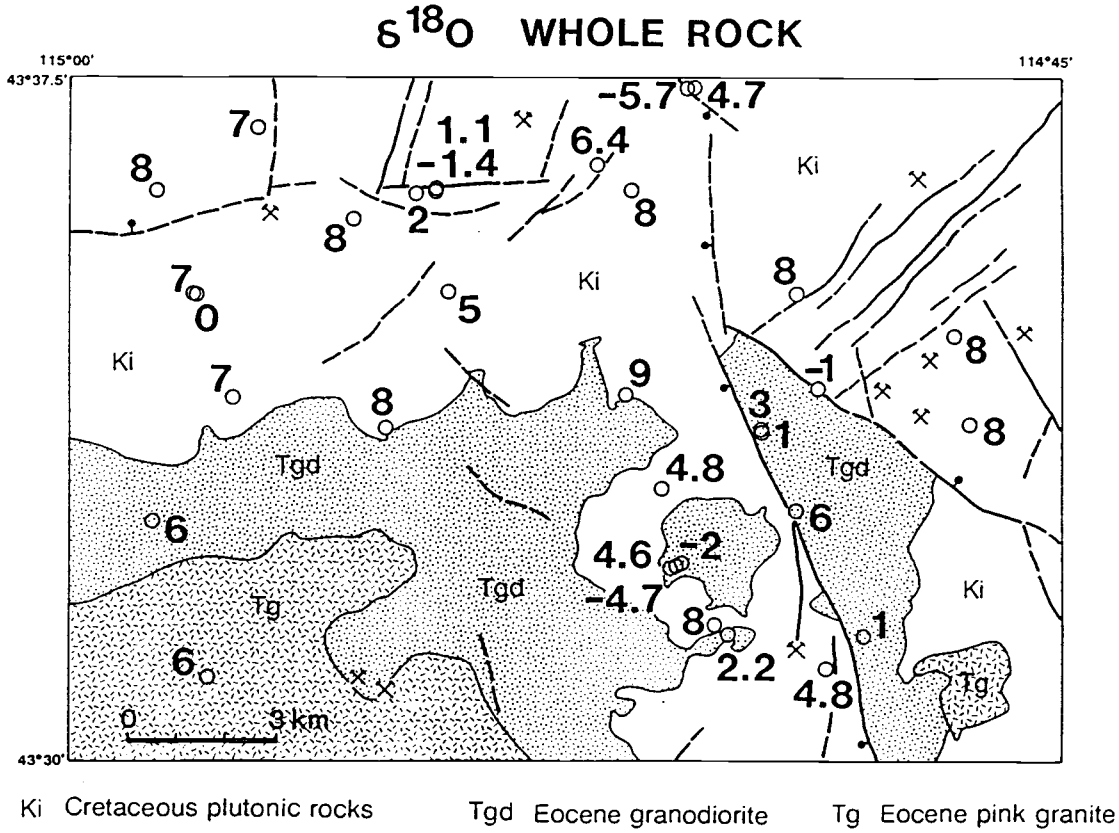

Figure 29. Simplified geologic map of the northern part of the study area showing locations of whole-rock $\delta^{18}O$ values.

contrast, Criss and Taylor (1983) demonstrated a positive correlation between plutons of pink granite and zones of meteoric-hydrothermal activity. This relationship is also observed in the study area, where the most widely propylitized rocks are those that rim the pink granite stock of Smoky Dome (i.e. the Eocene biotite-hornblende granodiorite unit). The adjacent Eocene granodiorites have whole-rock $\delta^{18}O$ values as low as -4.7 permil, indicative of extensive isotopic alteration.

In order to evaluate the importance of structural control on fluid movement and alteration, samples were collected within fault zones that contain altered rock (i.e. pre- or syn-alteration faults) and from nearby, less faulted and less intensely altered outcrops of the same rock unit. The $\delta^{18}O$ values of minerals and (or) whole-rock samples of these paired samples are plotted in Figure 30. All of the rocks have undergone ^{18}O depletion, but the rockswithin the fault zones show much greater amounts of depletion (e.g. whole-rock $\delta^{18}O$ values of -5.7 versus 4.7 permil in RL224 and RL225). This structural control of fluid movement, and thus locally steep $\delta^{18}O$ gradients, makes itimpossible to contour the isotopic data accurately at the density of present sampling. Also illustrated in Figure 30 is the amount of disequilibrium of a single mineral type at hand-sample scale. Less intensely altered, and more intensely altered ("pinked-up") potassium feldspars from the same sample (RL249) were analyzed and found to vary by 6.6 permil. The "pinked-up" potassium feldspar was present only along fractures in this rock. Thus, large amounts of disequilibrium are present at both hand-specimen and outcrop scale.

Effects of propylitization and "turbidization" on coexisting feldspars

Although numerous studies have outlined the isotopic

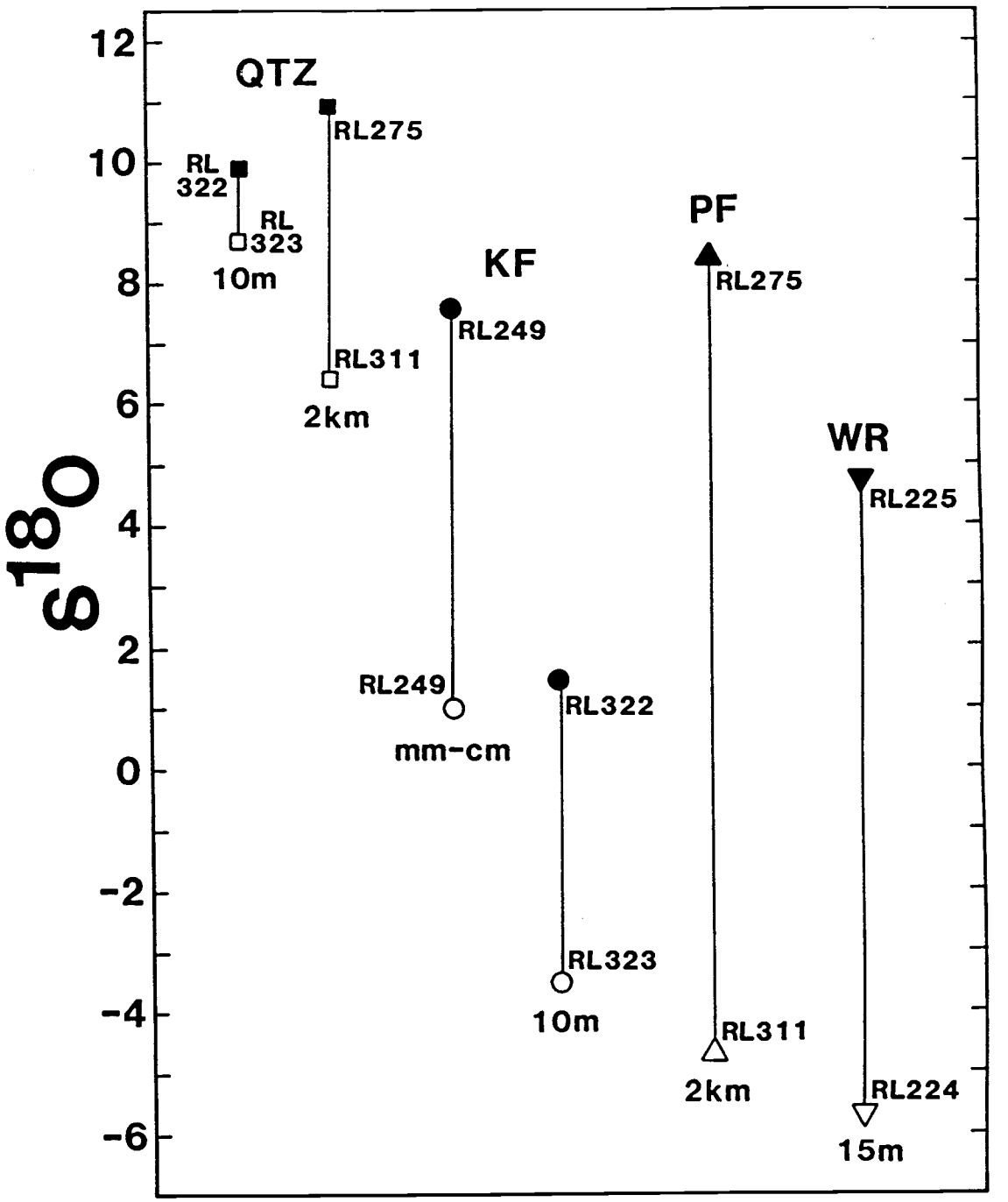

Figure 30. $\delta^{18}O$ values of whole-rock samples and minerals collected within (open symbols) and away from (filled symbols) faults and fractures. Distance between samples is listed below each pair. QTZ = quartz; KF = potassium feldspar; PF = plagioclase feldspar; WR = whole-rock sample.

effects of hydrothermal alteration on quartz and feldspar, few data exist for the isotopic values of coexisting potassium and plagioclase feldspar. In this study, the two feldspars were separated from several samples, and the results illustrated with a δ-δ plot in Figure 31. A 1:1 line, representing equilibrium conditions (neglecting the small fractionation factor between potassium feldspar and oligoclase), is included for reference. Feldspars from the study area range from having nearly identical $\delta^{18}O$ values (in the four freshest rocks), to variations up to 3.1 permil (RL322). The "pinked-up" potassium feldspar in RL249, discussed previously, was not plotted in this diagram because it was not evenly distributed throughout the sample. Included on this diagram is the one sample from Criss and Taylor (1983) in which potassium feldspar and plagioclase feldspar were analyzed separately (RH43a). The feldspars vary by 3.6 permil in this sample of propylitized Cretaceous granodiorite collected west of the study area.

Isotopic disequilibrium is indicated by those feldspar pairs that plot off of the 1:1 line. The two periods during which disequilibrium could develop are: 1) during initial cooling; and 2) during a later event that disturbed the isotopic system. Disequilibrium induced by cooling is an important consideration for plutonic rocks, given their relatively slow cooling rates. As noted by Javoy (1977), each mineral in a rock should behave almost independently upon cooling, because each has a different diffusion coefficient and diffusion activation energy. Quartz, for example, has an oxygen diffusion coefficient three orders of magnitude lower than potassium feldspar at 500°C (Giletti, 1986). When cooling from high temperatures, quartz and potassium feldspar will exchange oxygen at different rates, and cease exchanging at different temperatures. Although quartz and potassium feldspar may not be in equilibrium after slow cooling, a similar discrepancy is unlikely to prevail between pairs of coexisting plagioclase and potassium

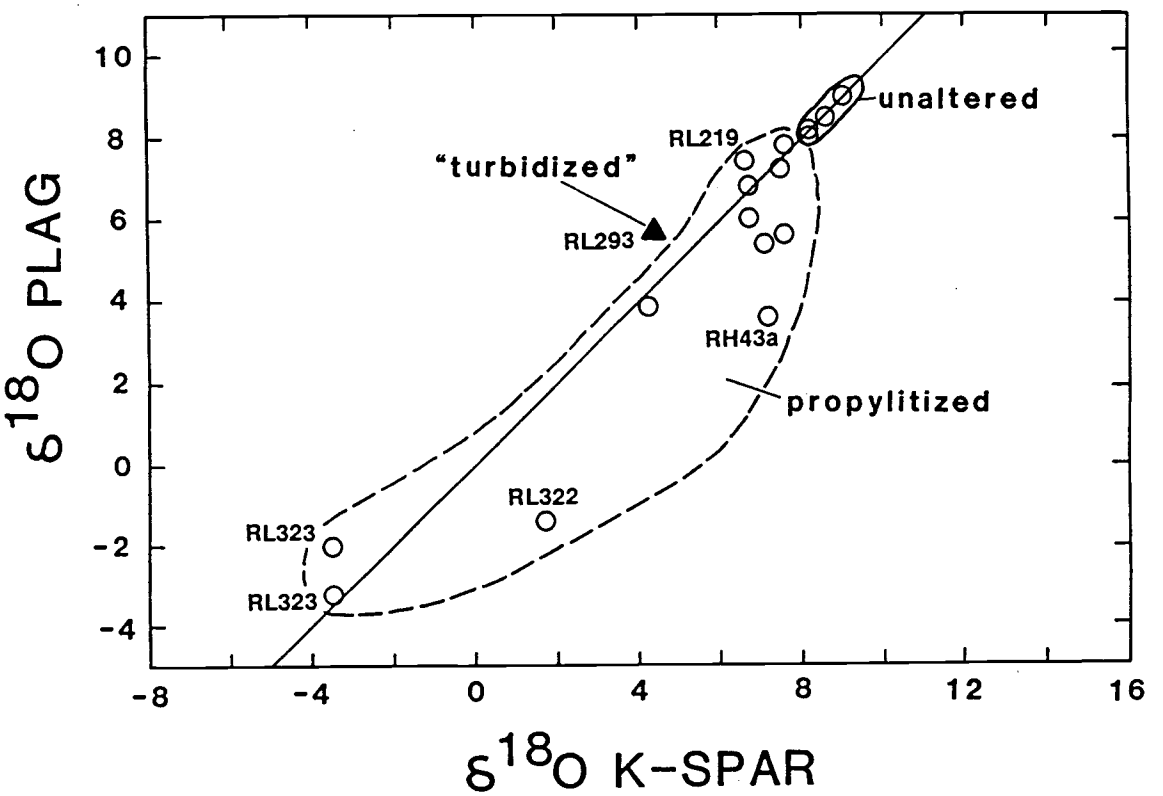

Figure 31. δ-δ plot of coexisting plagioclase and potassium feldspar of plutonic rocks from the study area.

feldspar. The diffusion rates of oxygen are similar between the feldspars (see compilation by Yund, 1983), and, thus, slow cooling should not produce significant differences between the two. Note also that disequilibrium is reflected by pairs with $\delta^{18}O$ values lower than normal feldspar values (<8.0 permil), which is suggestive of an open system in which low-^{18}O water of meteoric origin circulated.

Six samples plot below the 1:1 line (RL154, RL299, RL249, RL321, RL322, and RH43a), with plagioclase feldspar more depleted in ^{18}O than potassium feldspar. This relationship is not unexpected, because plagioclase feldspar in the propylitized samples appears more susceptable to replacement by hydrous secondary minerals (chiefly sericite and epidote) than potassium feldspar. These secondary minerals should be in isotopic equilibrium with the hydrothermal fluids present during their formation, which in this case was ^{18}O-depleted meteoric water. However, extreme depletion of ^{18}O in plagioclase feldspar is not accompanied by an abundance of hydrous secondary minerals, and in fact they are insignificant volumetrically. X-ray diffraction patterns of the plagioclase feldspar in RL322 indicate that it is nearly pure oligoclase, yet it has a $\delta^{18}O$ value of -1.4 permil. In this case, oxygen has clearly exchanged in the feldspar lattice. Isotopically similar characteristics prevail for potassium feldspar in this rock, although it is not as depleted as the plagioclase feldspar. Petrographically, the potassium feldspar in all of the propylitized rocks appears largely unaffected by alteration, except for minor clouding, yet it has $\delta^{18}O$ values as low as -3.5 permil. Similar observations have been made regarding potassium feldspars adjacent to Main-stage veins at Butte (Garlick and Epstein, 1966). Although only slightly turbid, they have $\delta^{18}O$ values as low as -0.6 permil, clearly indicating exchange of oxygen in the feldspar lattice without significant formation of secondary minerals.

The lowest $\delta^{18}O$ values of feldspar in the eastern

Soldier Mountains are those of secondary albite (RL323 = -3.2 permil; RL311 = -4.7 permil). This albite was probably in equilibrium with coexisting meteoric-hydrothermal fluid, and reflects complete cation exchange, as well as oxygen exchange. The correlation between cation and oxygen exchange is in accord with experimental results of O'Neil and Taylor (1967), which clearly showed enhanced oxygen exchange in feldspars when Na (or K) was also exchanging.

Under conditions of extreme propylitization (probably indicative of high water/rock ratios) potassium feldspar and plagioclase feldspar eventually achieved a state of near-isotopic equilibrium. Apparently this condition was reached in RL323, with coexisting potassium feldspar and pink albite (about An_5) having values of -3.5 and -3.2 permil, respectively. White and slightly more calcic plagioclase feldspar (about An_{11}) in the same rock is slightly heavier at -2.0 permil, and probably represents less intensely altered crystals that had not fully reached equilibrium with the hydrothermal fluid and coexisting potassium feldspar. Whereas plagioclase and potassium feldspar eventually approached equilibrium, this condition was not attained for quartz, regardless of the degree of propylitization.

Three samples plot above the 1:1 line in Figure 31, indicating isotopically heavier plagioclase feldspar than potassium feldspar (RL293, RL323, and RL219). In RL293 both feldspars are depleted in ^{18}O relative to the expected value of about 8 permil (plagioclase = 5.7 permil and potassium feldspar = 4.4 permil). Because both feldspars in the this sample of pink granite have lowered $\delta^{18}O$ values, it is likely that they exchanged oxygen with water that was at least partly meteoric in origin. The heavier plagioclase feldspar was anticipated, because the sample is of Eocene granite in which the pink potassium feldspar is more turbid than coexisting white plagioclase feldspar. Taylor (1967, 1968) and O'Neill and Taylor (1967) have noted the tendency for turbid feldspars to have exchanged oxygen. Additional

analyses are needed to confirm the lower $\delta^{18}O$ values of potassium feldspars in the pink granites, but these preliminary results indicate that the effects of "turbidization" on coexisting feldspars is opposite that of propylitization (i.e. potassium feldspar exchanges oxygen more readily than plagioclase feldspar during "turbidization"). The presence of one population of plagioclase feldspar in RL323 that plots above the 1:1 line probably results from these crystals having not fully equilibrated with the hydrothermal fluids, as discussed previously. The other sample that plots above the 1:1 line is more difficult to interpret. Plagioclase feldspar in RL219 has slightly higher $\delta^{18}O$ values than potassium feldspar, but is no less turbid than the potassium feldspar. The reason for this minor amount of disequilibrium is unknown.

In disequilibrium situations the relative exchange rates of oxygen in the two feldspars apparently differed. In cases where plagioclase feldspar has lower $\delta^{18}O$ values than potassium feldspar, its relative exchange rate was faster, probably reflecting a lower stability during alteration. Where potassium feldspar has the lower values, it was the least stable. The relative stability of the feldspars is determined to a large extent by temperature, which has a controlling effect on the composition of the hydrothermal fluid in equilibrium with the feldspars. Experimental work by Orville (1963) in the system $KAlSi_3O_8$-$NaAlSi_3O_8$-NaCl-KCl-H_2O indicates that the proportion of K to Na+K in the vapor phase that coexists with two alkali feldspars decreases with falling temperatures. Thus, at high temperatures K is partitioned into the vapor, and albite stability is favored over potassium feldspar; cooler temperatures stabilize potassium feldspar. This applies to both a diffusional process (Orville, 1963) and fluid transport process (Hemley and others, 1971). In the latter, a fluid equilibrated with two alkali feldspars will, upon migration to a cooler environment, produce potassic alteration. The exper-

imental work on the plagioclase system is not as complete, especially with regard to the effects of solid solution on feldspar stability. However, in general, a decrease in temperature stabilizes Na-feldspar relative to Ca-feldspar (Hemley and others, 1971, 1980; Orville, 1972). Thus, in the common case of rocks containing both potassium and plagioclase feldspar (oligoclase), albite may be stabilized at either higher or lower temperatures. These relationships are summarized as follows:

	High temperature	Low temperature
alkali feldspar	lower Na/K in fluid and albite stablized	higher Na/K in fluid and K-feldspar stablized
Ca-Na feldspar	lower Ca/Na in fluid and Ca-feldspar stablized	higher Ca/Na in fluid and albite stabilized

The temperature dependence of feldspar stability can be applied to hydrothermally altered rocks in the study area. The pink granite feldspar pair that plots above the 1:1 line in Figure 31 (i.e. potassium feldspar least stable) was probably subjected to alteration by fluids moving up a temperature gradient (a prograde process). This prograde alteration would stabilize plagioclase at the expense of potassium feldspar. Turbidity and concurrent oxygen exchange in the potassium feldspars is presumably a result of this alteration process. Evidence to support this hypothesis includes the following: 1) the lack of low temperature (propylitic) alteration assemblages in most of the pink granites (all of which contain turbid potassium feldspar), which is indicative of relatively high temperatures at the time of "turbidization"; 2) pervasive distribution of the turbid potassium feldspar in the Eocene granite, suggestive of an effective, high-temperature alteration process; and 3) the distribution of the altered rocks, which indicates that the pink granite was the center of the hydrothermal system, and thus could easily have been subjected to alteration under relatively high temperature conditions. Hemley and others (1980) and Carten (1986) have noted that prograde

processes take place in the lower and inner parts of a hydrothermal convective system.

Propylitic alteration in the plutonic rocks that surround (and pre-date) the pink granite has tended to deplete plagioclase feldspar in ^{18}O relative to potassium feldspar, and the feldspars plot below the 1:1 line on the δ-δ plot. Although potassium feldspar did exchange oxygen, its relative exchange rate was slower than that of plagioclase feldspar. Temperatures of alteration were presumably lower than those within the stocks of pink granite, and movement of heated hydrothermal fluids into these cooler rocks would have tended to stabilize potassium feldspar and albite relative to Ca-feldspar (Orville, 1963; Hemley and others, 1980). Thus, the presence of abundant secondary albiite in the propylitized rocks, and lesser amounts of secondary potassium feldspar, is consistent with the experimental data. The primary potassium feldspars in these rocks are less turbid, and have higher $\delta^{18}O$ values than coexisting plagioclase feldspars, which is compatible their having undergone lesser amounts of oxygen exchange. The movement of fluids from a high temperature regime to one of low temperature is a retrograde process, and is opposite the prograde process involved in "turbidization". Figure 32 is a schematic diagram illustrating these two processes and their proposed relationships to alteration type.

The effect of pressure on alkali feldspar equilibrium is opposite that of temperature. Lower pressures stabilize albite relative to potassium feldspar (Orville, 1963; Fournier, 1976). However, the effects of pressure change are much smaller than those of temperature, except at very low pressures (less than 200 bars). In the plagioclase system, a decrease in pressure stabilizes albite relative to Ca-feldspar (Orville, 1972), identical to the effect caused by a decrease in temperature. Because the vertical exposure of alteration in the eastern Soldier Mountains is limited to less than one kilometer, significant pressure gradients were

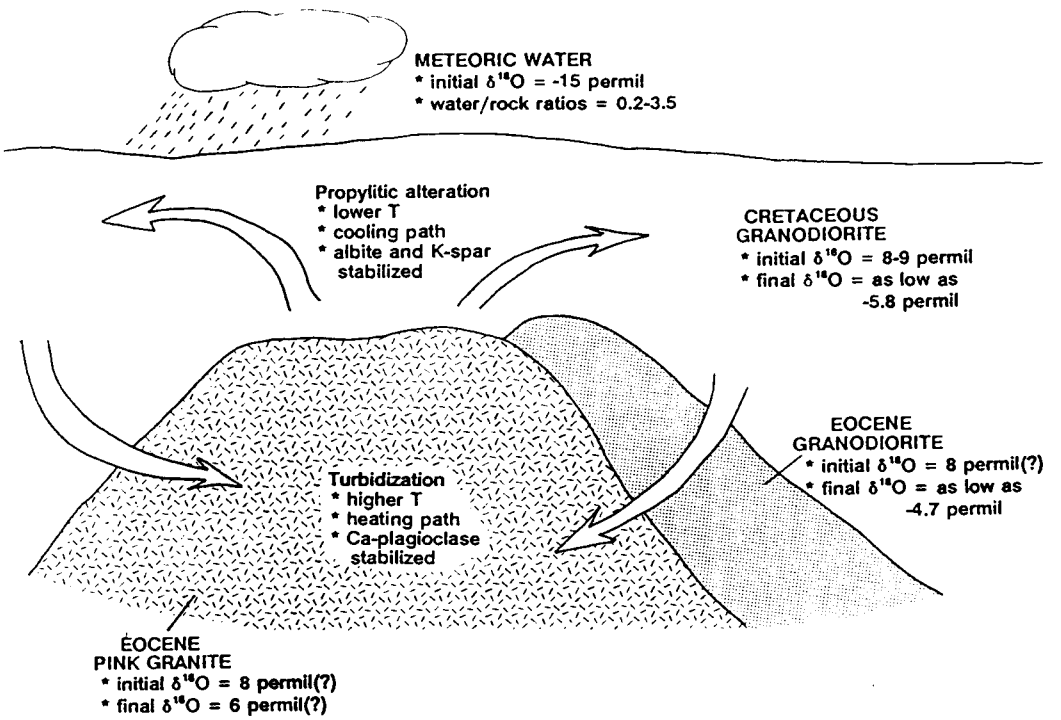

Figure 32. Schematic cross-section illustrating prograde alteration (turbidization) and retrograde (propylitic) alteration in the eastern part of the Soldier Mountains.

not likely to have been present. Thus, the effect of pressure on feldspar equilibria was probably minimal.

Effects of potassic alteration

The one sample of potassically altered Cretaceous granodiorite that was analyzed (RL230) does not show a shift in oxygen-isotope ratios of feldspar ($\delta^{18}O$ = 8.6 permil for potassium feldspar and 8.5 permil for plagioclase feldspar). Because only part of the sample was affected by this alteration, it is possible that the appropriate crystals were not separated and analyzed. However, it is more likely that this alteration involved high-temperature recrystallization related to intrusion of an Eocene stock that crops out 75 m from the sample site. The lack of a shift in $\delta^{18}O$ values, and the proximity of the Eocene pluton, indicate that the water involved in this recrystallization process was likely at high temperature and of magmatic origin. Assuming a temperature of 500°C, the composition of the water in equilibrium with feldspar of 8.5 permil would be about 6 permil, using the fractionation data of O'Neil and Taylor (1967). This contrasts with the -10 permil value for the least-shifted water of Eocene age that caused the propylitic alteration.

Effects of muscovite-quartz alteration

Muscovite-quartz alteration is characterized isotopically by relatively heavy muscovite (7.7 to 8.0 permil), and quartz that has probably been shifted to a higher $\delta^{18}O$ value (11.6 permil) from an original value near 10.2 permil. The relatively high $\delta^{18}O$ mineral values, in contrast to the propylitized samples, are the result of interaction with either magmatic fluids, or, less likely, meteoric waters that have been strongly shifted to heavier values as a result of low water/rock ratios. The $\Delta_{qtz\text{-}musc}$ value of 3.9

permil in RL168 indicates an alteration temperature of about 425°C, using the fractionation data of Botinga and Javoy (1973). This temperature is a maximum value, as some of the quartz in this sample may have retained its primary isotopic ratio of about 10.2 permil. Assuming that 425°C is the correct temperature, the water in equilibrium with the quartz and sericite must have had a $\delta^{18}O$ value of about 7 permil, using the fractionation factors provided by Botinga and Javoy (1973). This high $\delta^{18}O$ value is in contrast to the low-^{18}O meteoric-dominated waters that caused the ^{18}O shifts in the propylitized samples, and is similar in isotopic composition to that of water involved with the potassic alteration.

SUMMARY OF ALTERATION EFFECTS

Plutonic rocks in the eastern part of the Soldier Mountains have undergone propylitic, potassic, and muscovite-quartz alteration. In addition, feldspars in the pink granite have been "turbidized". A schematic diagram summarizing the effects of this hydrothermal alteration is presented in Figure 33. Muscovite-quartz alteration is Cretaceous in age and is localized along joints and fractures, some of which are filled with vein quartz. This alteration type involved relatively high-^{18}O fluids (about 7 permil) of probable magmatic origin. Altered rocks lost Na and Fe, and gained Ca and K. Potassic alteration is probably both Cretaceous and Eocene in age, but is areally limited. Potassic alteration adjacent to Eocene granodiorites resulted in recrystallization of existing minerals, but did not cause a shift in the oxygen isotope ratios of feldspars. The water involved in this process was probably magmatic in origin ($\delta^{18}O$ of about 6 permil). Little if any change took place in major-element compositions of these recrystallized rocks. Propylitic alteration is the most common alteration type in the eastern part of the Soldier Mountains. It

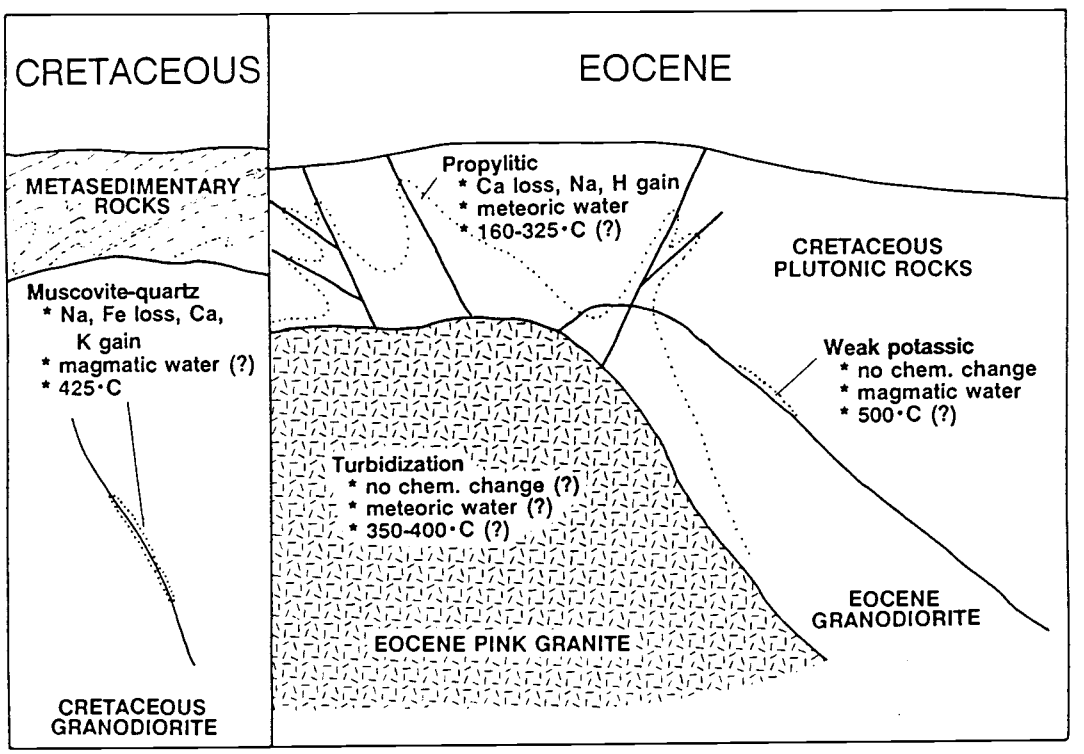

Figure 33. Schematic cross-section illustrating characteristics of hydrothermal alteration types of Cretaceous and Eocene age in the study area.

affected both Eocene and Cretaceous granodiorites and was most pronounced around the Eocene granites. In strongly propylitized rocks the elements Na and H were added and Ca was lost. Unaltered feldspars have $\delta^{18}O$ values of 8.0 to 9.0 permil, but in propylitized rocks the $\delta^{18}O$ values range down to -5.8 permil, indicating exchange with heated meteoric water. Whole-rock samples of Cretaceous granodiorite from within fault zones are as much as 10.4 permil lower than in adjacent unfaulted rocks. Some of the least-shifted meteoric water (about -10 permil) traversed these fault zones. Variable water/rock ratios of 0.2 to 3.5 can account for much of the range in $\delta^{18}O$ values in the propylitized rocks.

Most $\delta^{18}O$ values of coexisting feldspars fall near a 1:1 line on a δ-δ plot, but isotopic disequilibrium is indicated by several pairs that differ by up to 3.6 permil. In propylitized rocks the plagioclase feldspars typically have lower $\delta^{18}O$ values than do potassium feldspar. This effect is probably caused by faster isotopic exchange rates for the plagioclase feldspars that reflect lower mineral stabilities during hydrothermal alteration. In contrast, Eocene granite contains plagioclase feldspar <u>less</u> depleted in ^{18}O than coexisting pink, turbid potassium feldspar (values of 5.7 for plagioclase feldspar versus 4.4 permil for potassium feldspar). Fluid temperature was probably the most important variable controlling the relative stability of different feldspars during alteration. Fluids moving up a temperature gradient (prograde alteration) may have stabilized plagioclase relative to potassium feldspar during "turbidization" of the pink granites. In contrast, fluids moving down a temperature gradient as they moved up and out into the older rocks (retrograde alteration) stabilized albite and potassium feldspar relative to oligoclase, and caused widespread propylitic alteration.

MINES AND PROSPECTS

The study area includes portions of the Soldier, Rosetta, Big Smoky, Little Smoky, and Skeleton Creek mining districts. A number of small mines and prospects are present, but none have had significant production. The principal interest has been in gold, but minor amounts of lead and silver have also been produced. A simplified geologic map of the area and the location of known mines and prospects are shown in Figure 34; more precise locations are on Plate 1, and sample locations are on Plate 2.

Existing mines and prospects in the eastern part of the Soldier Mountains were visited and the mineralization at these localities related to specific geologic features such as rock type and structure. In this way, favorable structures and rock units could be identified for potential exploration. Twenty-five mineralized rock-chip samples were analyzed to characterize the metal types present and 188 stream-sediment samples were collected to identify metal-enriched areas that may not have been previously identified.

TEXAS STAR (D. MARIE) MINE

The Texas Star mine is located at the northern edge of Camas Praire in the southeastern part of the study area (Fig. 34). The underground workings were not extensive and are now inaccessible. According to R.E. Gibbons of Fairfield, Idaho (written comm., 1985), the property was located in 1891 by E.M. and H.S. Hego as the "Texas Star". Ross (1930) reported that in 1892 1.75 tons of ore were shipped from the Texas Star, which yielded 1.53 ounces of gold, 49.5 ounces of silver, and 1,651 pounds of lead. Continued work in 1893 produced 17.19 tons of ore yielding 75.2 ounces of gold, 132.3 ounces of silver, and 6,000 pounds of lead. According to R.E. Gibbons, a ten stamp mill was subsequently installed on the property, and underground

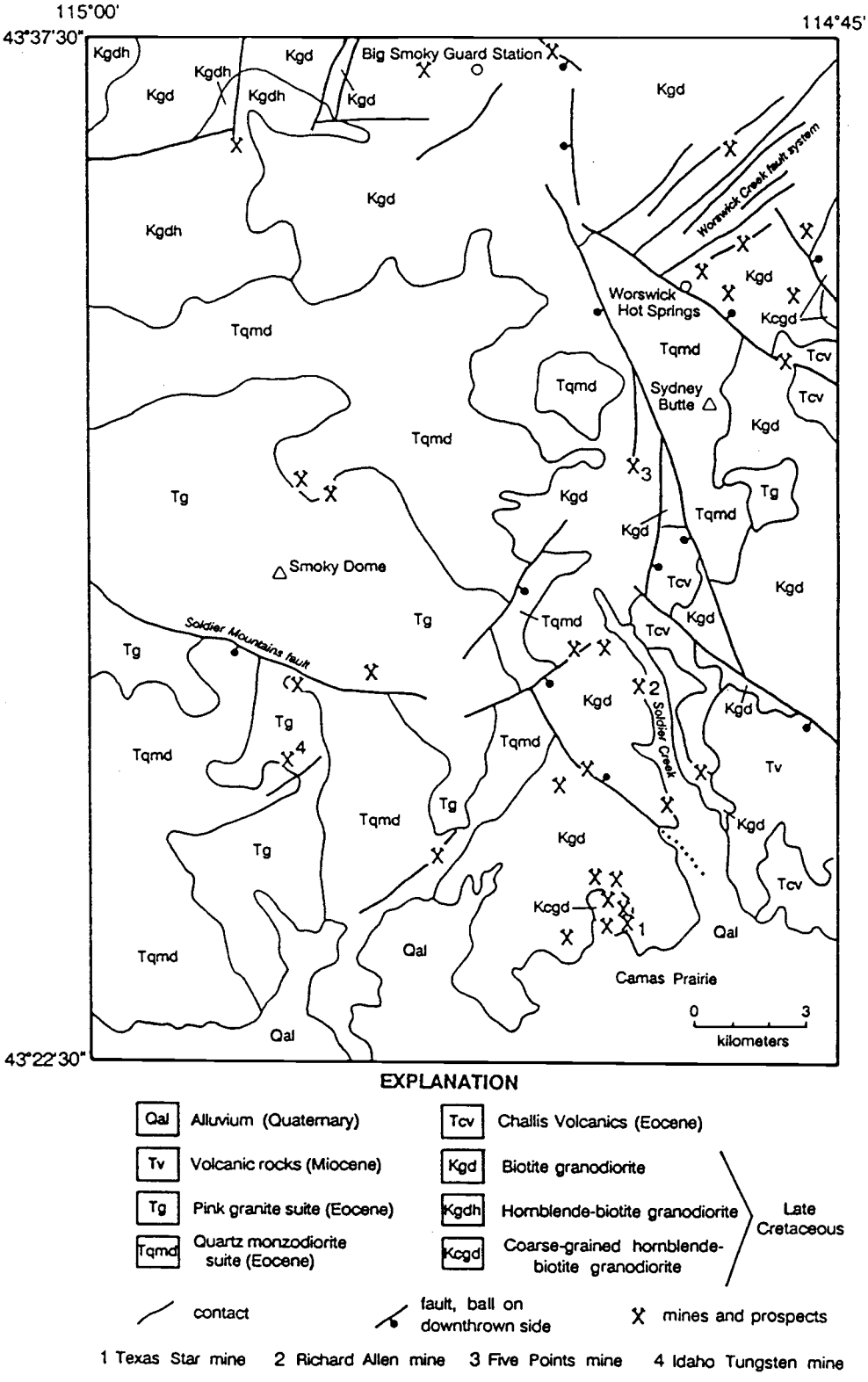

Figure 34. Simplified geologic map of the eastern part of the Soldier Mountains showing the locations of mines and prospects.

work was carried out which indicated that oxidized ore extended to a depth of 10 to 20 meters (30 to 60 feet). The oxidized zones of all known veins are reported to have been worked out, but records of the production from the mill, which was eventually removed, are not available. Subsequent work on the property is well summarized by R.E. Gibbons:

> "The ground stood idle for many years although the late Jack Wallace, a lifetime prospector of the local Soldier Mountain area, claimed, worked, and lived on the property for over twenty-five years, until his death in the late forties, apparently without success as his efforts didn't alter the landscape greatly, nor did he die a rich man."

The Texas Star mine, and a number of prospect pits present west and north of the mine, are in coarse-grained hornblende-biotite granodiorite. This unit belongs to the potassic suite of the Idaho batholith. It is similar texturally and mineralogically to the Hailey granodiorite unit of Schmidt (1962), which is exposed in the Hailey gold belt area to the east. The contact with the biotite granodiorite unit is poorly known, but is thought to be immediately east of the Texas Star mine. Veins of quartz, with lesser amounts of pyrite, galena, and magnetite, cross-cut the granodiorite. Molybdenite is sparingly present along quartz-free fractures. Alteration minerals include sericite, chlorite, calcite, and secondary potassium feldspar. A composite sample of granodiorite with molybdenite veinlets (RL36) contains 200 parts per million (ppm) Mo, and a composite sample of vein quartz with visible sulfides (RL333) contains 49 ppm Ag, 15 ppm Au, and 3.9 percent Pb. More complete analyses are listed in Table 17, along with sample descriptions, and sample locations are on Plate 2. A composite sample of vein quartz with sulfides from a prospect pit north of the Texas Star (RL35) contains 200 ppm Ag, 2.7 ppm Au, and 2.0 percent Pb.

	Ag	As	Au	B	Ba	Be	Bi	Cd	Co	Cr	Cu	Hg
RL05	3.0	20	0.80	20	1000	1	<1	0.6	<5	<10	50	0.02
RL24	0.10	<10	<0.05	10	1500	<1	<1	<0.1	<5	<10	5	<0.02
RL31	29	<10	2.4	10	70	2	28	0.7	<5	<10	80	0.08
RL34	0.1	<10	<0.05	<10	1000	1	<1	<0.1	<5	<10	5	0.02
RL35	200	100	2.7	10	50	1.5	590	1.3	<5	10	450	0.10
RL36	0.55	<10	0.05	<10	700	1	1	<0.1	10	50	70	0.02
RL61	35	<10	0.05	10	500	1	340	0.4	15	20	5000	0.02
RL63	37	10	<0.05	10	1000	1	120	2.9	<5	<10	20000	0.02
RL72B	<0.05	2.8	<0.05	<10	500	<1	<1	<0.05	<5	<10	8.4	<0.02
RL87	1.0	260	0.05	10	500	3	<1	<0.1	<5	<10	50	0.22
RL95	0.15	40	<0.05	10	300	1.5	1	<0.1	<5	20	10	0.26
RL118	0.10	20	<0.05	15	300	1.5	<1	<0.1	<5	20	10	0.04
RL151	0.15	<10	<0.05	10	1500	<1	<1	0.1	7	70	5	0.18
RL152	0.17	<1.0	<0.05	10	700	<1	<1	<0.05	<5	<10	9.6	0.12
RL153	0.09	<1.0	<0.05	10	700	<1	<1	<0.05	<5	<10	4.2	0.18
RL163	37	100	3.3	10	50	1	15	30	5	<10	1500	0.02
RL202	<0.05	<1.0	<0.05	<10	500	<1	<1	<.05	<5	<10	1	<0.02
RL203	0.9	<1.0	<0.05	15	500	<1	<1	0.90	<5	<10	130	0.04
RL226	<0.05	<1.0	<0.05	10	700	<1	<1	<0.05	<5	<10	2.1	<0.02
RL232	<0.05	1.2	<0.05	15	300	1	<1	<0.05	<5	<10	1	<0.02
RL236	<0.05	100	<0.05	15	70	1	<1	0.06	<5	<10	2.5	0.10
RL243	<0.05	<1.0	<0.05	10	1000	<1	<1	<0.05	<5	<10	0.8	<0.02
RL333	49	120	15	10	30	<1	6.8	19	<5	<10	1400	0.2
RL381	340	50	0.05	<10	300	<1	390	4.4	10	50	11000	–
CS01	1000	<200	<10	<10	2000	2	>1000	<20	50	100	10000	–

	La	Mo	Nb	Ni	Pb	Sb	Sc	Sr	V	Y	Zn	Zr
RL05	50	<0.5	<20	5	440	<2	<5	200	20	<10	140	70
RL24	70	<0.5	<20	<5	5	<2	5	1000	30	10	45	100
RL31	<20	12	<20	5	1500	<2	<5	<100	10	<10	290	20
RL34	50	1.5	<20	<5	10	<2	<5	500	15	<10	5	70
RL35	<20	20	<20	<5	20000	18	<5	<100	30	<10	250	70
RL36	100	200	<20	15	45	<2	7	500	70	10	70	50
RL61	<20	3.0	<20	10	110	<2	<5	100	30	<10	110	70
RL63	50	5.0	<20	<5	180	<2	<5	500	20	15	150	100
RL72B	30	3.4	<20	5	25	<1.2	<5	100	10	10	40	50
RL87	20	67	<20	5	10	16	<5	<100	30	<10	10	100
RL95	50	6.0	20	5	20	4	5	<100	50	10	15	100
RL118	50	6.5	20	5	20	4	<5	<100	20	10	15	100
RL151	70	0.5	<20	15	10	<2	10	1000	70	15	40	100
RL152	50	0.18	<20	<5	9.9	<1.2	<5	500	10	10	26	70
RL153	70	<0.15	<20	<5	16	<1.2	<5	300	<10	10	32	70
RL163	<20	15	<20	<5	2000	<2	<5	<100	15	<10	10000	20
RL202	30	1.8	<20	<5	5.0	<1.2	<5	300	<10	<10	17	30
RL203	50	0.32	<20	<5	94	<1.2	<5	200	15	<10	260	50
RL226	<20	<0.15	<20	<5	2.0	<1.2	<5	300	10	<10	27	70
RL232	100	<0.15	<20	<5	1.7	<1.2	<5	<100	15	<10	2.2	70
RL236	50	4.5	<20	<5	10	<1.2	<5	<100	15	<10	47	100
RL243	<20	0.26	<20	<5	8.9	<1.2	<5	150	10	<10	54	30
RL333	<20	<0.15	<20	<5	39000	<1.2	5	<100	10	<10	1600	30
RL381	50	480	<20	30	1800	<1.2	<5	100	20	<10	1400	70
CS01	<50	1500	<20	70	5000	<100	10	300	70	15	2000	300

Table 17. Mineralized samples from the eastern part of the Soldier Mountains. Analytical values are in parts per million (ppm). Analysts: J. Motooka, C. Taylor, R.J. Fairfield, L.S. Laudon, F.W. Tippitt, B. Bailey, O. Erlich, B. Roushey, and P.L. Hagemon.

Description of mineralized samples

RL05 Chip sample across silicified zone 1 m in width from prospect pit in biotite granodiorite
RL24 Composite sample of propylitized biotite granodiorite from roadcut
RL31 Composite sample of "high-graded" vein quartz from prospect pit in biotite granodiorite
RL34 Composite sample of sericitized biotite granodiorite from outcrop
RL35 Composite sample of "high-graded" vein quartz from prospect pit in coarse-grained hornblende-biotite granodiorite
RL36 Composite sample of "high-graded" coarse-grained hornblende-biotite granodiorite with sparse molybdenite veinlets from the mine dump at the Texas Star Mine
RL61 Chip sample across quartz vein 0.5 m in width from prospect pit in biotite-hornblende granodiorite
RL63 Composite sample of Cu-stained biotite granodiorite and quartz veins 1-3 cm in width from prospect pit
RL72B Chip sample across 20 m of outcrop of brecciated pink granite
RL87 Composite sample of "high-graded" vein quartz from the dump at the Idaho Tungsten mine
RL95 Chip sample across silicified outcrop 10 m in width
RL118 Composite sample of silicified rhyolite dike
RL151 Chip sample along 21 m (70 ft) of dacite dike in the upper adit of the Richard Allen mine
RL152 Chip sample along 14 m (47 ft) of biotite granodiorite in the upper adit of the Richard Allen mine
RL153 Chip sample along 12 m (40 ft) of biotite granodiorite in the upper adit of the Richard Allen mine
RL163 Composite sample of "high-graded" vein quartz from the dump at the Five Points mine
RL202 Composite sample of propylitized biotite granodiorite from mine dump
RL203 Chip sample across silicified zone and fault gouge 1 m in width above small caved adit in biotite granodiorite
RL226 Composite sample of propylitized and sericitized biotite granodiorite from outcrop
RL232 Composite sample of sericitized biotite granodiorite from outcrop
RL236 Chip sample across quartz vein 2 m in width from outcrop in biotite granodiorite
RL243 Composite sample of silicified rhyolite dike from roadcut
RL333 Composite sample of "high-graded" vein quartz from the dump at the Texas Star mine
RL381 Composite sample of "high-graded" vein quartz and biotite-hornblende granodiorite from prospect pit
CS01 Composite sample of "high-graded" vein quartz and biotite-hornblende granodiorite from prospect pit

Methods of determination are as follows: Atomic-absorption spectroscopy and inductively-coupled plasma spectroscopy for Ag, Au, Cu, Mo, Pb, Zn, As, Cd, Bi, and Sb; six-step semiquantitative emission spectroscopy for B, Ba, Be, Co, Cr, La, Nb, Ni, Sc, Sr, V, Y, and Zr.

Table 17 (continued). Mineralized samples from the eastern part of the Soldier Mountains.

RICHARD ALLEN MINE

The Richard Allen mine is located north of the Texas Star mine on the west side of Soldier Creek (Fig. 34). The property has been developed with several adits and prospects pits, but only the uppermost adit was accessible at the time of this study. According to the State Mine Inspector's reports from 1928 to 1939 (on file at the Idaho Geological Survey in Moscow, Idaho) the length of the underground workings is on the order of 300 meters (1,000 ft.). The amount of production from the Richard Allen mine is unknown, but it is unlikely that it was substantial.

The bedrock at the Richard Allen mine is biotite granodiorite of the sodic suite of the Idaho batholith. The granodiorite is cross-cut by dikes and sills of dacite which are probably Eocene in age. Exposures of quartz veins or other mineralized rock are not evident.

A geologic map of the uppermost adit at the Richard Allen mine is presented in Figure 35. Both the granodiorite and dacite in the adit are highly sheared and altered to clayey gouge, secondary muscovite, and chlorite. Most of the shears are subhorizontal and the shearing is pervasive; discrete faults are lacking. Because the shearing involves the dacite sills and dikes, at least some of the movement is likely Eocene or younger in age. Three composite chip samples were collected along the length of the upper adit (RL151, 152, and 153; Fig. 35, Table 17); all three contain less than 0.05 ppm Au.

FIVE POINTS (PERSERVERANCE) MINE

The Five Points mine is located north of the Richard Allen mine and southwest of Sydney Butte (Fig. 34). All of the workings are presently inaccessible. According to Ross (1930) the mine was developed by four tunnels with a total length of about 300 meters (1,000 feet). Development at

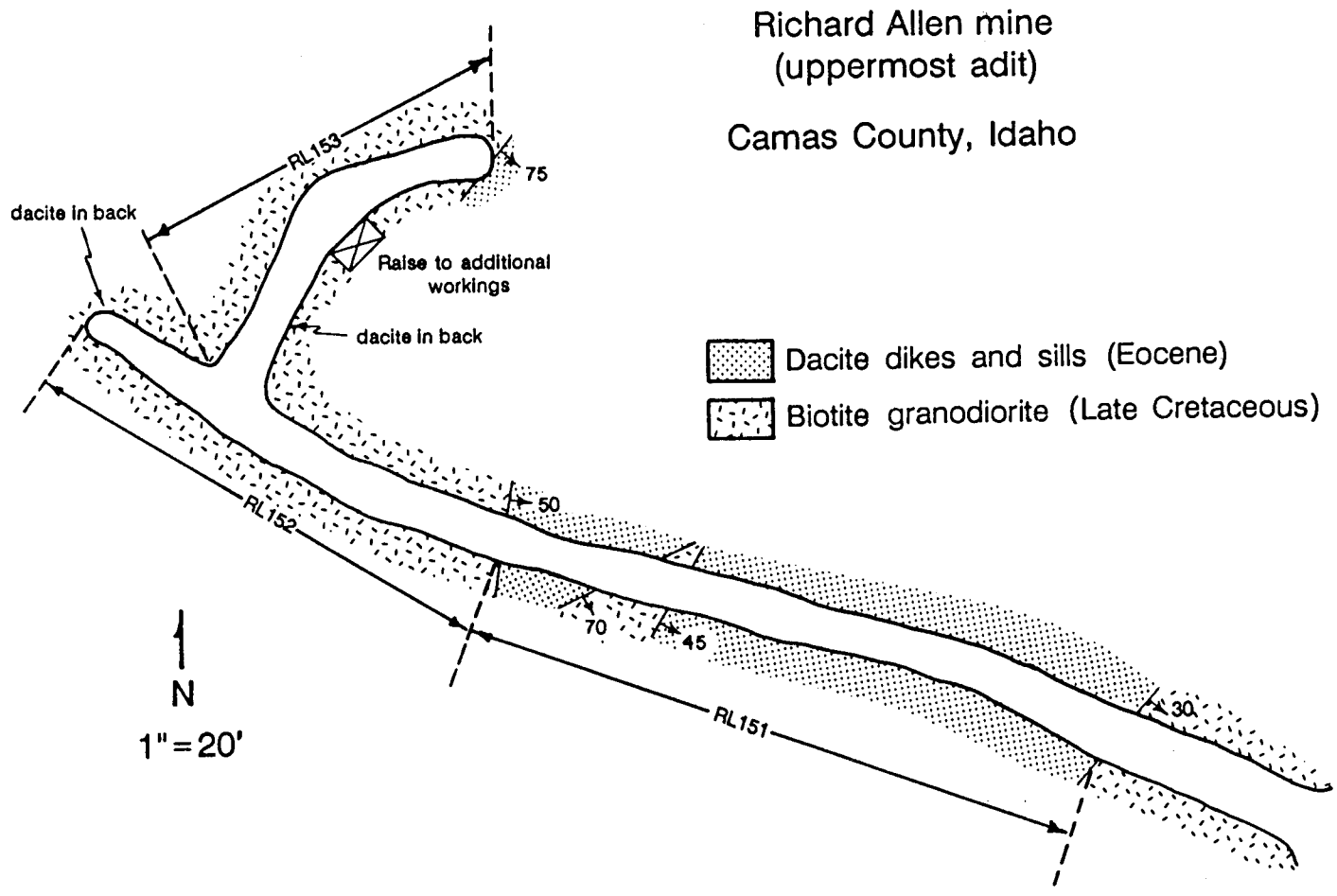

Figure 35. Geologic map of the upper adit of the Richard Allen Mine.

that time had been carried on intermitantly for several years. Recorded production from the Five Points mine is less than 1000 tons of ore that yielded between 100 and 500 ounces of Au and between 1000 and 5000 ounces of Ag (Mitchell and others, in press).

Bedrock at the mine is biotite granodiorite of the sodic suite of the Idaho batholith. A steeply dipping quartz vein at the mine strikes north-south, and appears to have been emplaced along the southern end of a fault that continues to the north along Five Points Creek. The vein is up to 1 meter in width and can be traced about 60 meters (200 feet) up the slope above the mine where it abruptly ends, possibly as a result of displacement along a low-angle fault. The granodiorite is altered to clay gouge, sericite, and chlorite. Galena and pyrite are present in dump samples of vein quartz. A composite sample of sulfide- and oxide-rich dump material was analyzed (RL163; Table 17) and found to contain 3.3 ppm Au, 37 ppm Ag, 0.2 percent Pb, and 1.0 percent Zn.

IDAHO TUNGSTEN MINE (SOLDIER MOUNTAIN DEPOSIT)

The Idaho Tungsten mine is located between Rough Creek and the East Fork of Corral Creek about five kilometers (3 miles) south of Smoky Dome (Fig. 34). The mine is hosted by pink biotite granite of Eocene age. Mineralization appears to be confined to narrow, chalcedonic quartz veins that contain sparse amounts of tungsten. Tungsten minerals were not recognized during this investigation, but according to Shannon (1926), ferberite is present in three narrow parallel veins one to 10 centimeters wide and about 50 centimeters apart. Cook (1956) has reported that one of the veins strikes about N 55 E and dips 50 degrees north and is within one of a set of fractures with a similar attitude that cut the granite in this area. This vein was explored with an adit about 60 meters (200 feet) in length, which is now caved. Production was limited to about 6.6 tons of

hand-sorted ore averaging about 4.4 percent WO_3 (Cook, 1956). A sample of vein material collected from the dump (RL87; Table 17) contains less than 50 ppm W.

UNNAMED MINES AND PROSPECTS IN CRETACEOUS PLUTONS

Several prospects pits and small caved adits are present within the biotite granodiorite unit of the sodic suite (Fig. 34, Plate 1). Those northeast of Worswick Hot Springs have been referred to as the Rosetta claim group (Umpleby, 1915). Deposits hosted in the biotite granodiorite unit are characterized by veins of quartz containing minor amounts of sulfides and gold. The granodiorites adjacent to the veins have undergone muscovite-quartz alteration. Chip samples were taken across four of these veins (RL05, RL31, RL203, and RL236; Table 17); two contain detectable amounts of Au (0.80 and 2.4 ppm) and two contain <0.05 ppm Au.

Copper mineralization is not common in the biotite granodiorite unit, but one prospect pit about 3.5 kilometers (2 miles) southwest of the Richard Allen mine contains small amounts of malachite and azurite. The copper minerals coat fractures and replace potassium feldspar. Sparse veinlets of quartz cross-cut the granodiorite; they are one to three centimeters in width and contain Fe-oxides and epidote. The feldspars and biotite are locally replaced by secondary albite, sericite, and chlorite. This mineralization may relate to the intrusion of biotite-hornblende granodiorite (of Eocene age) which is exposed one kilometer to the west. A composite sample rich in quartz and secondary copper minerals (RL63; Table 17) contains 37 ppm Ag, 5 ppm Mo, and 2.0 percent Cu.

A small exposure of the coarse-grained hornblende-biotite granodiorite unit of the potassic suite north of Camas Prairie contains an unusually large number of prospects (Fig. 34, Plate 1). The Texas Star mine is located near the easternmost exposures of this rock unit and the characteris-

tics of the various prospects are similar to those of the mine.

UNNAMED MINES AND PROSPECTS IN EOCENE PLUTONS

Mineralization is less common in rocks of Eocene age than in rocks of Cretaceous age. A small prospect pit has exposed a quartz vein within the biotite-hornblende granodiorite about three kilometers (2 miles) north of Smoky Dome (Fig. 34, Plate 1). Malachite coats fractures in the vein, which is 0.5 meters in width and trends east-west. A chip sample taken across the vein (RL61; Table 17) contains 0.05 ppm Au, 35 ppm Ag, and 0.5 percent Cu. A small prospect pit 700 meters to the southeast exposes a quartz vein 12 centimeters in width that is also stained with malachite. A claim notice at this prospect bears the name of Booker T. Phipps, a well-known bootlegger of the Fairfield area.

One of the more promising prospects in the area is between McMahan Creek and the West Fork of Threemile Creek, roughly midway between the Idaho Tungsten mine and the Texas Star mine (Fig. 34, Plate 1). A small prospect pit has exposed malachite-stained biotite-hornblende granodiorite that is cross-cut by numerous veinlets of quartz that are suggestive of a stockwork deposit. Chlorite, epidote, and Fe-oxides are abundant. Two collections of composite samples of the veined granodiorite were analyzed (RL381 and CS01; Table 17) and found to contain high concentrations of Ag (340 and 1000 ppm), Cu (1.1 and 1.0 percent) and Mo (480 and 1500 ppm). This prospect appears to be along a northeast-trending fault, but exposures in the area are poor and the existence of a fault is uncertain.

An extensive zone of brecciation 800 meters in length is present within the pink granite along the crest of the Soldier Mountains 3 kilometers (2 miles) southeast of Smoky Dome. The breccia consists of iron-stained, rounded, and angular fragments of both dike rock and fine- to coarsely-

crystalline granite as large as 1 meter across. The matrix is granite, and the rock has the appearance of an intrusion breccia. A chip sample taken across 20 meters of the breccia (RL72B; Table 17) did not reveal significant metal concentrations.

METAL CONTENT OF ALTERED ROCKS

Two samples of sericitized biotite granodiorite (RL34 and RL232), three samples of propylitized biotite granodiorite (RL24, RL202, and RL226), and a sample of silicified biotite granodiorite (RL95) were analyzed for metal content (Table 17). None of these samples contain appreciable amounts of metals. Two samples of silicified rhyolite dikes (RL118 and RL243) were also analyzed and found to have low metal contents (e.g. less than 0.05 ppm Au, Table 17).

RELATION OF MINERALIZATION TO ROCK UNIT

Mineralization in the eastern part of the Soldier Mountains is confined to plutonic rocks of Cretaceous and Eocene age (Fig. 34). Volcanic rocks of Eocene and Miocene age exposed in the eastern part of the area are unmineralized. The spatial relationship of mineralization to Cretaceous and Eocene plutons, and the lack of mineralization in Miocene rocks, indicates that mineralization in the eastern part of the Soldier Mountains is Eocene and older. Most of the mines and prospects are located in the Cretaceous plutons and the greatest density of mines and prospects is within the small exposure of the coarse-grained hornblende-biotite granodiorite unit at the northern edge of Camas Prairie. This unit belongs to the potassic suite of the Idaho batholith, which characteristically contains a greater number of mines and prospects than does the sodic suite. This greater tendency toward mineralization is evident in plutons of the potassic suite exposed to the east in the Hailey Gold Belt

area.

RELATIONSHIP OF MINERALIZATION TO STRUCTURE

Because of poor exposures, the relationship of mineralization to structure in the southern part of the area is not well established. However, most of the veins in this area do not appear to be related to large through-going faults. Instead, they appear to have been emplaced along small shears and joints within the granitic rocks; strike lengths of these structures are on the order of a few tens of meters. The faults recognized in the southern part of the area are relatively young, and either offset Eocene and Miocene volcanic rocks, or show topographic expression (e.g. the Soldier Mountains fault, Fig. 34). Because these faults offset Miocene rocks, it is likely that latest motion on these structures post-dated mineralization in the area.

Mineralization in the northern part of the area is more clearly related to larger structures. The Five Points mine is located on the southern end of a north-south fault (Fig. 34, Plate 1), the trace of which is marked by sheared biotite granodiorite along Five Points Creek. The Worswick Creek fault system is a pronounced set of northeast-trending faults in the northeastern part of the area (Fig. 34). Scattered prospects, collectively referred to as the Rosetta Claim group, are located within this fault system. The northeast trend of the Worswick Creek fault system is parallel to that of the trans-Challis fault system mapped to the north (Kiilsgaard and Lewis, 1985), which hosts several gold-bearing mineral deposits (Kiilsgaard and others, 1986).

STREAM-SEDIMENT ANALYSES

Stream-sediment samples collected in the study area were sieved to -80 mesh and analyzed by six-step semiquantitative spectrographic methods for Ag, B, Ba, Be, Co, Cr, Cu, La,

Nb, Ni, Pb, Sc, Sr, V, Y, and Zr at U.S. Geological Survey laboratories in Denver, Colorado. Concentrations of As, Bi, Cd, Sb, and Zn were determined either by atomic-absorption spectroscopy (samples RL01-RL186) or inductively-coupled plasma spectroscopy (samples RL200-LM32). The results are listed in Table 18, and sample locations are on Plate 2.

Low metal values were obtained throughout most of the study area. Of the 26 elements analyzed, five (Au, Mo, Sn, W, and Th) were below detection limits in all 188 samples. The concentration of Zn exceeds 150 ppm in only one sample (1200 ppm in RL251), which was collected from Carrie Leonard Creek in the extreme northeastern part of the area. This stream drains the Carrietown Ag-Pb-Zn district, which is part of the mineralized black shale belt of south-central Idaho (Hall, 1985; Darling, 1988). The same sample contains 5 ppm Ag, 30 ppm Cu, and 100 ppm Pb. Only four other samples contain concentrations of Ag above the detection limit of 0.5 ppm (RL135, RL312, RL332, and LM008). Sample RL135 from the North Fork of Soldier Creek contains 0.5 ppm Ag, as does sample RL312 from Williams Creek, southeast of Worswick Hot Springs. The latter sample also contains the highest concentration of Cu (50 ppm) in any stream-sediment sample collected in the study area. The other two samples with detectable amounts of Ag were collected from drainages in known mineralized areas. Sample RL332, which contains 0.5 ppm Ag, was collected from McCan Gulch a short distance below the Texas Star Mine and LM008, which contains 1.5 ppm Ag, was collected below the Five Points mine. The sample from McCan Gulch also contains 100 ppm Pb and LM008 contains 30 ppm Cu and 50 ppm Pb.

Concentrations of Cu in the stream-sediment samples ranged from 50 ppm to less than the 5 ppm detection limit. In addition to the samples mentioned previously, four contain 30 ppm Cu (RL343, RL350, RL351, and LM030). Sample LM030 was collected east of Smoky Dome Canyon on a tributary

	Ag	As	B	Ba	Be	Bi	Cd	Co	Cr	Cu	La	Nb	Ni	Pb	Sb	Sc	Sr	V	Y	Zn	Zr
RL01	<0.5	<10	10	500	1.5	<1	0.4	<5	20	7	70	20	5	30	<2	5	150	20	15	40	150
RL02	<0.5	<10	15	500	1.5	<1	0.3	<5	10	7	70	20	5	30	<2	5	150	20	15	40	200
RL09	<0.5	<10	10	700	1	<1	0.2	5	50	10	70	20	15	30	<2	7	300	50	15	60	150
RL11	<0.5	<10	10	700	1	<1	0.2	5	50	20	70	20	15	30	<2	7	300	50	15	50	200
RL12	<0.5	<10	10	500	1	<1	0.2	5	30	7	100	20	7	30	<2	7	200	30	15	35	200
RL13	<0.5	<10	10	700	1	<1	0.2	7	30	10	100	<20	15	30	<2	7	300	30	15	45	200
RL14	<0.5	<10	10	700	1	<1	0.3	5	30	10	50	20	10	30	<2	7	500	30	15	50	200
RL15	<0.5	<10	<10	700	1	<1	0.1	<5	20	5	50	<20	5	30	<2	5	300	20	10	25	100
RL18	<0.5	<10	10	700	1	<1	0.6	5	30	10	100	20	15	30	<2	5	300	30	15	50	200
RL41	<0.5	<10	15	500	3	<1	0.5	7	15	20	150	30	10	30	<2	5	150	30	50	100	300
RL54	<0.5	<10	10	500	1	<1	0.2	5	20	7	50	20	10	20	<2	5	200	30	15	40	150
RL55	<0.5	<10	10	500	1	<1	0.4	10	30	20	70	20	15	50	<2	10	300	100	30	90	200
RL57	<0.5	<10	10	500	1	<1	0.3	7	30	10	100	20	10	30	<2	7	300	70	20	70	150
RL60	<0.5	<10	<10	500	1.5	1	0.2	<5	30	10	50	<20	7	30	<2	5	200	30	15	40	200
RL68	<0.5	<10	10	500	1.5	<1	0.4	<5	15	7	100	20	5	30	<2	5	100	20	15	40	150
RL74	<0.5	<10	10	500	1.5	<1	0.2	5	30	7	70	20	5	30	<2	7	200	30	15	45	300
RL77	<0.5	<10	<10	500	1	<1	0.2	<5	15	5	70	20	<5	20	<2	5	300	30	15	70	200
RL78	<0.5	<10	10	700	1	<1	0.1	5	30	7	70	20	7	20	<2	7	300	50	20	75	200
RL82	<0.5	<10	<10	700	1	<1	0.1	5	20	<5	70	20	<5	15	<2	7	500	50	15	80	150
RL84	<0.5	<10	10	300	1	<1	0.2	<5	15	<5	100	20	5	20	<2	5	150	20	20	30	200
RL88	<0.5	<10	10	500	1.5	<1	0.2	5	30	7	70	20	10	20	<2	7	200	30	15	30	200
RL89	<0.5	<10	10	500	1	<1	0.2	7	50	7	100	20	20	20	<2	7	200	30	20	40	150
RL93	<0.5	<10	10	500	1	<1	0.1	<5	<10	<5	100	20	<5	20	<2	5	300	30	20	55	200
RL94	<0.5	<10	10	500	1	<1	0.2	<5	50	5	150	20	5	20	<2	7	300	50	20	60	200
RL98	<0.5	<10	10	500	1	<1	0.1	7	50	7	50	20	10	20	<2	7	200	50	20	35	300
RL99	<0.5	<10	10	500	1	1	0.2	7	70	7	70	20	15	20	<2	10	300	50	20	45	300
RL102	<0.5	<10	10	500	1	<1	0.2	<5	30	5	70	20	10	20	<2	5	500	30	15	60	150
RL103	<0.5	<10	10	500	<1	<1	0.2	5	30	7	70	20	7	20	<2	7	300	50	20	65	300
RL105	<0.5	<10	10	500	<1	<1	0.1	7	10	<5	70	30	<5	10	<2	10	500	70	30	100	200
RL106	<0.5	<10	10	500	1	<1	0.1	5	20	5	70	20	5	10	<2	7	500	50	30	65	200
RL109	<0.5	<10	10	500	2	1	0.3	<5	15	7	50	20	5	30	<2	5	200	20	15	55	200
RL110	<0.5	<10	10	500	2	1	0.4	<5	10	5	70	20	10	30	<2	<5	150	15	10	45	100

Table 18. Stream-sediment samples from the eastern part of the Soldier Mountains. Analytical values are in parts per million (ppm). Concentrations of Au, Mo, Sn, W, and Th were below their respective detection limits of 10, 5, 10, 50, and 100 ppm. Analysts: R.J. Fairfield, L.S. Laudon, C. Taylor, F.W. Tippitt, B. Bailey, and O. Erlich.

	Ag	As	B	Ba	Be	Bi	Cd	Co	Cr	Cu	La	Nb	Ni	Pb	Sb	Sc	Sr	V	Y	Zn	Zr
RL111	<0.5	<10	10	500	1.5	<1	0.3	5	30	10	50	<20	10	30	<2	5	200	20	15	55	200
RL112	<0.5	<10	10	500	1	<1	0.2	5	50	5	50	20	10	20	<2	5	200	30	20	40	500
RL114	<0.5	<10	<10	500	1.5	1	0.5	5	30	7	70	<20	10	30	<2	5	200	30	20	65	300
RL115	<0.5	<10	10	700	1	<1	0.2	5	50	7	70	30	10	20	<2	5	300	30	20	55	300
RL116	<0.5	<10	10	500	1	<1	0.3	7	100	10	70	20	20	20	<2	10	300	50	20	55	150
RL117	<0.5	<10	10	700	1	<1	0.2	10	100	10	100	20	20	15	<2	10	300	70	30	55	300
RL123	<0.5	<10	<10	700	1	<1	0.3	<5	30	7	50	<20	10	20	<2	5	300	30	10	35	150
RL124	<0.5	<10	10	700	1	1	0.5	7	50	10	70	20	15	50	<2	7	300	50	15	70	150
RL125	<0.5	<10	10	700	<1	1	0.3	<5	70	7	50	20	10	30	<2	7	500	50	15	60	150
RL126	<0.5	<10	10	700	1	<1	0.2	5	50	10	70	20	15	30	<2	7	500	50	15	55	200
RL127	<0.5	<10	10	700	1	<1	0.3	5	30	10	70	20	15	50	<2	7	300	50	15	85	150
RL128	<0.5	<10	10	500	1	<1	0.1	<5	20	7	150	20	5	20	<2	7	200	30	20	25	200
RL130	<0.5	<10	10	700	1.5	<1	0.3	5	20	10	70	20	10	30	<2	7	200	50	15	55	200
RL131	<0.5	<10	10	500	1	1	0.2	5	50	10	70	20	15	30	<2	7	200	30	20	40	150
RL132	<0.5	<10	10	700	1	<1	0.2	5	30	7	100	20	5	20	<2	7	300	50	20	50	200
RL133	<0.5	<10	10	500	1	1	0.2	7	50	15	100	<20	15	30	<2	7	300	70	30	50	300
RL134	<0.5	<10	10	500	1.5	1	0.4	5	20	7	70	20	10	30	<2	5	200	30	20	50	200
RL135	0.5	<10	15	500	1.5	1	0.6	<5	15	10	70	<20	10	50	<2	<5	150	20	20	45	200
RL136	<0.5	<10	10	300	1	<1	0.3	<5	<10	5	100	20	5	20	<2	<5	100	20	20	30	100
RL139	<0.5	<10	10	700	<1	<1	0.2	<5	10	5	50	<20	5	20	<2	5	300	20	10	55	150
RL144	<0.5	<10	10	700	<1	<1	0.1	10	150	7	100	20	20	15	<2	15	500	50	30	65	500
RL145	<0.5	<10	10	500	1	<1	0.1	7	50	10	70	20	15	20	<2	10	200	30	20	60	500
RL146	<0.5	<10	10	700	1	<1	0.1	5	30	7	70	20	15	15	<2	7	300	20	15	55	100
RL147	<0.5	<10	10	700	1	<1	0.1	<5	30	5	100	20	5	20	<2	5	300	70	20	45	200
RL149	<0.5	<10	10	700	1	<1	0.1	5	50	5	70	<20	15	20	<2	5	300	50	10	35	150
RL150	<0.5	<10	10	700	1	<1	0.2	5	30	7	70	20	10	30	<2	7	500	50	15	50	150
RL155	<0.5	<10	15	500	2	1	0.8	7	70	20	70	20	15	50	<2	7	200	50	30	70	150
RL156	<0.5	<10	<10	500	1.5	1	0.3	10	100	20	100	20	20	30	<2	10	300	70	20	80	300
RL157	<0.5	<10	20	500	1.5	<1	0.3	<5	20	10	50	<20	10	50	<2	5	200	20	15	40	150
RL162	<0.5	<10	10	700	<1	<1	0.1	5	30	5	100	20	5	20	<2	7	300	70	20	35	200
RL183	<0.5	<10	10	500	2	<1	0.2	<5	<10	5	50	20	5	30	<2	5	200	20	30	45	150
RL184	<0.5	<10	10	500	1	1	0.2	7	50	20	70	20	10	30	<2	7	200	50	20	45	300
RL185	<0.5	<10	10	500	1	1	0.2	5	30	20	100	30	10	20	<2	7	200	30	30	40	200
RL186	<0.5	<10	10	700	1	<1	0.7	5	20	10	50	<20	10	50	<2	7	500	30	10	85	200
RL200	<0.5	<1.0	10	700	<1	<1.0	0.17	5	10	7	70	<20	<5	15	<1.2	7	300	20	15	85	100

Table 18 (continued). Stream-sediment samples from the eastern part of the Soldier Mountains.

	Ag	As	B	Ba	Be	Bi	Cd	Co	Cr	Cu	La	Nb	Ni	Pb	Sb	Sc	Sr	V	Y	Zn	Zr
RL204	<0.5	<1.0	20	700	<1	<1.0	0.11	5	10	7	70	<20	<5	10	<1.2	7	200	30	10	100	150
RL205	<0.5	<1.0	15	1000	<1	<1.0	0.11	7	20	7	70	20	<5	15	<1.2	7	300	30	15	110	200
RL206	<0.5	<1.0	20	500	<1	<1.0	0.07	5	<10	7	50	<20	5	15	<1.2	5	150	20	10	110	100
RL211	<0.5	<1.0	<10	500	<1	<1.0	0.08	5	20	<5	70	20	<5	10	<1.2	5	200	30	15	97	150
RL212	<0.5	<1.0	10	700	<1	<1.0	0.10	5	30	5	70	<20	5	10	<1.2	5	200	20	10	81	100
RL213	<0.5	<1.0	<10	700	<1	<1.0	0.09	<5	10	<5	100	30	<5	10	<1.2	7	300	20	20	84	200
RL214	<0.5	<1.0	10	1000	<1	<1.0	0.13	5	50	5	50	20	5	10	<1.2	10	300	30	20	98	150
RL215	<0.5	<1.0	<10	700	<1	<1.0	0.12	7	30	<5	50	20	5	10	<1.2	10	200	30	15	91	100
RL216	<0.5	<1.0	10	1000	<1	<1.0	0.12	5	30	<5	50	20	5	20	<1.2	10	300	30	20	93	200
RL217	<0.5	<1.0	10	300	<1	<1.0	0.07	<5	50	5	50	<20	5	15	<1.2	5	100	20	<10	61	150
RL218	<0.5	<1.0	10	700	<1	<1.0	0.06	<5	20	5	100	20	5	15	<1.2	5	200	20	15	60	100
RL221	<0.5	<1.0	10	700	<1	<1.0	0.12	5	10	<5	20	20	<5	15	<1.2	5	200	30	20	83	150
RL222	<0.5	<1.0	20	700	<1	<1.0	0.10	<5	20	<5	50	20	5	20	<1.2	7	200	20	10	64	150
RL223	<0.5	<1.0	10	500	<1	<1.0	0.08	5	20	<5	100	<20	<5	<10	<1.2	7	200	20	15	110	100
RL228	<0.5	<1.0	10	700	<1	<1.0	0.13	10	100	10	70	<20	15	20	<1.2	15	300	50	30	71	150
RL229	<0.5	<1.0	15	500	<1	<1.0	0.08	7	50	5	50	<20	10	10	<1.2	7	200	30	15	62	100
RL233	<0.5	1.2	10	500	<1	<1.0	0.14	<5	10	7	50	<20	<5	15	<1.2	5	200	20	15	88	100
RL234	<0.5	1.5	15	500	<1	<1.0	0.17	<5	10	5	50	20	<5	20	<1.2	5	200	20	15	87	150
RL235	<0.5	<1.0	15	500	<1	<1.0	0.17	5	50	7	50	<20	7	20	<1.2	5	200	20	15	87	100
RL237	<0.5	1.5	10	300	<1	<1.0	0.11	7	50	7	70	<20	10	10	<1.2	7	200	30	15	89	100
RL238	<0.5	<1.0	10	200	1	<1.0	0.07	<5	<10	<5	50	<20	<5	10	<1.2	5	150	15	10	67	100
RL239	<0.5	<1.0	15	700	<1	<1.0	0.10	<5	15	5	50	<20	<5	20	<1.2	7	300	20	20	77	100
RL240	<0.5	<1.0	10	300	<1	<1.0	0.13	5	30	7	70	<20	5	10	<1.2	5	150	20	20	95	100
RL242	<0.5	<1.0	10	700	<1	<1.0	0.11	7	150	5	100	<20	15	15	<1.2	10	300	50	30	58	150
RL246	<0.5	<1.0	10	500	<1	<1.0	0.18	7	150	10	70	<20	15	20	<1.2	10	200	50	20	69	200
RL247	<0.5	2.0	10	300	<1	<1.0	0.11	5	70	7	50	<20	10	15	<1.2	5	150	20	10	66	100
RL250	<0.5	2.2	10	700	<1	<1.0	0.13	7	50	5	50	20	7	20	<1.2	7	200	20	15	62	150
RL251	5	300	20	500	1	<1.0	8.3	7	70	30	20	<20	15	100	7.4	10	150	30	20	1200	150
RL254	<0.5	3.0	10	500	<1	<1.0	0.31	7	50	15	50	<20	15	30	<1.2	7	100	20	15	84	150
RL259	<0.5	2.1	10	300	<1	<1.0	0.20	7	20	5	50	<20	7	10	<1.2	7	150	20	15	83	100
RL261	<0.5	1.9	20	500	1	<1.0	0.13	<5	10	5	50	<20	<5	10	<1.2	5	150	20	15	98	100
RL262	<0.5	<1.0	15	500	<1	<1.0	0.12	<5	15	5	70	20	5	15	<1.2	5	200	20	20	150	100
RL265	<0.5	1.1	10	500	1	<1.0	0.17	5	20	5	50	<20	5	<10	<1.2	7	200	20	10	89	200
RL268	<0.5	1.5	<10	500	<1	<1.0	0.10	10	150	10	50	<20	30	10	<1.2	10	200	50	15	87	150
RL269	<0.5	2.7	10	500	<1	<1.0	0.13	<5	10	5	50	<20	<5	20	<1.2	<5	150	20	10	84	70

Table 18 (continued). Stream-sediment samples from the eastern part of the Soldier Mountains.

	Ag	As	B	Ba	Be	Bi	Cd	Co	Cr	Cu	La	Nb	Ni	Pb	Sb	Sc	Sr	V	Y	Zn	Zr
RL270	<0.5	1.3	30	700	<1	<1.0	0.13	5	20	7	50	<20	5	20	<1.2	5	150	20	15	98	150
RL272	<0.5	<1.0	15	300	<1	<1.0	0.11	5	30	5	50	<20	5	10	<1.2	7	150	30	15	110	200
RL273	<0.5	<1.0	<10	500	<1	<1.0	0.09	10	150	10	50	<20	30	15	<1.2	10	200	50	15	110	150
RL276	<0.5	<1.0	10	300	1	<1.0	0.11	7	70	7	70	<20	20	15	<1.2	5	100	20	15	64	100
RL277	<0.5	<1.0	10	300	1	<1.0	0.28	<5	30	5	30	<20	5	20	<1.2	<5	150	20	10	71	100
RL283	<0.5	<1.0	15	300	1	<1.0	0.23	5	20	7	50	<20	7	20	<1.2	5	200	20	10	63	70
RL287	<0.5	2.3	15	300	<1	<1.0	0.57	5	20	<5	30	20	7	10	<1.2	5	100	20	10	100	100
RL288	<0.5	<1.0	15	700	<1	<1.0	0.10	<5	30	5	70	<20	<5	15	<1.2	7	200	20	15	95	70
RL289	<0.5	1.5	20	500	<1	<1.0	0.12	<5	20	<5	50	20	<5	<10	<1.2	7	300	20	15	96	150
RL300	<0.5	<1.0	10	300	1	<1.0	0.74	7	50	7	30	<20	10	30	<1.2	7	100	20	10	150	100
RL301	<0.5	1.8	15	500	1	<1.0	0.23	5	50	7	50	<20	10	30	<1.2	7	150	15	10	83	100
RL302	<0.5	<1.0	10	300	<1	<1.0	0.10	10	100	10	50	20	20	15	<1.2	10	150	50	20	72	200
RL303	<0.5	<1.0	20	300	1	<1.0	0.12	<5	<10	<5	70	<20	<5	10	<1.2	5	150	15	15	87	70
RL312	0.5	<1.0	15	500	<1	<1.0	0.16	7	70	50	70	<20	15	15	<1.2	10	300	50	20	89	150
RL313	<0.5	<1.0	10	500	<1	<1.0	0.15	5	50	20	70	20	10	10	<1.2	7	300	70	20	110	300
RL314	<0.5	<1.0	10	700	<1	<1.0	0.10	7	150	20	100	<20	15	<10	<1.2	10	300	100	20	70	100
RL315	<0.5	1.0	15	700	1	<1.0	0.14	<5	20	10	100	<20	<5	15	<1.2	5	500	50	20	88	150
RL316	<0.5	1.1	15	700	<1	<1.0	0.13	<5	30	5	100	<20	<5	15	<1.2	5	700	30	15	100	100
RL325	<0.5	<1.0	10	500	<1	<1.0	0.14	7	70	20	70	20	10	15	<1.2	10	200	50	30	69	1000
RL326	<0.5	1.9	10	700	<1	<1.0	0.13	5	50	7	150	<20	10	20	<1.2	7	200	50	20	61	200
RL327	<0.5	1.4	10	700	1	<1.0	0.30	7	50	15	30	<20	15	20	<1.2	7	150	70	20	92	150
RL328	<0.5	<1.0	10	700	<1	<1.0	0.64	7	50	20	70	<20	15	30	<1.2	10	300	50	20	160	70
RL329	<0.5	1.1	10	700	<1	<1.0	0.20	<5	30	5	70	<20	<5	20	<1.2	7	300	20	15	57	70
RL330	<0.5	1.6	20	1000	<1	<1.0	0.26	5	50	10	70	<20	10	20	<1.2	7	500	50	15	70	150
RL332	0.5	5.0	20	500	1	1.2	0.50	5	30	20	50	<20	<5	100	<1.2	5	200	30	15	95	100
RL334	<0.5	<1.0	15	500	1	<1.0	0.16	<5	30	5	100	<20	<5	15	<1.2	5	200	50	20	49	200
RL335	<0.5	<1.0	15	500	1	<1.0	0.13	7	50	20	70	<20	10	20	<1.2	7	200	50	20	73	150
RL336	<0.5	<1.0	15	500	<1	<1.0	0.11	<5	30	5	100	<20	<5	20	<1.2	5	200	20	15	50	300
RL337	<0.5	<1.0	10	700	<1	<1.0	0.10	5	100	7	50	20	20	10	<1.2	10	300	50	20	49	150
RL342	<0.5	<1.0	15	500	1	<1.0	0.07	5	100	5	70	<20	15	20	<1.2	10	300	50	15	53	150
RL343	<0.5	<1.0	20	700	<1	<1.0	0.09	15	150	30	100	<20	50	15	<1.2	15	300	70	30	76	300
RL344	<0.5	1.8	15	700	<1	<1.0	<0.05	10	150	10	100	<20	30	15	<1.2	15	300	70	30	57	150
RL346	<0.5	<1.0	20	500	<1	<1.0	0.08	7	150	10	50	<20	30	15	<1.2	10	200	50	15	60	150
RL347	<0.5	<1.0	20	700	<1	<1.0	0.05	10	200	20	100	<20	30	15	<1.2	15	300	100	30	56	300
RL348	<0.5	<1.0	15	500	<1	<1.0	0.05	7	150	10	100	<20	20	20	<1.2	10	300	50	20	55	150

Table 18 (continued). Stream-sediment samples from the eastern part of the Soldier Mountains.

	Ag	As	B	Ba	Be	Bi	Cd	Co	Cr	Cu	La	Nb	Ni	Pb	Sb	Sc	Sr	V	Y	Zn	Zr
RL350	<0.5	<1.0	10	700	<1	<1.0	0.10	10	200	30	100	20	30	15	<1.2	15	300	70	20	70	200
RL351	<0.5	<1.0	<10	500	<1	<1.0	<0.05	15	300	30	30	<20	50	10	<1.2	10	300	70	10	51	100
RL352	<0.5	<1.0	<10	700	<1	<1.0	0.05	7	100	10	50	<20	20	10	<1.2	10	300	50	15	46	100
RL353	<0.5	<1.0	10	700	<1	<1.0	0.14	10	200	20	70	<20	30	15	<1.2	15	300	100	20	73	200
RL357	<0.5	<1.0	10	700	<1	<1.0	0.11	5	70	10	100	<20	<5	15	<1.2	10	300	70	20	65	300
RL358	<0.5	<1.0	10	700	<1	<1.0	0.09	7	100	15	50	<20	20	15	<1.2	7	200	70	15	62	200
RL359	<0.5	<1.0	10	700	<1	<1.0	<0.05	7	100	5	70	<20	20	15	<1.2	15	500	70	30	44	200
RL360	<0.5	<1.0	15	500	<1	<1.0	<0.05	7	100	7	70	<20	30	10	<1.2	7	150	30	15	49	200
RL361	<0.5	2.6	15	300	<1	<1.0	0.14	<5	30	<5	150	<20	5	20	<1.2	<5	100	15	10	50	70
RL363	<0.5	1.2	10	700	1	<1.0	0.12	5	50	7	70	<20	7	20	<1.2	7	200	30	20	48	150
RL364	<0.5	3.3	15	500	1.5	<1.0	0.19	<5	30	7	70	20	<5	30	<1.2	5	200	70	20	47	300
RL365	<0.5	1.6	10	700	1	<1.0	0.08	<5	50	5	150	<20	<5	20	<1.2	7	200	30	30	45	150
RL366	<0.5	1.3	20	300	<1	<1.0	0.14	<5	50	7	50	20	<5	20	<1.2	7	150	30	20	53	1000
RL368	<0.5	<1.0	15	500	<1	<1.0	0.09	5	50	7	100	<20	<5	10	<1.2	7	150	50	15	42	300
RL369	<0.5	2.0	10	500	<1	<1.0	0.11	<5	50	7	70	20	<5	15	<1.2	7	150	50	30	48	500
RL370	<0.5	<1.0	10	500	<1	<1.0	0.08	5	70	10	50	20	<5	15	<1.2	7	150	50	15	52	1000
RL371	<0.5	1.9	15	500	<1	<1.0	0.07	5	70	5	50	<20	20	20	<1.2	7	150	50	15	49	150
RL380	<0.5	<1.0	15	700	<1	<1.0	0.12	7	70	10	70	<20	20	10	<1.2	7	200	50	20	66	500
RL382	<0.5	<1.0	10	700	<1	<1.0	0.35	7	70	20	70	<20	20	30	<1.2	7	200	50	15	96	500
LM001	<0.5	<1.0	10	1000	<1	<1.0	0.13	5	20	5	70	20	<5	15	<1.2	7	500	30	20	81	200
LM002	<0.5	<1.0	10	300	<1	<1.0	0.11	<5	<10	5	70	<20	<5	10	<1.2	<5	200	20	10	75	100
LM003	<0.5	<1.0	20	1000	<1	<1.0	0.10	<5	10	<5	70	<20	<5	15	<1.2	7	200	20	20	110	100
LM004	<0.5	<1.0	<10	500	<1	<1.0	0.20	5	30	5	100	<20	<5	15	<1.2	7	300	20	20	77	100
LM005	<0.5	<1.0	10	700	<1	<1.0	0.15	7	50	7	50	20	5	10	<1.2	10	300	30	15	110	150
LM006	<0.5	<1.0	10	700	<1	<1.0	0.11	7	70	7	70	20	7	10	<1.2	10	300	50	20	82	150
LM007	<0.5	<1.0	<10	700	<1	<1.0	0.14	7	70	7	70	<20	10	10	<1.2	10	200	30	20	84	100
LM008	1.5	<1.0	10	700	<1	<1.0	0.13	<5	20	30	70	<20	<5	50	<1.2	5	200	20	15	65	100
LM009	<0.5	1.0	15	500	<1	<1.0	0.18	7	70	10	100	<20	10	15	<1.2	10	300	50	20	77	70
LM010	<0.5	<1.0	<10	500	<1	<1.0	0.12	5	70	7	100	<20	5	10	<1.2	7	150	30	20	65	150
LM011	<0.5	<1.0	10	500	<1	<1.0	0.13	10	100	10	70	30	10	15	<1.2	15	200	70	30	69	700
LM012	<0.5	<1.0	15	300	<1	<1.0	0.12	5	50	7	50	<20	10	20	<1.2	<5	150	20	10	60	100
LM013	<0.5	<1.0	15	300	<1	<1.0	0.11	7	70	7	50	<20	10	10	<1.2	5	150	30	10	74	150
LM014	<0.5	<1.0	10	500	<1	<1.0	0.09	7	70	5	50	<20	10	10	<1.2	7	200	30	15	89	150
LM015	<0.5	<1.0	10	500	<1	<1.0	0.09	5	30	10	70	20	7	10	<1.2	7	300	50	30	87	150
LM016	<0.5	<1.0	15	500	<1	<1.0	0.11	7	50	7	50	20	15	15	<1.2	7	150	30	15	59	100

Table 18 (continued). Stream-sediment samples from the eastern part of the Soldier Mountains.

	Ag	As	B	Ba	Be	Bi	Cd	Co	Cr	Cu	La	Nb	Ni	Pb	Sb	Sc	Sr	V	Y	Zn	Zr
LM017	<0.5	<1.0	10	500	<1	<1.0	0.10	7	100	10	50	<20	20	15	<1.2	7	150	30	10	55	150
LM018	<0.5	<1.0	<10	700	<1	<1.0	0.15	10	150	15	70	<20	20	15	<1.2	15	200	50	15	71	300
LM019	<0.5	<1.0	15	700	<1	<1.0	0.23	7	70	10	70	<20	7	20	<1.2	10	200	50	15	52	200
LM020	<0.5	<1.0	15	700	<1	<1.0	0.16	<5	20	5	70	<20	<5	10	<1.2	5	150	20	10	97	100
LM021	<0.5	<1.0	10	500	<1	<1.0	0.09	<5	20	<5	50	<20	<5	10	<1.2	5	150	30	20	75	100
LM022	<0.5	<1.0	10	700	<1	<1.0	0.14	<5	10	5	50	<20	<5	15	<1.2	5	200	20	15	79	100
LM023	<0.5	<1.0	20	500	1	<1.0	0.47	7	70	10	50	20	10	30	<1.2	7	200	50	20	69	150
LM024	<0.5	<1.0	15	500	1	<1.0	0.22	<5	20	7	70	<20	5	20	<1.2	<5	100	20	15	47	70
LM025	<0.5	<1.0	15	300	1	<1.0	1.2	5	15	7	50	<20	<5	20	<1.2	5	100	20	15	87	150
LM026	<0.5	2.0	20	500	1	<1.0	0.41	5	30	10	70	<20	5	30	<1.2	5	100	20	15	58	100
LM027	<0.5	1.1	20	200	1	<1.0	0.36	5	<10	7	50	<20	7	20	<1.2	<5	<100	15	10	61	30
LM028	<0.5	1.9	15	300	<1	<1.0	0.31	5	10	7	50	<20	5	20	<1.2	<5	<100	20	10	54	150
LM029	<0.5	1.2	20	700	1	<1.0	0.71	<5	30	10	100	20	<5	30	<1.2	7	150	30	20	96	150
LM030	<0.5	<1.0	10	500	<1	<1.0	0.23	<5	20	10	30	<20	5	20	<1.2	<5	100	15	10	71	100
LM031	<0.5	1.4	20	500	1	1.0	0.94	7	100	30	70	20	20	30	<1.2	10	150	50	30	140	150
LM032	<0.5	<1.0	10	700	<1	<1.0	0.14	7	70	15	70	<20	15	15	<1.2	10	200	50	20	67	100

Table 18 (continued). Stream-sediment samples from the eastern part of the Soldier Mountains.

of Boardman Creek. The other three samples were collected in the extreme southwestern part of the area on tributaries of Ear Creek and the West Fork of Corral Creek. Concentrations of Pb range from 100 to less than 10 ppm. In addition to the samples mentioned previously, six contain 50 ppm Pb. These samples are RL55 (Sampson Creek), RL124 (tributary of the East Fork of Threemile Creek), RL135 (South Fork of Soldier Creek), RL155 (tributary of Boardman Creek), RL157 (tributary of Boardman Creek), and RL186 (East Fork of Threemile Creek).

DISCUSSION

Rock type, and to a lesser extent structure, have influenced the formation of mineralized areas in the eastern part of the Soldier Mountains. Most of the mines and prospects are hosted by granodiorites of the Late Cretaceous Idaho batholith. Although the highest density of prospects is within the coarse-grained hornblende-biotite granodiorite unit (potassic suite), the majority of the mineralized areas are hosted by the more widespread biotite granodiorite unit (sodic suite).

Mineralization within the sodic suite is characterized by gold-bearing quartz veins which contain minor amounts of pyrite, galena, and sphalerite. Quartz-muscovite (sericitic) alteration is common alongside these veins. This mineralization, as discussed in a preceeding section on hydrothermal alteration, is probably Late Cretaceous in age and related to the final stages of emplacement and cooling of the Idaho batholith. In general, the structures along which the veins formed are not large, but exceptions exist (e.g. at the Five Points mine).

The mineralization within the potassic suite is similar to that of the sodic suite. However, in addition to gold and galena, molybdenite is present, and the host rocks have locally undergone potassic alteration. As with the sodic

suite, this mineralization is probably Late Cretaceous in age.

The mineralization within the Eocene plutonic rocks differs from that in the Cretaceous plutonic rocks. Mineralization in the pink granite suite is limited to a small number of quartz veins and the presence of minor amounts of tungsten. Mineralized areas within the quartz monzodiorite suite are characterized by veins or stockworks(?) rich in Cu, Mo, and Ag. Because these mineralized areas are Cu-rich, and hosted by plutonic rocks of intermediate composition, they are similar to the porphyry-copper deposits such as those associated with Laramide-age intrusions of the southwestern United States (Titley and Beane, 1981). However, the mineralized areas do not appear to be extensive, nor are they associated with widespread hydrothermal alteration, as is the case in the porphyry-type deposits. The one Cu-rich sample from within a Cretaceous unit (sample RL63 with 2.0 percent Cu) is from a prospect only one kilometer away from the Eocene biotite-hornblende granodiorite unit of the quartz monzodiorite suite (Plate 2). The Cu mineralization at this locality is probably related to intrusion of the Eocene granodiorite, rather than to mineralization during the Late Cretaceous.

The mineral potential of the eastern part of the Soldier Mountains is moderate to low relative to other areas in the Idaho batholith. However, potential does exist for additional discoveries of vein-type gold deposits within the Cretaceous plutonic rocks. The rocks of the potassic suite are more favorable than those of the sodic suite, but they are not areally extensive. Favorable structures include the north-south trending fault north of the Five Points mine, and the series of northeast-trending faults of the Worswick Creek fault system northeast of Worswick Hot Springs. Plutonic rocks of the Eocene pink granite suite are not likely to contain substantial mineralization. The potential does exist for porphyry-type Cu-Mo-Ag mineralization in

rocks of the quartz monzonite suite. However, none of the areas of known mineralization are on the scale of typical porphyry systems.

The results of the stream-sediment sampling are not encouraging with regard to the discovery of previously unidentified metal-rich areas. Overall, metal values are below those reported for other areas of the Idaho batholith (e.g. the Tenmile roadless area southeast of Lowman; Kiilsgaard, 1983b). However, the drainage of Williams Creek, south of Worswick Hot Springs, yielded relatively high Cu and Ag values (50 and 0.5 ppm, respectively) and is worthy of further study.

CONCLUSIONS

The eastern part of the Soldier Mountains is principally underlain by plutonic rocks of Cretaceous and Eocene age. Eocene volcanic rocks correlative with the Challis Volcanics, and Miocene volcanic rocks in part correlative with the Idavada Volcanics, are locally preserved. Numerous faults with steep dips are present; those with northeast trends appear to be the oldest and have localized the emplacement of Eocene dike swarms. North-south- to northwest-trending faults exhibit topographic expression and are interpreted as Basin and Range structures. However, some of these faults may have been the site of recurrent movement since Cretaceous time.

The Cretaceous plutonic rocks in the study area are part of the Idaho batholith. Three intrusive phases are present: 1) coarse-grained hornblende-biotite granodiorite; 2) hornblende-biotite granodiorite; and 3) biotite granodiorite. The coarse-grained phase contains large books of biotite and belongs to a potassic suite of plutons that are more widely exposed east of the study area. The hornblende-biotite granodiorite and biotite granodiorite phases contain small "shreddy" biotite books and belong to a sodic suite of plutons present largely north and west of the study area. Relative to the sodic suite, the potassic suite is enriched in LIL elements such as K, Rb, Cs, U, and B, as well as compatible elements such as Mg, Sc, Co, and Cr. The sodic suite is enriched in Na, Al, Sr, Ba, LREE, and Zr, and was probably derived from one or more sources relatively more depleted, but more felsic, than the source of the potassic suite. Within-suite variations in major- and trace-element abundances are minimal, and can be explained by minor amounts of crystal segregation and (or) restite segregation. Rocks of the sodic suite have relatively uniform initial $^{87}Sr/^{86}Sr$ ratios (0.7072 ± 0.0003) but variable ϵ_{Nd} values (-6.8 ± 1 for the biotite granodiorite unit and -19.5 for the

hornblende-biotite granodiorite unit). The lower ϵ_{Nd} value for the hornblende-biotite granodiorite unit is most easily explained by an older source for this unit relative to other rocks of the sodic suite.

Because of the abundance of granodiorite, and lack of gabbro and diorite, the mass contribution from the mantle in the Cretaceous rocks in the eastern part of the Soldier Mountains is probably minor. However, heat transfer through the process of underplating of mantle-derived magmas may have been important in forming melts from the lower crust, which then coalesced to form the Cretaceous plutons. Alternatively, crustal thickening and anatexis resulting from the stacking of thrust plates during the Sevier Orogeny may have resulted in Cretaceous plutonism and the formation of the Idaho batholith.

Four intrusive phases of Eocene plutonic rocks are present in the eastern part of the Soldier Mountains. All are epizonal and are associated with dike swarms. The earliest three units are the most mafic; they range from diorite to granite in composition and are collectively referred to as the quartz monzodiorite suite. The youngest phase is pink biotite granite, the plutons of which are referred to as the pink granite suite. Both suites are present throughout central Idaho and are the intrusive equivalents of the Challis Volcanics. The pink granite suite has silica contents in excess of 70 percent, whereas those of the quartz monzodiorite suite range from 48 to 70 percent. The quartz monzodiorite suite is further subdivided geochemically into mafic and intermediate subgroups. On the basis of field relations, CaO and Sr content, MgO/(MgO + FeO*) ratios, and initial $^{87}Sr/^{86}Sr$ ratios, the two suites cannot be related by fractional crystallization. However, large ranges in MgO, Sc, Cr, and Co content indicate that fractional crystallization of mafic minerals was important in controlling at least some of the chemical variability within the mafic subgroup of the quartz monzodiorite suite.

Differing parental magma composition may also have contributed to diverse compositions of the mafic subgroup. A relatively large variation in Ba content of the pink granite suite probably is a result of removal or accumulation of variable amounts of potassium feldspar. These variations in trace-element concentrations in the Eocene plutons are in contrast to the limited compositional variations determined for the Cretaceous plutons.

Mixing between the two Eocene suites has not been extensive, but some hybrid pink granites were generated which contain mafic inclusions and have SiO_2 contents of less than 72 percent. The pink granite suite has geochemical affinities with A-type granites, but is not as enriched in Zr, Nb, Y, and Ce. By analogy to other A-type granites, the pink granite probably originated from partial melting of lower crustal rocks under high temperature and vapor-absent conditions.

The Challis Volcanics in the eastern part of the Soldier Mountains are characterized by lava flows of rhyodacite, dacite, and andesite. A K-Ar age determination of 49.9 $\pm$ 0.6 Ma on hornblende from a rhyodacite flow is the best estimate of the age of these rocks. The next youngest volcanic unit is the tuff of Cannonball Mountain, which was dated at 10.2 $\pm$ 0.3 Ma (K-Ar on sanidine). This tuff is a peralkaline rhyolite (comendite), and is unlike typical Miocene rhyolite in the region, which is metaluminous or peraluminous. Also present are exposures of rhyolite tuff that correlate with the Gwin Spring Formation, the type section of which is exposed in the Mount Bennett Hills 20 km south of the study area. Overlying the Gwin Spring Formation is a series of porphyritic olivine basalt flows. Ages of these flows are not precisely known, but most (or all) are probably between 9.4 and 6.4 Ma. The youngest rocks in the area are composed of poorly consolidated arkose and interbedded water-lain ash of Late Miocene (?) or Pliocene (?) age that were deposited in a small basin on Cretaceous

biotite granodiorite.

Plutonic rocks in the eastern part of the Soldier Mountains have undergone propylitic, potassic, and muscovite-quartz alteration. In addition, the feldspars in the pink granite have been "turbidized". Muscovite-quartz alteration is Cretaceous in age ($^{40}Ar/^{39}Ar$ plateau of 70.3 $\pm$ 0.4 on muscovite) and is localized along joints and fractures, some of which are filled with vein quartz. This alteration type involved relatively high-^{18}O fluids (about 7 permil) of probable magmatic origin. Altered rocks were depleted in Na and Fe, and were enriched in Ca and K.

Following a period of uplift, hydrothermal activity resumed in Eocene time, concurrent with the intrusion of the epizonal plutons. Disturbance of Ar systematics in Cretaceous rocks by Eocene plutons was pronounced. Hornblende was the least affected, and potassium feldspar more so. Biotite was the most strongly affected, and underwent resetting to Eocene ages. Potassic alteration occurred locally, but propylitization was the predominant and widespread alteration type. Propylitic alteration around the youngest plutons (the pink granites) was particularly pronounced, and both Eocene and Cretaceous plutons were affected. Faults and joint surfaces served as conduits for fluid circulation. Concurrent(?) movement of heated oxygenated fluids within the cooling plutons of pink granite caused "turbidization" of potassium feldspar, which simultaneously imparted an overall pink color to these rocks. The fluids involved in this process were hotter (perhaps 350-400°C) than those associated with the peripheral propylitic zone, and movement of the fluids was apparently along grain boundaries and microfractures rather than along the larger through-going structures.

In strongly propylitized rocks the elements Na and H were added and Ca was depleted. Unaltered feldspars have $\delta^{18}O$ values of 8.0 to 9.0 permil, but in propylitized rocks the $\delta^{18}O$ values range down to -5.8 permil, indicating ex-

change with heated meteoric water. Whole-rock samples of Cretaceous granodiorite from within fault zones are as much as 10.4 permil lower than in adjacent unfaulted rocks.

Most $\delta^{18}O$ values of coexisting feldspars fall near a 1:1 line on a δ-δ plot, but isotopic disequilibrium is indicated by several pairs that differ by up to 3.6 permil. Plagioclase feldspars in propylitized rocks typically have lower $\delta^{18}O$ values than do potassium feldspars. This effect is probably caused by faster isotopic exchange rates for the plagioclase feldspars, which in turn reflect the lower stability of plagioclase feldspar during hydrothermal alteration. In contrast, Eocene granite contains plagioclase feldspar <u>less</u> depleted in ^{18}O than coexisting pink, turbid potassium feldspar (5.7 permil versus 4.4 permil). Fluid temperature was probably the most important variable controlling the relative stability of different feldspars during alteration. Fluids moving up a temperature gradient (prograde alteration) may have stabilized plagioclase relative to potassium feldspar during "turbidization" of the pink granites. In contrast, fluids moving down a temperature gradient as they moved up and out into the older rocks (retrograde alteration) stabilized albite and potassium feldspar relative to oligoclase, and caused widespread propylitic alteration.

Potassic alteration is probably both Cretaceous and Eocene in age, but is limited in areal extent. Potassic alteration adjacent to Eocene granodiorites resulted in recrystallization of existing minerals, but did not cause a shift in the oxygen isotope ratios of feldspars. The water involved in this process was probably magmatic in origin ($\delta^{18}O$ of about 6 permil). Little if any change took place in major-element compositions of these recrystallized rocks.

Rock type, and to a lesser extent structure, have influenced the development of mineralized areas in the eastern part of the Soldier Mountains. Most of the mines and prospects are hosted by granodiorites of the Late Creta-

ceous Idaho batholith. Although the highest density of prospects is within the coarse-grained hornblende-biotite granodiorite unit of the potassic suite, the majority of the mineralized areas are hosted by the more widespread biotite granodiorite unit of the sodic suite.

Mineralization within the sodic suite is characterized by gold-bearing quartz veins that contain minor amounts of pyrite, galena, and sphalerite. Quartz-muscovite alteration is common alongside these veins. This mineralization is probably Late Cretaceous in age and related to the final stages of emplacement and cooling of the Idaho batholith. The mineralization within the potassic suite is similar to that of the sodic suite. However, in addition to gold and galena, molybdenite is present, and the host rocks have locally undergone potassic alteration. As with the sodic suite, this mineralization is probably Late Cretaceous in age.

Despite a clear association between pink granite plutons and widespread propylitic alteration, mineralization in the pink granite suite is limited to a small number of quartz veins and the presence of minor amounts of tungsten. None of the veins in the older rocks surrounding the pink granite are known to be related to the intrusion of these plutons. Mineralized areas within the quartz monzodiorite suite are characterized by veins or stockworks(?) rich in Cu, Mo, and Ag. Although these mineralized areas are geochemically similar to porphyry-copper deposits, they do not appear to be extensive, nor are they associated with widespread hydrothermal alteration, as is the case in the porphyry-type deposits.

The mineral potential of the eastern part of the Soldier Mountains is moderate to low relative to other areas in central Idaho. However, reasonable possibilities exist for additional discoveries of vein-type gold deposits within the plutonic rocks of Cretaceous age. The rocks of the potassic suite are more favorable than those of the sodic suite, but

they are not extensively exposed. Favorable structures for mineralization include the north-south trending fault north of the Five Points mine, and the series of northeast-trending faults of the Worswick Creek fault system northeast of Worswick Hot Springs. Plutonic rocks of the Eocene pink granite suite are not likely to contain substantial mineralization. The potential does exist for porphyry-type Cu-Mo-Ag mineralization in rocks of the quartz monzonite suite. However, none of the known areas of mineralization are of the size or intensity that is characteristic of major porphyry systems.

REFERENCES

Alderton, D.H.M., Pearce, J.A., and Potts, P.J., 1980, Rare earth element mobility during granite alteration: evidence from southwest England: Earth and Planetary Science Letters, v. 49, p. 149-165.

Aliberti, E.A., and Manduca, C.A., 1988, A transect across an island arc-continent boundary in west-central Idaho, in Link, P.K., and Hackett, W.R., eds., Guidebook to the geology of central and southern Idaho: Idaho Geological Survey Bulletin 27, p. 99-107.

Allen, R.M., Jr., 1952, Geology and mineralization of the Volcano district, Elmore County, Idaho: Economic Geology, v. 47, no. 8., p. 815-821.

Anders, E., and Ebihara, M., 1982, Solar-system abundances of the elements: Geochimica et Cosmochimica Acta, v. 46, p. 2363-2380.

Anderson, A.L., 1934a, Geology of the Pearl-Horseshoe Bend gold belt, Idaho: Idaho Bureau of Mines and Geology Pamphlet 32, 70 p.

Anderson, A.L., 1934b, A preliminary report on recent block faulting in Idaho: Northwest Science, v. 8, p. 17-28.

Anderson, A.L., 1947, Geology and ore deposits of Boise Basin, Idaho: U.S. Geological Survey Bulletin 944-C, 319 p.

Anderson, A.L., 1952, Multiple emplacement of the Idaho batholith: Journal of Geology, v. 60, p. 255-265.

Anderson, J.L., 1983, Proterozoic anorogenic plutonism of North America: Geological Society of America Memoir 161, p. 133-154.

Armstrong, R.L., 1974, Geochronometry of the Eocene volcanic-plutonic episode in Idaho: Northwest Geology, v. 3, p. 1-15.

Armstrong, R.L., 1975, The geochronometry of Idaho: Isochron/West, no. 14, p. 1-50.

Armstrong, R.L., Leeman, W.P., and Malde, H.E., 1975, K-Ar dating, Quaternary and Neogene volcanic rocks of the Snake River Plain, Idaho: American Journal of Science, v. 275, p. 225-251.

Armstrong, R.L., Taubeneck, W.H. and Hales, P.O., 1977, Rb-Sr and K-Ar geochronometry of Mesozoic granitic rocks and their Sr isotopic composition, Oregon, Washington, and Idaho: Geological Society of America Bulletin, v. 88, p. 397-411

Arth, J.G., and Hanson, G.N., 1975, Geochemistry and origin of the early Precambrian crust of northeastern Minnesota: Geochimica et Cosmochimica Acta, v. 39, p. 325-362.

Baker, J.H., 1985, Rare earth and other trace element mobility accompanying albitization in a Proterozoic granite, W. Bergslagen, Sweden: Mineralogical Magazine, v. 49, p. 107-115.

Bateman, P.C., Clark, L.D., Huber, N.D., Moore, J.G., and Rinehart, C.D., 1963, The Sierra Nevada batholith, a synthesis of recent work across the central part: U.S. Geological Survey Professional Paper 414D, 46 p.

Bennett, E.H., 1980a, Granitic rocks of Tertiary age in the Idaho batholith and their relation to mineralization: Economic Geology, v. 75, p. 278-288.

Bennett, E.H., 1980b, Reconnaissance geology and geochemistry of the Trinity Mountain-Steel Mountain area, Elmore County, Idaho: Idaho Bureau of Mines and Geology Open-File Report 80-11, 56 p.

Bennett, E.H, and Knowles, C.R., 1985, Tertiary plutons and related rocks in central Idaho, in McIntyre, D.H., ed., Symposium on the geology and mineral deposits of the Challis 1 x 2 degree quadrangle, Idaho: U.S. Geological Survey Bulletin 1658A-S, chap. F, p. 81-95.

Berry, A.L., Dalrymple, M.A., and Von Essen, J.C., compilers, 1976, Summary of miscellaneous potassium-argon age measurements, U.S. Geological Survey, Menlo Park, California, for the years 1972-1974: U.S. Geological Survey Circular 727, 13 p.

Best, M.G., Armstrong, R.L., Graustein, W.C., Embree, G.F., and Ahlborn, R.L., 1974, Mica granites of the Kern Mountains pluton, eastern White Pine County, Nevada: remobilized basement of the Cordilleran miogeosyncline?: Geological Society of America Bulletin, v. 85, p. 1277-1286.

Bickford, M.E., Chase, R.B., Nelson, B.K., Shuster, R.D., and Arruda, E.C., 1981, U-Pb studies of zircon cores and overgrowths, and monazite: implications for age and petrogenesis of the northeastern Idaho batholith: Journal of Geology, v. 89, p. 433-457.

Bond, J.G., compiler, 1978, Geologic map of Idaho: Idaho Bureau of Mines and Geology, scale 1:500,000.

Bonnichsen, Bill, 1987, Pre-Cenozoic geology of the West Mountain-Council Mountain-New Meadows area, west-central Idaho, in Vallier, T.L. and Brooks, H.C., eds., Geology of the Blue Mountains region of Idaho, Oregon, and Washington: the Idaho batholith and its border zone: U.S. Geological Survey Professional Paper 1436, p. 151-170.

Bonnichsen, Bill, and Citron, G.P., 1982, The Cougar Point Tuff, southwestern Idaho and vicinity, in Bonnichsen, Bill, and Breckenridge, R.M., eds., Cenozoic Geology of Idaho: Idaho Bureau of Mines and Geology Bulletin 26, p. 255-282.

Boone, G.M., 1969, Origin of clouded red feldspars: petrologic contrasts in a granite porphyry intrusion: American Journal of Science, v. 267, p. 633-668.

Borg, I.Y., and Smith, D.K., 1969, Calculated X-ray powder patterns for silicate minerals: Geological Society of America Memoir 122.

Bottinga, Y., and Javoy, M., 1983, Comments on oxygen isotope geothermometry: Earth and Planetary Science Letters, v. 20., p. 250-265.

Brooks, H.C., and Vallier, T.L., 1978, Mesozoic rocks and tectonic evolution of eastern Oregon and western Idaho, in Howell, D.G., and McDougall, K.A., eds., Mesozoic Paleogeography of the Western United States: Society of Economic Paleontologists and Mineralogists, Pacific Section, Pacific Coast Paleogeography Symposium 2, p. 133-145.

Buddington, A.F., 1959, Granite emplacement with special reference to North America: Geological Society of America Bulletin, v. 70, p. 671-647.

Carten, R.B., 1986, Sodium-calcium metasomatism: chemical, temporal, and spatial relationships at the Yerington, Nevada, porphyry copper deposit: Economic Geology, v. 81, p. 1495-1519.

Chappell, B.W. and White, A.J.R., 1974, Two contrasting granite types: Pacific Geology, v. 8, p. 173-174.

Chappell, B.W., White, A.J.R., and Wyborn, D., 1987, The importance of residual source material (restite) in granite petrogenesis: Journal of Petrology, v. 28, p. 1111-1138.

Clemens, J.D., Holloway, J.R., and White, A.J.R., 1986, Origin of an A-type granite: experimental constraints: American Mineralogist, v. 71, p. 317-324.

Cluer, J.K. and Cluer, B.L., 1986, The late Cenozoic Camas Prairie rift, south-central Idaho: Contributions to Geology, University of Wyoming, Laramie, v. 24, no. 1, p. 91-101.

Collins, W.J., Beams, S.D., White, A.J.R., and Chappell, B.W., 1982, Nature and origin of A-type granites with particular reference to southeastern Australia: Contributions to Mineralogy and Petrology, v. 80, p. 189-200.

Coney, P.J., 1980, Cordilleran metamorphic core complexes: an overview, in Crittenden, M.D., Jr., Coney, P.J., and Davis, G.H., eds., Cordilleran metamorphic core complexes: Geological Society of America Memoir 153, p. 7-31.

Conrad, W.K., 1984, The mineralogy and petrology of compositionally zoned ash flow tuffs, and related silicic volcanic rocks, from the McDermitt caldera complex, Nevada-Oregon: Journal of Geophysical Research, v. 89, p. 8639-8664.

Cook, E.F., 1956, Tungsten deposits of south-central Idaho: Idaho Bureau of Mines and Geology Pamphlet 108, 40 p.

Criss, R.E., 1981, An $^{18}O/^{16}O$, D/H and K-Ar study of the southern half of the Idaho batholith: Ph.D. Thesis, California Institute of Technology, Pasadena, California, 401 p.

Criss, R.E., and Champion, D.E., 1984, Magnetic properties of granitic rocks from the southern half of the Idaho batholith: influences of hydrothermal alteration and implications for aeromagnetic interpretation: Journal of Geophysical Research, v. 89, no. B8, p. 7061-7076.

Criss, R.E., and Fleck, R.J., 1987, Petrogenesis, geochronology, and hydrothermal systems of the northern Idaho batholith and adjacent areas based on $^{18}O/^{16}O$, D/H $^{87}Sr/^{86}Sr$, K-Ar, and $^{40}Ar/^{39}Ar$ studies, in Vallier, T.L., and Brooks, H.C., eds., Geology of the Blue Mountains Region of Oregon, Idaho, and Washington: the Idaho batholith and its border zone: U.S. Geological Survey Professional Paper 1436, p. 95-137.

Criss, R.E., Lanphere, M.A., and Taylor, H.P., Jr., 1982, Effects of regional uplift, deformation, and meteoric-hydrothermal metamorphism on K-Ar ages of biotites in the southern half of the Idaho batholith: Journal of Geophysical Research, v. 87, p. 7029-7046.

Criss, R.E., and Taylor, H.P., Jr., 1983, An $^{18}O/^{16}O$ and D/H study of Tertiary hydrothermal systems in the southern half of the Idaho batholith: Geological Society of America Bulletin, v. 94, p. 640-663.

Cullers, R.L., and Graf, J.L., 1984, Rare earth elements in igneous rocks of the continental crust: intermediate and silicic rocks -- ore petrogenesis, in Henderson, Paul, ed., Rare Earth Element Geochemistry, p. 775-316.

Dalrymple, G.B., Alexander, E.C., Jr., Lanphere, M.A., and Kraker,G.P., 1981, Irradiation of samples for $^{40}Ar/^{39}Ar$ dating using the Geological Survey TRIGA reactor: U.S. Geological Survey Professional Paper 1176, 55 p.

Darling, R.S., 1987, The geology and ore deposits of the Carrietown silver-lead-zinc district, Blaine and Camas Counties, Idaho: M.S. Thesis, Idaho State University, Pocatello, Idaho, 168 p.

Darling, R.S., 1988, Ore deposits of the Carrietown silver-lead-zinc district, Blaine and Camas Counties, Idaho, in Link, P.K., and Hackett, W.R., eds., Guidebook to the geology of central and southern Idaho: Idaho Geological Survey Bulletin 27, p. 193-200.

Dover, J.H., 1983, Geologic map and sections of the central Pioneer Mountains, Blaine and Custer Counties, central Idaho: U.S. Geological Survey Miscellaneous Investigations Series Map I-1319, scale 1:48,000.

Ekren, E.B., McIntyre, D.H., and Bennett, E.H., 1984, High-temperature, large-volume, lavalike ash-flow tuffs without calderas in southwestern Idaho: U.S. Geological Survey Professional Paper 1272, 76 p.

Ekren, E.B., McIntyre, D.H., Bennett, E.H., and Marvin, R.F., 1982, Cenozoic stratigraphy of Western Owyhee County, Idaho, in Bonnichsen, Bill, and Breckenridge, R.M., eds., Cenozoic Geology of Idaho: Idaho Bureau of Mines and Geology Bulletin 26, p. 215-236.

Ferry, J.M., 1985, Hydrothermal alteration of Tertiary igneous rocks from the Isle of Skye, northwest Scotland, II. Granites: Contributions to Mineralogy and Petrology, v. 91, p. 283-304.

Fisher, F.S., McIntyre, D.H., and Johnson, K.M., 1983, Geologic map of the Challis 1 x 2 degree quadrangle, Idaho: U.S. Geological Survey Open-File Report 83-523, scale 1:250,000.

Fleck, R.J. and Criss, R.E., 1985, Strontium and oxygen isotopic variations in Mesozoic and Tertiary plutons of central Idaho: Contributions to Mineralogy and Petrology, v. 90, p 291-308.

Fournier, R.O., 1976, Exchange of Na^+ and K^+ between water vapor and feldspar phases at high temperature and low vapor pressure: Geochimica et Cosmochimica Acta, v. 40., p. 1553-1561.

Garlick, G.D., and Epstein, S., 1966, The isotopic compositions of oxygen and carbon in hydrothermal minerals at Butte, Montana: Economic Geology, v. 61, p. 1325-1335.

Gehlen, W.T., 1983, The geology and mineralization of the eastern part of the LIttle Smoky Creek mining district, Camas County, Idaho: M.S. Thesis, University of Idaho, Moscow, Idaho, 136 p.

Geslin, J.K., 1986, The Permian Dollarhide Formation and Paleozoic Carrietown sequence in the SW 1/4 of the Buttercup Mountain quadrangle, Blaine and Camas Counties, Idaho: M.S. Thesis, Idaho State University, Pocatello, Idaho, 116 p.

Giletti, B.J., 1986, Diffusion effects on oxygen isotope temperatures of slowly cooled igneous and metamorphic rocks: Earth and Planetary Science Letters, v. 77, p. 218-228.

Gromet, P.L., and Silver, L.T., 1983, Rare earth element distributions among minerals in a granodiorite and their petrogenetic implications: Geochimica et Cosmochimica Acta, v. 47, p. 925-939.

Hall, W.E., 1985, Stratigraphy and mineral deposits in Middle and Upper Paleozoic Rocks of the black-shale mineral belt, central Idaho, in McIntyre, D.H, ed., Symposium on the geology and mineral deposits of the Challis 1 x 2 degree quadrangle, Idaho: U.S. Geological Survey Bulletin 1658A-S, chap. J., p. 117-132.

Hamilton, Warren, 1963, Metamorphism in the Riggins region, western Idaho: U.S. Geological Survey Professional Paper 436, 95 p.

Hanson, G.N., 1978, The application of trace elements to the petrogenesis of igneous rocks of granitic composition: Earth and Planetary Science Letters, v. 38, p. 26-43.

Harrison, T.M., 1981, Diffusion of ^{40}Ar in hornblende: Contributions to Mineralogy and Petrology, v. 78, p. 324-331.

Harrison, T.M., and McDougall, I., 1980, Investigations of an intrusive contact, northwest Nelson, New Zealand-I. Thermal, chronological, and isotopic constraints: Geochimica et Cosmochimica Acta, v. 44, p. 1985-2003.

Heier, K.S., 1973, Geochemistry of granulite facies rocks and problems of their origins: Philosophical Transactions, Royal Society London, A, v. 273, p. 429-442.

Heller, P.L., Bowder, S.S., Chambers, H.P., Coogan, J.C., Hagen, E.S., Shuster, M.W., and Winslow, N.S., 1986, Time of initial thrusting in the Sevier orogenic belt, Idaho-Wyoming and Utah: Geology, v. 14, p. 388-391.

Hemley, J.J., Montoya, J.W., Marinenko, J.W., and Luce, R.W., 1980, Equilibria in the system Al_2O_3-SiO_2-H_2O and some general implications for alteration/mineralization processes: Economic Geology, v. 75, p. 210-228.

Hemley, J.J., Montoya, J.W., Nigrini, A., and Vincent, H.A., 1971, Some alteration reactions in the system CaO-Al_2O_3-SiO_2-H_2O: Society Mining Geology Japan, Special Issue 2, Proc. IMA-IAGOD meetings, 1970, p. 58-63.

Honjo, Norio, McElwee, K.R., Duncan, R.A., and Leeman, W.P., 1986, K-Ar ages of volcanic rocks from the Magic Reservoir eruptive center, Snake River Plain, Idaho: Isochron/West, no. 46, p. 15-19.

Hooper, P.R., 1982, The Columbia River Basalts: Science, v. 215, p. 1463-1468.

Hoover, A.L., 1987, Transect across the Salmon River suture, South Fork of the Clearwater River, western Idaho -- rare earth element, geochemical, structural, and metamorphic study: M.S. Thesis, Oregon State University, Corvallis, Oregon, 138 p.

Huppert, H.E., and Sparks, R.S.J., 1988, The generation of granitic magmas by intrusion of basalt into continental crust: Journal of Petrology, v. 29, p. 599-624.

Hyndman, D.W., 1981, Controls on source and depth of emplacement of granitic magma: Geology, v. 9, p. 244-249.

Hyndman, D.W., 1983, The Idaho batholith and associated plutons, Idaho and western Montana, in Roddick, J.A., ed., Circum-Pacific plutonic terrances: Geological Society of America Memoir 159, p. 213-240.

Hyndman, D.W., 1984, A petrographic and chemical section through the northern Idaho batholith: Journal of Geology, v. 92, p. 83-102.

Hyndman, D.W., and Foster, D.A., 1988, The role of tonalites and mafic dikes in the generation of the Idaho batholith: Journal of Geology, v. 96, p. 31-46.

Irvine, T.N., and Baragar, W.R.A., 1971, A guide to the chemical classification of the common volcanic rocks: Canadian Journal of Earth Science, v. 8, p. 523-548.

Jacob, T.M., 1985a, Reconnaissance geology of the House Mountain metamorphic rocks, Elmore County, Idaho: Geological Society of America Abstracts with Programs, v. 17, no. 7, p. 227.

Jacob, T.M., 1985b, Reconnaissance geology of House Mountain, Elmore County, Idaho, M.S. thesis, University of Idaho, Moscow, Idaho, 134 p.

Javoy, M., 1977, Stable isotopes and geothermometry: Journal Geological Society London, v. 133, p. 609-639.

Johnson, K.M., Lewis, R.S., Bennett, E.H., and Kiilsgaard, T.H., 1988, Cretaceous and Tertiary intrusive rocks of south-central Idaho, in Link, P.K., and Hackett, W.R., eds., Guidebook to the geology of central and southern Idaho: Idaho Geological Survey Bulletin 27, p. 55-86.

Kerrich, R., and Kamineni, D.C., 1988, Characteristics and chrononology of fracture-fluid infiltration in the Archean, Eye Dashwa Lakes pluton, Superior Province: evidence from H, C, O-isotopes and fluid inclusions: Contributions to Mineralogy and Petrology, v. 99, p. 430-445.

Kiilsgaard, T.H., 1983a, Geologic map of the Ten Mile West Roadless Area, Boise and Elmore Counties, Idaho: U.S. Geological Survey Miscellaneous Field Studies Map MF-1500-A, scale 1:62,500.

Kiilsgaard, T.H., 1983b, Geochemical map of the Ten Mile West Roadless Area, Boise and Elmore Counties, Idaho: U.S. Geological Survey Miscellaneous Field Studies Map MF-1500-B, scale 1:62,500.

Kiilsgaard, T.H., Fisher, F.S. and Bennett, E. H., 1986, The trans-Challis fault system and associated precious metal deposits, Idaho: Ecomomic Geology, v. 81, p. 721-724.

Kiilsgaard, T.H., Freeman, V.L., and Coffman, J.S., 1970, Mineral resources of the Sawtooth Primitive area, Idaho: U.S. Geological Survey Bulletin 1319-D, 174 p.

Kiilsgaard, T.H., and Lewis, R.S., 1985, Plutonic rocks of Cretaceous age and faults in the Atlanta lobe of the Idaho batholith, in McIntyre, D.H, ed., Symposium on the geology and mineral deposits of the Challis 1 x 2 degree quadrangle, Idaho: U.S. Geological Survey Bulletin 1658A-S, chap. B, p. 29-42.

Lameyre, Jean, and Bowden, Peter, 1982, Plutonic rock type series: discrimination of various granitoid series and related rocks: Journal of Volcanology and Geothermal Research, v. 14, p. 169-186.

Leeman, W.P., 1982a, Geology of the Magic Reservoir area, Snake River Plain, Idaho, in Bonnichsen, Bill, and Breckenridge, R.M., eds., Cenozoic Geology of Idaho: Idaho Bureau of Mines and Geology Bulletin 26, p. 369-376.

Leeman, W.P., 1982b, Rhyolites of the Snake River Plain-Yellowstone Plateau Province, Idaho and Wyoming: a summary of petrogenetic models, in Bonnichsen, Bill, and Breckenridge, R.M., eds., Cenozoic Geology of Idaho: Idaho Bureau of Mines and Geology Bulletin 26, p. 203-212.

Leeman, W.P., 1982c, Tectonic and magmatic significance of strontium isotopic variations in Cenozoic volcanic rocks from the western United States: Geological Society of America Bulletin, v. 93, p. 487-503.

Leeman, W.P., Menzies, M.A., Matty, P.J., and Embree, G.F., 1985, Strontium, neodymium and lead isotopic compositions of deep crustal xenoliths from the Snake River Plain: evidence for Archean basement: Earth and Planetary Science Letters, v. 75, p. 354-368.

Leeman, W.P., and Vitaliano, C.J., 1976, Petrology of McKinney Basalt, Snake River Plain, Idaho: Geological Society of America Bulletin, v. 87, p. 1777-1792.

LeMaitre, R.W., 1984, A proposal by the IUGS Subcommission on the systematics of igneous rocks for a chemical classification of volcanic rocks based on the total alkali silica diagram: Australian Journal of Earth Science, v. 31, p. 243-255.

Lewis, R.S., 1984, Geology of the Cape Horn Lakes quadrangle, south-central Idaho: M.S. Thesis, University of Washington, Seattle, Washington, 91 p.

Lewis, R.S., Kiilsgaard, T.H., Bennett, E.H., and Hall, W.E., 1987, Lithologic and chemical characteristics of the central and southeastern part of the southern lobe of the Idaho batholith, in Vallier, T.L., and Brooks, H.C., eds., Geology of the Blue Mountains region of Oregon, Idaho, and Washington -- the Idaho batholith and its border zone: U.S. Geological Survey Professional Paper 1436, p. 171-196.

Link, P.K., Mahoney, J.B., Burton, B.R., Ratchford, Edward, Turner, R.J.W., and Otto, B.R., 1987, Introduction to the geology of the central Idaho black shale mineral belt: Northwest Geology, v. 16, p. 61-84.

Link, P.K., Skipp, Betty, Hait, M.H., Jr., Janecke, Susanne, and Burton, B.R., 1988, Structural and stratigraphic transect of south-central Idaho: a field guide to the Lost River, White Knob, Pioneer, Boulder, and Smoky Mountains, in Link, P.K., and Hackett, W.R., eds., Guidebook to the geology of central and southern Idaho: Idaho Geological Survey Bulletin 27, p. 5-42.

Loiselle, M.C., and Wones, D.R., 1979, Characteristics and origin of anorogenic granites: Geological Society of America Abstracts with Programs, v. 11, p. 468.

Lund, Karen, 1984, Tectonic history of a continent-island arc boundary -- west-central Idaho: Ph.D. Thesis, Pennsylvania State University, University Park, Pennsylvania, 207 p.

Lund, Karen, and Snee, L.W., 1988, Metamorphism, structural development, and age of the continent-island arc juncture in west-central Idaho, in Ernst, W.G., ed., Metamorphism and Crustal Evolution of the Western United States, Rubey Volume 7, Prentice-Hall, Inc., p. 297-331.

Luthy, S.T., 1981, Petrology of Cretaceous and Tertiary intrusive rocks, Red Mountain - Bull Trout Point area, Boise, Valley and Custer counties, Idaho: M.S. Thesis, University of Montana, Missoula, Montana, 119 p.

Macdonald, R., 1974, Nomenclature and petrochemistry of the peralkaline oversaturated extrusive rocks, in Bailey, D.K, Barberi, F., and Macdonald, R., eds., Oversaturated Peralkaline Rocks: Bulletin volcanologique, v. 38, no. 3, p. 498-516.

Malde, H.E., Powers, H.A., and Marshall, C.H., 1963, Reconnaissance geologic map of west-central Snake River Plain, Idaho: U.S. Geological Survey Miscellaneous Investigations Series Map I-373, scale 1:125,000.

Manduca, C.C.A., 1988, Geology and geochemistry of the oceanic arc-continent boundary in the western Idaho batholith near McCall: Ph.D. Thesis, California Institute of Technology, Pasadena, California, 272 p.

Martin, R.F., and LaLonde, A., 1979, Turbidity in K-feldspars: causes and implications: Geological Society of America Abstracts with Programs, v. 11, p. 472-473.

McCarthy, T.S., and Hasty, R.A., 1976, Trace element distribution patterns and their relationship to the crystallization of granitic melts: Geochimica et Cosmochimica Acta, v. 40, p. 1351-1358.

McDowell, S.D., and Elders, W.A., 1980, Authigenic layer silicate minerals in borehole Elmore 1, Salton Sea geothermal field, California, U.S.A.: Contributions to Mineralogy and Petrology, v. 74, p. 293-310.

McIntyre, D.H., Ekren, E.B., and Hardyman, R.F., 1982, Stratigraphic and structural framework of the Challis Volcanics in the eastern half of the Challis 1 degree by 2 degree quadrangle, Idaho, in Bonnichsen, Bill, and Breckenridge, R.M., eds., Cenozoic Geology of Idaho: Idaho Bureau of Mines and Geology Bulletin 26, p. 3-22.

Miller, C.F., and Bradfish, L.J., 1980, An inner Cordilleran belt of muscovite-bearing plutons: Geology, v. 8, p. 412-416.

Miller, C.F., Watson, E.B., and Harrison, T.M., 1988, Perspectives on the source, segregation and transport of granitoid magmas: Transactions of the Royal Society of Edinburgh, Earth Sciences, v. 79, p. 135-156.

Miller, E.L., and Gans, P.B., 1989, Cretaceous crustal structure in the hinterland of the Sevier thrust belt, western U.S. Cordillera: Geology, v. 17, p. 59-62.

Mitchell, V.E., and others, in press, Mines and prospects of the Hailey quadrangle, second edition: Idaho Geological Survey Mines and Prospects Map Series, scale 1:250,000.

Mittlefehldt, D.W., and Miller, C.F., 1983, Geochemistry of the Sweetwater Wash pluton, California: implications for "anomalous" trace element behavior during differentiation of felsic magmas: Geochimica et Cosmochimica Acta, v. 47, p.109-124.

Moye, F.J., Hackett, W.R., Blakley, J.D., and Snider L.G., 1988, Regional geologic setting and volcanic stratigraphy of the Challis Volcanic field, central Idaho, in Link, P.K., and Hackett, W.R., eds., Guidebook to the Geology of Central and Southern Idaho: Idaho Geological Survey Bulletin 27, pp. 87-98

Myers, 1982, Geology of the Harpster area, Idaho County, Idaho: Idaho Bureau of Mines and Geology Bulletin 25, 46 p.

Nash, W.P., and Crecraft, H.R., 1985, Partition coefficients for trace elements in silicic magmas: Geochimica et Cosmochimica Acta, v. 49, p. 2309-2322.

Noble, D.C., and Parker, D.F., 1974, Peralkaline silicic volcanic rocks of the western United States, in Bailey, D.K, Barberi, F., and Macdonald, R., eds., Oversaturated Peralkaline Rocks: Bulletin volcanologique, v. 38, no. 3, p. p. 803-836.

Noyes, H.J., Frey, F.A., and Wones, D.R., 1983, A tale of two plutons: geochemical evidence bearing on the origin and differentiation of the Red Lake and Eagle Peak plutons, central Sierra Nevada, California: Journal of Geology, v. 91, p. 487-509.

Onash, C.M., 1987, Temporal and spatial relations between folding, intrusion, metamorphism, and thrust faulting in the Riggins area, west-central Idaho, in Vallier, T.L. and Brooks, H.C., eds., Geology of the Blue Mountains region of Idaho, Oregon, and Washington -- the Idaho batholith and its border zone: U.S. Geological Survey Professional Paper 1436, p. 139-150.

O'Neil, J.R., and Taylor, H.P., Jr., 1967, The oxygen isotope and cation exchange chemistry of feldspars: American Mineralogist, v. 52, p. 1414-1437.

O'Neill, J. M., and Lopez, D.A., 1985, Character and regional significance of the Great Falls tectonic zone, east-central Idaho and west-central Montana: American Association of Petroleum Geologists Bulletin, v. 69, p. 437-447.

O'Neill, R.L., and Pavlis, T.L., 1985, Superposition of Cenozoic extension on Mesozoic compressional structures of the Pioneer Mountains, central Idaho: Geological Society of America Abstracts with Programs, v. 17, p. 397-398.

O'Neill, R.L., and Pavlis, T.L., 1988, Superposition of Cenozoic extension on Mesozoic compressional structures in the Pioneer Mountains metamorphic core complex, central Idaho: Geological Society of America Bulletin, v. 100, p. 1833-1845.

Orville, P.M., 1963, Alkali ion exchange between vapor and feldspar phases: American Journal of Science, v. 261, p. 201-237.

Orville, P.M., 1972, Plagioclase cation exchange equilibria with aqueous chloride solution: results at 700°C and 2000 bars in the presence of quartz: American Journal of Science, v. 272, p. 234-272.

Otto, B.R., and Turner, R.J.W., 1987, Stratigraphy and structure of the Milligen Formation, Sun Valley area, Idaho: Northwest Geology, v. 17, p. 95-103.

Parsons, Ian, 1978, Feldspars and fluids in cooling plutons: Mineralogical Magazine, v. 42, p. 1-17.

Parsons, Ian, and Brown, W.L., 1984, Feldspars and the thermal history of igeneous rocks, in Brown, W.L., ed., Feldspars and Feldspathoids, D. Reidel Publishing Co., p. 317-371.

Patino-Douce, A.E., and Humphreys, E.D., 1989, Thermal evolution of the crust and anatexis in the Late Mesozoic Cordillera of western North America and their bearing on Cenozoic tectonics: Geological Society of America Abstracts with Programs, v. 21, no. 5, p. 128.

Pavlis, T.L., and O'Neill, R.L., 1987, Comment on "Extensional deformation with northwest vergence, Pioneer core complex, central Idaho": Geology, v. 15, p. 283-284.

Pichavant, M., 1981, An experimental study of the effect of boron on a water-saturated haplogranite at 1 kbar vapour pressure: Contributions to Mineralogy and Petrology, v. 76, p. 430-439.

Piper, A.M., 1924, Ground water for irrigation on Camas Prairie, Camas and Elmore Counties, Idaho: Idaho Bureau of Mines and Geology Pamphlet 15, 46 p.

Pitcher, W.S., 1987, Granites and yet more granites forty years on: Geologische Rundschau, v. 76, no. 1, p. 51-79.

Reid, R.R., 1963, Reconnaissance geology of the Sawtooth Range: Idaho Bureau of Mines and Geology Pamphlet 129, 37 p.

Reid, R.R., 1987, Structural geology and petrology of a part of the Bitterroot lobe of the Idaho batholith, in Vallier, T.L., and Brooks, H.C., eds., Geology of the Blue Mountains region of Oregon, Idaho, and Washington -- the Idaho batholith and its border zone: U.S. Geological Survey Professional Paper 1436, p. 37-58.

Robie, R.A., Bethke, P.M., and Beardsley, K.M., 1967, Selected X-ray crystallographic data, molar volumes, and densities of minerals and related substances: U.S. Geological Survey Bulletin 1248, 87 p.

Ross, C.P., 1930, Geology and ore deposits of the Seafoam, Alder Creek, Little Smoky, and Willow Creek Mining Districts, Custer and Camas Counties, Idaho: Idaho Bureau of Mines and Geology Pamphlet 33, 26 p.

Rudnick, R.L., McLennan, S.M., and Taylor, S.R., 1985, Large ion lithophile elements in rocks from high pressure granulite facies terranes: Geochimica et Cosmochimica Acta, v. 49, p. 1645-1655.

Russell, C.W., 1987, Mafic complexes on the western margin of the Idaho batholith: Geological Society of America Abstracts with Programs, v. 19, no. 5, p. 330.

Rytuba, J.J., and McKee, E.H., 1984, Peralkaline ash flow tuffs and calderas of the McDermitt volcanic field, southeast Oregon and north central Nevada: Journal of Geophysical Research, v. 89, no. B10, p. 8616-8628.

Schmidt, D.L., 1962, Quaternary geology of the Bellevue area in Blaine and Camas Counties, Idaho: U.S. Geological Survey Open-File Report 62-120, 92 p.

Schmincke, H.U., 1974, Volcanological aspects of peralkaline silicic welded ash-flow tuffs, in Bailey, D.K, Barberi, F., and Macdonald, R., eds., Oversaturated Peralkaline Rocks: Bulletin volcanologique, v. 38, no. 3, p. 594-636.

Shannon, E.V., 1926, The minerals of Idaho: Smithsonian Institution, United States National Museum Bulletin 131, 483 p.

Shuster, R.D., and Bickford, M.E., 1985, Chemical and isotopic evidence for the petrogenesis of the northeastern Idaho batholith: Journal of Geology, v. 93, p. 727-742.

Simmons, F.C., and Hedge, C.E., 1978, Minor-element and Sr-isotope geochemistry of Tertiary stocks, Colorado Mineral Belt: Contributions to Mineralogy and Petrology, v. 67, p. 379-396.

Skipp, Betty, 1987, Basement thrust sheets in the Clearwater Orogenic zone, central Idaho and western Montana: Geology, v. 15, p. 220-225.

Skipp, Betty, Hall, W.E., and Link, P.K., 1986, Pre-middle Eocene extension in south-central Idaho -- the Wood River allochthon: Geological Society of America Abstracts with Programs, v. 18, no. 6, p. 753.

Skipp, Betty, and Hait, M.H., Jr., 1977, Allochthons along the northeast margin of the Snake River Plain, Idaho: 29th Annual Field Conference, Wyoming Geological Association Guidebook, p. 499-515.

Skipp, Betty, and Hall, W.E., 1980, Upper Paleozoic paleotectonics and paleogeography of Idaho, in Fouch, T.D., and Magathan, E.R., eds., Paleogeography of west-central United States: Society of Economic Paleontologists and Mineralogists, Rocky Mountain Paleogeography Symposium 1, Denver, Colorado, p. 387-422.

Smith, C.L., 1966, Geology of eastern Mount Bennett Hills, Camas, Gooding, and Lincoln Counties, Idaho: Ph.D. Thesis, University of Idaho, Moscow, Idaho, 129 p.

Smith, J.V., 1974, Feldspar Minerals, v. 1, Crystal Structure and Physical Properties, Springer-Verlag, 627 p.

Smitherman, J.R., 1985, Geology of the Stibnite roof pendant, Valley County, Idaho: M.S. Thesis, University of Idaho, Moscow, Idaho, 62 p.

Snee, L.W., 1982, Emplacement and cooling of Pioneer batholith, southwestern Montana: Ph.D. Thesis, Ohio State University, Columbus, Ohio, 320 p.

Snee, L.W., Sutter, J.F., and Kelly, W.C., 1988, Thermochronology of economic mineral deposits: dating the stages of mineralization at Panasqueira, Portugal, by high-precision $^{40}Ar/^{39}Ar$ age spectrum techniques on muscovite: Economic Geology, v. 83, p. 335-354.

Spear, D.B., and King, J.S., 1982, The geology of Big Southern Butte, Idaho, in Bonnichsen, Bill, and Breckenridge, R.M., eds., Cenozoic Geology of Idaho: Idaho Bureau of Mines and Geology Bulletin 26, p. 395-404.

Stewart, D.E., 1987, Geology of the northern half of the Baker Peak quadrangle, Blaine and Camas counties, Idaho: M.S. thesis, Idaho State University, Pocatello, Idaho, 113 p.

Streckeisen, A.L., and others, 1973, Plutonic rocks -- classification and nomenclature recommended by the IUGS Subcommission on the systematics of igneous rocks: Geotimes, v. 18, no. 10, p. 26-30.

Streckeisen, A.L., 1978, Classification and nomenclature of volcanic rocks, lamprophyres, carbonatites, and melitic rocks, Neues Jahrbuch fur Mineralogie, Abhandlungen, v. 134, p. 1-14.

Sutherland, D.S., 1974, Petrography and mineralogy of the peralkaline silicic rocks, in Bailey, D.K, Barberi, F., and Macdonald, R., eds., Oversaturated Peralkaline Rocks: Bulletin volcanologique, v. 38, no. 3, p. 517-547.

Sutter, J.F., Snee, L.W., and Lund, K., 1984, Metamorphic, plutonic, and uplift history of a continent-island arc suture zone, west-central Idaho: Geological Society of America Abstracts with Programs, v. 16, no. 6, p. 670-671.

Swanson, D.A., Wright, T.L, Hooper, P.R., and Bentley, R.D., 1979, Revisions in stratigraphic nomenclature of the Columbia River Basalt: U.S. Geological Survey Bulletin 1457-G, 59 p.

Tarney, J., and Windley, B.F., 1977, Chemistry, thermal gradients and evolution of the lower continental crust: Journal Geological Society of London, v. 134, p. 153-172.

Taubeneck, W.H., 1971, Idaho batholith and its southern extension: Geological Society of America Bulletin, v. 82, p. 1899-1928.

Taylor, H.P., Jr., 1967, Origin of red-rock granophyres: EOS, American Geophysical Union Transactions, v. 48, p. 245-246.

Taylor, H.P., Jr., 1968, The oxygen isotope geochemisty of igneous rocks: Contributions to Mineralogy and Petrology, v. 19, p. 1-71.

Taylor, H.P., Jr., 1979, Oxygen and hydrogen isotope relationships in hydrothermal mineral deposits, in Barnes, H.L., ed., Geochemistry of Hydrothermal Ore Deposits, John Wiley and Sons, p. 236-277.

Taylor, H.P., Jr., and Margaritz, M., 1976, An oxygen and hydrogen isotope study of the Idaho batholith: EOS, American Geophysical Union Transactions, v. 43, p. 57, p. 350.

Taylor, H.P., Jr., and Margaritz, M., 1978, Oxygen and hydrogen isotope studies of the cordilleran batholiths of western North America, in Robinson, B.W., ed., Stable isotopes in the earth sciences: New Zealand Department of Scientific and Industrial Research Bulletin, v. 220, p. 151-173.

Tilling, R.I., 1973, Boulder batholith Montana: a product of two contemporaneous but chemically distinct magma series: Geological Society of America Bulletin, v. 84, p. 3879-3900.

Titley, S.R., and Beane, R.E., 1981, Porphyry copper deposits, part 1, geologic settings, petrology and tectogenesis: Economic Geology, 75th Anniversary Volume, p. 214-234.

Tuttle, O.F., 1952, Origin of the contrasting mineralogy of extrusive and plutonic salic rocks: Journal of Geology, v. 60, p. 107-124.

Tuttle, O.F., and Bowen, N.L., 1958, Origin of granite in the light of experimental studies in the system $NaAlSi_3O_8$-$KAlSi_3O_8$-SiO_2-H_2O: Geological Society of America Memoir 74, 153 p.

Umpleby, J.B., 1915, Ore deposits in the Sawtooth quadrangle, Blaine and Custer Counties, Idaho: U.S. Geological Survey Bulletin 580, p. 221-249.

Vallier, T.L., and Engebretson, D.C., 1984, The Blue Mountains island arc of Oregon, Idaho, and Washington: an allochthonous terrane from the ancestral Pacific Ocean?, in Howell, D.G., and others, eds., Proceedings of the Circum-Pacific Terrane Conference: Stanford University Publications in the Geological Sciences, v. 18, p. 197-199.

Wall, V.J., Clemens, J.D., and Clarke, D.B., 1987, Models for granitoid evolution and source compositions: Journal of Geology, v. 95, p. 731-749.

Watson, E.B., 1979, Zircon saturation in felsic liquids: experimental results and applications to trace element geochemistry: Contributions to Mineralogy and Petrology, v. 70, p. 407-419.

Watson, E.B., and Harrison, T.M., 1983, Zircon saturation revisited: temperature and composition effects in a variety of crustal magma types: Earth and Planetary Science Letters, v. 64, p. 295-304.

Whalen, J.B., Currie, K.L., and Chappell, B.W., 1987, A-type granites: geochemical characteristics, discrimination and petrogenesis: Contributions to Mineralogy and Petrology, v. 95, p. 407-419.

White, A.J.R., and Chappell, B.W., 1977, Ultrametamorphism and granitoid genesis: Tectonophysics, v. 43, p. 7-22.

Wickham, S.M., 1987, Crustal anatexis and granite petrogenesis during low-pressure regional metamorphism: the Trois Seigneurs Massif, Pyrenees, France: Journal of Petrology, v. 28, part 1, p. 127-169.

Wust, S.L., 1985, Problematic tectonic relations of the Pioneer Window, central Idaho: Geological Society of America Abstracts with Programs, v. 17, p. 272.

Wust, S.L., 1987, Reply on "Extensional deformation with northwest vergence, Pioneer core complex, central Idaho": Geology, v. 15, p. 284.

Wust, S.L. and Link, P.K., 1988, Field Guide to the Pioneer Mountains Core Complex, South-Central Idaho, in Link, P.K., and Hackett, W.R., eds., Guidebook to the Geology of Central and Southern Idaho: Idaho Geological Survey Bulletin 27, p. 43-54.

Yoder, H.S., Jr., and Tilley, C.E., 1962, Origin of basalt magmas: an experimental study of natural and synthetic rock systems: Journal of Petrology, v. 3, p. 342-532.

Yund, R.A., 1983, Diffusion in feldspars, in Ribbe, P.H., ed., Feldspar Mineralogy, Reviews in Mineralogy, v. 2, Mineralogical Society of America, p. 203-222.

Zen, E-an, and Hammarstrom, J.A., 1984, Magmatic epidote and its petrologic significance: Geology, v. 12, p. 515-518.

Zen, E-an, 1988, Thermal modelling of stepwise anatexis in a thrust-thickened sialic crust: Transactions of the Royal Society of Edinburgh, Earth Sciences, v. 79, p. 223-235.